NEW EVOLUTIONARY ALGORITHMS AND THEIR APPLICATION TO ELECTRIC POWER SYSTEM OPERATIONAL ENGINEERING

by

Zakareya Hasan

Submitted in partial fulfillment of the requirements
for the degree of Doctor of Philosophy

at

Dalhousie University
Halifax, Nova Scotia
September 2017

This dissertation is lovingly dedicated to my family for their support, encouragement, understanding, and constant love.

Table of Contents

List of Tables

List of Figures

Abstract

In this research work, models will be developed for optimal dispatch problems applied in a smart grid environment. The models will be used to solve optimal dispatch problems and other problems such as: optimal power flow , unit commitment and short term hydrothermal scheduling for a smart grid environment. The main objectives of smart grid include the optimization of energy production, minimization of the production cost, integration of renewable energy resources and implementation of real time pricing and billing. Each problem will be effected by the objectives of the smart grid and the tools used to implement these objectives such as demand side management (DSM) and load forecasting. There are many constraints in the problems treated such as generators capacity, ramp rate limit, and prohibited operational zones. This research will define the changes in all these constraints. There is also the problem of valve point effects for thermal driven units which will change the fuel cost equation of the generators, which categorizes it as non-smooth and non-convex problem. The second objective of this work will be selecting a suitable algorithm or algorithms to solve the problems with different constraints. The algorithms tested are population based and are inspired by nature. A new heuristic optimization technique called Khums optimization algorithm is introduced and tested on some of the problems treated.

Acknowledgements

It is a pleasure to thank those who made this thesis possible. To a few of them I offer my words of gratitude.

I would like to express my gratitude and sincere thanks and appreciation to my thesis supervisor Dr. M.E. El-Hawary for his great assistance and guidance throughout the thesis work.

Special acknowledgement for my family for their support, motivations and providing me all the time required to reach this point.

Chapter 1

Introduction

1.1 Motivation

In the conventional power network, the economic dispatch problem shown in Fig (1.1) is to allocate the demand load at a specific time to the available generation units with small integration of renewable energy usually considered as a negative load. The generation should always match the load to maintain the frequency of the system and also to satisfy customer needs.

There are no current means of two-way communication between the power producing organization and consumers and it is difficult for the producers to control the loads individually. The nature of the electrical load is effected by the development, and in general it is increasing. In the past, the load increasing problem usually lead to an expensive solution by installing new power plants.

New power network known as smart grid is proposed as a natural development of the massive development in communication systems which facilitates smart decision making [34]. Smart grid (SG) was introduced in [119] and although, there is no standard definition of the smart grid, the European Technology Platform defines it as: "an electrical network that can intelligently integrate the actions of all users connected to it, generators, consumers and those that do both in order to efficiently deliver sustainable, economic and secure electricity supplies" [63].

The main objectives of smart grids are implementation of real time pricing and billing, integration of renewable resources in the network, integration of plugin hybrid electrical vehicles (PHEVs) and electrical vehicles (EVs) with the management system, optimization of energy production, reducing production costs and the greenhouse gases emissions (GHGs) and finally insure the two-way information flow between the utility and consumers. This power network allows the utility to accommodate consumer load commands easily through the advanced metering infrastructure installed in this network as shown in Fig (1.2).

In power systems with appreciable renewable energy and incentivising consumer driven load curtailment implementation of real time pricing are proposed as a smart grid function.

The problem of load increasing at the peak hours can be solved in SG network by controlling the consumption of the consumer (load side) and keeping the same power generation capacity which saves a significant amount of costs.

Fig (1.2) shows also that there is considerable contribution of the renewable energy resources in the SG, which requires developing a more realistic model. This model should deals with the intermittent behavior of these type of energy sources.

Demand side management (DSM) is one of the tools proposed to achieve some of the SG objectives [63]. DSM is the sum of all measures used by the utility to control the user side load at peak times to insure the reliability and sustainability of power generation and to save the large sums of money that will be used in building new power plants.

The economic dispatch problem will be effected by the presence of DSM measures and the significant contribution of the renewable energy resources. In order to address the problem, a mathematical model for the renewable energy resources and a mathematical model for the demand side management load reduction for the economic dispatch problem should be developed. In this thesis the renewable power source under consideration are the wind turbine and the demand side management measures under consideration. The DSM measures will be applied to reduce the load at peak times.

1.2 Thesis Objective

Solving the economic dispatch for smart grid network will allow other power system operational problems because ED is a main part of these problems such as: optimal power flow, unit commitment and the short term hydrothermal scheduling. The objectives of this thesis are:

1. Develop a mathematical model for the economic dispatch problem for smart grid that can account for the significant contribution of the renewable energy source represented by the wind turbines and account for the application of demand side management represented by the load reduction at peak load times.

2. Develop or select a mathematical cost model for the wind turbine units that can deal with the intermittent nature and can be used to solve the economic dispatch problem.

3. Develop mathematical cost models for the load reduction at peak times that can be used to solve the economic dispatch problem.

4. Use the model for economic dispatch for the smart grid to solve the optimal power flow [52], the unit commitment [75] and the short term hydrothermal scheduling [36].

5. Develop new modern optimization algorithm to solve one or more of the four problems and compare it with other algorithms in the literature.

1.3 Thesis Contribution

The contributions of this thesis can be stated as follows:

1. Propose and test a new mathematical optimization algorithm known as the Khums optimization algorithm.

2. Develop a mathematical model for the economic dispatch problem for smart grid accounts for the significant contribution of wind energy and accounts for the application of the load reduction at peak load times and use it to model and solve the optimal power flow problem, the unit commitment problem and the short term hydrothermal scheduling problem.

3. Propose, test and study mathematical cost models for the load reduction at peak times that can be used to solve the economic dispatch problem. The proposed models are the negative load cost model, the probabilistic cost model based on Normal Distribution, probabilistic cost model based on Exponential Distribution and probabilistic cost model based on Weibull Distribution.

4. Study the different cost model proposed in literature for the wind turbine and select the probabilistic model based on the result obtained to deal with the intermittent nature of the wind turbine.

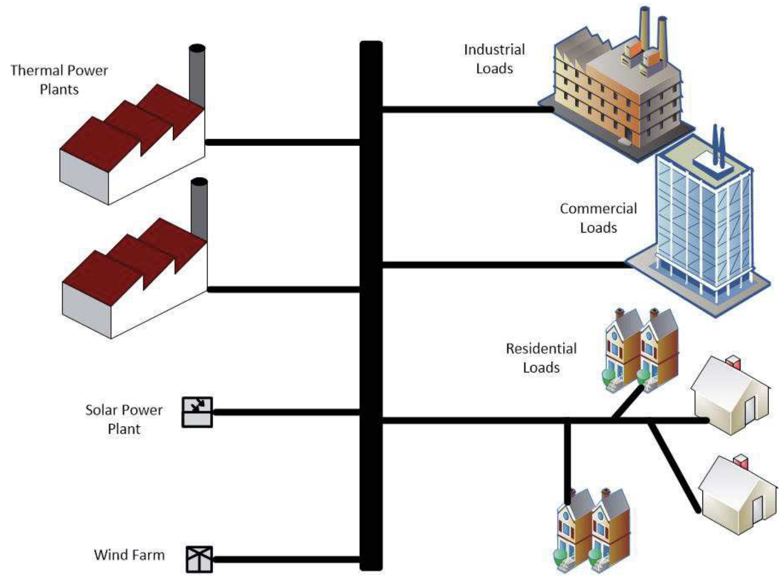

Figure 1.1: Economic dispatch problem for conventional power network

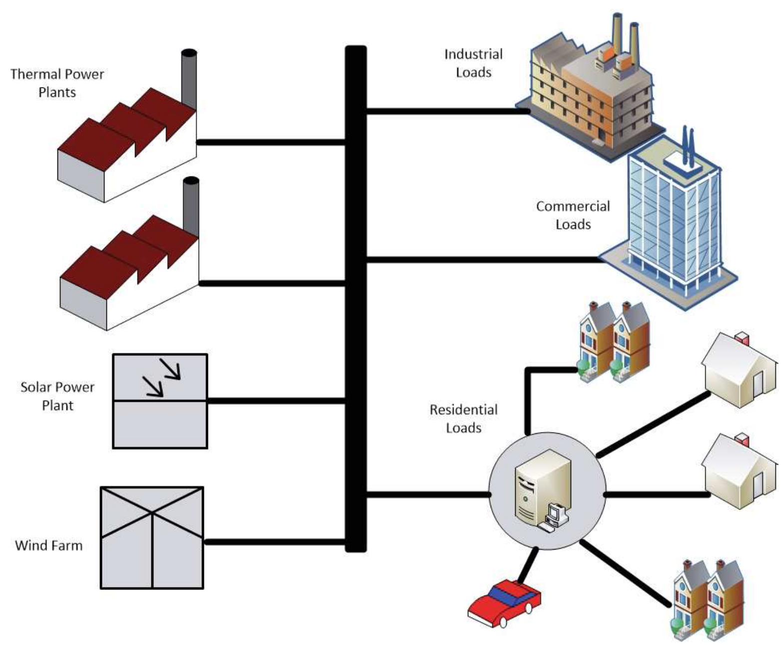

Figure 1.2: New economic dispatch problem for Smart Grid

1.4 Thesis Outline

This thesis is organized to eleven chapters and three appendices as follows:

Chapter 1 This chapter includes the motivation, the objectives of the thesis, the major contributions and the thesis outline.

Chapter 2 This chapter contains literature reviews for the power system operation problems considered in this thesis starting by the economic dispatch problem, then the unit commitment problem, the hydrothermal scheduling and the optimal power flow problem.

Chapter 3 This chapter will cover the mathematical modeling of economic dispatch problem for smart grid network with different constraint and taking account for both the wind energy significant contribution and load reduction at peak load times.

Chapter 4 This chapter briefly review the modern optimization algorithms used in this thesis to study the developed or selected model for the different components such as the wind turbine and the load reduction model and solve the power system operation problems. These algorithms include the Black hole optimization algorithm, the Biogeography based optimization algorithm, the Differential evolution algorithm and the Genetic algorithm.

Chapter 5 This chapter covers a new optimization algorithm known as the Khums optimization algorithm.

Chapter 6 This chapter covers the study of the two proposed cost model for the wind turbine in literature, compare them and solve the economic dispatch problem incorporating wind energy.

Chapter 7 This chapter covers the development of four mathematical cost model for the load reduction at peak load and compare the solution of the problem using the negative load model and the probabilistic model based on Normal distribution.

Chapter 8 Unit commitment for smart grid is formulated in this chapter and solved for four units benchmark test system and ten units benchmark test system with different constraints and including both the wind turbines and the load reduction at peak loads.

Chapter 9 Hydrothermal scheduling for smart grid is formulated in this chapter and solved for two different benchmark test system with different constraints and including both wind turbines and the load reduction at peak loads.

Chapter 10 Optimal power flow for smart grid is formulated in this chapter and solved for IEEE 30 bus benchmark test system with different constraints and including both wind turbines and the load reduction at peak loads.

Chapter 11 This chapter includes the conclusion and the suggestion for future work.

Appendix A This appendix covers the mathematical proof of wind turbine probabilistic cost model based on Weibull Distribution.

Appendix B This appendix covers the mathematical proof of load reduction probabilistic cost model based on normal Distribution, exponential Distribution and Weibull Distribution.

Appendix C This appendix contains the data of most of the benchmark test systems used in this thesis.

Chapter 2

Literature Review

2.1 Introduction

In this chapter, a literature review will be made for the four power system operation problems under consideration in this thesis and they include the economic dispatch, the unit commitment, the short term hydrothermal scheduling and the optimal power flow problems.

2.2 Economic Dispatch

Economic dispatch (ED) is finding the minimum cost of generating electrical energy while satisfying the load demand and the system constraints. There are many constraints such as generators capacity, ramp rate limits, prohibited operation zones [8].

A modern generation unit has input-output characteristics which are highly non-linear because of the valve point effect and ramp rate limits and discontinuities due to prohibited operational zones[7].

Methods proposed for solving the ED problem can be classified like most engineering problems into deterministic methods and stochastic methods[135].

Deterministic methods such as lambda iteration method, gradient methods, base point, and participation factors method as mentioned in [124] assume that the cost curve is continuous and monotonically increasing (convex and smooth objective). This assumption may lead to unfeasible solutions or may lead to suboptimal solution which means that the conventional methods fails in solving such problems with non-smooth and non-convex objectives.

Dynamic programming proposed also to solve the economic dispatch problem [124] and it dose not impose any restriction on the objective function or the constrains but it suffers from the curse of dimensionality.

Stochastic optimization algorithms proposed for solving the economic dispatch are metaheuristic optimization algorithms which either population based like genetic algorithm and biogeography based optimization algorithm or trajectory based like the simulating annealing and evolutionary strategy[135].

Metaheuristic optimization algorithms propose a feasible solution to the problem because they impose no restriction on the nature of the objective functions or constraints. They also provide fast, easy and optimal or near optimal solution.

The drawbacks of using the meta-heuristic algorithms are the lack of theoretical basis which make it not clear for some readers, different search may lead to different solutions, and Optimal solution is not guaranteed.

Simulated Annealing was proposed to solve the economic dispatch to overcome the conventional methods drawbacks in [125]. The algorithm is powerful and can find the optimal and near optimal solution. On the other hand the algorithm is slow.

Genetic algorithm was proposed to solve the economic dispatch with two phases to improve the performance of the algorithm and to obtain better solutions [80]. The algorithm was also proposed to solve the economic dispatch with valve point effect considered in [120]. Then it was proposed to solve the economic dispatch in large scale systems [19] because it is faster and more robust compare with lambda iteration. The problem was solved for a system with ramp rate limits and prohibited operation zones. The main disadvantage of using genetic algorithm lies in the premature convergence which may lead to local optima in dealing with highly correlated optimization parameters or in other words highly epistatic objective functions [40].

Evolutionary programming (EP) was proposed to solve the non-smooth fuel cost function economic dispatch problem because it can overcome the GA algorithm convergence problem and SA high processing time problem [133]. EP proposed to solve the environmentally constrained economic dispatch problem and solution acceleration techniques is proposed and used to enhance the speed and robustness of the algorithm [121]. To enhance the performance of the EP algorithm in solving the economic dispatch problem with non-convex cost curve, two modification were proposed to the adaptation bases in [103].

The Particle Swarm Optimization (PSO) algorithm was proposed to solve the economic dispatch problem with prohibited operation zones and ramp rate limits constraints and the valve point effect is considered in the fuel cost functions in [40]. The main difficult problem in using the particle swarm optimization is the process of choosing the inertia weight factor and the acceleration constants coefficients because the non proper selection may lead to unfeasible solutions [70].

Differential Evolution (DE) was proposed to solve the economic dispatch problem with valve point effects, fuel switching and prohibited operating zones because it is an extremely powerful and simple evolutionary algorithm with great convergence characteristics and requires few control parameters [87]. It was also proposed to solve the economic environmental dispatch problem considering emissions as constraints and as a second objective function of a multiobjective optimization problem [86].

Artificial neural networks were proposed to find the real time optimal dispatch of thermal power plant units considering the operation requirements and the network power losses [24]. The disadvantage of the neural network applied in economic dispatch problem is that it may fail to converge to an equilibrium point. To overcome this problem a modified Hopfield network was proposed to solve the economic dispatch problem where the internal parameters of the Hopfield network are calculated in a way guarantee the convergence to an equilibrium point [22].

Biogeography based optimization algorithm was proposed to solve the convex and non-convex economic dispatch problem with ramp rate limit, prohibited operation zones, power losses, valve point effect and multi-fuel option. This algorithm is easy to implement and has good convergence performance compare to other evolutionary algorithms in solving economic dispatch problem [9, 76]. But like other algorithms it cannot guarantee the optimal solution where it can get the optimal or near optimal solution. Based on the no free lunch theorems, there is no best universal algorithm for all optimization algorithms, which encourages the researcher to find the best optimization algorithm for a specific optimization problem.

In order to improve the performance of evolutionary algorithms, hybrid algorithms were proposed to solve the economic dispatch problem.Two hybrid algorithms GGA and GAA2 based on genetic algorithm and simulated annealing were proposed to solve the environmental economic dispatch problem [118]. A DE/BBO algorithm proposed to improve the solution quality and the convergence speed [8]. BBO/ES hybrid algorithm proposed to solve the economic dispatch problem where equality and inequality constraints, transmission losses and valve point effect were considered [91].

2.3 Unit Commitment

The unit commitment (UC) problem is defined as: finding the minimum cost schedule of a set of generators by turning each one either ON or OFF over a given time horizon to meet the demand load and satisfy different operational constraints [98].

Three components are associated with the total unit commitment cost and they are: the operation cost, start up cost, and shut down cost. There are many constraints in the unit commitment problem such as spinning reserve, minimum uptime, minimum downtime, crew, must run and fuel constraints [129]. The problem is a nonlinear, large scale, mixed integer combinatorial optimization problem with constrains.

Several methods were proposed to solve the unit commitment problem. Conventional methods such as exhaustive enumeration, Priority List, Mixed integer programming, Dynamic Programming, Branch-Bound, Interior Point optimization, decomposition technique and Lagrangian Relaxation were used to solve the UC problem.

Exhaustive enumeration will evaluate all possible combination of ON and OFF schedule of the problem which for N_g generation units and T period equal to $(2^{N_g}-1)^T$. For a small system consisting of four generation units, scheduled for 24 hours and using a supercomputer that do forty thousand trillion operation per second, it will take around 13345.155 years to complete all the possible combinations. Hence, it is not suitable for solving the UC problem because of the curse of dimensionality[129].

Priority list is fast and simple method for solving the UC problem and there are no curse of dimensionality in it, but it is highly heuristic and usually achieves schedules with relatively high operating cost [129].

Dynamic Programming (DP) [129] can reduce the number of possible combinations of the ON and OFF schedule in UC problem by eliminating the non feasible solutions. DP can handle the different constraints of unit commitment problem but it suffer from the curse of dimensionality for large systems.

Branch-and-bound techniques proposed to solve the unit commitment problem with startup costs, demand constraint, reserve constraint, minimum up constraint and minimum down time constraint. This method does not require a priority ordering of the units like the priority list method [21]. The applications using this method are limited to small sized systems because the computation time will increase exponentially with the size of UC problem.

Interior Point optimization/ cutting plane methods have good convergence characteristics and the parameter tuning is not a critical issue compared to sub-gradient and bundle methods [74].

Mixed Integer programming guarantees convergence to the optimal solution in a finite number of steps while providing a feasible and accurate modeling framework [15]. This method was applied to small systems and the approximation done limit the solution space.

Lagrange Relaxation (LR) is the most realistic and efficient method for large scale systems [140, 20]. The drawbacks of LR method is that the convergence to a feasible solution after a limited number of iterations is not guaranteed and it is inherently sub optimal.

Metaheuristic algorithms were proposed as solution methods to the unit commitment problem to cover the shortcomings of the classical methods and search for the optimal solution. These methods are inspired by nature and they include: Expert Systems [79], Simulated Annealing (SA) [102], Artificial Neural Networks [97], Genetic Algorithm (GA) [114], Ant Colony Search Algorithm (ACSA) [132, 110], Tabu Search (TS) method [140] and Biogeography Based Optimization (BBO) [75]. These algorithms do not impose any restriction on the nature of the objective function or constraints but do not guarantee the global optimal solution all the time because they may converge to near optimal solution.

The expert system method is mainly used for search and optimization because it reduces the complexity in calculation and reduces computation time. The main problem in this method arises if a new schedule is different from schedule in the database.

Simulated Annealing was proposed to solve the UC problem to overcome the conventional algorithms weakness that may converges to global optimum solution. The drawback of the SA is it may converge to a local optimal solution if the annealing scheduling is not selected carefully and It will take much time to reach the solution.

Artificial Neural networks method can accommodate more complicated constraints and the solution convergence is rapid and has a good quality. The main disadvantage of the artificial neural networks is the computation time which increases exponentially with size of the problem [1].

Genetic Algorithm is a general purpose stochastic and parallel search method based on the mechanics of natural selection and natural genetics. GA is mainly used for search and optimization and one of the frequently algorithm applied for solving the unit commitment problem. This algorithm has the potential of obtaining near optimal global solution, obtain accurate result within short time and the constraints are included easily.

Ant Colony Search Algorithm (ACSA) algorithm is a powerful tool to solve optimization problems in power systems such as economic dispatch and unit commitment inspired by the ants behavior in finding the shortest bath between the nets and the food source. ACSA is successfully applied to solve the unit commitment in [110]. An improved ACSA which use artificial ants with memory and not completely blind and to insure solution optimality, the state transition, global updating rule and local updating rule were introduce[132]. The improve d algorithm produce lower cost but with higher execution time compared with the conventional ACSA. Also as the agent number increase the cost decrease and the execution time increase [132].

Tabu search algorithm is an iterative improvement procedure that uses a short term memory of recent solutions to escape from local optima to a better near global or global solution. The main disadvantages of the Tabu search algorithm are the long processing time and the possibility of trapping on a local optima is significant [1].

Biogeography Based Optimization (BBO) is a global evolutionary optimization algorithm such as GA and Particle Swarm optimization (PSO) algorithms which is inspired by the study of distribution of species in Habitats. BBO is simple in concept, fast and easy to implement in solving the unit commitment problem compared with other evolutionary algorithms, but like other algorithms it cannot grantee the optimal solution where it can get the optimal or near optimal solution [75].

2.4 Hydrothermal Scheduling

The hydrothermal scheduling (HTS) problem is finding the optimal power allocation of the load among the available thermal unit and hydro units for a period of time and the objective is to minimize the thermal units total fuel cost. There are many constraints in the HTS problem such as real power balance, thermal generation unit power limit constraints and hydro generation unit power limit constraint, water discharge rate, spillage discharge rate, starting storage volume and ending storage volume [124].

Various classical methods such as Lagrange relaxation and dynamic programming were used to solve the HT problem. First order gradient methods were used for long-term and short-term hydrothermal scheduling of multi storage hydroelectric and multi thermal systems[2]. Direct method which treats constraints as subspaces and the solution is automatically restricted within the limiting subspaces was used to solve the long-term and short-term hydrothermal scheduling problems [96].

Multi pass dynamic programming (MPDP) technique with successive approximations is used to solve the daily hydrothermal scheduling problem [57]. The combination is used to reduce the long computation time and the large storage memory requirement. Extended differential dynamic programming and mixed coordination was used to solve short-term scheduling of hydrothermal scheduling [115]. The variational feedback nature of the control strategy is used to handle unpredictable changes in natural inflow. Mixed-integer is used to solve the short term hydrothermal scheduling problem [84]. The main problem of the dynamic programing is the curse of dimensionality [124, 126].

The Lagrangian relaxation technique was presented to solve the short term hydrothermal scheduling problem with cascaded reservoirs and discrete hydro constraints in [45]. Dual problem formulation based Lagrange relaxation method presented to solve the short term hydrothermal scheduling problem [94]. Lagrangian multipliers correction procedure called optimal distance method is used short-term hydro-thermal coordination procedures based on the Lagrangian relaxation technique [93]. Lagrange relaxation techniques overcome the dimensionality problem for large network but they required special measures to get a feasible solution if the objective function is not convex and the algorithm iterative process may oscillate [18].

Modern algorithms were used to solve the HT problem because they are easy to implement and can handle the nonlinear or non-convex objectives or constraint and they can find the optimal or near optimal solutions .

The Simulated Annealing algorithm was proposed to solve short term hydrothermal scheduling because it overcome the drawback of Lagrange relaxation and dynamic programming [126]. Coarse grained parallel simulated annealing algorithm proposed to modify the speed of the algorithm [127]. The weakness of the SA algorithm lies on the annealing scheduling were it should be selected carefully or the obtained solution will lies on the local optimal solution and if the annealing scheduling was well selected, it will cost a lot of computation time.

Evolutionary Programming (EP) algorithm [134] was proposed to overcome the drawback of simulation annealing in solve the short-term hydrothermal scheduling problem.

Genetic Algorithm was also proposed to overcome the drawback of the conventional method and the drawback of the simulating annealing algorithm in solving the short term hydrothermal scheduling problem [85, 130, 44].

Evolution Strategies were used to solve the short-term hydrothermal scheduling [123]. Decomposition is not required in this algorithm like the previous algorithm were the evolutionary algorithm is used to optimize the hydroelectric subsystem and the conventional method to solve the thermal system like in [85].

The Hopfield Neural Networks were proposed to overcome the problem of long time required to solve the hydrothermal scheduling problem by other methods [72]. Heuristic rule is used to deal with the situations were some of the practical constraints was violated. A two-phase neural network based optimization method were proposed to solved short-term scheduling of a hydrothermal power system and does not required a heuristic rule and has the ability to generate feasible solutions[81].

The Bacterial Foraging Algorithm was used to solve the HT problem as [35, 36, 37]. A new modification was proposed to solve the poor convergence properties and high execution time requirements problems in the algorithm specially in dynamic environment and high dimension search space.

The Particle Swarm Optimization Algorithm was proposed to solve the HTS problem [136] because the PSO algorithm is easy to implement and have a high computational efficiency. The algorithm required high population size and high generation in order to get a reasonable solution which will cost a lot of computation time. A small population-based particle swarm optimization approach proposed to solve the problem of high computation time in short-term hydrothermal scheduling by using a small population size[138]. Time varying acceleration coefficient based particle swarm optimization with constriction factor and inertia weight approach was applied to determine the optimal hourly schedule of power generation in a hydrothermal power system [23].

The Imperialistic Competition Algorithm based optimization technique was presented for solving the short-term economic emission dispatch problem in a hydrothermal system with cascaded reservoirs [68].

The Teaching Learning Based Optimization techniques was applied to solve short-term scheduling of a hydrothermal power system with cascaded reservoirs and the delay of water transport between the cascaded reservoirs are also taken in to consideration [89].

The Grey Wolf Optimization Algorithm was used to solve short-term hydrothermal scheduling problems which provide enough diversity for finding better solutions [113].

Searching for better convergence and less execution time, the Symbiotic Organisms Search algorithm was proposed to solve the short-term hydrothermal generation scheduling in [59].

2.5 Optimal Power Flow

Optimal power flow (OPF) is one of the most important optimization problems in power system operation and control that has been studied widely in the past few decades. The main objective used in the OPF problem is to reduce the generation cost with or without reducing the system losses subjected to different equality constraints such as full AC power flow, DC power flow and steady state security. The problem is also subject to inequality constraints such as active/reactive power generation limits, bus voltage limits and control limits.

As an optimization problem, OPF is classified as nonlinear and non-convex optimization problem as result of the process of selecting both the objective function and system constraints. It is also a large scale optimization problem because of the large number of variables dealt with even in small systems.

Variables in this problem are classified as state and control variables. State variables are continuous and include the bus voltage magnitude, the bus voltage phase angle, the bus injected active and the reactive power. The control variables are a mix of continuous variable and discrete variables. The control variables include the generation voltage magnitude, the generation active power, the generation reactive power and the setting of network control devices such as the transformers tap changers and switching devices.

Many classical optimization algorithms were proposed as methods of solution to the OPF problem since the introduction of the problem by Carpentier in 1962[14] such as gradient methods[26, 5, 38, 31, 13, 88], Newton methods[112, 56], sequential linear programing[4], sequential quadratic programing[12, 16] and interior point methods[117]. All these methods assume that the objective function is continuous and monotonically increasing and linearize both the objective function and the system constraints around the selected operating point. But, the OPF problem is highly nonlinear and non-convex optimization problem which means that it has more than one optimal solution. Furthermore, modern generation units have input-output characteristics which are highly nonlinear because of the valve point effect and ramp rate limits and discontinuous due to prohibited operation zones. Hence, using the classical methods with the new units may lead to infeasible solutions or may lead to suboptimal solutions.

Evolutionary algorithms (EA) were used frequently in the engineering optimization methods to overcome the weakness of the conventional methods in finding the global optimal solution while satisfying the different constraints. EA are metaheuristic optimization algorithms which is usually inspired by nature. They are also derivative free and dynamic robust algorithms. These algorithms can be applied to any problem that can be formulated as an optimization problem.

Genetic Algorithm (GA)[55], Particle Swarm optimization algorithm (PSO)[29, 62], Evolutionary Programming (EP)[39], Differential Evolution (DE)[108], Ant Colony Optimization (ACO)[27], and Biogeography Based Optimization (BBO)[100] are example of metaheuristic optimization algorithm.

GA is the most widely used and the oldest metaheuristic algorithm and it is relies on natural selection for solving optimization problems[101]. GA is a population based optimization algorithm which apply basically to main operation for generating the new solutions which is: crossover and mutation. The offspring solution generated after the two operation will replace the old population. Lai et al.[69] presents an improved genetic algorithm to solve the OPF problem using a dynamical hierarchy of the coding system which has the ability to code a large number of control variables in a practical system. Zhang et al.[137] used an integer/float mixed coding GA for optimizing the power system reactive power. Real coded GA is easier and straightforward and it is utilized to solve the OPF problem in recent papers[109, 41].

PSO is a population based algorithm which is inspired by swarm intelligence of animals such as birds and fish schooling. Kim et al.[66] used straightforward parallelization of PSO algorithm to overcome higher computing time to find optimal point. Hajian-Hoseinabadi et al.[46] used a modified particle swarm optimization algorithm for solving the OPF problems. The main distinction of this approach is in using particles worth experience instead of the best previous experience. Zhang and Liu [139] utilize the PSO method to deal with the reactive power optimization problem in power system.

Evolutionary programming is population based algorithm proposed by Lawrance Fogel [39] based on finite state machine. Wong and Yuryevich [128] applied evolutionary programming for solving the optimal power flow problem with highly non-linear generator input output cost curves. Tangpatiphan and Yokoyama [116] applied an improved Evolutionary Programming algorithm for the OPF with steady state voltage stability which utilize the crossover techniques from real coded genetic algorithm.

Differential evolution is a simple population based algorithm which create the new candidate solutions basically from adding a scaled amount of the difference between two or more vectors in the population to a third vector [101]. Liang et al.[71] propose a modified DE algorithm to overcome the disadvantage of premature convergence generated from not using a large population in solving optimal reactive power flow problems. Abou El Ela et al. [32] utilize the DE algorithm to solve the optimal power flow problem.

Ant colony optimization is a population based algorithm inspired by the ants food searching. Kalil et al. [60] apply the ACO algorithm to solve the optimal reactive power in order to improve voltage stability, transmission loss and voltage profile monitoring. Gasbaoui and Allaoua [42] utilize the ACO algorithm for solving the OPF combinatorial problem.

Biogeography based optimization (BBO) is population based algorithm which simulate the process of how species migrate between islands, how new species arise, and become extinct [100]. Bhattacharya and Chattopadhyay[10] employ the BBO algorithm to solve OPF problems with generators that have both convex or non-convex fuel cost characteristics. Roy et al. [92] present the BBO algorithm for solving the OPF considering generators valve point effect.

The Harmony Search (HS) algorithm proposed in [43] is relies on musical processes in concept. Khazali and Kalantar[65] ues HS algorithm to solve the optimal reactive power dispatch with power transmission loss, voltage stability and voltage profile as separate objective functions. Sivasubramani and Swarup [105] apply the HS algorithm for optimal power flow (OPF) problem as a multi-objective optimization problem with generation fuel cost, power transmission loss and voltage stability index as three objective functions.

Chapter 3

Economic Dispatch Problem for Smart Grid

3.1 Introduction

Economic dispatch (ED) is finding the minimum cost of generating electrical energy while satisfying the load demand and the system constraints.In power systems with appreciable renewable energy and incentivising consumer driven load curtailment, implementation of real time pricing is proposed as a smart grid function. In smart grid network, the economic dispatch problem will be affected by the presence of demand side managements (DSM) measures due to the advanced metering infrastructure installed in this network, and the significant contribution of the renewable energy resources. This chapter proposes the formulation of economic dispatch problem for smart grid network, and define the different equality and inequality constraints.

3.2 Smart Grid Economic Dispatch Mathematical Formulation

Smart grid is shown in Fig(3.1) where renewable energy contribution is significant and there are means of two-way communication between the utility and the consumer through the smart meters installed in the network which ease the process of DSM measures. In this work the renewable power source under consideration is the wind turbine and the demand side management measures under consideration are the changing of the loads shape measures by load management programs. The DSM measures will be applied to reduce the load at peak times. Hence, the ED problem at smart grid defined as the allocation of the load demand on the available generation units (thermal and wind) and choose the cheapest area or consumers to apply DSM measures (load reduction) while satisfying the unit constraints and the system constraints. The general formulation of the ED optimization problem can be stated as follows:

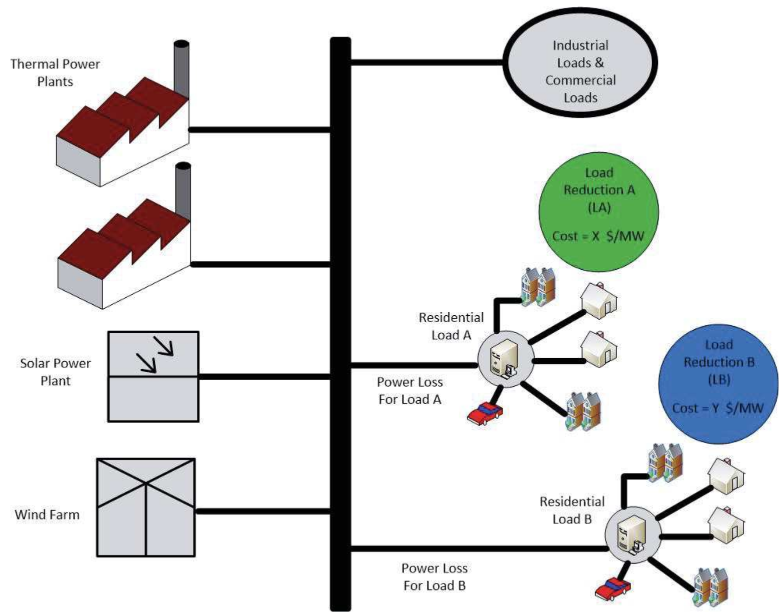

Figure 3.1: Effect of DSM on the economic dispatch problem for Smart Grid

$$min \;\; J \tag{3.1}$$

$$J = FC + W_{cost} + LR_{cost} \tag{3.2}$$

Where J is the objective function, FC is the total fuel cost of thermal generation units, W_{cost} is the total cost of wind power generation and LR_{cost} is the total cost of load reduction. W_{cost} model and LR_{cost} model will be discussed in chapter (6) and (7) respectively.

$$FC = \sum_{i=1}^{N_x} a_i\, P_i^2 + b_i\, P_i + c_i \tag{3.3}$$

Where FC is the total fuel cost of generators, N_x is the number of generator units, P_i is the output power of generation unit i, a_i, b_i and c_i are the fuel cost coefficients. The fuel cost equation considering the valve point effect is given by:

$$FC = \sum_{i=1}^{N_x} a_i\, P_i^2 + b_i\, P_i + c_i + \left| e_i \, \sin(f_i \; (P_i^{min} - P_i)) \right| \tag{3.4}$$

Where e_i, f_i are the fuel cost coefficients and P_i^{min} is the minimum active output power of the i^{th} generating unit.

3.3 Equality Constraints

3.3.1 Real Power Balance Constraint

Equation (3.5) represents the equality constraint in the problem, where the P_D represent the total load demand and P_L is the power losses.

$$\sum_{i=1}^{N_x} P_i + \sum_{j=1}^{N_w} w_j + \sum_{k=1}^{N_d} L_k = P_D + P_L \tag{3.5}$$

$$P_L = \sum_{h=1}^{N_t} \sum_{m=1}^{N_t} P_h\, B_{hm}\, P_m + B_{h0}\, P_h + B_{00} \tag{3.6}$$

Where w_j available wind power for the j^{th} wind turbine, L_k is the available load reduction from area k and N_d is the total number of load reduction areas. $N_t = N_x + N_w$, B_{hm}, B_{h0} and B_{00} are the Power loss coefficients.

3.4 Inequality Constraints

3.4.1 Generator Power Limit Constraint

Generation units are restricted by their limits in term of generation active power as follows:

$$P_i^{min} \leq P_i \leq P_i^{max} \quad i = 1, 2 \cdots, N_x \tag{3.7}$$

Where P_i^{min} and P_i^{max}, are the minimum active output power, maximum active output power of the i^{th} generating unit respectively.

3.4.2 Ramp Rate Limit Constraint

$$\begin{aligned} P_{i\ now} - P_{i\ new} &\leq DR_i \\ P_{i\ new} - P_{i\ now} &\leq UR_i \end{aligned} \tag{3.8}$$

Where DR_i is the down ramp limit of the i^{th} generator and UR_i is the up ramp limit of the i^{th} generator.

3.4.3 Prohibited Operating Zone Constraint

$$\begin{aligned} P_i^{min} \leq P_i &\leq P_{i,1}^l \\ P_{i,1}^u \leq P_i &\leq P_{i,2}^l \\ P_{i,2}^u \leq P_i &\leq P_{i,3}^l \\ &\vdots \\ P_{i,j_x}^u \leq P_i &\leq P_i^{max} \\ i &= 1, 2 \cdots, N_x \\ j_x &= 1, 2 \cdots, m_i \end{aligned} \tag{3.9}$$

where P_{i,j_x}^l, P_{i,j_x}^u are the lower and upper bound of the j_x^{th} prohibited zone of the i^{th} generation unit respectively, and m_i is the total number of prohibited operating zones of the i^{th} generation unit.

3.4.4 Wind Turbine Power Limit Constraint

$$0 \leq w_j \leq w_j^r \quad j = 1, 2 \cdots, N_w \tag{3.10}$$

Here w_j^r, is the rated active power output of the j^{th} wind turbine unit and N_w is the total number of wind turbine units.

3.4.5 Load Reduction Power Limit Constraint

$$L_k^{min} \leq L_k \leq L_k^{max} \quad k = 1, 2 \cdots, N_d \tag{3.11}$$

Here L_k^{min} and L_k^{max}, are the minimum active power reduction, maximum active power reduction of the k^{th} area respectively.

3.5 Summary

In this chapter, a formulation of economic dispatch problem for smart grid network is proposed, and the different equality and inequality constraints was defined. The objective function and the constraints were modified based on the significant contribution of both wind energy and load reduction. The cost models will be discussed in detail in chapter (6) for wind turbine and chapter (7) for load reduction.

Chapter 4

Metaheuristic Optimization Algorithms

4.1 Population Based Modern Optimization Algorithm

Metaheuristic optimization algorithms are usually population based algorithms where we start with some random candidate solutions to solve the optimization problem. Some algorithms like the evolutionary strategy algorithm and the simulating annealing algorithm require only one single candidate solution, whereas most of the algorithms require a group of candidate solutions like the genetic algorithms and the particle swarm optimization algorithm. The pseudo code of the population based metaheuristic algorithms is shown in (1). This chapter introduce the metaheuristic optimization algorithms that have been used in this thesis to solve the power system operation problems and these algorithms are: black hole algorithm, biogeography based optimization, differential Evolution and genetic algorithm.

Algorithm 1 Metaheuristic Algorithm

```
Initialization
Generate a random set of solutions
Calculate the fitness of each habitat
Save the Optimal solution
while not (termination criterion) do
    Execute the Algorithm
    Calculate the fitness of each habitat
    Save the Optimal solution
end while
return
```

4.2 Black Hole Algorithm

The black hole algorithm (BH) is a population based algorithm inspired by the black hole phenomenon[53] and has common features with other population based algorithms such as genetic algorithm(GA), particle swarm optimization(PSO), differential evolution (DE), etc. A candidate solution in the BH algorithm is represented by a star and the best candidate solution is selected to be a black hole. Two operations in the proposed algorithm are used to evolve the population toward the optimality: star absorption and star sucking.

4.2.1 Star Absorption

It is the operation of moving the stars towards the black hole under the black hole absorbing force and in the optimization method it is equivalent to recombination in other evolutionary algorithms. For example crossover in GA, crossover in DE, migration in BBO, etc. Star absorption can be formulated as follows:

$$X_i^{t+1} = X_i^t + r\ (X_{BH} - X_i^t) \tag{4.1}$$

where X_i^{t+1} and X_i^t are the location i^{th} star (candidate solution) at iteration t and $t+1$ respectively, X_{BH} is the location of the black hole(best candidate solution) and r is random number in the interval [0,1].

4.2.2 Star Sucking

During the moving operation of stars toward the black hole, there is a probability of crossing the event horizon which is the point of no return. If a star (candidate solution) crosses the event horizon it will be sucked by the black hole (best solution) and the new solution will be generated in order to keep a constant number of candidate solutions. The radius of the event horizon in the BH algorithm calculated as follows:

$$R = \frac{f_{BH}}{\sum_{i=1}^{N} f_i} \tag{4.2}$$

where f_{BH} is the fitness value of the black hole, f_i is the fitness value of the i^{th} star and N is the number of stars. If the distance between the candidate solution and the best solution is less than R, that candidate solution will be replaced by new solution. The pseudo code for the BH algorithm is shown in Algorithm (2).

Algorithm 2 Black Hole Algorithm

Initialize a random population of stars (X_i and $i \in [1, N]$ and $X_i = [x_{1i} \cdots x_{mi}]$)
Calculate the fitness of each star
$X_{BH} \leftarrow$ Optimal solution
while not (termination criterion) **do**
    for each star X_i and $i \in [1, N]$ **do**
        $X_i^{t+1} \leftarrow X_i^t + r\ (X_{BH} - X_i^t)$
    end for
    $R \leftarrow \frac{f_{BH}}{\sum_{i=1}^{N} f_i}$
    for each individual X_i and $i \in [1, N]$ **do**
        $D_i \leftarrow \sqrt{(x_{1BH} - x_{1i})^2 + \cdots (x_{mBH} - x_{mi})^2}$
        if $D_i < R$ **then**
            $X_i \leftarrow$ Randomly generated individual
        end if
    end for
    Calculate the fitness of each star
    $X_{BH} \leftarrow$ Optimal solution
end while
return

4.3 Biogeography Based Optimization

Biogeography based optimization (BBO) method is a population based algorithm proposed by Simon in [100]. BBO is inspired by the study of distribution of species in Habitats. The mathematical model was developed by MacArthur and Edward Wilson as pointed in [100]. In BBO Islands represent a feasible candidate solution. The solutions will be ranked using two variables: immigration rate λ (bad) and emigration μ (good) rate. The fitness is defined in BBO as the habitat suitability index (HIS) and there are two main operations in this algorithm: migration and mutation. The pseudo code for the BH algorithm is shown in Algorithm (3).

Algorithm 3 BBO Algorithm

```
Initialize the BBO parameters
Generate a random set of habitats( I_i and i ∈ [1, N])
Calculate the fitness (HSI) of each habitat
Calculate and map μ and λ
I_Best ← Optimal solution
while not (termination criterion) do
    Migration process
    Mutation process
    Fitness, μ and λ Calculation and mapping
    I_Best ← Optimal solution
end while
return
```

4.3.1 Migration

Migration is the process of probabilistically sharing information between habitats using the λ and μ rates. We modify each solution based on other solutions by first randomly selecting an island to be modified (poor island) using the immigration rate λ (bad). After that using the emigration rate μ (good) we select a source of modification (good island). Then we randomly select a feature from the good island to modify the poor island.

4.3.2 Mutation

A rarely severely destructive events can extremely change the HSI of a habitat and can cause the species count to deviate from its equilibrium point [100]. In mutation a randomly new candidate solution will be generated to replace the old one using the selected mutation rate.

4.4 Differential Evolution

Differential evolution (DE) is a population based optimization algorithm introduced by Ken Price and Rainer Storn[106]. The motivation of the algorithm was a result of developing a solution to the Chebyshev polynomial coefficients and the optimization of digital filter coefficients. This algorithm uses three operations to generate new candidate solutions: mutation, crossover and selection [111]. The pseudo code for the DE method shown in Algorithm (4).

4.4.1 Mutation

In the mutation process a new candidate solution is created by modifying a randomly selected solution as shown generally in the Equation (4.3):

$$v_i = \begin{cases} x_{r_1} + F \times (x_{r_2} - x_{r_3}) & r < pf \\ x_{r_1} + \frac{(F+1)}{2} \times (x_{r_2} - x_{r_1} + x_{r_3} - x_{r_1}) & r \geq pf \end{cases} \tag{4.3}$$

Where F is the step size parameter, pf is the mutation rate, r_i is random integer and x_{r_i} is the candidate solution in the population which has a position r_i.

4.4.2 Crossover

In the crossover process the old and new solutions generated in mutation are merged as shown in (4.4) to generate new population.

$$u_i = \begin{cases} v_i & r < co \\ x_i & r \geq co \end{cases} \tag{4.4}$$

Where co is the crossover probability.

4.4.3 Selection

The selection process is done by implementing (4.5) which chooses between the parents and the children based on the fitness function.

$$x_i = \begin{cases} u_i & f(u_i) < f(x_i) \\ x_i & f(u_i) \geq f(x_i) \end{cases} \tag{4.5}$$

Algorithm 4 Differential Evolution

Initialize the DE parameters$\{F, pf, co\}$
Generate a random set of individual(x_i, v_i^0 $i \in [1, N]$)
Calculate the fitness of each individual
while not (termination criterion) **do**
    for each individual x_i and $i \in [1, N]$ **do**
        $r_1 \leftarrow$ random integer $\in [1, N]$
        $r_2 \leftarrow$ random integer $\in [1, N]$ and $r_2 \neq r_1$
        $r_3 \leftarrow$ random integer $\in [1, N]$ $r_3 \neq r_2 \neq r_1$
        $r \leftarrow$ random number
        if $r < pf$ **then**
            $v_i \leftarrow x_{r_1} + F \times (x_{r_2} - x_{r_3})$
        else
            $v_i \leftarrow x_{r_1} + \frac{(F+1)}{2} \times (x_{r_2} - x_{r_1} + x_{r_3} - x_{r_1})$
        end if
        $r \leftarrow$ random number
        if $r < co$ **then**
            $u_i \leftarrow v_i$
        else
            $u_i \leftarrow x_i$
        end if
        Calculate the fitness of u_i
        if $f(u_i) < f(x_i)$ **then**
            $x_i \leftarrow u_i$
        end if
    end for
end while
return

4.5 Genetic Algorithm

GA is a population based optimization algorithm proposed by John Holland [135] which is inspired by the biological evolution based on theory of natural selection of Darwin. This algorithm uses three operations to generate a new candidate solution: reproduction, crossover and mutation [90]. The pseudo code for the GA method shown in Algorithm (5).

4.5.1 Reproduction

In this process the mating pool is generated from the good solutions from the population. This process uses the roulette wheel selection or other methods to choose the best parents to generate a new child through the crossover and mutation process.

4.5.2 Crossover

This process will decide how much of genetic information will be shared between the parents and offspring using one of the methods such as: single point crossover, multiple point crossover, uniform crossover or other methods. The crossover process is done randomly based on the crossover probability p_c which is usually selected between $[0.7, 1]$.

4.5.3 Mutation

In GA the mutation process is simply done for each member of the population generated after the crossover process. If the member has n bits and the probability of mutation is p_m, then we flip the zero to one and vice versa randomly based on p_m.

Algorithm 5 GA Algorithm

```
Initialize the GA parameters
Generate a random set of individual( x_i and i ∈ [1, N])
Calculate the fitness of each individual
while not (termination criterion) do
    Reproduction process
    for each individual x_i and i ∈ [1, N]  do
        if r < p_c then
            Crossover process
        end if
    end for
    for each individual x_i and i ∈ [1, N]  do
        if r < p_m then
            Mutation process
        end if
    end for
    Calculate the fitness of each individual
end while
return
```

4.6 Summary

In this chapter, black hole algorithm, biogeography based optimization, differential Evolution and genetic algorithm were introduced. All these algorithms are population based. The main processes were explained and the pseudo codes were presented. These algorithms will be used to solve the power system operations under consideration in this thesis.

Chapter 5

Khums Optimization Algorithm (KOA)

5.1 Introduction

In Islamic tradition, Khums and Zakat are religious taxes paid by believers to the Islamic government and are required religious obligations. These taxes help the needy in the Islamic nation. Khums is the 20% tax paid generally on income and other earnings depending on the Islamic group tradition. Like charity on all the world, helping the poor people will help society to become safer, stable and create a better future for all individuals by reducing the gap between the rich and poor [95]. This is similar to the Christian tithing tradition which is one tenth of annual produce or earnings, formerly taken as a tax for the support of the church and clergy. Next sections will cover the Khums optimization algorithm, then the KOA algorithm main operations: collection and distributions and finally, the KOA simulation results compared with other algorithms.

5.2 Khums Optimization Algorithm

There are two processes in Khums: collection and distribution. In collection believers will pay the 20% of their profit with certain conditions based on the Islamic group and in distribution the money will be distributed among the different eligible Khums receivers like the orphans, poor and wayfarers which also based on the Islamic group. In the Khums optimization algorithm (KOA), each solution is considered as a Khums paying person. The solutions are ranked based on the earnings each person have and this is decided based on the objective function. High income people are considered as good solution and poor profit or no profit persons are considered as poor solution which required a help and support from the community. In KOA in order to generally simulate the process, there are two operations: collection and distribution. In the collection process the 20% will be taken from all the solution based on the profit they gain where higher profit persons will pay more than the poor or nonprofit persons. The distribution process here will be based on the earnings where the poor solution will get more help from the Khums money. The pseudo code for the KOA optimization method is shown in Algorithm (6).

5.2.1 Collection Process

In this process, the rich individuals (good solutions) who must pay the 20% tax from their earnings were identified and ranked based on their profit. By cutting this tax from the good solutions we create new solutions as shown in (5.1).

$$X_i^{new} = X_i^{old}\ (1 - K_r\ R(i)) \tag{5.1}$$

$$R(i) = \frac{N - i}{N} \tag{5.2}$$

Where X_i^{new} is the new solution generated after the collection process, X_i^{old} is the old solution, K_r is the Khums tax rate and $R(i)$ is rate between 0 and 1 define the best $(R = 1)$ and the poor solution$(R = 0)$ in a population where the solution is sorted from the best to the worst. The pseudo code for the collection process is shown in Algorithm (7).

5.2.2 Distribution Process

In this step the poor solutions are identified and classified based on their needs where the larger in need will get more support. By supporting these individuals, new solutions will be created as shown in (5.3).

$$X_i^{new} = X_i^{old} + X_m\ K_r\ P(i) \tag{5.3}$$

$$P(i) = 1 - R(i) \tag{5.4}$$

Where m is a random integer between 0 and the number of population, $P(i)$ is rate between 0 and 1 define the rich $(P = 0)$ and the poor solution$(P = 1)$ in a population where the solution is sorted from the best to the worst. The function of R and P is not the only way of representing these variables and it could be any function that serve the same purpose. The pseudo code for the distribution process is shown in Algorithm (8).

Algorithm 6 KOA Algorithm

Initialize the KOA parameters
Generate a random set of individual(x_i and $i \in [1, N]$)
Calculate the fitness of each individual
Calculate the R and P of each individual
$x_{best} \leftarrow$ Optimal solution
while not (termination criterion) **do**
    Collection process
    $x_i \leftarrow x_i \cup x_{best}$
    $x_{best} \leftarrow$ Optimal solution
    Distribution Process
    $x_i \leftarrow x_i \cup x_{best}$
    $x_{best} \leftarrow$ Optimal solution
end while
return

Algorithm 7 Collection process

for each individual x_i and $i \in [1, N]$ **do**
$X_i^{new} = X_i^{old}\ (1 - K_r\ R(i))$
    Calculate the fitness of each individual
    Mapping R and P of each X_i
end for
return

5.3 Simulation Results

To explore the performance of the algorithm, it was first applied on 14 benchmark from the literature and compare the performance with other methods. Then the KOA algorithm was applied to solve an engineering problem and the result was compared with other algorithms in literature. The code used in the first part is from

Algorithm 8 Distribution Process

for each individual x_i and $i \in [1, N]$ **do**
    $m \leftarrow$ random integer $\in [1, N]$
$X_i^{new} = X_i^{old} + X_m\ K_r\ P(i)$
    Calculate the fitness of each individual
    Mapping R and P of each X_i
end for
return

http://academic.csuohio.edu/simond/bbo/ and the only modification was adding the KOA algorithm.

5.3.1 Benchmark Test

Fourteen common benchmark functions and eight population based optimization algorithms were used to test the performance of the KOA algorithm. The algorithms are: ant colony optimization (ACO) [28], biogeography-based optimization (BBO) [100], differential evolution (DE) [107], evolutionary strategy (ES) [101, 6], genetic algorithm (GA) [135, 101, 6], probability-based incremental learning (PBIL) [99], particle swarm optimization (PSO) [135, 101] , stud genetic algorithm (StudGA) [101, 30]. The evolutionary algorithms parameters can be found in [100]. In KOA, the Khums tax rate K_r is chosen to be 0.2 based on Table 5.1, where the performance and the CPU time present a compromise solution. For all algorithms, The population size is 50, the elitism parameter is 2 and the number of generation is 50. Table 5.2 represents the normalized mean minimum optimization results of the benchmark functions for 100 monte carlo simulation where 1 represents the minimum value. The performance of the KOA algorithm was the best in solving all the benchmark except the Fletcher benchmark function and the Rastrigin benchmark function. Table 5.3 presents the normalized best minimum optimization results of the benchmark functions for for 100 Monte Carlo simulation. In this table also the KOA algorithm outperform the other algorithms in all benchmark except the Fletcher benchmark function and the Rastrigin benchmark function. The mean CPU time of the algorithms shows that the PIBL algorithm is the best in term of speed and that the KOA is the third in the rank.

Table 5.1: Normalized mean minimum optimization results of the benchmark functions for the koa optimization algorithm with different K_r for 100 monte carlo simulation

	$KOA_{0.1}$	$KOA_{0.2}$	$KOA_{0.25}$	$KOA_{0.6}$
Ackley	2	1	1	6
Fletcher	1	1	1	1
Griewank	3	1	1	90
Penalty1	16	1	1	9.15E+07
Penalty2	11	1	4	4.07E+07
Quartic	203	1	5	4.27E+05
Rastrigin	1	1	1	2
Rosenbrock	2	1	1	13
Schwefel	7	2	1	2
Schwefel2	11	1	1	819
Schwefel3	5	1	1	32
Schwefel4	3	1	1	22
Sphere	16	1	2	547
Step	15	1	2	573
Mean CPU	1.14	1.12	1.17	1.00

Table 5.2: Normalized mean minimum optimization results of the benchmark functions for the koa and other algorithm for 100 monte carlo simulation of each algorithm

	ACO	BBO	DE	ES	GA	KOA	PBIL	PSO	StudGA
Ackley	6	3	5	7	6	1	8	6	3
Fletcher	10	1	4	10	4	13	9	8	1
Griewank	11	8	18	90	36	1	196	71	7
Penalty1	7.63E+08	3.68E+05	2.61E+06	3.68E+08	4.81E+06	1	8.28E+08	5.76E+07	999
Penalty2	2.45E+08	4.22E+05	3.63E+06	1.55E+08	5.85E+06	1	3.15E+08	4.06E+07	3.40E+04
Quartic	9.09E+04	8412	3.69E+04	1.18E+06	7.94E+04	1	1.43E+06	2.58E+05	3770
Rastrigin	4	1	4	6	4	2	6	5	1
Rosenbrock	92	5	13	113	23	1	94	27	6
Schwefel	2	1	5	6	2	1	7	7	1
Schwefel2	477	273	642	745	505	1	754	513	413
Schwefel3	20	3	9	33	15	1	25	19	4
Schwefel4	22	23	27	34	29	1	36	28	19
Sphere	587	46	117	1255	422	1	1285	452	46
Step	101	43	107	735	228	1	1253	433	37

Table 5.3: Normalized best minimum optimization results of the benchmark functions for the koa and other algorithm for 100 monte carlo simulation of each algorithm

	ACO	BBO	DE	ES	GA	KOA	PBIL	PSO	StudGA
Ackley	5	3	5	8	6	1	9	7	3
Fletcher	19	1	7	23	4	16	18	16	1
Griewank	5	4	10	58	10	1	148	50	3
Penalty1	27	135	1.07E+04	4.54E+07	184	1	6.60E+08	4.90E+06	42
Penalty2	3	32	3.81E+05	6.65E+07	6.56E+04	1	1.20E+08	8.98E+06	29
Quartic	3.90E+04	2727	4.43E+04	2.17E+06	1.63E+04	1	9.99E+05	2.16E+05	318
Rastrigin	6	1	5	9	5	2	9	7	1
Rosenbrock	41	2	7	70	7	1	54	13	3
Schwefel	223	85	778	869	125	1	1229	926	70
Schwefel2	326	203	482	754	305	1	1018	617	386
Schwefel3	30	2	13	42	14	1	49	22	4
Schwefel4	22	20	33	45	22	1	42	27	14
Sphere	622	37	114	1924	225	1	1556	467	28
Step	66	24	93	847	83	1	1582	498	24
Mean CPU	3.44	2.06	2.95	2.12	2.43	2.10	1.00	3.29	2.43

5.3.2 Economic Dispatch Solution

The general procedure to solve the economic dispatch problem using any metaheuristic algorithm is shown in Procedure (3).

Procedure 1: Economic Dispatch Solution

1. Initialize the algorithm parameters (population size, no of generations, no of iteration, mutation rate, cross over rate, khums rate).
2. Generate a set of feasible solutions where each solution consist of output power generation for each unit that satisfy the different economic dispatch constraints required in the problem.
3. Calculate the objective function.
4. Save the best solution.
5. Apply the algorithm operations on the set of the solutions.
6. Check the feasibility of the generated solutions and repeat steps (3-4).
7. Repeat steps (5-6) until the termination criterion is achieved.

5.3.3 ED Problem with Valve Point Effect

Two test system were used to test the efficiency and performance of the KOA algorithm in comparison with other algorithms in the literature. Three and Thirteen generating units with quadratic cost function, and the effects of valve-point loading is considered. The unit characteristics cost coefficients, and generators operating limits are shown in Appendix (C.1.2) and Appendix (C.1.4). The result shown is a result of Monte Carlo simulation of 100 iteration for both system. For the three generation system the population and generation are 100. The best minimum cost equal to 8234.09 \$/h and the mean minimum cost equal to 8244.4407 \$/h. In the case of the thirteen generation system the population was 300 and the generation was 100. The best minimum cost equal to 17965.8138 \$/h and the mean minimum cost equal to 17974.5619 \$/h. In both cases the KOA algorithm succeed in solving the problem with small percentage difference than the best solution less than or equal to 0.011%. This work has been reported in [51].

Table 5.4: Optimal results for three machine system with valve point effect

Algorithm	KOA	GA[82]	BBO[77]	SOS[82]
P_1	300.24	300	300.2829	300.27
P_2	149.7725	150	149.7377	400
P_3	400	400	399.9794	149.73
P_D	850	850	850	850
Total Cost (\$/h)	8234.09	8234.6	8234.0777	8234.07

Table 5.5: Optimal results for thirteen machine system with valve point effect

Algorithm	KOA	BBO[78]	FAPSO-NM[83]	PSO[17]
P_1	627.41	627.4094	628.32	538.561
P_2	223.99	223.9911	222.75	299.355
P_3	149.42	149.4163	149.6	75.037
P_4	109.78	60	109.87	159.734
P_5	109.83	109.7842	109.87	60.078
P_6	109.85	109.8296	109.87	109.864
P_7	109.86	109.8499	109.87	109.913
P_8	60.00	109.8591	60	159.753
P_9	109.86	109.8632	109.87	60.069
P_{10}	40.00	40	40	40.035
P_{11}	40.00	40	40	77.561
P_{12}	55.00	55	55	55.042
P_{13}	55.00	55	55	55
P_D	1800	1800.0028	1800.02	1800.002
Total Cost $/h	17965.814	17965.8098	17963.84	18014.16

5.4 Conclusion

In this chapter, a new optimization algorithm called Khums optimization algorithm is introduced. KOA has two operations to search for optimal solution, collection and distribution. In collection, new solution will be generated from cutting the tax from the solutions based on their profit and in distribution, the generated solution will be as result from distributing these tax among the poor solutions. The algorithm was applied to solve 14 benchmark from the literature and compare the performance with other methods. Then the KOA algorithm is applied to solve the economic dispatch with valve point effect for two systems. The results show that the new algorithm can be applied to solve practical optimization problems. Although, KOA has a better performance on solving the benchmark systems but we can not conclude that it is better than other algorithms based on the no free lunch theorem. Three interesting modification can be studied in the future. The first modification is about the khums tax rate where it is assumed in this work to be constant 20%. The khums rate can be random but within this range and a comparison between the performance of the algorithm based on these two tax rates observed. The second modification is in the way of ranking the good solutions and poor solutions. Other methods can be used to study the effects on the performance of the algorithms. Finally, the last modification can be done by adding the effects of death of tax payers and the effect of joining new tax payers which is similar to mutation process in other algorithms which may effect the performance of the algorithm and need to be studied as future work.

Chapter 6

Wind Turbine Cost Model

6.1 Introduction

Among the renewable energy (RE) sources, wind energy is one popular and most used in the modern power system network. Like other RE sources wind energy suffers from intermittency and uncertainty of availability but with a higher rate [61]. Integrating such a RE source in the power system increases the complexity of the economic dispatch problem and finding a suitable wind turbine cost model becomes important to achieving reliable and efficient optimal solution [61].

Many algorithms were proposed to deal with the intermittent behavior of the wind turbines because of the impacts of merging significant wind power capacity on conventional generation, reserve levels and emissions as shown in [25].

The conventional approach models the intermittent resources as negative load [122]. Model Predictive Control proposed in [131] is used for dispatching the available generation with the objective of minimizing the total production cost.

A probabilistic model for the wind turbine output based on the Weibull probability density function is used in [54], which accounts for both overestimation and underestimation of available wind power. The probabilistic method used to model and solve the economic dispatch problem with random wind power constraint using a penalty function and interior point method [141].

This chapter will cover both wind turbine cost models, the negative load model and the probabilistic model based on weibull distribution. It is assumed that the anticipated (forecast) wind power output is available in the studies of this thesis.

6.2 Wind Turbine Cost Model as a Negative Load

In this model all the forecast wind power will be used to calculate the new load by subtracting the wind power from the total load as done in [122]. There will be no dispatching for the wind power with other power generator to decide the optimal power allocation among all of them. Wind turbine cost model as a negative load in the economic dispatch problem is shown in (6.1).

$$W_{Cost} = \sum_{m=1}^{N_w} d_m \; w_m^{sc} \tag{6.1}$$

where W_{Cost} is the total wind power generation cost for N_w units, w_m^{sc} is the scheduled wind power for the m^{th} wind turbine, d_m is the cost coefficients and usually called direct cost coefficient.

6.3 Wind Turbine Cost Model as a Probabilistic Model

In this model the wind turbine is treated as a normal power generation units with a cost function modeled using the Weibull distribution and the objective function will be to minimize the total cost of both the thermal generation units and the wind turbine units. The total wind cost W_{Cost} is consists of the sum of three components: direct cost, underestimate cost and overestimate cost as shown in (6.2).

$$W_{Cost} = \sum_{m=1}^{Nw} C_{d\,m} + C_{p\,m} + C_{r\,m} \tag{6.2}$$

where W_{Cost} is the total cost of wind power, N_w is the number of wind turbines, $C_{d\,m}$ is direct cost for wind turbine m, $C_{p\,m}$ is underestimate cost for wind turbine m and $C_{r\,m}$ is overestimate cost for wind turbine m. A detailed total wind power cost is shown in (6.3), which show that there are two components depends on the expected value of exceeding or not exceeding the scheduled value. In both cases there will be a cost to be paid, hence there will be an effect on the total cost. A more detailed expression is shown in (6.3).

$$W_{Cost} = \sum_{m=1}^{Nw} d_m \; w_m^{sc} + kp_m \; E_m^{ue} + kr_m \; E_m^{oe} \tag{6.3}$$

where w_m^{sc} is the scheduled wind power for the m^{th} wind turbine, w_m available wind power for the m^{th} wind turbine, E_m^{ue} is the expected value of $w_m > w_m^{sc}$ for the m^{th} wind turbine, E_m^{oe} is the expected value of $w_m < w_m^{sc}$ for the m^{th} wind turbine, d_m, kp_m and kr_m are the direct, penalty, and reserve cost coefficients for the m^{th} wind turbine respectively. A detailed proof of the model is found in [73] and in Appendix A. The underestimation and overestimation expected values are shown in (6.4) and (6.5) respectively.

$$\begin{aligned} E_m^{ue} &= (w_r - w_m^{sc})\ (e^{-(\frac{V_r}{c})^k} - e^{-(\frac{V_o}{c})^k}) + (w_m^{sc} + \frac{w_r}{h})\ (e^{-(\frac{V_r}{c})^k} - e^{-(\frac{V_m^{sc}}{c})^k}) \\ &+ \frac{w_r\ c}{V_{in}\ h}\ [\Gamma(1+\frac{1}{k}, (\frac{V_m^{sc}}{c})^k) - \Gamma(1+\frac{1}{k}, (\frac{V_r}{c})^k)] \end{aligned} \tag{6.4}$$

$$\begin{aligned} E_m^{oe} &= w_m^{sc}\ (1 - e^{-(\frac{V_m^{sc}}{c})^k} + e^{-(\frac{V_o}{c})^k}) + \frac{w_r}{h}\ (e^{-(\frac{V_{in}}{c})^k} - e^{-(\frac{V_m^{sc}}{c})^k}) \\ &- \frac{w_r\ c}{V_{in}\ h}\ [\Gamma(1+\frac{1}{k}, (\frac{V_{in}}{c})^k) - \Gamma(1+\frac{1}{k}, (\frac{V_m^{sc}}{c})^k)] \end{aligned} \tag{6.5}$$

where w_r is the wind turbine rated power, V_r is the wind turbine rated speed, V_{in} is the wind turbine cut in speed, V_o is the wind turbine cut out speed, c is the scale factor of the Weibull distribution, k is the shape factor of the Weibull distribution, and $h = \frac{V_r}{V_{in}} - 1$.

In order to study the effect of the shape factor k and scale factor c on the performance of the model, a plot of the overestimate expected power, underestimate expected power and total wind cost at different scale factor and shape factor is shown in Fig(6.1) to Fig(6.6). The wind turbine model parameters are shown in Appendix (C.1.5).

The scale factor c usually proportional to mean wind speed and it is proportional to wind generated power. It is observed in Fig(6.1) as c increase the overestimate expected power will decrease which means that the probability that the overestimation forecasting error decrease at higher forecast power and this will decrease the overestimation cost.

The situation is opposite in Fig(6.2), where E_{ue} increase with the increase in c at low forecast power which indicate that as c increase the probability of underestimate forecast power increase.

Since, at low forecast power the underestimate expected power is higher than the overestimate expected power and at high forecast power the situation is opposite, the total wind forecast will follow the underestimate cost at low forecast power and follow the overestimate expected power at high forecast power as shown in Fig(6.3).

The change in the shape factor k did not show significant difference in the overestimate expected power or the underestimate expected power or the total wind cost as shown in the Fig(6.4) to Fig(6.6).

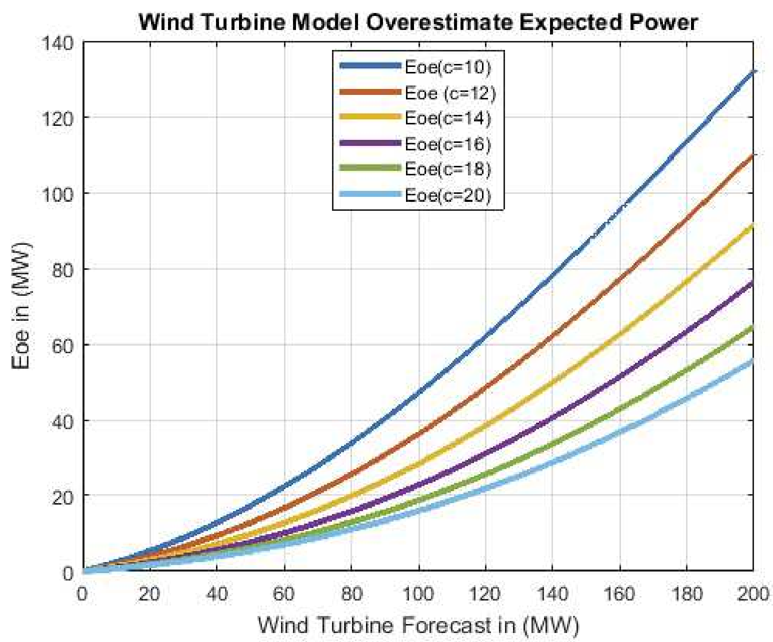

Figure 6.1: Wind turbine model overestimate expected power for different scale factor (c)

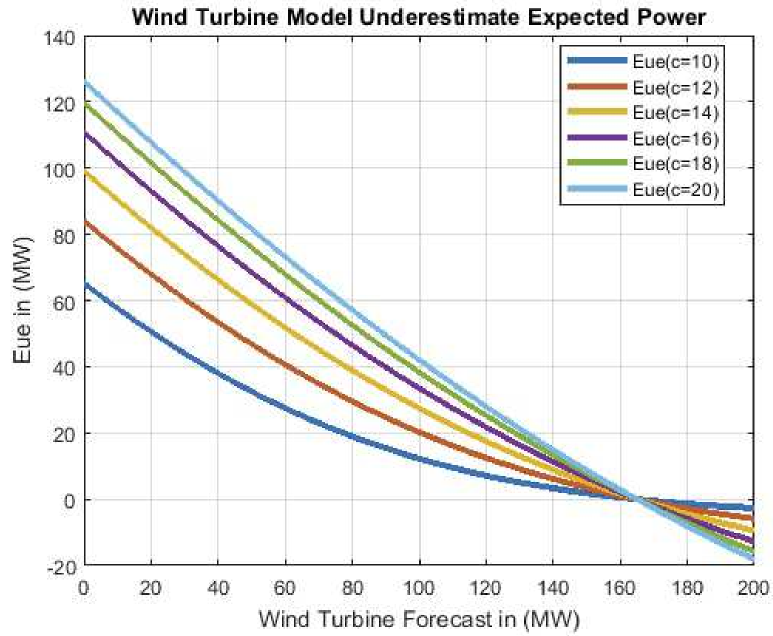

Figure 6.2: Wind turbine model underestimate expected power for different scale factor (c)

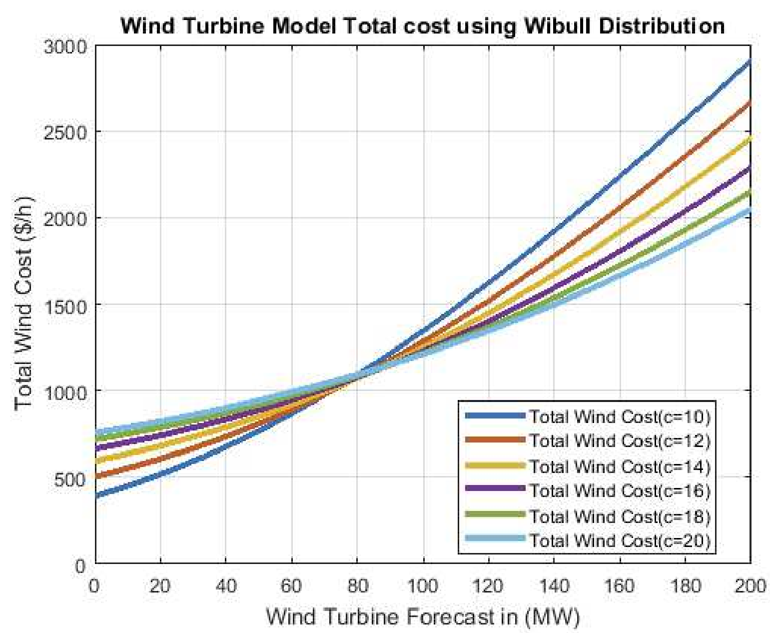

Figure 6.3: Wind turbine model total cost (W_{Cost}) for different scale factor (c)

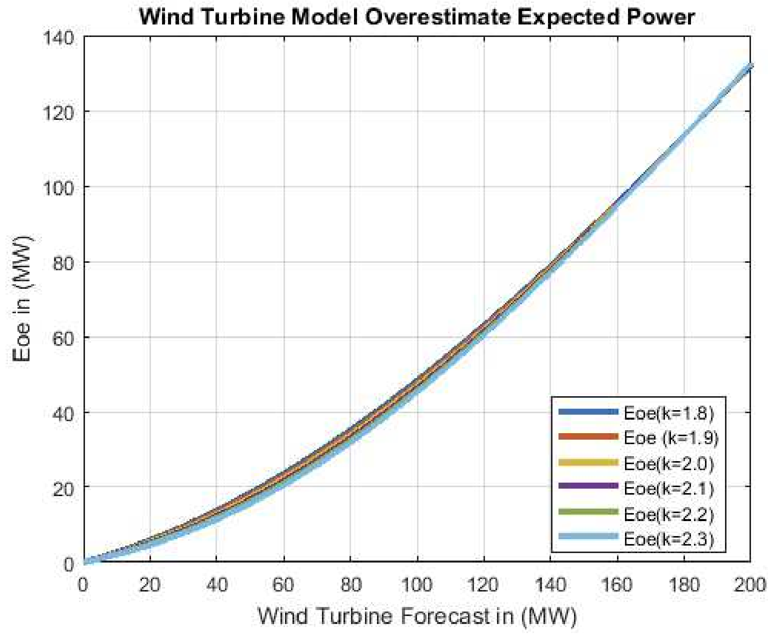

Figure 6.4: Wind turbine model overestimate expected power for different shape factor (k)

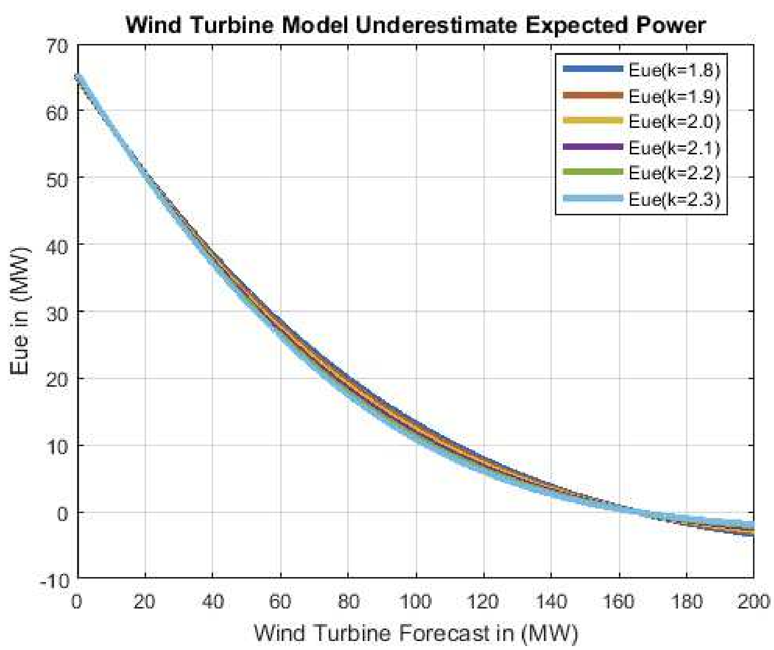

Figure 6.5: Wind turbine model underestimate expected power for different shape factor (k)

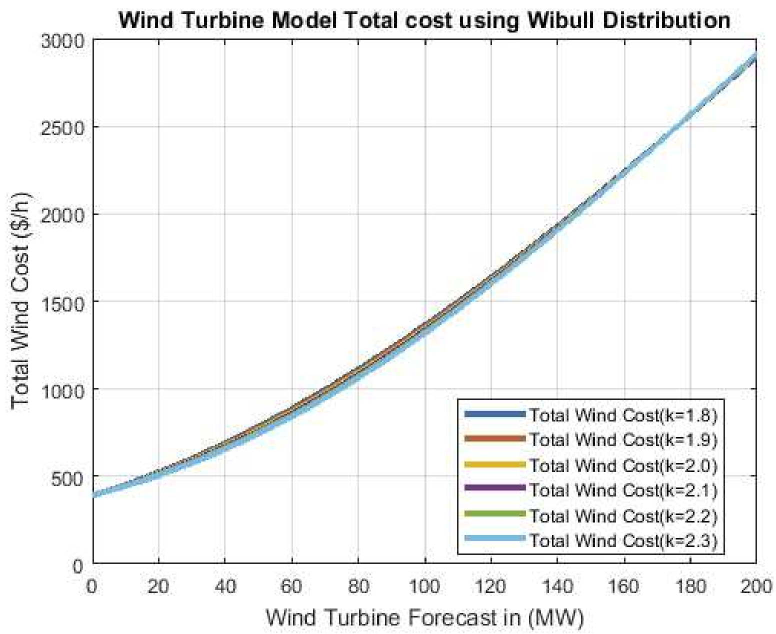

Figure 6.6: Wind turbine model total cost (W_{Cost}) for different shape factor (k)

6.3.1 Economic Dispatch Solution Incorporating Wind Energy

The general procedure to solve the economic dispatch problem incorporating wind energy using any metaheuristic algorithm is shown in Procedure (2).

Procedure 2: Economic Dispatch Solution

1. Initialize the algorithm parameters (population size, no of generations, no of iteration, mutation rate, cross over rate, khums rate).
2. Generate a set of feasible solutions where each solution consist of output power generation for each thermal unit and the wind power which generated randomly based on the forecast. The solutions satisfy the different economic dispatch constraints required in the problem.
3. The direct cost, overestimation cost and the under estimation cost for wind power are calculated for all the solutions.
4. Calculate the objective function.
5. Save the best solution.
6. Apply the algorithm operations on the set of the solutions.
7. Check the feasibility of the generated solutions and repeat steps (3-5).
8. Repeat steps (6-7) until the termination criterion is achieved.

6.4 Comparison Of Wind Turbine Probabilistic Model With Negative Model in Economic Dispatch Problem

The Differential evolution (DE) algorithm will be used to do a comparison between the two wind turbine cost models proposed in the last sections and will be used to solve the economic dispatch problem.

The economic dispatch problem will be solved with and without the valve point effect considering different constrains such as generators capacity, ramp rate limit, and prohibited operation zones. The probabilistic wind cost model and the negative load wind cost model will be used to model the significant integration of wind energy in the problem to study them and to select the suitable model among them. Three test systems with different constraints will be used to select the best cost model for the wind turbine.

All the DE parameters were selected based on the experience of solving the problem. For the first two test systems, the selected number of generations and population size are 40 and 40 respectively and for the third system are 30 and 30 respectively. The other evolutionary algorithm parameters are shown in Table (6.1). This work has been reported in [48].

Table 6.1: Parameters for BBO and DE

Algorithm	**co**	**pf**	**F**
BBO	-	0.005	-
DE	0.5	0.005	0.9

6.4.1 Test System 1

This system consists of three generation units with quadratic cost functions and a wind turbine. The units characteristics cost coefficients and generators operating limits are shown in Appendix (C.1.1) and the wind turbine cost model is shown in Appendix (C.1.5).

The total cost obtained is shown in Fig(6.7) for different scale factors c where the figure vertical axis represents the total cost ($/h) and the horizontal axis represents the wind power forecast in (MW). The total cost decrease as c increase and finally it matches the negative load model at $c = 20$.It is clear that the probabilistic model and the negative load model are similar for low forecast power and for each c value curve there is a critical wind power point represents the separation between the two models curves. From that point the probabilistic model cost start to be constant and will continue to the end of the wind power forecast range. This is because the model will select the critical wind power always if the forecast power is grater or equal to it.

The objective function cost curve is shown in Fig(6.8) which further explains the behavior of the total cost curve. At the critical wind forecast point the negative load model and the probabilistic model start to separate, where the negative load model cost become high and the probabilistic cost model keep a constant cost. As c value increase the critical wind forecast point point increase and the two model become equivalent.

Since no significant change in the wind cost model happens in the change of the shape factor k in the selected range, it is expected that the total cost curve and the objective function cost curve will not change significantly as result of change in k as shown in Fig(6.9) and Fig(6.10) respectively.

To appreciate the benefits of using the probabilistic model, let assume that there was a forecasting error of 6% of total capacity (9.9 MW) at $P_w = 68$ MW and c=12. Table (6.2) shows the calculation of total cost resulted from the overestimation and the underestimation forecasting error. In both cases the probabilistic model succeed in getting the lower cost compared to negative load model.

Table 6.2: Total cost under 6% of total wind turbine capacity forecasting error

	Overestimate error		
Model	Forecast Power	scheduled Power	Total Cost ($/h)
Probabilistic	68+9.9=77.9 MW	70 MW	8119+10 (70-68)-8 (70-68)=8123
Negative Load	68+9.9=77.9 MW	77.9 MW	8109+10 (77.9-68)-8 (77.9-68)=8128.8
	Underestimate error		
Model	Forecast Power	scheduled Power	Total Cost ($/h)
Probabilistic Model	68-9.9=58.1 MW	58.1 MW	8130+6 (68-58.1)-8 (68-58.1)=8110.2
Negative Load Model	68-9.9=58.1 MW	58.1 MW	8130+6 (68-58.1)-8 (68-58.1)=8110.2

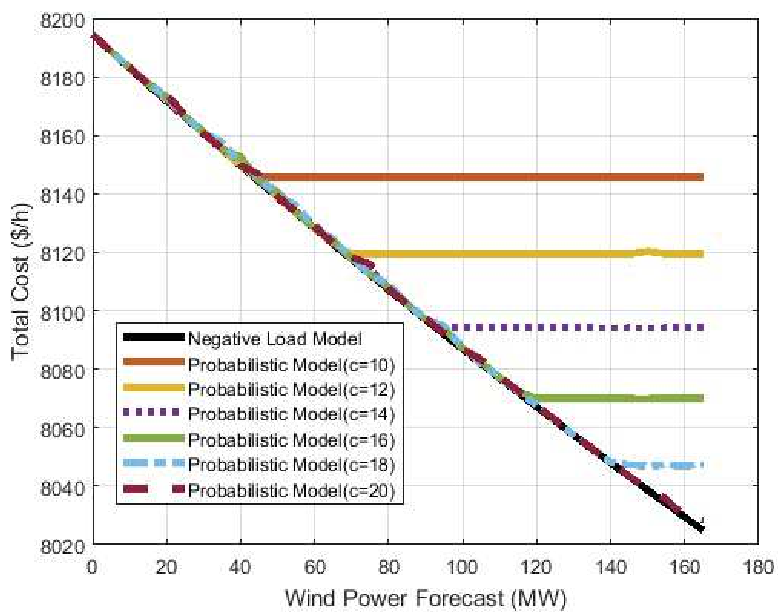

Figure 6.7: Total cost for three generator quadratic cost functions and with wind power for different scale factor (c)

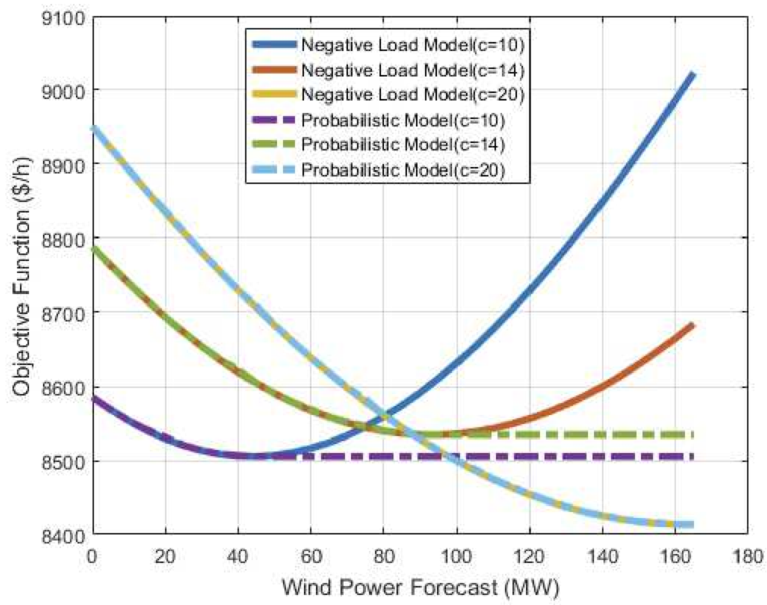

Figure 6.8: Objective function cost for three generator quadratic cost functions and with wind power for different scale factor (c)

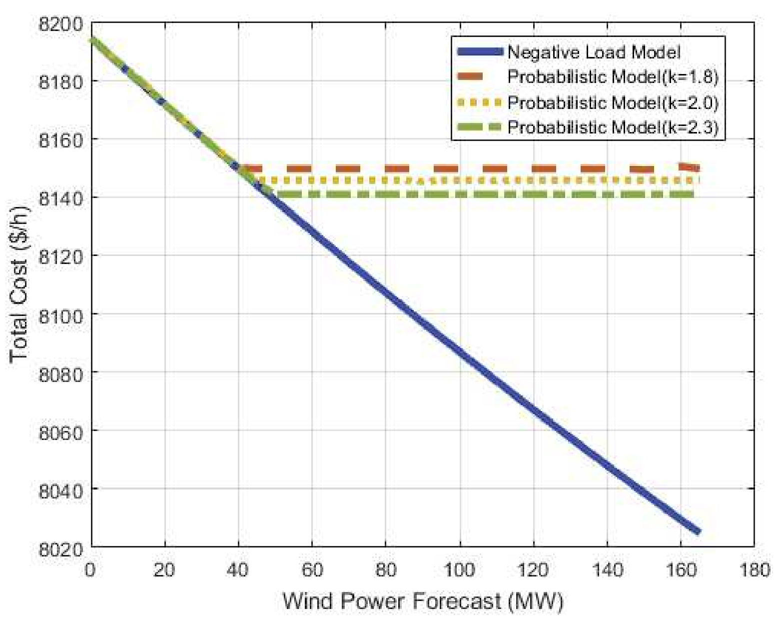

Figure 6.9: Total cost for three generator quadratic cost functions and with wind power for different shape factor (k)

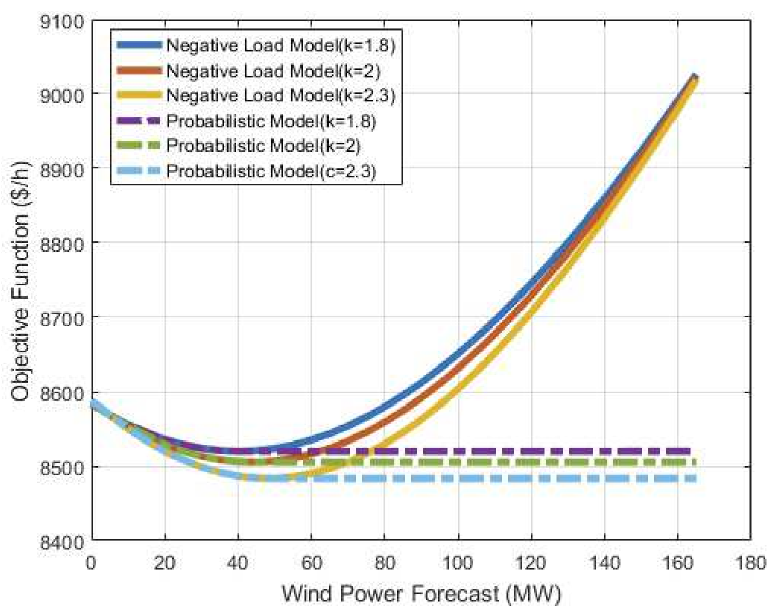

Figure 6.10: Objective function cost for three generator quadratic cost functions and with wind power for different shape factor (k)

6.4.2 Test System 2

This system consists of three generation units with quadratic cost functions and the effects of valve-point loading is considered. All the equality and inequality constraints are considered. The units characteristics cost coefficients, and generators operating limits are shown in Appendix (C.1.2) and the wind turbine cost model is shown in Appendix (C.1.5).

The effect of valve point non-linearity is obvious on the total cost curves using both models as shown in Fig (6.11) to Fig (6.12). Like the case without valve point effect, as c increase the total cost curves using the probabilistic model follow the total cost using negative load model and the picture is more clear if you see it from the objective function window as shown in Fig (6.13). At low wind power forecast the total cost using probabilistic model is equivalent to the total cost using negative load model.

It is clear from Fig (6.13) that like the previous case there is a critical wind forecast power, where the objective function cost based on the probabilistic model will be almost constant with a small change within a small range because of the valve point effect and the objective function cost using the negative load model will be increasing as the wind forecast power increase.

The performance of the total cost using different k values is shown in Fig (6.14) to Fig (6.15) where it is obvious that like the previous case the change in the total cost due to the change in k is small compare to the case of changing the value of c. This fact is also clear in the objective function cost plot at different k values shown in Fig (6.16).

It is important to clarify the fact that the values of c and k are decided by the site chosen and we cannot change them, but we change them here to understand the behavior of the probabilistic model at different values.

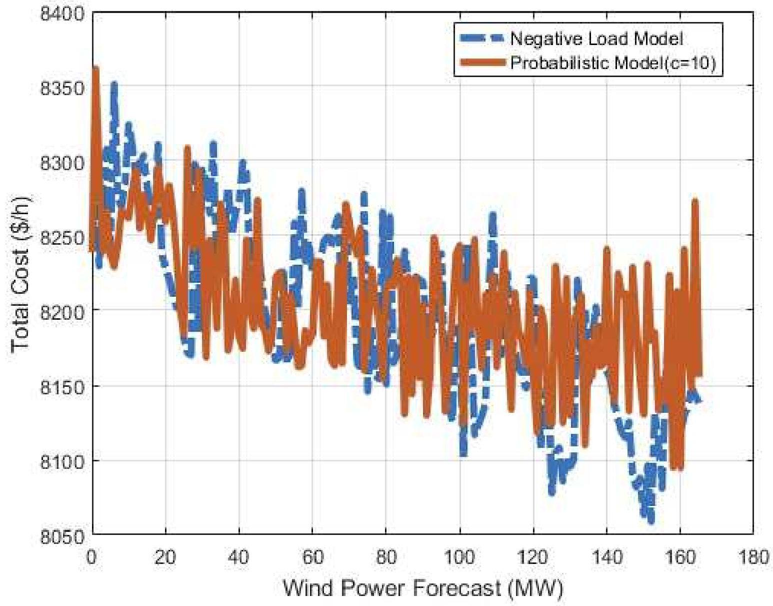

Figure 6.11: Total cost for three generation units with quadratic cost functions and the effects of valve-point loading is considered and with wind power at scale factor (c=10)

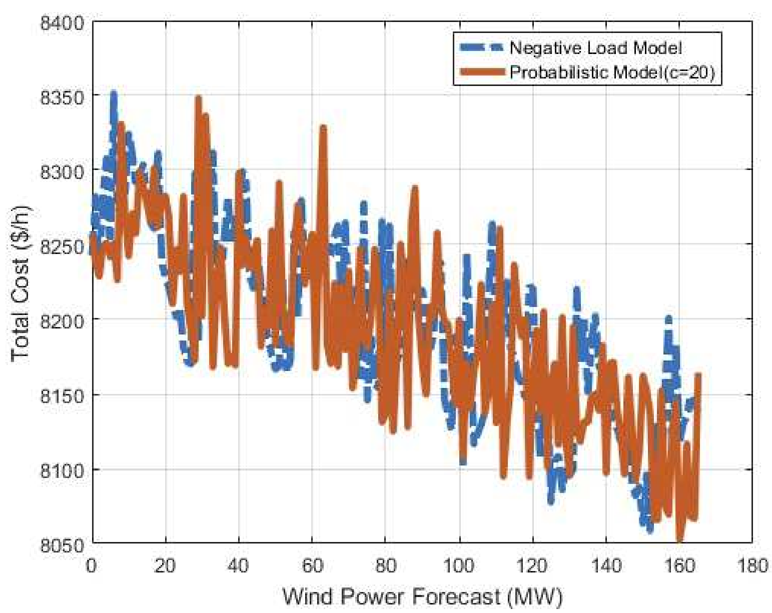

Figure 6.12: Total cost for three generation units with quadratic cost functions and the effects of valve-point loading is considered and with wind power at scale factor (c=20)

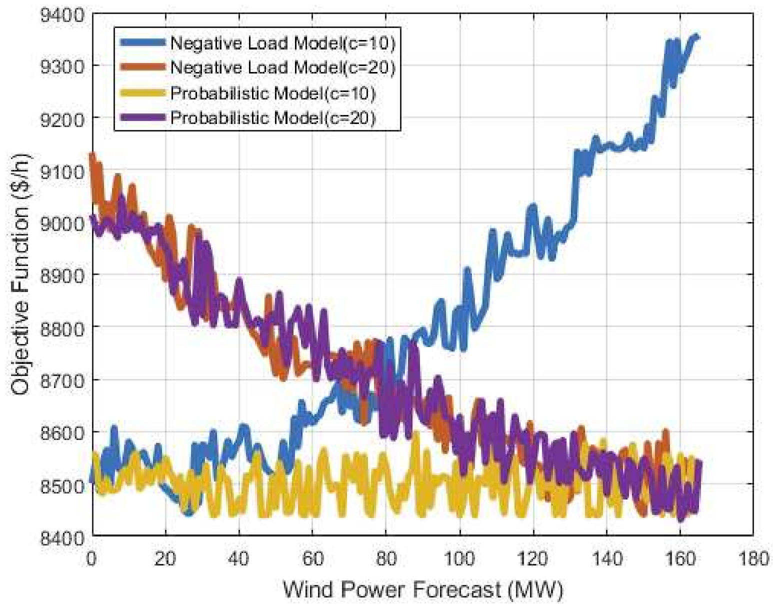

Figure 6.13: Objective function for three generation units with quadratic cost functions and the effects of valve-point loading is considered and with wind power at different scale factor (c)

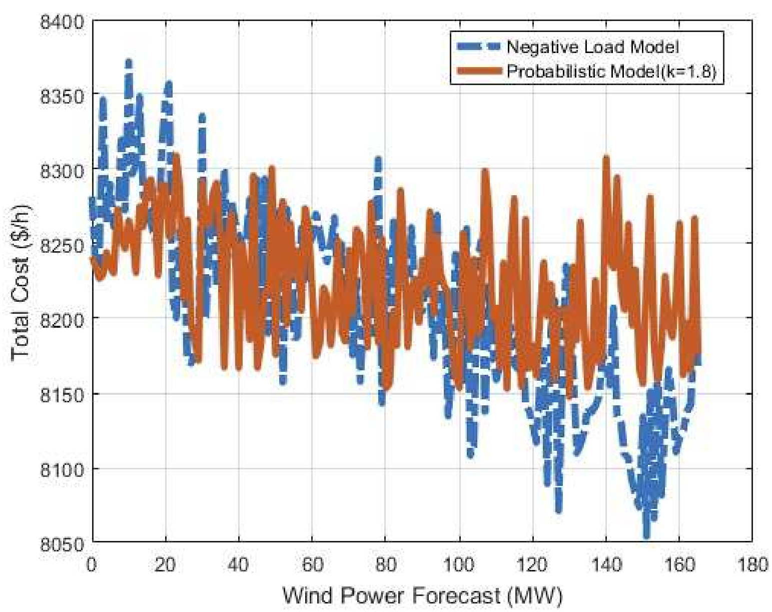

Figure 6.14: Total cost for three generation units with quadratic cost functions and the effects of valve-point loading is considered and with wind power at shape factor (k=1.8)

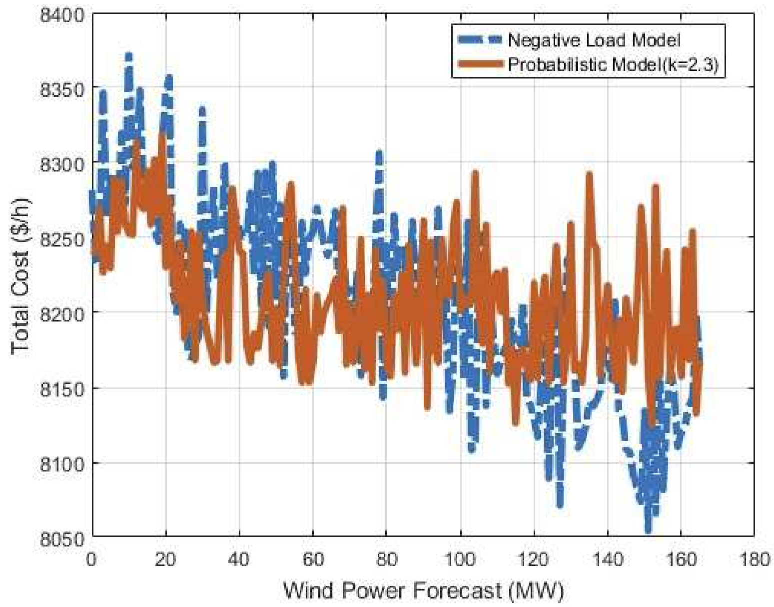

Figure 6.15: Total cost for three generation units with quadratic cost functions and the effects of valve-point loading is considered and with wind power at shape factor (k=2.3)

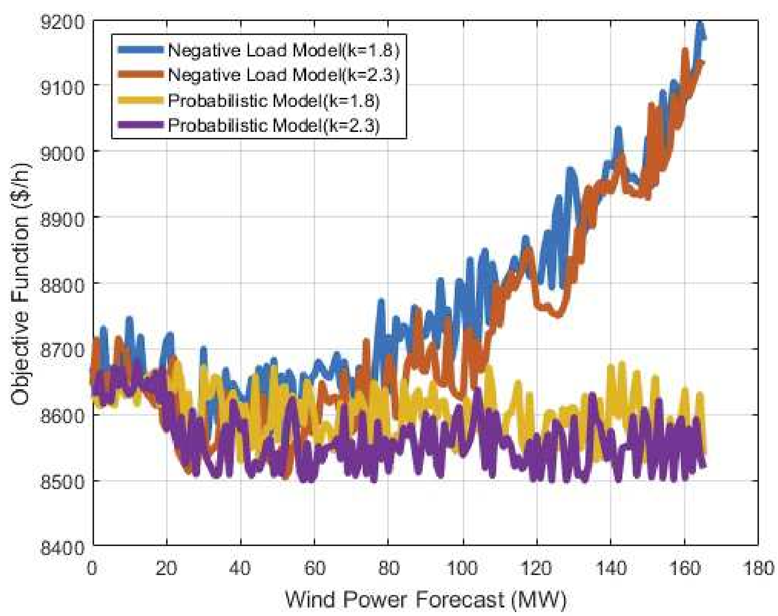

Figure 6.16: Objective function for three generation units with quadratic cost functions and the effects of valve-point loading is considered and with wind power at different shape factor (k)

6.4.3 Test System 3

This test system consists of six generation units with quadratic cost functions, transmission losses, ramp rates limits and prohibited operating zones of these thermal units. The unit characteristics of cost coefficients, and generators operating limits are shown in Appendix (C.1.3) and the wind turbine cost model is shown in Appendix (C.1.5). The difference between this test system and the previous ones is the presence of ramp rate limits, presence of the losses, the generation units number and the absence of the valve point effect.

The general performance of the total cost using the probabilistic model is like the previous cases and more clear than the case of valve point effect as shown in Fig (6.17). As the scale factor value increase the probabilistic model critical wind power point move down and the total cost using probabilistic model become equivalent to the total cost using negative load model.

In the objective function cost curve shown in Fig (6.18), as the c value increase the wind forecast critical point increase and the objective function cost based on probabilistic model become equivalent to the objective function based on negative load model. At low wind forecast both models are almost equivalent and as c increase in the low forecast reign the objective function cost increase.

The total cost using probabilistic model increase as shape factor k increase like the previous cases but the change is very small compared to the change in scale factor c as shown in Fig (6.19).

The objective function cost for different value of shape factor k is shown in Fig (6.20), where there is no significant change in the critical point of the wind forecast but as k increase the objective function cost is decreased as the forecast power increase.

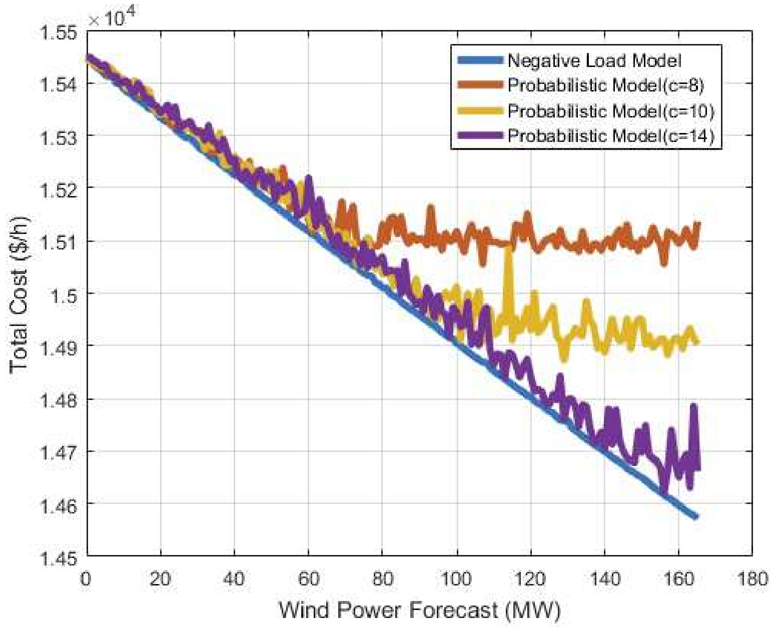

Figure 6.17: Total cost for six generator with wind power considering the prohibited operation zones and the ramp rate limits for different scale factor (c).

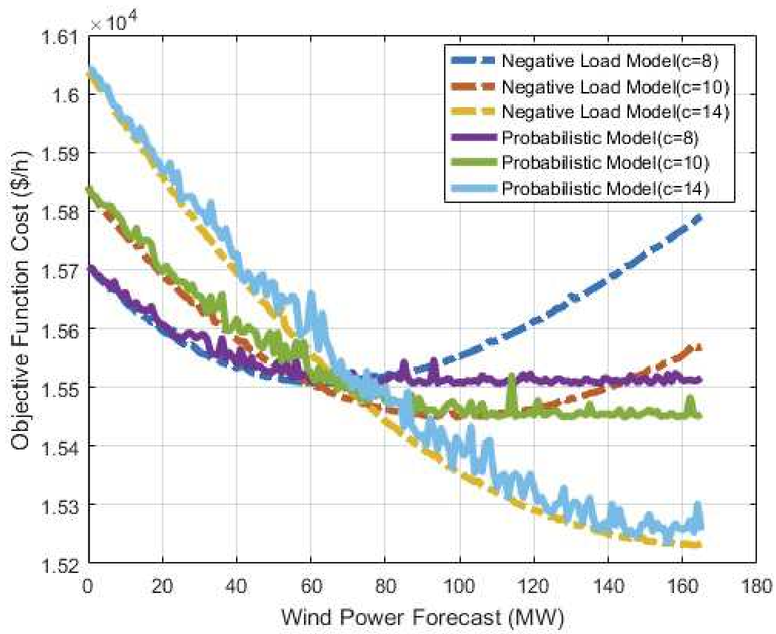

Figure 6.18: Objective function cost for six generator with wind power considering the prohibited operation zones and the ramp rate limits for different scale factor (c)

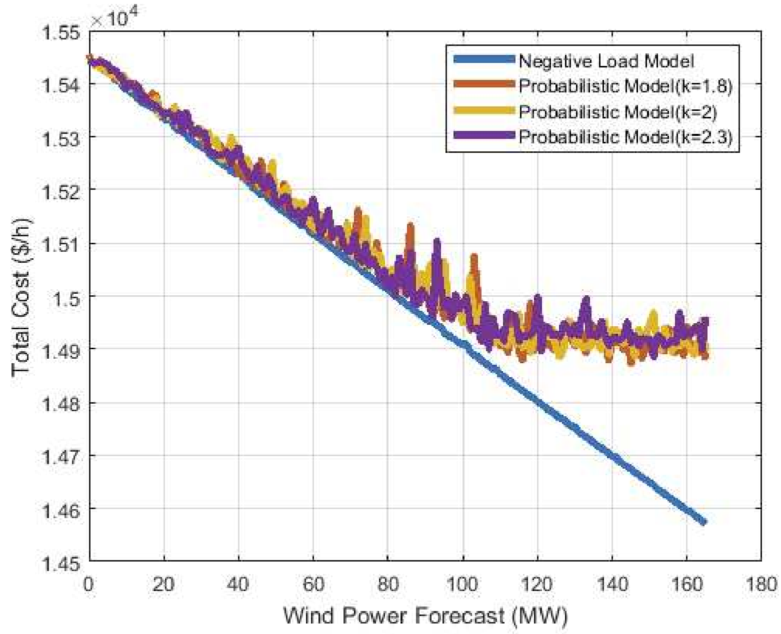

Figure 6.19: Total cost for six generator with wind power considering the prohibited operation zones and the ramp rate limits for different shape factor (k)

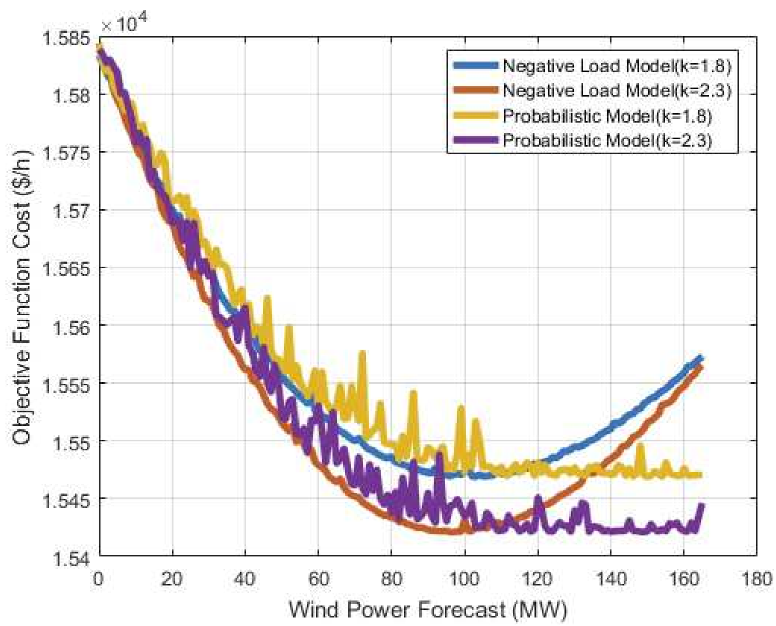

Figure 6.20: Objective function cost for six generator with wind power considering the prohibited operation zones and the ramp rate limits for different shape factor (k)

6.5 Economic Dispatch Incorporating Wind Energy Solution

This section proposes a group of Evolutionary Algorithms: Black Hole (BH) algorithm, Biogeography Based Optimization (BBO) algorithm, Differential Evolution (DE) algorithms and Khums optimization algorithm (KOA) to solve the economic dispatch problem incorporating wind energy (EDIW) uncertainty. For all the algorithms, the selected number of generation, population size and number of iteration for the first system systems are 100, 100 and 20 respectively. On the other hand the selected number of generation, population size and number of iteration for the second system systems are 100, 200 and 20 respectively. The optimization algorithm parameters are shown in Table (6.1). This work has been reported in [49] without the KOA algorithm.

6.5.1 Test System 1

This system consists of three generation units with quadratic cost functions and the effects of valve-point loading is considered. All the equality and inequality constraints are considered. The units characteristics cost coefficients, and generators operating limits are shown in Appendix (C.1.2) and the wind turbine cost model is shown in Appendix (C.1.5).

The general performance of the total cost using the probabilistic wind turbine cost model for a fixed value of c and k obtained in section (6.4), is equivalent to the negative load model in the low load forecast power and remain equivalent to it till the forecast reach a certain wind power forecast point called the critical wind power forecast point and after that, no increase in the scheduled wind power will be obtained by the wind probabilistic cost model as the forecast increase. Due to the presence of valve point effect nonlinearity there is a fluctuation on the objective function and total cost performance in a range around a mean value which make the problem difficult to solve as shown in Fig (6.11) and Fig (6.13).

Four algorithms were used to solve the problem at three wind forecasting points as shown in Table (6.3). DE and KOA algorithms succeeded in solving the problem in all the forecasted points and show the general performance expected. BBO and BH fails in the last forecast (165 MW) in finding the minimum point compared to DE and KOA, where the total cost obtained is small but the objective function value is high which indicate that there is a high overestimation error. DE succeed in finding the minimum cost with minimum objective value in all wind forecast values and KOA find the wind forecast critical region.

Table 6.3: Optimal results for test system 1 obtained by using BBO, BH, DE and KOA ($P_D = 850MW$)

Wind Power Forecast	0 MW				50 MW				165 MW			
Algorithm	BBO	BH	DE	KOA	BBO	BH	DE	KOA	BBO	BH	DE	KOA
P_1 (MW)	299.75	498.94	300.27	299.46	399.98	399.19	399.20	399.38	298.76	399.19	399.20	398.80
P_2 (MW)	151.10	99.87	149.73	151.12	151.50	99.85	99.87	149.76	149.15	99.90	149.73	149.59
P_3 (MW)	399.15	251.19	400.00	399.42	249.99	324.40	324.40	250.98	322.06	249.61	249.60	249.03
P_W (MW)	0.00	0.00	0.00	0.00	48.53	26.57	26.53	49.88	80.03	101.30	51.47	52.59
Fuel Cost ($/h)	8236.09	8241.19	8234.07	8235.28	7795.78	7954.29	7954.28	7768.87	7511.74	7284.58	7741.24	7741.11
C_d ($/h)	0.00	0.00	0.00	0.00	388.25	212.54	212.28	399.04	640.21	810.38	411.76	420.68
C_p ($/h)	390.96	390.96	390.96	390.96	199.61	277.24	277.36	195.33	113.81	71.32	190.36	186.92
C_r ($/h)	0.00	0.00	0.00	0.00	166.40	76.14	76.02	172.76	338.36	480.24	180.37	185.79
Total cost ($/h)	8236.09	8241.19	8234.07	8235.28	8184.03	8166.83	8166.56	8167.91	8151.95	8094.96	8152.99	8161.80
Objective Function ($/h)	8627.05	8632.15	8625.03	8626.23	8550.04	8520.20	8519.95	8536.00	8604.12	8646.52	8523.72	8534.50

Table 6.4: Comparison of algorithms results of test system 1

Wind Power Forecast	0 MW				50 MW				165 MW			
Algorithm	BBO	BH	DE	KOA	BBO	BH	DE	KOA	BBO	BH	DE	KOA
Minimum total cost ($/h)	8236.09	8241.19	8234.07	8235.28	8184.03	8166.83	8166.56	8167.91	8151.95	8094.96	8152.99	8161.80
Average total cost ($/h)	8270.43	8243.39	8241.41	8243.14	8239.15	8177.90	8177.24	8183.89	8190.86	8161.71	8174.51	8215.67
Maximum total cost ($/h)	8319.19	8265.90	8264.77	8252.22	8296.58	8228.64	8225.61	8208.36	8239.80	8246.64	8228.01	8282.26
Standard deviation ($/h)	25.24	6.05	6.17	3.87	32.94	19.09	18.61	10.32	22.54	37.68	22.76	33.40

6.5.2 Test System 2

This test system consists of six generation units with quadratic cost functions, transmission losses, ramp rates limits and prohibited operating zones of these thermal units. The unit characteristics of cost coefficients, and generators operating limits are shown in Appendix (C.1.3) and the wind turbine cost model is shown in Appendix (C.1.5).

The results support the previous result obtained by Test system 3 in section (6.4) which show that the probabilistic model at constant c and constant k will act as negative load model for low forecast till the forecast value reach the critical point where the probabilistic model will stop following the negative load model and the schedule wind power value be fixed and equal to the critical wind forecast point as the wind power forecast increase because the overestimate forecast error will increase.

It is obvious that all algorithms have almost the same total cost and objective function cost at first wind forecast point, and in the second forecast point DE and BBO are slightly better than other algorithms.

In the last forecast point, although the BBO has the highest total cost but it has the lowest objective function cost which means that BBO has the best point. DE can compete because the objective cost difference between it and between the BBO is small (3.24 \$/h) but the total cost difference is large (23.17 \$/h). This is not correct because of the overestimation cost will be more than the saving since the DE scheduled wind power is higher than BBO scheduled wind power by 4.69 MW and the overestimation cost is 10 \$/MW.

Table 6.5: Optimal results for test system 2 obtained by using BBO, BH, DE and KOA ($P_D = 1263MW$)

Wind Power Forecast	0 MW				50 MW				165 MW			
Algorithm	BBO	BH	DE	KOA	BBO	BH	DE	KOA	BBO	BH	DE	KOA
P_1 (MW)	447.74	448.26	447.50	443.95	438.54	430.33	438.69	430.13	421.16	436.53	415.33	439.23
P_2 (MW)	173.08	173.86	173.31	175.50	166.71	160.50	166.61	168.05	160.54	177.54	171.37	168.18
P_3 (MW)	264.31	263.79	263.46	258.86	253.86	250.02	256.41	251.03	247.10	240.52	250.64	245.03
P_4 (MW)	138.41	137.71	139.07	136.97	130.00	126.46	131.37	146.00	132.05	100.63	125.01	93.00
P_5 (MW)	165.40	164.85	165.47	170.78	164.05	166.95	157.53	162.00	137.05	138.40	139.50	125.00
P_6 (MW)	87.03	87.51	87.14	89.97	72.00	93.38	74.46	68.00	73.00	68.21	64.43	93.00
P_W (MW)	0.00	0.00	0.00	0.00	49.99	47.58	50.00	49.68	102.99	112.41	107.68	110.89
P_L (MW)	12.97	12.98	12.96	13.03	12.15	12.23	12.06	11.89	10.88	11.24	10.96	11.33
Fuel Cost (\$/h)	15449.91	15449.93	15449.90	15450.64	14777.81	14813.08	14776.96	14785.13	14074.54	13957.44	14013.80	13987.97
C_d (\$/h)	0.00	0.00	0.00	0.00	399.91	380.67	400.00	397.47	823.88	899.28	861.45	887.09
C_p (\$/h)	390.96	390.96	390.96	390.96	194.99	202.65	194.96	195.95	68.42	53.44	60.71	55.73
C_r (\$/h)	0.00	0.00	0.00	0.00	173.27	161.99	173.33	171.83	492.29	561.58	526.40	550.15
Total cost (\$/h)	15449.91	15449.93	15449.90	15450.64	15177.72	15193.74	15176.96	15182.59	14898.42	14856.72	14875.25	14875.06
Objective Function (\$/h)	15840.87	15840.89	15840.86	15841.60	15545.99	15558.39	15545.24	15550.37	15459.13	15471.74	15462.37	15480.94

Table 6.6: Comparison of algorithms results of test system 2

Wind Power Forecast	0 MW				50 MW				165 MW			
Algorithm	BBO	BH	DE	KOA	BBO	BH	DE	KOA	BBO	BH	DE	KOA
Minimum total cost (\$/h)	15449.91	15449.93	15449.90	15450.64	15177.72	15193.74	15176.96	15182.59	14898.42	14856.72	14875.25	14875.06
Average total cost (\$/h)	15450.00	15450.35	15449.90	15454.79	15181.76	15201.67	15194.79	15214.80	14915.28	14910.10	14919.45	14973.70
Maximum total cost (\$/h)	15450.57	15453.77	15449.90	15459.92	15189.38	15221.54	15217.65	15247.02	14932.78	14931.85	14953.99	15054.00
Standard deviation (\$/h)	0.15	0.93	0.00	2.67	2.74	7.06	13.62	16.11	8.52	15.26	19.49	53.47

6.6 Conclusion

In this chapter, two wind turbine cost models proposed in the literature in solving the economic dispatch problem were introduced and they are: negative load model and the probabilistic wind turbine cost model. Differential evolution is used to compare between the probabilistic wind turbine cost model and the negative load model in solving the economic dispatch problem. Three test systems were used to compare the behavior of the probabilistic model with the negative load model. Then several metaheuristic optimization algorithms used to solve two systems at three different wind forecast points to test the probabilistic model results obtained in the previous section were DE used to solve the problem. The second objective is to show complete solution for the problem at different wind forecast solution using different algorithms.

For all the cases it is clear that the behavior of the probabilistic model at low wind forecast will be equivalent or following the negative load model till the forecast wind power reaches a critical point where in the objective function cost the negative load will start to become costly compared to the probabilistic model which will schedule the wind at fix power equal to the critical wind power forecast even if the wind power forecast is increase to a higher value because the overestimation forecast error is high and the overestimation cost is also high. The probabilistic model is better than the negative load model if the wind power generation capacity is significant compared to the total generation capacity because the probabilistic model account for both the overestimation and underestimation forecasting error and the negative load did not account. Also using the probabilistic model you have the flexibility to get many models including the negative load model by adjusting the direct cost, reserve cost and penalty cost.

Chapter 7

Load Reduction Cost Model

7.1 Introduction

Load reduction proposed in this thesis as a smart grid function, is the incentivising consumer driven load curtailment implementation of real time pricing. Finding a suitable model for load reduction at peak times is important to get a correct solution to the economic dispatch problem. The conventional network models it as negative load because it is easy to deal with it in solving the the ED problem, but due to the size of load reduction power contribution, this model may lead to an incorrect result and financial loss due to errors in forecasting. To overcome the load reduction forecasting error problem, probabilistic modeled is proposed in this chapter because it accounts for both overestimation and underestimation of available load reduction.

7.2 Load Reduction Cost Model as a Negative Load

This model is the used model in the conventional power networks because it is easier to handle it in solving the economic dispatch problem. The load reduction power is assumed to be constant, and the only change in the ED problem will be modifying the total demand by cutting the load reduction amount.

The drawbacks of this model are due to the errors of overestimating and underestimating the load reduction amount in the forecasting stage which lead to inaccurate economic dispatch solution and lose of money. Load reduction cost modeled as a negative load in the economic dispatch problem is shown in (7.1).

$$LR_{cost} = \sum_{k=1}^{Nd} h_k \; L_k \tag{7.1}$$

Here LR_{cost} is the total cost of load reduction, N_d is the number of load reduction areas, L_k is the power reduced from area k, h_k is the load reduction cost coefficients.

7.3 Probabilistic Model for Load Reduction

The probabilistic model is a more realistic option in dealing with the forecasting errors, because it accounts for both overestimation and underestimation error. The main drawback is the complexity of handling it in the economic dispatch problem. The probabilistic Load reduction cost model in the economic dispatch problem is shown in (7.2).

$$LR_{cost} = \sum_{i=1}^{N_d} L_{cost}^{D} + L_{cost}^{ue} + L_{cost}^{oe} \tag{7.2}$$

Where LR_{cost} is the total cost of load reduction, N_d is the number of load reduction units, L_{cost}^{D} is the direct cost, L_{cost}^{ue} is the load reduction underestimate forecast error cost and L_{cost}^{oe} is the load reduction overestimate forecast error cost.

$$LR_{cost} = \sum_{i=1}^{N_d} h_i \; L_i^{sc} + kue_i \; EL_i^{ue} + koe_i \; EL_i^{oe} \tag{7.3}$$

Here L_i is the available load reduction from area i, L_i^{sc} is the scheduled (forecast) load reduction power for the i^{th} area, EL_i^{ue} is the expected value of $Li > L_i^{sc}$ for the i^{th} area, EL_i^{oe} is the expected value of $Li < L_i^{sc}$ for the i^{th} area, h_i, kue_i and koe_i are the available, penalty, and reserve cost coefficients for the i^{th} area respectively. EL_i^{ue} and EL_i^{oe} are calculated based on the probability distribution of load reduction at the targeted area. Since, the consumer behavior probability distribution is not known yet in this specific issue, the load reduction model is formulated for three probability distributions: Normal distribution, Exponential distribution and Weibull distribution. Then the model formulated using Normal distribution will be used in this thesis because it is the most common choice for unknown distribution random variables and it is used in many fields.

7.3.1 Load Reduction Model Based on Normal Distribution

Assume that load reduction Power is L and $L \sim N(\mu, \sigma^2)$ and that the Load reduction Power $L \in [L_{min}\ L_{max}]$. The overestimate and underestimate expected values are shown in (7.4) and (7.5) respectively. A detailed proof of the model is found in Appendix (B).

$$EL^{oe} = (L^{sc} - \mu)\ (F(L^{sc}) - F(L_{min})) + \frac{\sigma}{\sqrt{2\pi}} \left[\exp^{\frac{-(L^{sc}-\mu)^2}{2\,\sigma^2}} - \exp^{\frac{-(L_{min}-\mu)^2}{2\,\sigma^2}} \right] \quad (7.4)$$

$$EL^{ue} = (\mu - L^{sc})\ (F(L_{max}) - F(L^{sc})) - \frac{\sigma}{\sqrt{2\pi}} \left[\exp^{\frac{-(L_{max}-\mu)^2}{2\,\sigma^2}} - \exp^{\frac{-(L^{sc}-\mu)^2}{2\,\sigma^2}} \right] \quad (7.5)$$

Figures (7.1) to (7.3) show the load reduction model overestimation cost, underestimation cost and total cost at different mean values (μ) assuming that the load reduction is active and the load reduction cost model data are shown in Appendix (C.5). As the mean value increase, the overestimation cost decrease and the underestimation cost increase. Also, it is clear that the overestimation cost equal to zero before the mean value and the underestimation cost equal to zero after the mean value. This explains the load reduction total cost behavior shown in Fig(7.3), where the load reduction total cost increase at low power forecast value as the mean value (μ) increase and it decrease at high power forecast value as the mean value increase.

The standard deviation value (σ) effect on the load reduction cost model is generally increase the cost at the region near the mean value as the standard deviation increase as shown in Fig(7.4) to Fig(7.6).

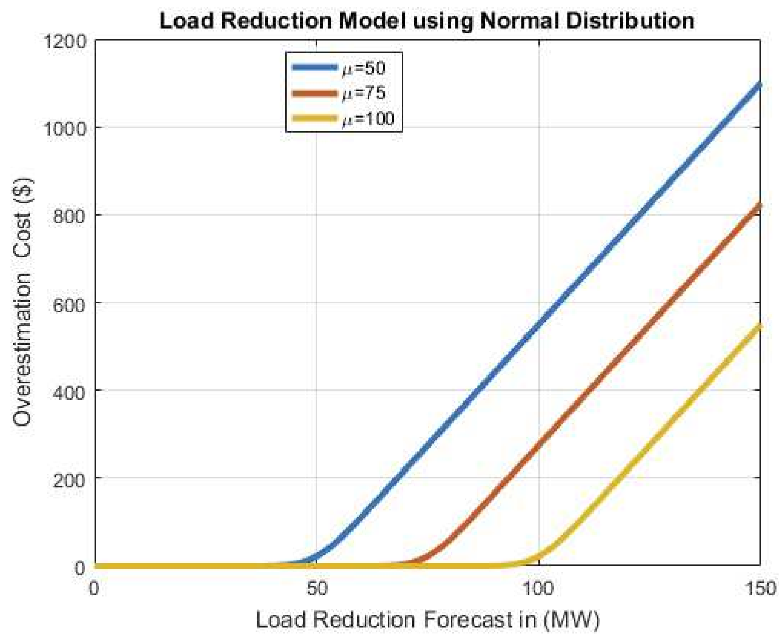

Figure 7.1: Load reduction model overestimate cost for different mean (μ)

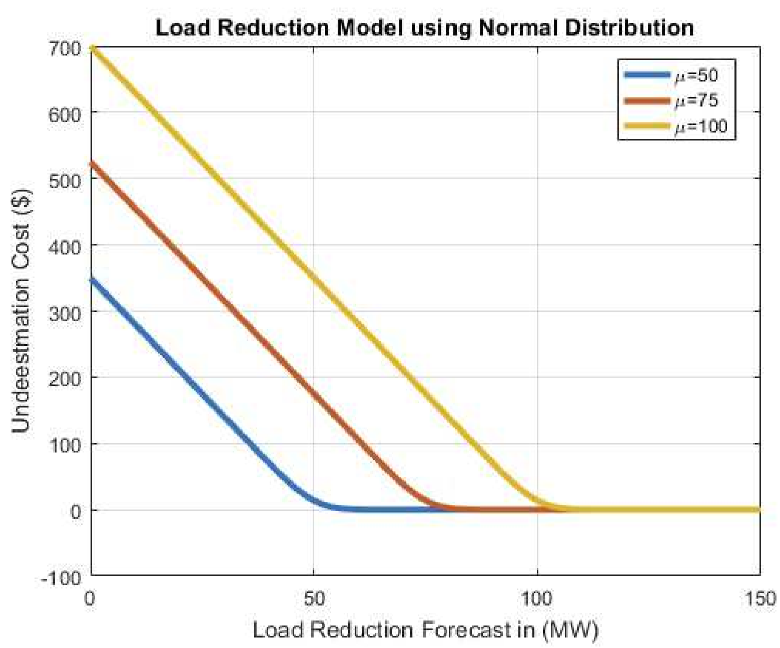

Figure 7.2: Load reduction model underestimate cost for different mean (μ)

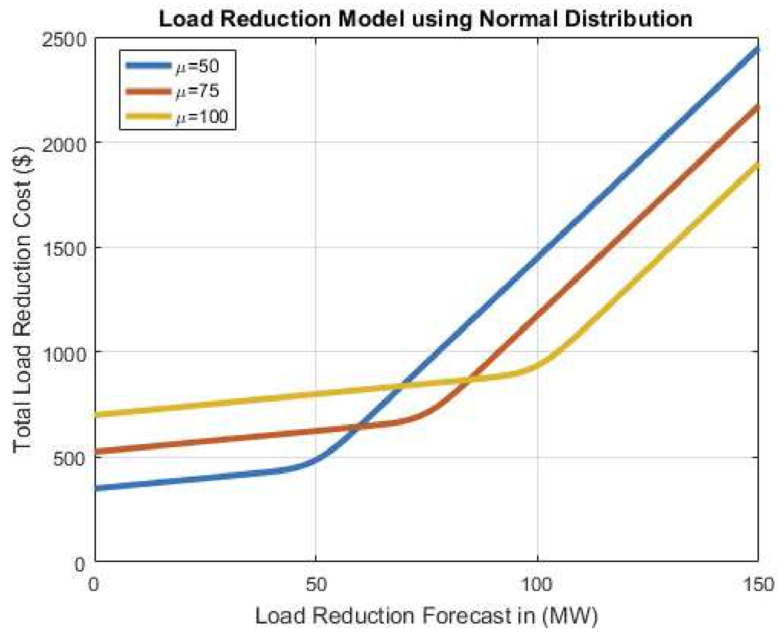

Figure 7.3: Load reduction model Total cost for different mean (μ)

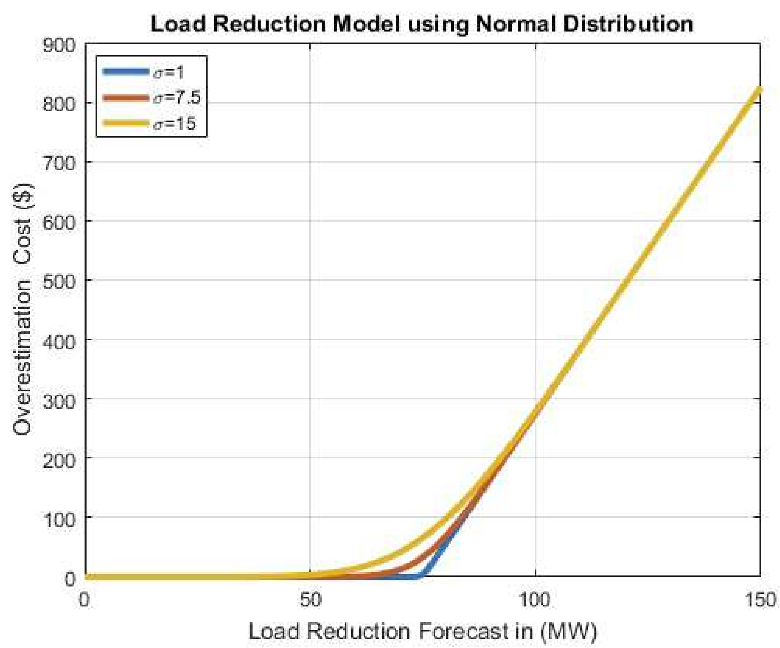

Figure 7.4: Load reduction model overestimate cost for different variance (σ^2)

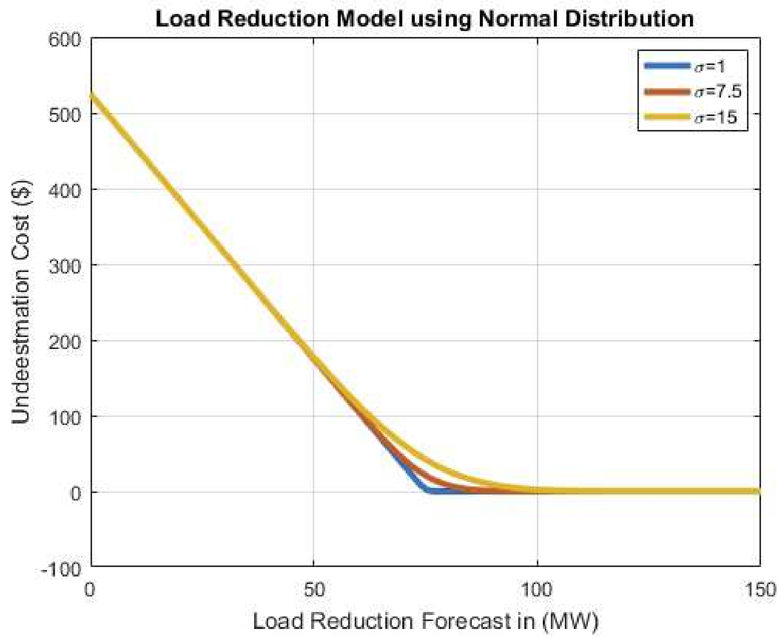

Figure 7.5: Load reduction model underestimate cost for different variance (σ^2)

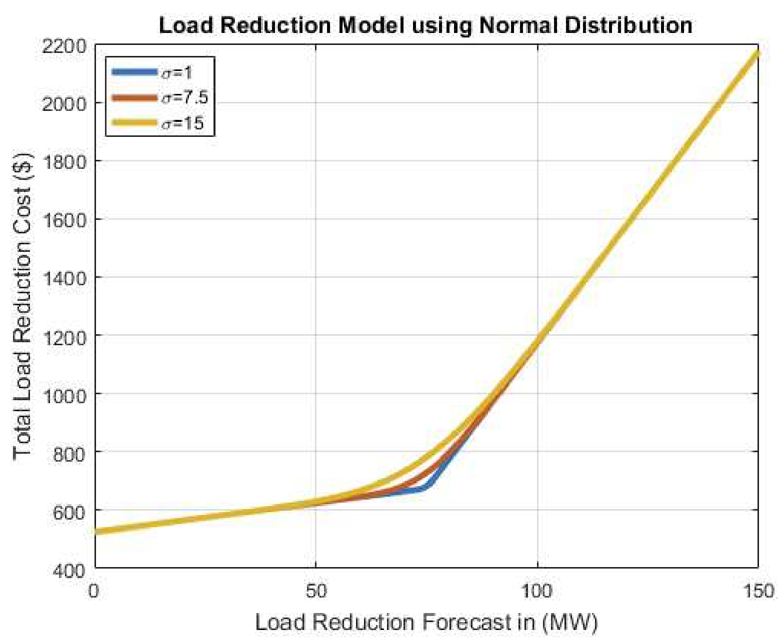

Figure 7.6: Load reduction model Total cost for different variance (σ^2)

7.3.2 Load Reduction Model Based on Exponential Distribution

Assume that load reduction Power is L and $L \sim Exp(\lambda)$ and that the Load reduction Power $L \in [L_{min}\ L_{max}]$. The overestimate and underestimate expected value are shown in (7.6) and (7.7) respectively. A detailed proof of the model is found in Appendix (B).

$$EL^{oe} = (L^{sc} - L_{min})\ e^{-\lambda\ L_{min}} - \frac{1}{\lambda}(F(L^{sc}) - F(L_{min})) \tag{7.6}$$

$$E_{ue} = (L^{sc} - L_{max})\ e^{-\lambda\ L_{max}} - \frac{1}{\lambda}(F(L^{sc}) - F(L_{max})) \tag{7.7}$$

7.3.3 Load Reduction Model Based on Weibull Distribution

Assume that load reduction Power is L and $L \sim W(c,k)$ and that the Load reduction Power $L \in [L_{min}\ L_{max}]$. The overestimate and underestimate expected value are shown in (7.8) and (7.9) respectively. A detailed proof of the model is found in Appendix (B).

$$EL^{oe} = L^{sc}\ (F(L^{sc}) - F(L_{min})) - c\ (\Gamma(1+\frac{1}{k},(\frac{L_{min}}{c})^k) - \Gamma(1+\frac{1}{k},(\frac{L^{sc}}{c})^k)) \tag{7.8}$$

$$E_{ue} = c\ (\Gamma(1+\frac{1}{k},(\frac{L^{sc}}{c})^k) - \Gamma(1+\frac{1}{k},(\frac{L_{max}}{c})^k)) - L^{sc}\ (F(L_{max}) - F(L^{sc}) \tag{7.9}$$

7.3.4 Economic Dispatch Solution Incorporating Wind Energy and Load Reduction

The general procedure to solve the economic dispatch problem incorporating wind energy and load reduction is active using any metaheuristic algorithm is shown in Procedure (3).

Procedure 3: Economic Dispatch Solution

1. Initialize the algorithm parameters (population size, no of generations, no of iteration, mutation rate, cross over rate, khums rate).
2. Generate a set of feasible solutions where each solution consist of output power generation for each thermal unit, the wind power which generated randomly based on the forecast and the load reduction power which generated randomly based on the forecast. The solutions satisfy the different economic dispatch constraints required in the problem.
3. The direct cost, overestimation cost and the under estimation cost for wind power and load reduction power are calculated for all the solutions.
4. Calculate the objective function.
5. Save the best solution.
6. Apply the algorithm operations on the set of the solutions.
7. Check the feasibility of the generated solutions and repeat steps (3-5).
8. Repeat steps (6-7) until the termination criterion is achieved.

7.4 Comparison Of Load Reduction Probabilistic Model With Negative Model in Economic Dispatch Problem Without Wind Energy

To analyze the difference between the load reduction negative load cost model and the load reduction probabilistic cost model based on normal distribution and to select the suitable model among them, economic dispatch problem will be solved with and without the valve point effect considering different constraints such as generators capacity, ramp rate limit, and prohibited operation zones.

Three test systems were used to study the difference between the two models. The first system is composed of three generation units with generation capacity constraints. The generation units cost coefficients and capacity limits are shown in Appendix (C.1.1). To observe the effect of valve point nonlinearity, a three machine system shown in Appendix (C.1.2) is used and to observe the prohibited operation zones, ramp rate limit and power losses, a six machine system shown in Appendix (C.1.3) is used. The systems were modified by assuming that the systems operate at peak value and the load reduction program is active. The demand load for the first and the second system are 1000 MW and for the third system is 1400 MW.

The load reduction probabilistic cost model and the load reduction negative load cost model will be used to model the load reduction in the problem. KOA algorithm were used to solve the problem with Khums tax rate selected to be $K_r = 0.2$. For the three test systems, the selected number of generations and population size are 50 and 50. The load reduction cost model data are shown in Appendix (C.5).

The performance of load reduction probabilistic cost model and the load reduction negative load cost model are shown in Fig(7.7) for three machine test system. The effect of valve point nonlinearity on the performance is shown in Fig(7.9) and the effect of prohibited operation zone and ramp rate limit is shown in Fig(7.11).

The general response obtained, as expected to be similar in general to the response obtained in Chapter (6). The two models are equivalent in the lower load reduction forecast values till the forecast value reach a critical point and it is here equal to the mean value μ. After that the load reduction probabilistic cost model will stop increasing by always scheduling a load reduction value near the mean value because of the high overestimation forecasting error cost. On the other hand, the negative load reduction cost model increase as the forecast increase which may result in high loss of money due to the load reduction overestimation forecasting error.

Total cost can mislead the decision maker as shown in Fig (7.8), Fig (7.10) and Fig (7.12) where the negative load model always have the lowest price. But as shown before in Table (6.2) in Chapter (6) that even though that the negative load model produce lower cost but due to small overestimation forecasting error and by calculating the cost of this error, the new total cost is higher in the case of negative load model compare to the probabilistic model.

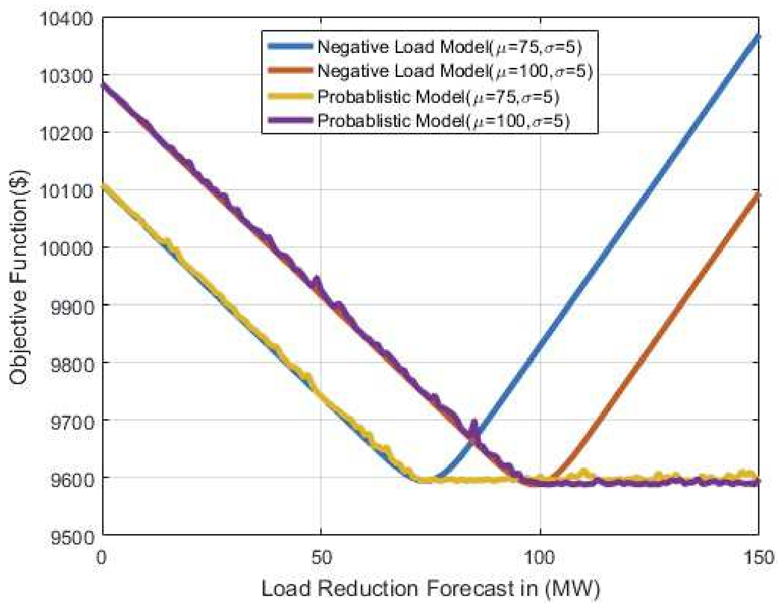

Figure 7.7: Objective function cost for three generator quadratic cost functions and with load reduction power at different mean value (μ)

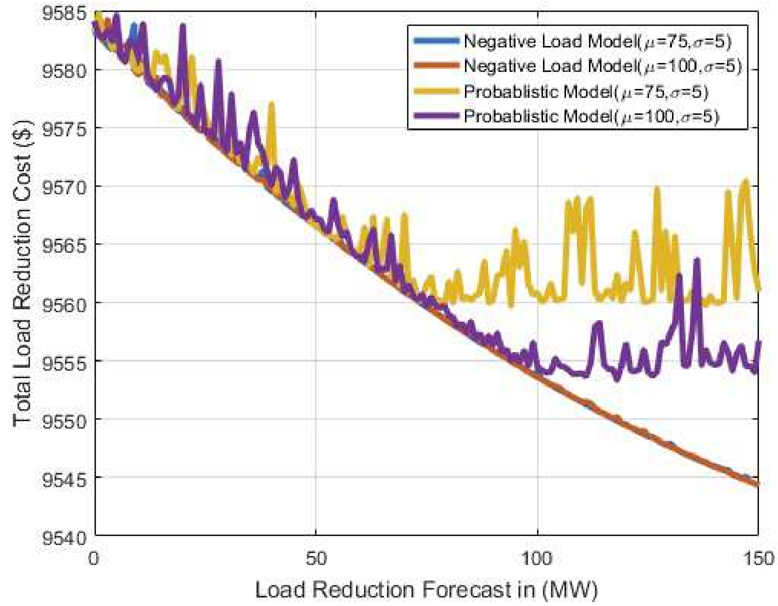

Figure 7.8: Total cost for three generator quadratic cost functions and with with load reduction power at different mean value (μ)

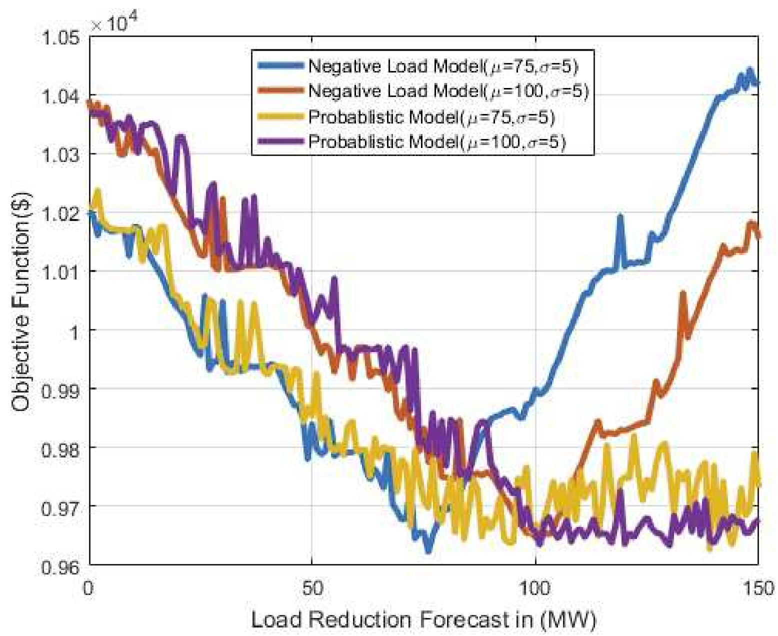

Figure 7.9: Objective function for three generation units with quadratic cost functions and the effects of valve-point loading is considered and with load reduction power at different mean value (μ)

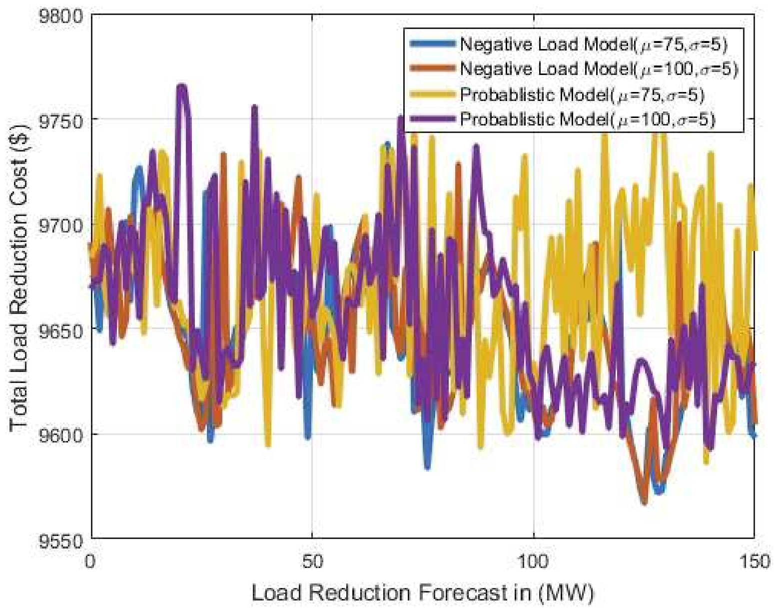

Figure 7.10: Total cost for three generation units with quadratic cost functions and the effects of valve-point loading is considered and with load reduction power at different mean value (μ)

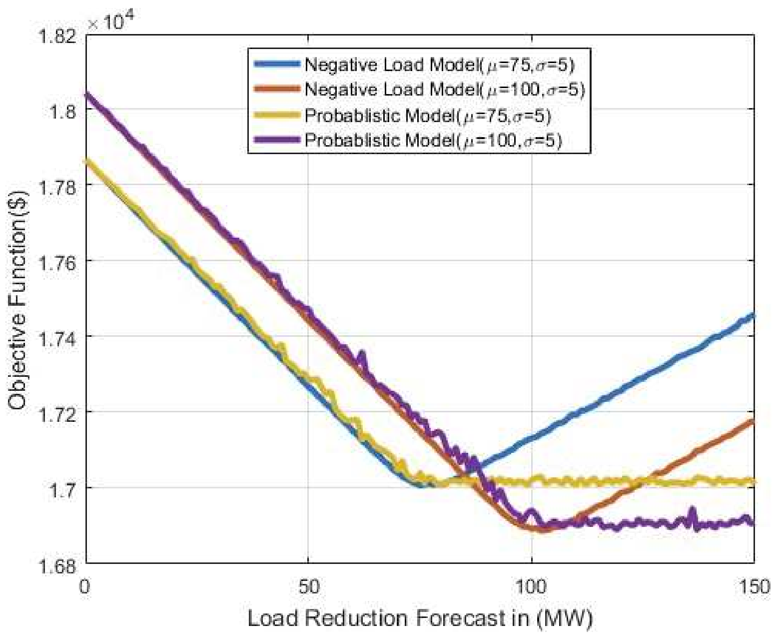

Figure 7.11: Objective function cost for six generator with load reduction considering the prohibited operation zones and the ramp rate limits at different mean value (μ)

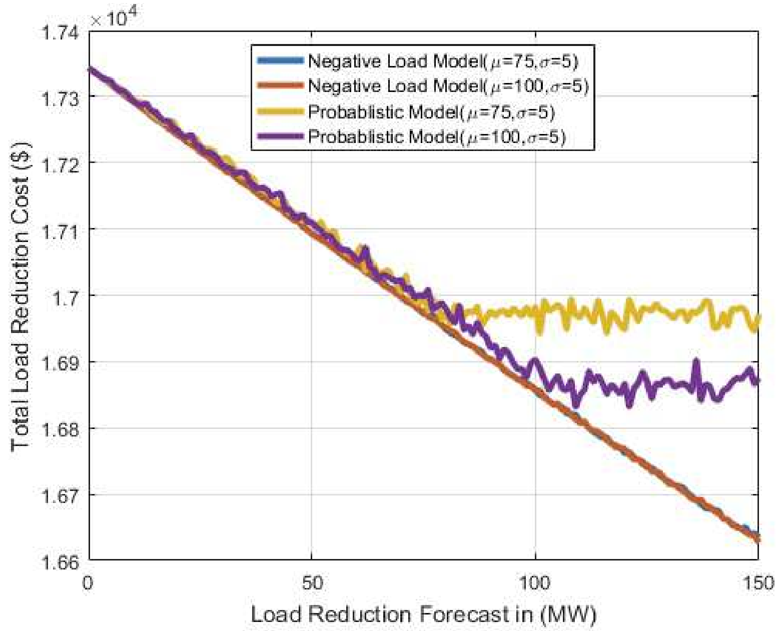

Figure 7.12: Total cost for six generator with load reduction considering the prohibited operation zones and the ramp rate limits at different mean value (μ)

7.5 Comparison Of Load Reduction Probabilistic Model With Negative Model in Economic Dispatch Problem With Wind Energy

There are four possible combination for the wind turbine operation cost model and load reduction operation cost model as shown in Table(7.1).

Table 7.1: Possible combination for the wind turbine operation cost model and load reduction operation cost model

Cost Model Option	wind Turbine	Load Reduction
1	Negative	Negative
2	Negative	Probablistic
3	Probablistic	Negative
4	Probablistic	Probablistic

Like the last section (Section (7.4)), three Test systems were used to study the difference between the two models. The first system is composed of three generation units with generation capacity constraints. The generation units cost coefficients and capacity limits are shown in Appendix (C.1.1). To observe the effect of valve point nonlinearity, a three generating units system shown in Appendix (C.1.2) is used and to observe the prohibited operation zones, ramp rate limit and power losses, a six machine system shown in Appendix (C.1.3) is used. The systems were modified by adding wind turbine to each system and assuming that the system operate at peak value and the load reduction program is active. The load reduction cost model data and the wind turbine cost model are shown in Appendix (C.5). The demand load for the first and the second system are 1000 MW and for the third system is 1400 MW.

DE algorithm were used to solve the problem and the optimization parameters are shown in Table (7.2). For the three test systems, the selected number of generations and population size are 50 and 50 respectively.

Table 7.2: Parameters for DE

Algorithm	**co**	**pf**	**F**
DE	0.5	0.005	0.9

The objective function cost for three generation unit system with quadratic cost functions, with one wind turbine unit and with load reduction for all possible combination of models is shown in Fig(7.13) from different views. The effect of valve point nonlinearity on the objective function cost is shown in Fig(7.15) and the effect of prohibited operation zones and the effect of ramp rate limit on the objective function cost is shown in Fig(7.17). In general, it is clear that the probabilistic-probabilistic option is the lowest cost option most of the time or the second lowest and the difference between it and the lowest option is not high.

The bottom view of the objective function cost shown in Fig(7.13e), Fig(7.15e) and Fig(7.17e) support the general behavior of the probabilistic model mentioned in Section (7.4), but in two dimension. There are two critical points, one for the wind forecast and one for the load reduction forecast. The minimum region area depends on the critical points values.

If the forecast value is low then the best model is the negative load model for that variable and if the forecast value is high for any variable, then the best model is the probabilistic model.

It is like a road map for the operator or dispatcher to decide based on the forecasting data, the preferred model. Table (7.3) shows the different combination based on the forecasting data.

Table 7.3: Different model combination for wind turbine cost model and load reduction cost model based on forecasting data

Forecast		
wind Turbine	Load Reduction	Model Combination
Low	Low	Negative-Negative (N-N)
Low	High	Negative-Probablistic (N-P)
High	Low	Probablistic-Negative (P-N)
High	High	Probablistic-Probablistic (P-P)

Based on the observation mentioned before about the probabilistic-probabilistic option is the lowest or the second lowest most of the times and the difference is not high, the probabilistic-probabilistic option present a good and competitive choice for all the cases if the dispatcher need to work with one model for the wind turbines and one model for the load reduction models and avoid the complexity if the cost difference is not significant.

Total cost of all the four combinations is shown in Fig(7.14), Fig(7.16) and Fig(7.18) for the cases. Although, the probabilistic-probabilistic option is higher in total cost in all the time intervals but it is the least expensive if the forecast error occurred, because it is obtained based on the objective function cost which account for overestimation and underestimation forecasting error.

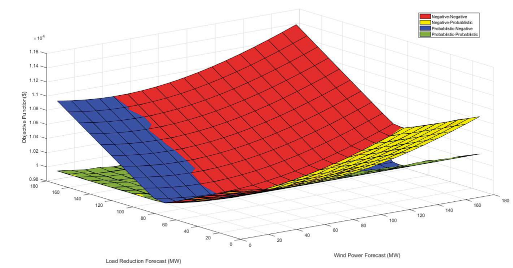

(a) 0° View

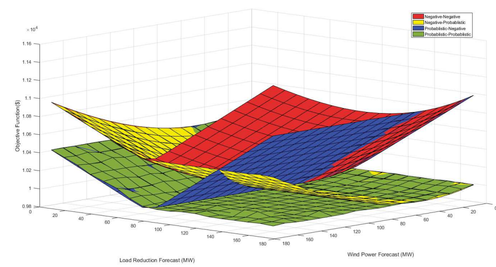

(b) 180° View

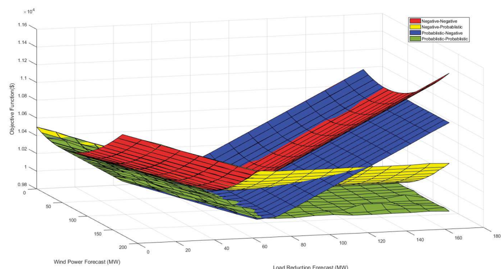

(c) Side view

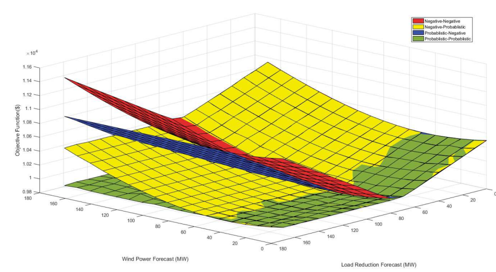

(d) Another side view

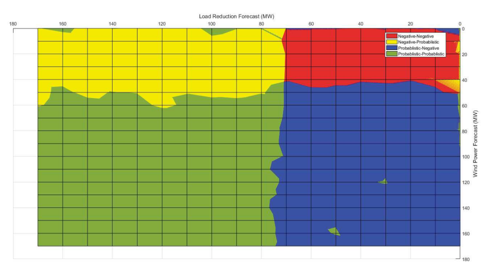

(e) Bottom view

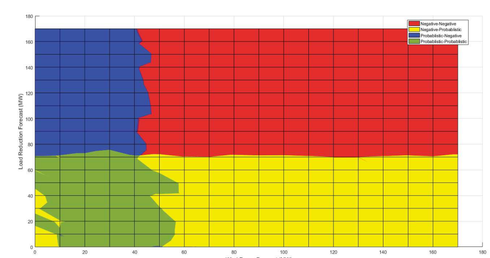

(f) Top view

Figure 7.13: Objective function cost for three generator with quadratic cost functions and with load reduction power and with wind energy included for all the possible combination of models

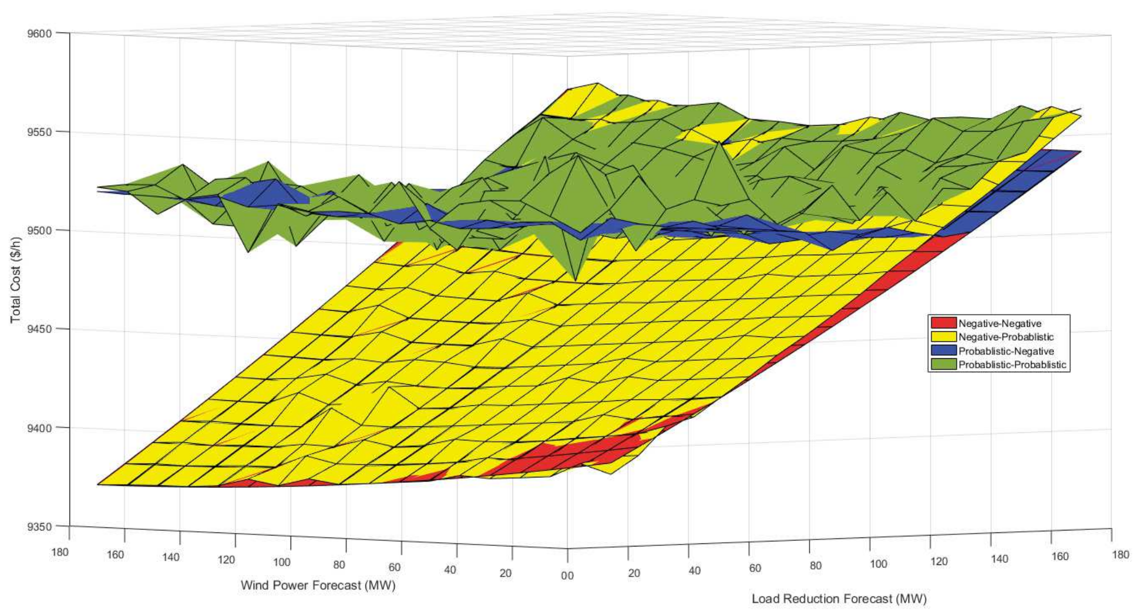

Figure 7.14: Total cost for three generator with quadratic cost functions and with load reduction power and with wind energy included for all the possible combination of models

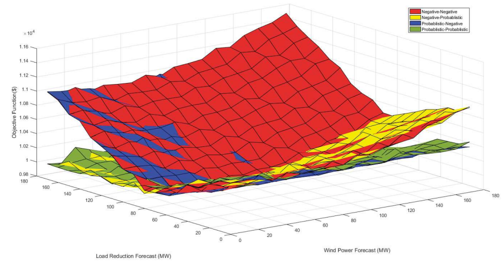

(a) 0° View

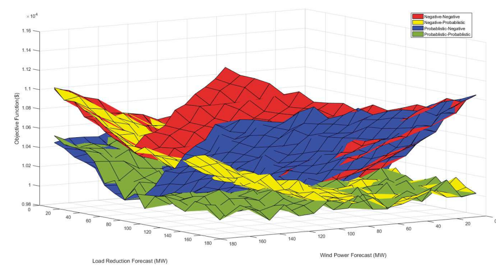

(b) 180° View

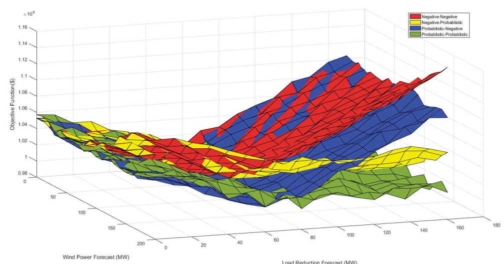

(c) Side view

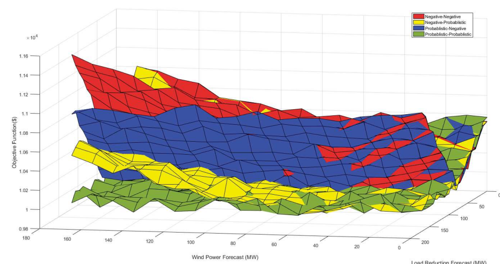

(d) Another side view

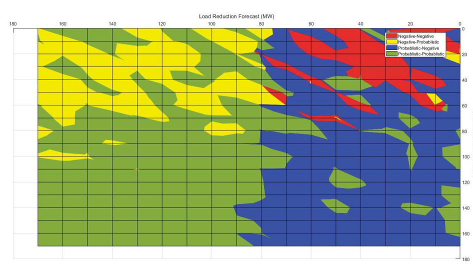

(e) Bottom view

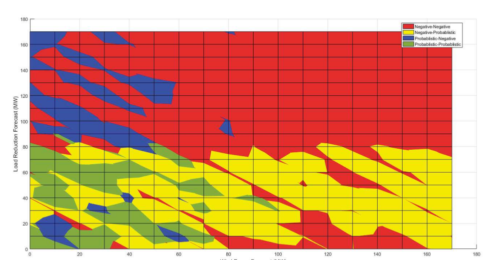

(f) Top view

Figure 7.15: Objective function cost for three generation units with quadratic cost functions and the effects of valve-point loading is considered and with load reduction power and with wind energy included for all the possible combination of models

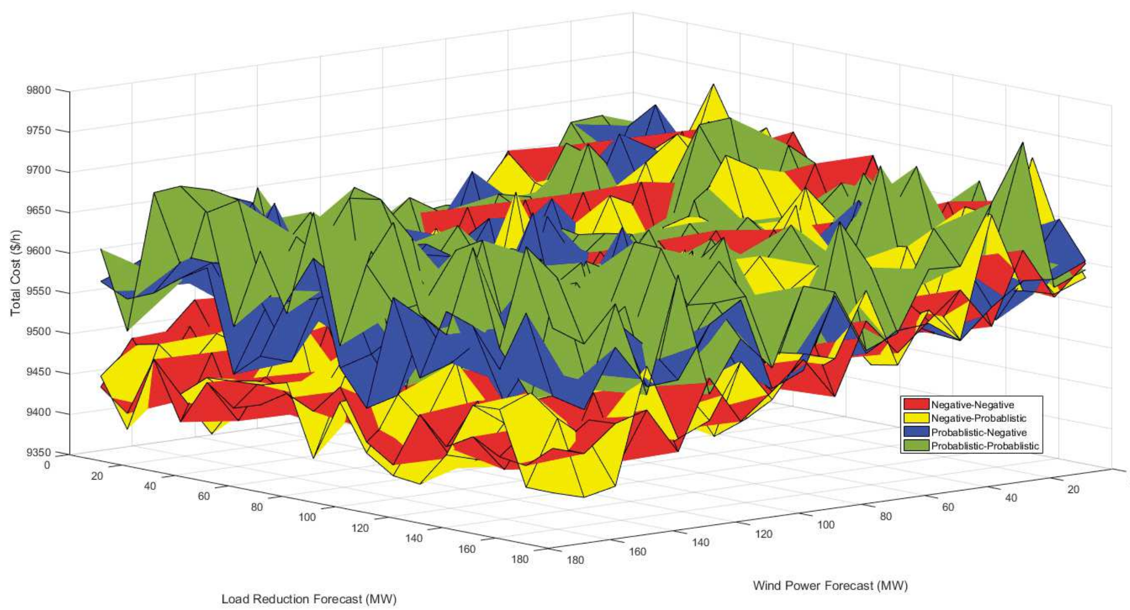

Figure 7.16: Total cost for three generation units with quadratic cost functions and the effects of valve-point loading is considered and with load reduction power and with wind energy included for all the possible combination of models

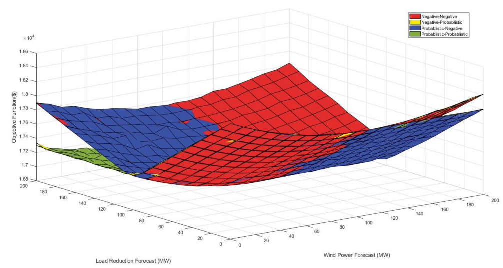

(a) 0° View

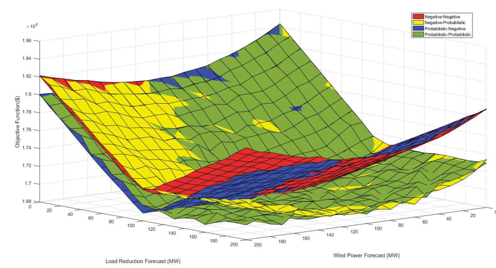

(b) 180° View

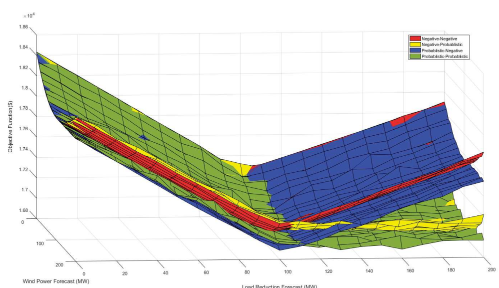

(c) Side view

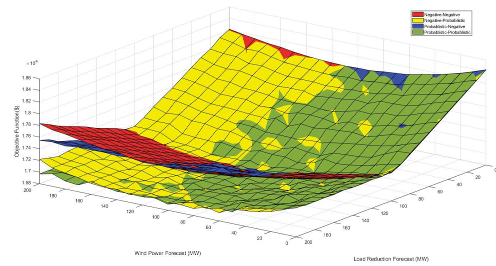

(d) Another side view

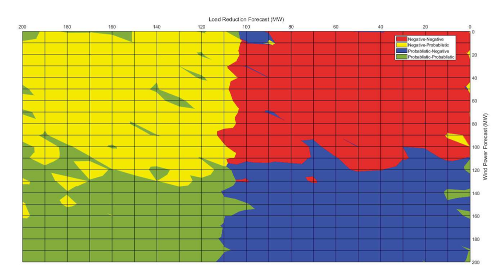

(e) Bottom view

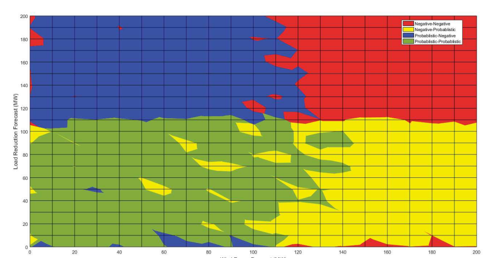

(f) Top view

Figure 7.17: Objective function cost for six generator considering the prohibited operation zones and the ramp rate limits and with load reduction power and with wind energy included for all the possible combination of models

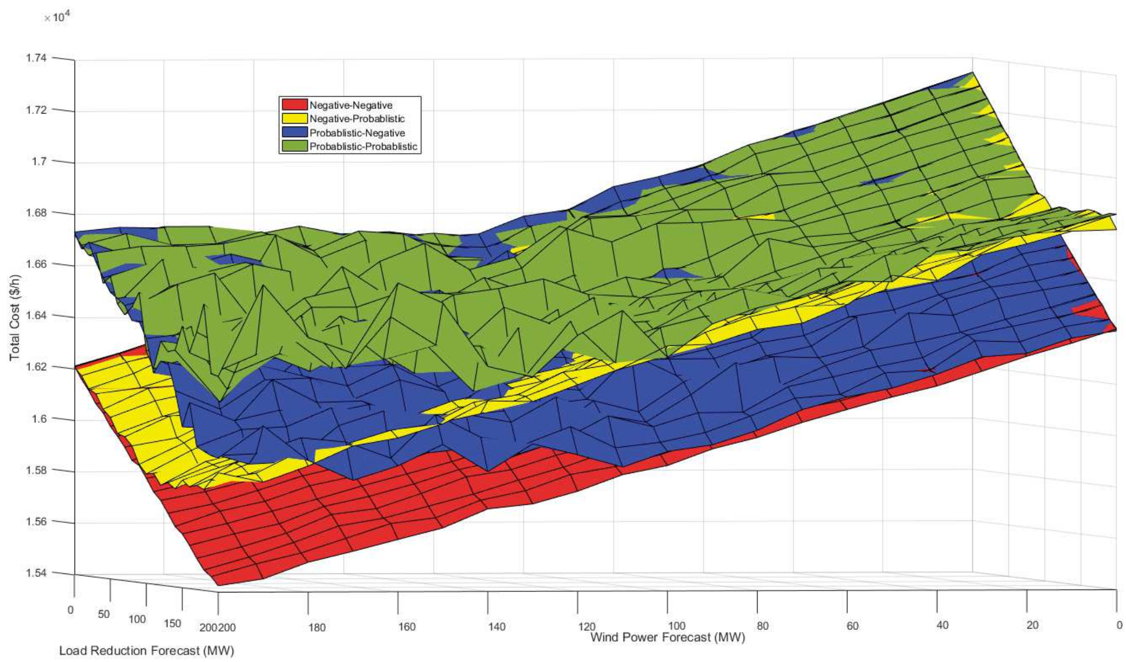

Figure 7.18: Total cost for six generator considering the prohibited operation zones and the ramp rate limits and with load reduction power and with wind energy included for all the possible combination of models

7.6 Conclusion

In this chapter two models were presented for the load reduction as demand side management measure for economic dispatch problem in smart grid network at peak load time and they are the negative load cost model and the probabilistic cost model based on Normal distribution. The first model is the model used in the conventional network. The load reduction probabilistic cost model is proposed in this chapter and in this thesis to model the load reduction to minimize the effect of load reduction forecasting error in smart grid network. The general response of the objective function and the total cost function obtained without wind energy, is similar in general to the response obtained in Chapter (6).

The general response of of the objective function and the total cost function obtained with wind energy is more complex and result into four possible model combinations: N-N, N-P, P-N and P-P.

Among the four combinations, P-P are the most reliable in dealing with the forecasting errors because it is either the cheapest choice or the second cheapest choice in the objective function for the three test systems in the four regions. Hence, in all the next chapters the P-P model will be used to model the wind energy and the load reduction.

Chapter 8

Unit Commitment Problem For Smart Grid

8.1 Introduction

Finding the ON/OFF schedule of a set of generators over a time horizon in a way that minimizes the operation cost is the definition of unit commitment problem. The time horizon usually is 24 hours of day or 168 hours of a week [129].

The integration of a significant amount of renewable energy and the integration of load reduction as demand side management measure increase the complexity of the problem and introduce many challenges in finding the optimal solution which accounts for the intermittent behavior of renewable resources and the error in the forecasting of the available renewable power and the forecasting of the amount of load reduction at peak loads.

In the conventional network, the wind power modeled as negative load because of the small contribution of it compared to the thermal units. Load reduction is also modeled as negative load due to the small contribution compared with the capacity of the system.

In the smart grid and based on its objectives, there will be a significant contribution of renewable energy which helps in minimizing production costs and the greenhouse gases emissions (GHGs). In this chapter, unit commitment will be modeled and solved for smart grid network by assuming significant integration of wind energy to the network and the load reduction programs are active.

8.2 Smart Grid Unit Commitment Mathematical Formulation

Suppose that there are N generation units that will feed the demand load over T periods. The unit commitment objective function can be written as:

$$min\ C_{th} + C_{wind} + C_{LR} \tag{8.1}$$

where C_{th} is the total thermal unit commitment cost, C_{wind} is the total wind power generation cost and C_{LR} is the total load reduction cost.

8.2.1 Thermal Power Generation Cost

The thermal unit commitment cost compose of the fuel cost and the start up cost as shown in (8.2)[129, 64].

$$C_{th} = \sum_{t=1}^{T}\sum_{j=1}^{N}[F(P_j(t)) + SC_j(t)] \tag{8.2}$$

where C_{th} is the total unit commitment cost for N units in T periods (hours), $F(P_j(t))$ is the fuel cost function for unit j at period t and $SC_j(t)$ is the start up cost for unit j at period t. The fuel cost function is shown in (8.3)[129, 64].

$$F(P_j) = a_j P_j^2 + b_j P_j + c_j \tag{8.3}$$

where a_j, b_j, c_j are the fuel cost coefficients of generator j, P_j is the the output power of generator j and $F(P_j)$ is the fuel cost of unit j. Start up cost is a function of time, where time will decide the start up cost price. Cold start up cost is considered if the unit is off for a long period, whereas a hot start up cost is considered if it is off for a short period. the start up cost is defined as follows [64]:

$$SC_j(t) = \begin{cases} C_j^{hot} & T_j^{off} \leq T_j^{down} + T_j^{cold} \\ C_j^{cold} & T_j^{off} > T_j^{down} + T_j^{cold} \end{cases} \tag{8.4}$$

where $SC_j(t)$ is the start up cost for unit j, T_j^{off} is the continuous off time duration of generating unit j, T_j^{down} is the minimum down time of unit j, T_j^{cold} is the cold start hours of unit j, C_j^{hot} is the hot start cost for unit j and C_j^{cold} is the cold start cost for unit j.

8.2.2 Wind Power Generation Cost

There are two cost model shown in Chapter (6): the negative load model and the probabilistic model. Based on these models, the total wind cost for N_w units and in T periods can be calculated as follows:

$$C_{wind} = \sum_{t=1}^{T} W_{Cost}^{t} \tag{8.5}$$

Where W_{Cost}^{t} is the total wind power generation cost.

8.2.3 Load Reduction Cost

There are two main cost model proposed in Chapter (7): the negative load model and the probabilistic model. The probabilistic cost model was formulated to normal distribution, weibull distribution, and exponential distribution. Based on the selected model, the total wind cost for T periods can be calculated as follows:

$$C_{LR} = \sum_{t=1}^{T} LR_{Cost}^{t} \tag{8.6}$$

Where LR_{Cost}^{t} is the total cost of load reduction.

8.3 Equality Constraints

8.3.1 Real Power Balance Constraint

The total power generated from thermal and wind units should equal the load demand at each period of time as shown in (8.7), where the P_D represents the total load demand.

$$\sum_{i=1}^{Nx} P_i + \sum_{j=1}^{Nw} w_j = P_D - \sum_{k=1}^{Nd} L_k \tag{8.7}$$

Where w_j available wind power for the j^{th} wind turbine and L_k is the available load reduction from area k.

8.4 Inequality Constraints

8.4.1 Spinning Reserve Constraint

The total amount of generation available from all units synchronized in the system minus the demand power and the losses of the system is the spinning reserve. The importance of the spinning reserve is that when a unit or more is lost the system frequency will not drop. Spinning reserve is specified as a percentage of peak load or enough of making up the loss of the largest unit loaded on the system. Spinning reserve should be distributed around the system to avoid transmission limitations [129, 64].

$$\sum_{j=1}^{N} P_j^{max} \geq P_D + P_R \tag{8.8}$$

P_j^{max} is the maximum power generated from unit j, P_D is the total demand power and P_R is the required spinning reserve.

8.4.2 Minimum Up Time Constraint

If the unit is turned on it should not turned off before a minimum up time [64].

$$T_j^{ON} \geq T_j^{up} \tag{8.9}$$

$T_j^{ON}$is the continuous ON time duration and T_j^{up} is the minimum up time for unit j.

8.4.3 Minimum Down Time Constraint

If the unit is turned off it should not turned on before a minimum down time [64].

$$T_j^{OFF} \geq T_j^{down} \tag{8.10}$$

$T_j^{OFF}$is the continuous OFF time duration and T_j^{down} is the minimum down time for unit j.

8.4.4 Generator Power Limit Constraint

Generation units are restricted by their limits in term of generation active power as follows:

$$P_j^{min} \leq P_j \leq P_j^{max} \quad j = 1, 2 \cdots, N \tag{8.11}$$

where P_j^{min}, P_j^{max}, are the minimum active power output, maximum active power output of the j^{th} generating unit respectively.

8.4.5 Wind Turbine Power Limit Constraint

$$0 \leq w_j \leq w_j^r \quad j = 1, 2 \cdots, Nw \tag{8.12}$$

Here w_j^r, is the rated active power output of the j^{th} wind turbine unit.

8.4.6 Load Power Limit Constraint

$$L_k^{min} \leq L_k \leq L_k^{max} \quad k = 1, 2 \cdots, Nd \tag{8.13}$$

Here L_k^{min}, L_k^{max}, are the minimum active power reduction, maximum active power reduction of the k^{th} unit respectively.

8.5 Unit Commitment Solution Incorporating Wind Energy and Load Reduction

The general procedure to solve the unit commitment problem incorporating wind energy and load reduction measures are active at peak loads using any metaheuristic algorithm is shown in Procedure (4).

Procedure 4: Unit Commitment Solution

1. Initialize the algorithm parameters (population size, no of generations, no of iteration, mutation rate, cross over rate).
2. Generate a set of feasible solutions where each consist of a set of ON/OFF schedules, and on each hour in any schedule there are the wind power and the load reduction power, both generated randomly based on the forecast.
3. The economic dispatch is calculated using Quadratic programing for all the solutions.
4. The direct cost, overestimation cost and the under estimation cost for wind power and load reduction power are calculated for all the solutions.
5. Calculate the objective function.
6. Save the best solution.
7. Apply the Algorithm operations on the set of the solutions.
8. Check the feasibility of the generated solutions and repeat steps (3-6).
9. Repeat steps (7-8) until the termination criterion is achieved.

8.6 Unit Commitment Solution Incorporating Wind Energy and Load Reduction using BBO and GA

In this section, a numerical example will be shown using the new unit commitment model for two test systems assuming that the wind energy is included and the load reduction is active. The wind energy cost model and the load reduction cost model are the probabilistic based on Weibull distribution and probabilistic based on Normal distribution respectively.

BBO and GA were selected to solve the unit commitment because of their ability to operate on the binary numbers easily and directly without creating many violations in the unit commitment problem. The parameters for the BBO and GA algorithms are selected as shown in Table (8.1).

For the first test cases the selected number of generation, population size and number of iteration are 50, 50 and 10 respectively and for the second test system it is 200, 200 and 10 respectively. The wind turbine cost model parameters and the load reduction cost model parameters are shown in Table (8.2) and Table (8.3) respectively. This work has been reported in [50].

Table 8.1: BBO and GA parameters for unit commitment problem

Algorithm	CO	pf
BBO	-	0.005
GA	0.75	0.005

Table 8.2: Wind turbine data for unit commitment problem

Test System	k	c	k_p	k_r	d	V_i	V_r	V_0	W_r
1 & 2	2	10	6	11	8	5	15	45	165

Table 8.3: Load reduction cost model data for unit commitment problem

System	h	kue	koe	μ	σ	$L_{min}(MW)$	$L_{max}(MW)$
1 & 2	9	7	11	75	5	0	90

8.6.1 Test System 1

This system consists of four thermal generation units, a wind turbine and load reduction measures are active at peak loads. The study is for eight periods of time and the spinning reserve for the thermal units is assumed to be 10% of the demand at each period. The data and load demand are shown in Appendix(C.2.1).

The evolutionary algorithm parameters, the wind turbine cost model data and the load reduction cost model data are shown in Table (8.1), Table (8.2) and Table (8.3) respectively.

Table (8.5) lists the optimum schedule obtained using the proposed algorithms without including the wind energy and the load reduction measures are not active. It is obvious that the minimum total cost generated by the proposed algorithms is lower than that obtained using other algorithms as shown in Table (8.4) and Figure (8.1). Also, both algorithms succeed in getting the same minimum total cost when the wind turbine is not included.

Table (8.6) and Figure (8.2) show the optimum results with the wind energy included based on the probabilistic model and the load reduction measures are not active. Table (8.7) and Figure (8.3) shows the show the optimum results without the wind energy and the load reduction measures are active. Finally, Table (8.8) and Figure (8.4) show the optimum results with the wind energy and the load reduction measures are active.

It is obvious that, the objective function cost and the total cost obtained by the BBO algorithm is lower than that obtained using the GA algorithm for this test system in all the cases except the first case shown in Table (8.5). Also, The total cost decreases with the merging of wind energy and applying the load reduction measures.

The rule is to choose the solution with lower objective function cost because as the objective function cost decrease, the overestimation cost and the underestimation cost decrease. If both the objective function and the total cost are together smaller for one algorithm solution, then the obtained solution in that case is the best compared to the other solution.

Table 8.4: Minimum cost for BBO, GA, LR, PSO-LR, B.SMP, and A.SMP without wind energy for test system 1

Method	Minimum Cost ($)
BBO	**74528.67**
GA	**74528.67**
LR [64]	75232
PSO-LR [64]	74808
B.SMP [64]	74812
A.SMP [64]	74812

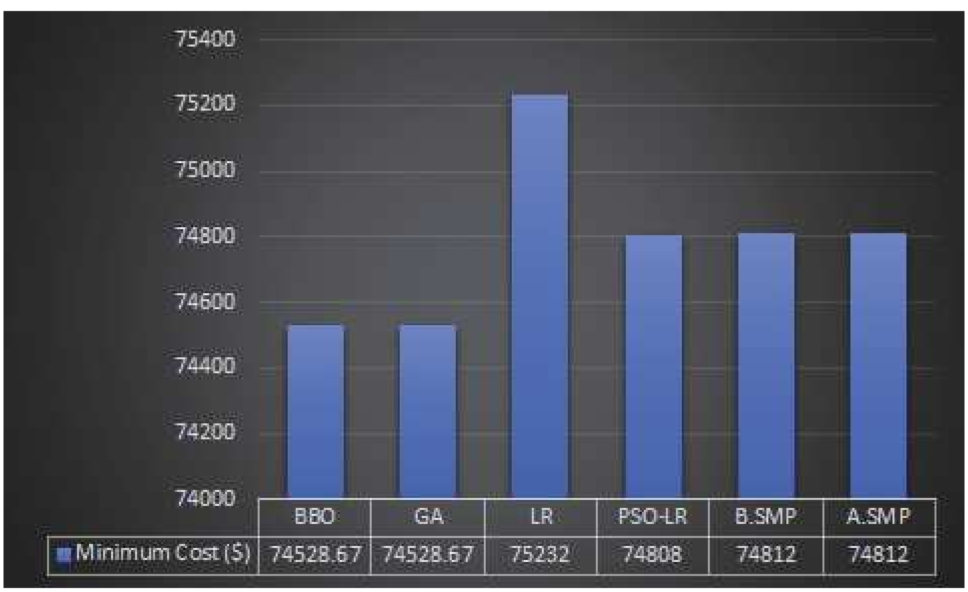

Figure 8.1: Minimum cost for BBO, GA, LR, PSO-LR, B.SMP, and A.SMP without wind energy for test system 1

Table 8.5: Optimal results of four thermal generation units with eight periods of time and the spinning reserve for the thermal units is assumed to be 10% of the demand at each period without wind energy and without load reduction

Algorithm	**BBO**				**GA**			
Time	**U1**	**U2**	**U3**	**U4**	**U1**	**U2**	**U3**	**U4**
1	300.00	150.00	0.00	0.00	300.00	150.00	0.00	0.00
2	300.00	205.00	25.00	0.00	300.00	205.00	25.00	0.00
3	300.00	250.00	30.00	20.00	300.00	250.00	30.00	20.00
4	300.00	215.00	25.00	0.00	300.00	215.00	25.00	0.00
5	276.19	123.81	0.00	0.00	276.19	123.81	0.00	0.00
6	196.19	83.81	0.00	0.00	196.19	83.81	0.00	0.00
7	202.86	87.14	0.00	0.00	202.86	87.14	0.00	0.00
8	300.00	200.00	0.00	0.00	300.00	200.00	0.00	0.00
Fuel Cost ($)	74378.64571				74378.6457			
Start-Up Cost ($)	150.0200				150.0200			
Total Cost ($)	74528.6657				74528.6657			
Objective Function Cost ($)	74528.6657				74528.6657			

Table 8.6: Optimal results of four thermal generation units, a wind turbine and load reduction is not active at peak loads for eight periods of time and the spinning reserve for the thermal units is assumed to be 10% of the demand at each period

Algorithm	**BBO**					**GA**					Forecast
Time	**U1**	**U2**	**U3**	**U4**	w_m^{sc}	**U1**	**U2**	**U3**	**U4**	w_m^{sc}	w_m^F
1	300.00	150.00	0.00	0.00	0.00	300.00	150.00	0.00	0.00	0.00	0.00
2	300.00	210.00	0.00	20.00	0.00	300.00	205.00	25.00	0.00	0.00	0.00
3	300.00	250.00	30.00	20.00	0.00	300.00	250.00	30.00	20.00	0.00	0.00
4	300.00	175.52	25.00	0.00	39.48	300.00	172.53	25.00	0.00	42.47	50.00
5	244.62	108.03	0.00	0.00	47.35	246.54	108.98	25.00	0.00	19.48	50.00
6	163.30	67.37	0.00	0.00	49.33	157.84	64.64	25.00	0.00	32.52	50.00
7	134.21	60.00	0.00	0.00	95.79	83.97	60.00	0.00	0.00	146.03	165.00
8	244.35	107.89	0.00	0.00	147.76	279.02	125.22	0.00	0.00	95.76	165.00
Fuel Cost ($)	67653.3505					68949.0726					
Start-Up Cost ($)	150.0200					150.0200					
C_{dm} **($)**	3037.7037					2690.0729					
Total Cost ($)	70841.0743					71789.1654					
Objective Function Cost ($)	74659.0291					75557.0800					

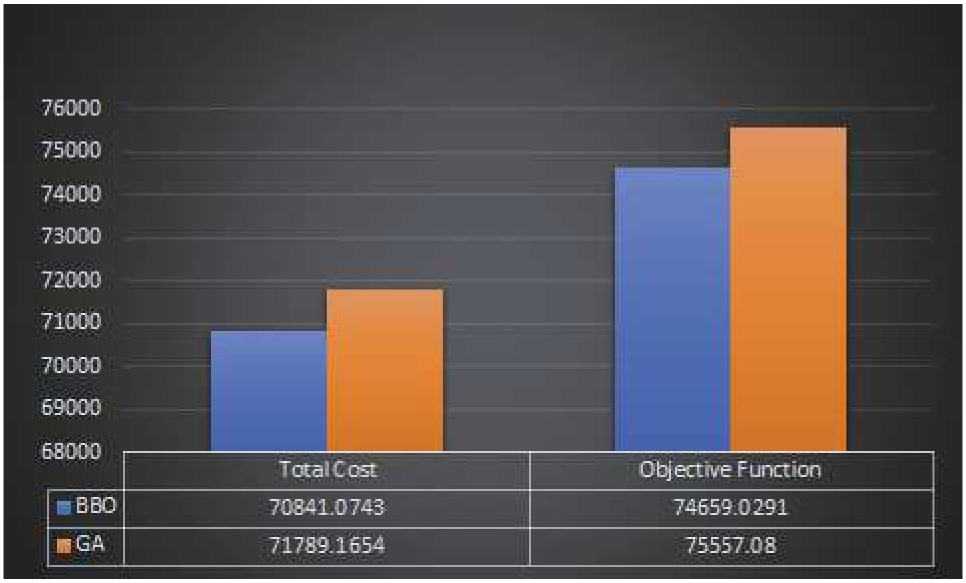

Figure 8.2: Optimal results of four thermal generation units, a wind turbine and load reduction is not active at peak loads for eight periods of time and the spinning reserve for the thermal units is assumed to be 10% of the demand at each period

Table 8.7: Optimal results of four thermal generation units without wind energy and the load reduction is active at peak loads for eight periods of time and the spinning reserve for the thermal units is assumed to be 10% of the demand at each period

Algorithm	**BBO**					**GA**					Forecast
Time	**U1**	**U2**	**U3**	**U4**	L_m^{sc}	**U1**	**U2**	**U3**	**U4**	L_m^{sc}	L_m^F
1	300.00	150.00	0.00	0.00	0.00	300.00	150.00	0.00	0.00	0.00	0
2	295.07	133.25	25.00	0.00	76.69	296.37	133.90	25.00	0.00	74.73	81
3	300.00	165.28	25.00	20.00	89.72	300.00	203.24	25.00	20.00	51.76	90
4	300.00	146.25	25.00	0.00	68.75	300.00	145.52	25.00	0.00	69.48	72
5	276.19	123.81	0.00	0.00	0.00	276.19	123.81	0.00	0.00	0.00	0
6	196.19	83.81	0.00	0.00	0.00	196.19	83.81	0.00	0.00	0.00	0
7	202.86	87.14	0.00	0.00	0.00	202.86	87.14	0.00	0.00	0.00	0
8	300.00	200.00	0.00	0.00	0.00	300.00	200.00	0.00	0.00	0.00	0
Fuel Cost ($)	70013.6561					70737.9757					
Start-Up Cost ($)	150.0200					150.0200					
L_{cost}^D **($)**	2116.4364					1763.7309					
Total Cost ($)	72280.1125					72651.7266					
Objective Function Cost ($)	75152.01011					75514.52764					

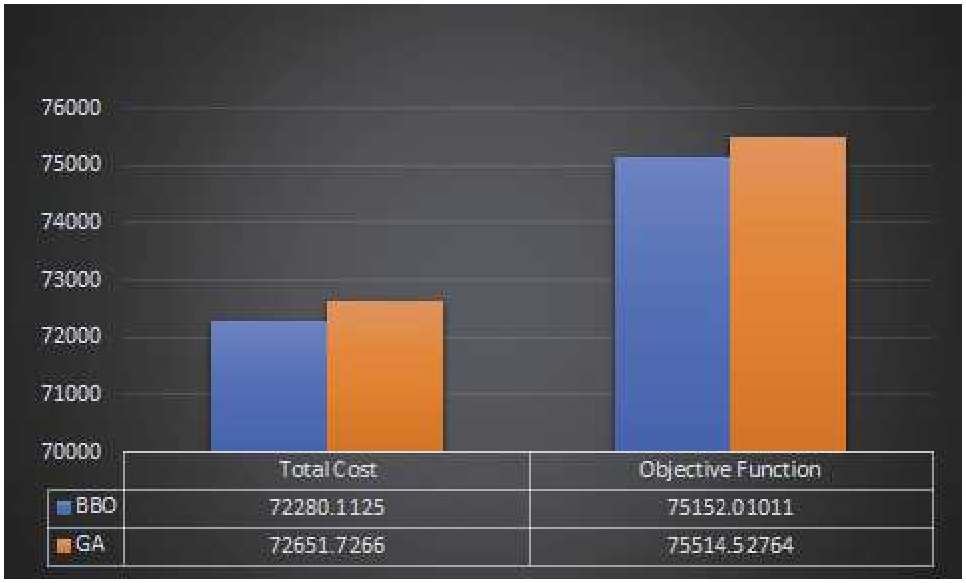

Figure 8.3: Optimal results of four thermal generation units without wind energy and the load reduction is active at peak loads for eight periods of time and the spinning reserve for the thermal units is assumed to be 10% of the demand at each period

Table 8.8: Optimal results of four thermal generation units, a wind turbine and load reduction is active at peak loads for eight periods of time and the spinning reserve for the thermal units is assumed to be 10% of the demand at each period

Algorithm	**BBO**						**GA**						Forecast	
Time	**U1**	**U2**	**U3**	**U4**	w_m^{sc}	L_m^{sc}	**U1**	**U2**	**U3**	**U4**	w_m^{sc}	L_m^{sc}	w_m^F	L_m^F
1	300.00	150.00	0.00	0.00	0.00	0.00	300.00	150.00	0.00	0.00	0.00	0.00	0.00	0.00
2	300.00	181.09	25.00	0.00	0.00	23.91	300.00	200.20	25.00	0.00	0.00	4.80	0.00	81.00
3	300.00	195.65	25.00	20.00	0.00	59.35	300.00	178.71	25.00	20.00	0.00	76.29	0.00	90.00
4	294.56	132.99	0.00	0.00	47.08	65.37	300.00	162.22	0.00	0.00	46.06	31.72	50.00	72.00
5	265.66	118.54	0.00	0.00	15.80	0.00	256.16	113.79	0.00	0.00	30.05	0.00	50.00	0.00
6	187.04	79.23	0.00	0.00	13.73	0.00	163.24	67.33	0.00	0.00	49.43	0.00	50.00	0.00
7	148.86	60.15	0.00	0.00	80.99	0.00	156.46	63.94	0.00	0.00	69.60	0.00	165.00	0.00
8	243.18	107.31	0.00	0.00	149.51	0.00	261.86	116.65	0.00	0.00	121.49	0.00	165.00	0.00
Fuel Cost ($)	65805.8885						66294.5325							
Start-Up Cost ($)	150.0200						150.0200							
C_{dm} **($)**	2456.8569						2532.9931							
L_{cost}^D **($)**	1337.6590						1015.2560							
Total Cost ($)	69750.4245						69992.8016							
Objective Function Cost ($)	76642.3054						76920.9708							

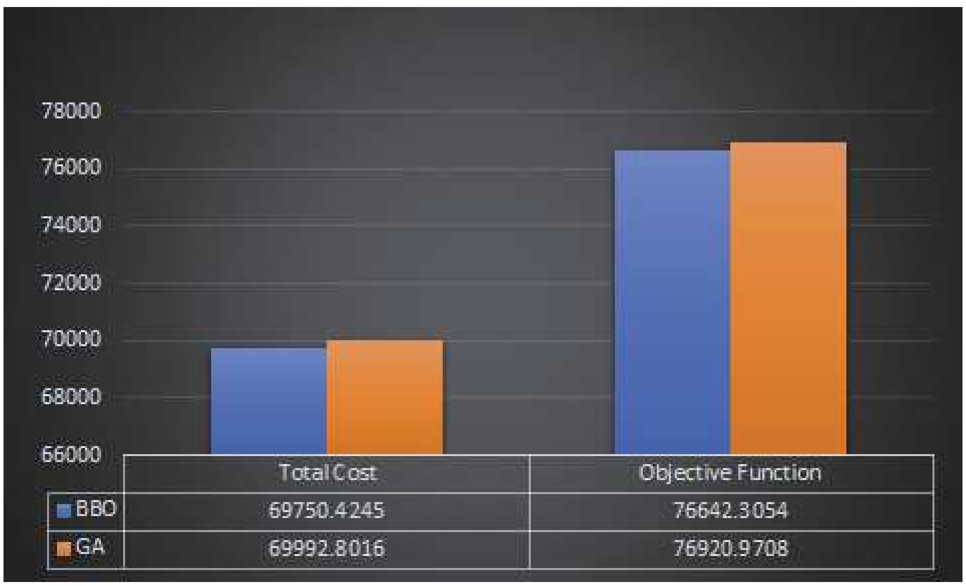

Figure 8.4: Optimal results of four thermal generation units, a wind turbine and load reduction is active at peak loads for eight periods of time and the spinning reserve for the thermal units is assumed to be 10% of the demand at each period

8.6.2 Test System 2

This system consists of ten thermal generation units, a wind turbine and load reduction measures are active at peak loads. The study is for twenty-four periods of time and the spinning reserve on the thermal units is assumed to be 10% of the demand at each period. The data and load demand are shown in Appendix(C.2.2) and The evolutionary algorithm parameters, the wind turbine cost model data and the load reduction cost model data are shown in Table (8.1), Table (8.2) and Table (8.3) respectively.

Table(8.10) lists the optimum schedule obtained using the proposed algorithms without the wind energy and the load reduction is not active. BBO get better solution compared to GA and both succeed in finding lower cost compared to other algorithms except A.SMP [64] and B.SMP [64] as shown in Table (8.9) and illustrated in Figure (8.5).

Table(8.11) shows the optimum results with the wind energy included and the load reduction measures are not active where The BBO algorithm again gets better solution compared to GA in both the objective function cost and the total cost as shown in Figure (8.6).

Table(8.12) shows the optimum results without the wind energy included and the load reduction measures are active and Table(8.13) shows the optimum results with the wind energy included and the load reduction measures are active. GA obtained better solution compare to BBO in both the objective function cost and the total cost as shown in Figure (8.7) and Figure (8.8) respectively.

Table 8.9: Minimum cost for BBO, GA, LR, PSO-LR, B.SMP, and A.SMP without wind energy for test system 2

Method	**Minimum Cost ($)**
BBO	565092.46
GA	565249.50
LR [64]	565825.00
DP [64]	565825.00
GA [64]	565852.00
B.SMP [64]	564017.73
A.SMP [64]	563937.26

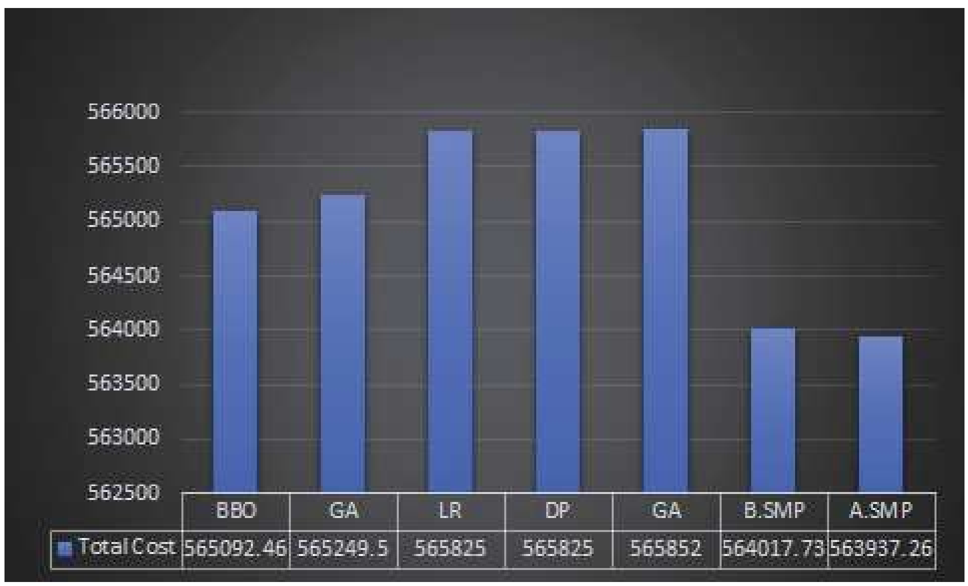

Figure 8.5: Minimum cost for BBO, GA, LR, PSO-LR, B.SMP, and A.SMP without wind energy for test system 2

Table 8.10: Optimal results of ten thermal generation units with twenty-four periods of time and the spinning reserve on the thermal units is assumed to be 10% of the demand at each period without wind energy and the load reduction measures are not active

Algorithm	**BBO**										**GA**									
Time	**U1**	**U2**	**U3**	**U4**	**U5**	**U6**	**U7**	**U8**	**U9**	**U10**	**U1**	**U2**	**U3**	**U4**	**U5**	**U6**	**U7**	**U8**	**U9**	**U10**
1	455.00	245.00	0.00	0.00	0.00	0.00	0.00	0.00	0.00	0.00	455.00	245.00	0.00	0.00	0.00	0.00	0.00	0.00	0.00	0.00
2	455.00	295.00	0.00	0.00	0.00	0.00	0.00	0.00	0.00	0.00	455.00	295.00	0.00	0.00	0.00	0.00	0.00	0.00	0.00	0.00
3	455.00	265.00	130.00	0.00	0.00	0.00	0.00	0.00	0.00	0.00	455.00	265.00	130.00	0.00	0.00	0.00	0.00	0.00	0.00	0.00
4	455.00	345.00	130.00	0.00	0.00	20.00	0.00	0.00	0.00	0.00	455.00	340.00	130.00	0.00	25.00	0.00	0.00	0.00	0.00	0.00
5	455.00	395.00	130.00	0.00	0.00	20.00	0.00	0.00	0.00	0.00	455.00	390.00	130.00	0.00	25.00	0.00	0.00	0.00	0.00	0.00
6	455.00	365.00	130.00	130.00	0.00	20.00	0.00	0.00	0.00	0.00	455.00	360.00	130.00	130.00	25.00	0.00	0.00	0.00	0.00	0.00
7	455.00	410.00	130.00	130.00	25.00	0.00	0.00	0.00	0.00	0.00	455.00	410.00	130.00	130.00	25.00	0.00	0.00	0.00	0.00	0.00
8	455.00	455.00	130.00	130.00	30.00	0.00	0.00	0.00	0.00	0.00	455.00	455.00	130.00	130.00	30.00	0.00	0.00	0.00	0.00	0.00
9	455.00	455.00	130.00	130.00	95.00	0.00	25.00	10.00	0.00	0.00	455.00	455.00	130.00	130.00	100.00	20.00	0.00	10.00	0.00	0.00
10	455.00	455.00	130.00	130.00	162.00	33.00	25.00	0.00	0.00	10.00	455.00	455.00	130.00	130.00	162.00	33.00	25.00	0.00	0.00	10.00
11	455.00	455.00	130.00	130.00	162.00	73.00	25.00	0.00	10.00	10.00	455.00	455.00	130.00	130.00	162.00	73.00	25.00	10.00	0.00	10.00
12	455.00	455.00	130.00	130.00	162.00	80.00	25.00	43.00	10.00	10.00	455.00	455.00	130.00	130.00	162.00	80.00	25.00	43.00	10.00	10.00
13	455.00	455.00	130.00	130.00	162.00	33.00	25.00	0.00	10.00	0.00	455.00	455.00	130.00	130.00	162.00	33.00	25.00	10.00	0.00	0.00
14	455.00	455.00	130.00	130.00	95.00	0.00	25.00	0.00	10.00	0.00	455.00	455.00	130.00	130.00	85.00	20.00	25.00	0.00	0.00	0.00
15	455.00	455.00	130.00	130.00	30.00	0.00	0.00	0.00	0.00	0.00	455.00	455.00	130.00	130.00	30.00	0.00	0.00	0.00	0.00	0.00
16	455.00	310.00	130.00	130.00	25.00	0.00	0.00	0.00	0.00	0.00	455.00	310.00	130.00	130.00	25.00	0.00	0.00	0.00	0.00	0.00
17	455.00	260.00	130.00	130.00	25.00	0.00	0.00	0.00	0.00	0.00	455.00	260.00	130.00	130.00	25.00	0.00	0.00	0.00	0.00	0.00
18	455.00	360.00	130.00	130.00	25.00	0.00	0.00	0.00	0.00	0.00	455.00	360.00	130.00	130.00	25.00	0.00	0.00	0.00	0.00	0.00
19	455.00	455.00	130.00	130.00	30.00	0.00	0.00	0.00	0.00	0.00	455.00	455.00	130.00	130.00	30.00	0.00	0.00	0.00	0.00	0.00
20	455.00	455.00	130.00	130.00	162.00	33.00	25.00	10.00	0.00	0.00	455.00	455.00	130.00	130.00	162.00	0.00	25.00	23.00	10.00	10.00
21	455.00	455.00	130.00	130.00	85.00	20.00	25.00	0.00	0.00	0.00	455.00	455.00	130.00	130.00	95.00	0.00	25.00	0.00	10.00	0.00
22	455.00	455.00	130.00	0.00	0.00	25.00	25.00	10.00	0.00	0.00	455.00	360.00	130.00	130.00	0.00	0.00	25.00	0.00	0.00	0.00
23	455.00	425.00	0.00	0.00	0.00	20.00	0.00	0.00	0.00	0.00	455.00	315.00	130.00	0.00	0.00	0.00	0.00	0.00	0.00	0.00
24	455.00	345.00	0.00	0.00	0.00	0.00	0.00	0.00	0.00	0.00	455.00	345.00	0.00	0.00	0.00	0.00	0.00	0.00	0.00	0.00
Fuel Cost	561692.4647										562129.5031									
Start-Up Cost	3400.00										3120.0000									
Total Cost	565092.4647										565249.5031									
Objective Function Cost	565092.4647										565249.5031									

Table 8.11: Optimal results of ten thermal generation units, a wind turbine and the load reduction measures are not active for twenty-four periods of time and the spinning reserve on the thermal units is assumed to be 10% of the demand at each period

Algorithm	**BBO**											**GA**											Forecast
Time	**U1**	**U2**	**U3**	**U4**	**U5**	**U6**	**U7**	**U8**	**U9**	**U10**	w_m^{sc}	**U1**	**U2**	**U3**	**U4**	**U5**	**U6**	**U7**	**U8**	**U9**	**U10**	w_m^{sc}	w_m^F
1	455.00	245.00	0.00	0.00	0.00	0.00	0.00	0.00	0.00	0.00	0.00	455.00	245.00	0.00	0.00	0.00	0.00	0.00	0.00	0.00	0.00	0.00	0.00
2	455.00	295.00	0.00	0.00	0.00	0.00	0.00	0.00	0.00	0.00	0.00	455.00	295.00	0.00	0.00	0.00	0.00	0.00	0.00	0.00	0.00	0.00	0.00
3	455.00	385.00	0.00	0.00	0.00	0.00	0.00	0.00	10.00	0.00	0.00	455.00	265.00	130.00	0.00	0.00	0.00	0.00	0.00	0.00	0.00	0.00	0.00
4	455.00	359.21	130.00	0.00	0.00	0.00	0.00	0.00	0.00	0.00	5.79	455.00	344.64	130.00	0.00	0.00	0.00	0.00	0.00	0.00	0.00	20.36	30.00
5	455.00	281.36	130.00	130.00	0.00	0.00	0.00	0.00	0.00	0.00	3.64	455.00	384.98	130.00	0.00	25.00	0.00	0.00	0.00	0.00	0.00	5.02	30.00
6	455.00	333.54	130.00	130.00	25.00	0.00	0.00	0.00	0.00	0.00	26.46	455.00	455.00	130.00	0.00	50.54	0.00	0.00	0.00	0.00	0.00	9.46	30.00
7	455.00	383.44	130.00	130.00	25.00	0.00	0.00	0.00	0.00	0.00	26.56	455.00	388.11	130.00	130.00	25.00	0.00	0.00	0.00	0.00	0.00	21.89	60.00
8	455.00	409.26	130.00	130.00	25.00	0.00	0.00	0.00	0.00	0.00	50.74	455.00	417.73	130.00	130.00	25.00	0.00	0.00	0.00	0.00	0.00	42.27	60.00
9	455.00	455.00	130.00	130.00	48.28	0.00	25.00	0.00	0.00	0.00	56.72	455.00	455.00	130.00	130.00	65.69	0.00	0.00	10.00	0.00	0.00	54.31	60.00
10	455.00	455.00	130.00	130.00	90.54	20.00	25.00	0.00	0.00	0.00	94.46	455.00	455.00	130.00	130.00	140.26	20.00	0.00	10.00	0.00	10.00	49.74	100.00
11	455.00	455.00	130.00	130.00	149.31	20.00	25.00	10.00	0.00	0.00	75.69	455.00	455.00	130.00	130.00	162.00	30.06	25.00	0.00	10.00	0.00	52.94	100.00
12	455.00	455.00	130.00	130.00	129.08	20.00	25.00	10.00	0.00	0.00	145.92	455.00	455.00	130.00	130.00	126.43	20.00	25.00	0.00	10.00	0.00	148.57	165.00
13	455.00	455.00	130.00	130.00	76.30	20.00	0.00	0.00	0.00	0.00	133.70	455.00	455.00	130.00	130.00	128.71	20.00	25.00	0.00	0.00	0.00	56.29	165.00
14	455.00	455.00	130.00	130.00	74.39	20.00	0.00	0.00	0.00	0.00	35.61	455.00	455.00	130.00	130.00	64.55	20.00	0.00	0.00	0.00	0.00	45.45	70.00
15	455.00	422.12	130.00	130.00	25.00	0.00	0.00	0.00	0.00	0.00	37.88	455.00	415.32	130.00	130.00	25.00	0.00	0.00	0.00	0.00	0.00	44.68	70.00
16	455.00	240.85	130.00	130.00	25.00	0.00	0.00	0.00	0.00	0.00	69.15	455.00	280.89	130.00	130.00	25.00	0.00	0.00	0.00	0.00	0.00	29.11	70.00
17	455.00	211.27	130.00	130.00	25.00	0.00	0.00	0.00	0.00	0.00	48.73	455.00	213.70	130.00	130.00	25.00	0.00	0.00	0.00	0.00	0.00	46.30	70.00
18	455.00	297.13	130.00	130.00	25.00	0.00	0.00	0.00	0.00	0.00	62.87	455.00	291.90	130.00	130.00	25.00	0.00	0.00	0.00	0.00	0.00	68.10	70.00
19	455.00	444.85	130.00	130.00	25.00	0.00	0.00	0.00	0.00	0.00	15.15	455.00	415.43	130.00	130.00	25.00	0.00	0.00	0.00	0.00	0.00	44.57	70.00
20	455.00	455.00	130.00	0.00	162.00	80.00	25.00	49.00	10.00	10.00	24.00	455.00	455.00	130.00	130.00	132.71	20.00	25.00	0.00	10.00	10.00	32.29	50.00
21	455.00	455.00	130.00	0.00	162.00	32.46	25.00	0.00	10.00	0.00	30.54	455.00	455.00	130.00	0.00	162.00	24.84	25.00	10.00	0.00	0.00	38.16	50.00
22	455.00	455.00	0.00	0.00	96.06	20.00	25.00	0.00	0.00	0.00	48.94	455.00	455.00	0.00	0.00	117.86	20.00	25.00	0.00	0.00	0.00	27.14	50.00
23	455.00	420.00	0.00	0.00	25.00	0.00	0.00	0.00	0.00	0.00	0.00	455.00	420.00	0.00	0.00	25.00	0.00	0.00	0.00	0.00	0.00	0.00	0.00
24	455.00	345.00	0.00	0.00	0.00	0.00	0.00	0.00	0.00	0.00	0.00	455.00	345.00	0.00	0.00	0.00	0.00	0.00	0.00	0.00	0.00	0.00	0.00
Fuel Cost	537264.4644											540310.8040											
Start-Up Cost	3170.0000											3230.0000											
C_{dm} **($)**	7940.3943											6693.2187											
Total Cost	548374.8588											550234.0227											
Objective Function Cost	565092.4647											565249.5031											

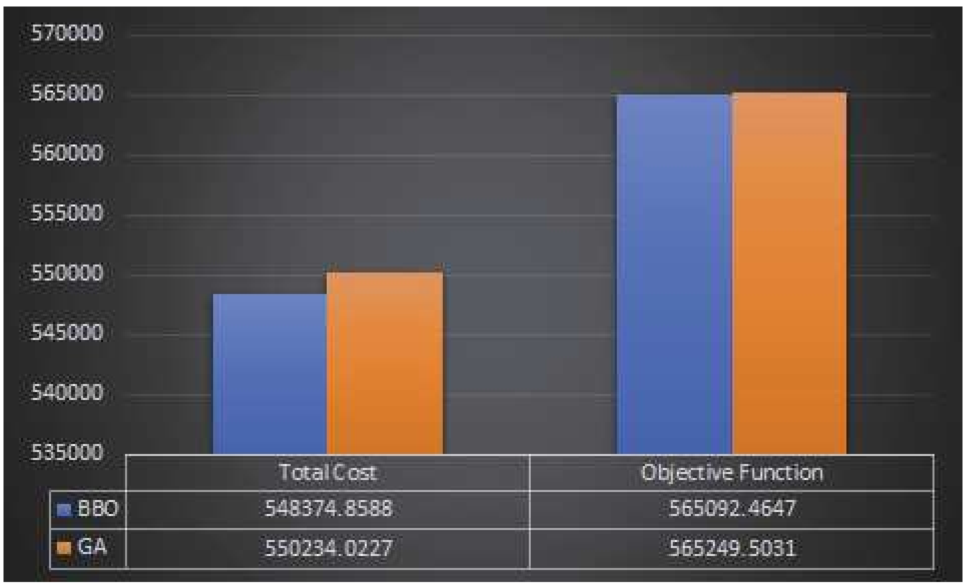

Figure 8.6: Optimal results of ten thermal generation units, a wind turbine and the load reduction measures are not active for twenty-four periods of time and the spinning reserve on the thermal units is assumed to be 10% of the demand at each period

Table 8.12: Optimal results of ten thermal generation units without wind energy and the load reduction measures are active at peak loads for twenty-four periods of time and the spinning reserve on the thermal units is assumed to be 10% of the demand at each period

Algorithm	**BBO**											**GA**											Forecast
Time	**U1**	**U2**	**U3**	**U4**	**U5**	**U6**	**U7**	**U8**	**U9**	**U10**	L_m^{sc}	**U1**	**U2**	**U3**	**U4**	**U5**	**U6**	**U7**	**U8**	**U9**	**U10**	L_m^{sc}	L_m^F
1	455.00	245.00	0.00	0.00	0.00	0.00	0.00	0.00	0.00	0.00	0.00	455.00	245.00	0.00	0.00	0.00	0.00	0.00	0.00	0.00	0.00	0.00	0.00
2	455.00	295.00	0.00	0.00	0.00	0.00	0.00	0.00	0.00	0.00	0.00	455.00	295.00	0.00	0.00	0.00	0.00	0.00	0.00	0.00	0.00	0.00	0.00
3	455.00	265.00	130.00	0.00	0.00	0.00	0.00	0.00	0.00	0.00	0.00	455.00	265.00	130.00	0.00	0.00	0.00	0.00	0.00	0.00	0.00	0.00	0.00
4	455.00	235.00	130.00	130.00	0.00	0.00	0.00	0.00	0.00	0.00	0.00	455.00	235.00	130.00	130.00	0.00	0.00	0.00	0.00	0.00	0.00	0.00	0.00
5	455.00	260.00	130.00	130.00	25.00	0.00	0.00	0.00	0.00	0.00	0.00	455.00	285.00	130.00	130.00	0.00	0.00	0.00	0.00	0.00	0.00	0.00	0.00
6	455.00	360.00	130.00	130.00	25.00	0.00	0.00	0.00	0.00	0.00	0.00	455.00	360.00	130.00	130.00	25.00	0.00	0.00	0.00	0.00	0.00	0.00	0.00
7	455.00	410.00	130.00	130.00	25.00	0.00	0.00	0.00	0.00	0.00	0.00	455.00	410.00	130.00	130.00	25.00	0.00	0.00	0.00	0.00	0.00	0.00	0.00
8	455.00	455.00	130.00	130.00	30.00	0.00	0.00	0.00	0.00	0.00	0.00	455.00	455.00	130.00	130.00	30.00	0.00	0.00	0.00	0.00	0.00	0.00	0.00
9	455.00	455.00	130.00	130.00	95.00	0.00	25.00	0.00	0.00	10.00	0.00	455.00	455.00	130.00	130.00	85.00	20.00	25.00	0.00	0.00	0.00	0.00	0.00
10	455.00	455.00	130.00	130.00	162.00	24.37	25.00	10.00	0.00	0.00	8.63	455.00	455.00	130.00	130.00	123.93	20.00	25.00	0.00	10.00	0.00	51.07	81.00
11	455.00	455.00	130.00	130.00	141.84	20.00	25.00	10.00	10.00	0.00	73.16	455.00	455.00	130.00	130.00	162.00	67.36	25.00	10.00	10.00	0.00	5.64	90.00
12	455.00	455.00	130.00	130.00	162.00	72.71	25.00	10.00	10.00	10.00	40.29	455.00	455.00	130.00	130.00	162.00	70.82	25.00	10.00	10.00	10.00	42.18	90.00
13	455.00	455.00	130.00	130.00	162.00	26.84	25.00	10.00	0.00	0.00	6.16	455.00	455.00	130.00	130.00	115.65	20.00	25.00	0.00	10.00	0.00	59.35	76.50
14	455.00	455.00	130.00	130.00	85.00	20.00	25.00	0.00	0.00	0.00	0.00	455.00	455.00	130.00	130.00	85.00	20.00	25.00	0.00	0.00	0.00	0.00	0.00
15	455.00	455.00	130.00	130.00	30.00	0.00	0.00	0.00	0.00	0.00	0.00	455.00	455.00	130.00	130.00	30.00	0.00	0.00	0.00	0.00	0.00	0.00	0.00
16	455.00	310.00	130.00	130.00	25.00	0.00	0.00	0.00	0.00	0.00	0.00	455.00	310.00	130.00	130.00	25.00	0.00	0.00	0.00	0.00	0.00	0.00	0.00
17	455.00	260.00	130.00	130.00	25.00	0.00	0.00	0.00	0.00	0.00	0.00	455.00	260.00	130.00	130.00	25.00	0.00	0.00	0.00	0.00	0.00	0.00	0.00
18	455.00	360.00	130.00	130.00	25.00	0.00	0.00	0.00	0.00	0.00	0.00	455.00	360.00	130.00	130.00	25.00	0.00	0.00	0.00	0.00	0.00	0.00	0.00
19	455.00	455.00	130.00	130.00	30.00	0.00	0.00	0.00	0.00	0.00	0.00	455.00	455.00	130.00	130.00	30.00	0.00	0.00	0.00	0.00	0.00	0.00	0.00
20	455.00	455.00	130.00	130.00	88.99	20.00	25.00	10.00	0.00	0.00	86.01	455.00	455.00	130.00	130.00	162.00	20.18	25.00	0.00	10.00	0.00	12.82	90.00
21	455.00	455.00	130.00	130.00	75.00	20.00	25.00	10.00	0.00	0.00	0.00	455.00	455.00	130.00	130.00	75.00	20.00	25.00	0.00	10.00	0.00	0.00	0.00
22	455.00	455.00	0.00	0.00	145.00	20.00	25.00	0.00	0.00	0.00	0.00	455.00	455.00	0.00	0.00	145.00	20.00	25.00	0.00	0.00	0.00	0.00	0.00
23	455.00	420.00	0.00	0.00	25.00	0.00	0.00	0.00	0.00	0.00	0.00	455.00	420.00	0.00	0.00	25.00	0.00	0.00	0.00	0.00	0.00	0.00	0.00
24	455.00	345.00	0.00	0.00	0.00	0.00	0.00	0.00	0.00	0.00	0.00	455.00	345.00	0.00	0.00	0.00	0.00	0.00	0.00	0.00	0.00	0.00	0.00
Fuel Cost	557526.8976											557722.5808											
Start-Up Cost	3170.00											3110.00											
L_{cost}^D **($)**	1928.2282											1539.4357											
Total Cost	562625.1258											562372.0165											
Objective Function Cost	573926.9713											573755.5840											

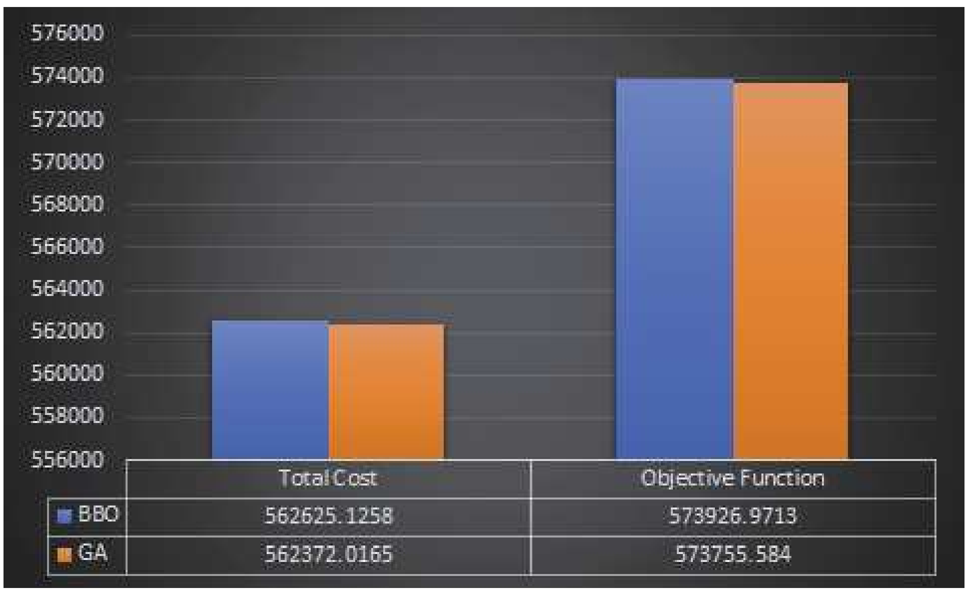

Figure 8.7: Optimal results of ten thermal generation units without wind energy and the load reduction measures are active at peak loads for twenty-four periods of time and the spinning reserve on the thermal units is assumed to be 10% of the demand at each period

Table 8.13: Optimal results of ten thermal generation units, a wind energy and the load reduction measures are active at peak loads for twenty-four periods of time and the spinning reserve on the thermal units is assumed to be 10% of the demand at each period

Algorithm	**BBO**												**GA**												Forecast	
Time	**U1**	**U2**	**U3**	**U4**	**U5**	**U6**	**U7**	**U8**	**U9**	**U10**	L_m^{sc}	L_m^{sc}	**U1**	**U2**	**U3**	**U4**	**U5**	**U6**	**U7**	**U8**	**U9**	**U10**	L_m^{sc}	L_m^{sc}	w_m^F	L_m^F
1	455.00	245.00	0.00	0.00	0.00	0.00	0.00	0.00	0.00	0.00	0.00	0.00	455.00	245.00	0.00	0.00	0.00	0.00	0.00	0.00	0.00	0.00	0.00	0.00	0.00	0.00
2	455.00	295.00	0.00	0.00	0.00	0.00	0.00	0.00	0.00	0.00	0.00	0.00	455.00	295.00	0.00	0.00	0.00	0.00	0.00	0.00	0.00	0.00	0.00	0.00	0.00	0.00
3	455.00	265.00	130.00	0.00	0.00	0.00	0.00	0.00	0.00	0.00	0.00	0.00	455.00	265.00	130.00	0.00	0.00	0.00	0.00	0.00	0.00	0.00	0.00	0.00	0.00	0.00
4	455.00	348.06	130.00	0.00	0.00	0.00	0.00	0.00	0.00	0.00	16.94	0.00	455.00	345.32	130.00	0.00	0.00	0.00	0.00	0.00	0.00	0.00	19.68	0.00	30.00	0.00
5	455.00	276.71	130.00	130.00	0.00	0.00	0.00	0.00	0.00	0.00	8.29	0.00	455.00	260.09	130.00	130.00	0.00	0.00	0.00	0.00	0.00	0.00	24.91	0.00	30.00	0.00
6	455.00	356.61	130.00	130.00	25.00	0.00	0.00	0.00	0.00	0.00	3.39	0.00	455.00	332.90	130.00	130.00	25.00	0.00	0.00	0.00	0.00	0.00	27.10	0.00	30.00	0.00
7	455.00	363.40	130.00	130.00	25.00	0.00	0.00	0.00	0.00	0.00	46.60	0.00	455.00	353.91	130.00	130.00	25.00	0.00	0.00	0.00	0.00	0.00	56.09	0.00	60.00	0.00
8	455.00	455.00	130.00	130.00	28.23	0.00	0.00	0.00	0.00	0.00	1.77	0.00	455.00	425.81	130.00	130.00	25.00	0.00	0.00	0.00	0.00	0.00	34.19	0.00	60.00	0.00
9	455.00	455.00	130.00	130.00	86.23	20.00	0.00	0.00	10.00	0.00	13.77	0.00	455.00	455.00	130.00	130.00	54.08	20.00	0.00	0.00	0.00	0.00	55.92	0.00	60.00	0.00
10	455.00	455.00	130.00	130.00	127.92	20.00	25.00	10.00	0.00	0.00	31.70	15.38	455.00	455.00	130.00	130.00	143.87	20.00	25.00	0.00	0.00	10.00	15.91	15.23	100.00	81.00
11	455.00	455.00	130.00	130.00	145.70	20.00	25.00	10.00	0.00	0.00	74.29	5.00	455.00	455.00	130.00	130.00	101.73	20.00	25.00	0.00	0.00	10.00	81.26	42.01	100.00	90.00
12	455.00	455.00	130.00	130.00	162.00	62.10	25.00	10.00	10.00	0.00	58.43	2.47	455.00	455.00	130.00	130.00	121.15	20.00	25.00	0.00	0.00	10.00	141.53	12.31	165.00	90.00
13	455.00	455.00	130.00	130.00	106.63	20.00	25.00	10.00	0.00	0.00	36.60	31.77	455.00	455.00	130.00	130.00	54.70	20.00	25.00	0.00	0.00	0.00	75.18	55.12	165.00	76.50
14	455.00	455.00	0.00	130.00	150.09	20.00	25.00	10.00	0.00	0.00	54.91	0.00	455.00	455.00	130.00	130.00	69.53	20.00	0.00	0.00	0.00	0.00	40.47	0.00	70.00	0.00
15	455.00	455.00	0.00	130.00	100.83	20.00	0.00	0.00	0.00	0.00	39.17	0.00	455.00	405.51	130.00	130.00	25.00	0.00	0.00	0.00	0.00	0.00	54.49	0.00	70.00	0.00
16	455.00	390.01	0.00	130.00	25.00	0.00	0.00	0.00	0.00	0.00	49.99	0.00	455.00	303.42	130.00	130.00	25.00	0.00	0.00	0.00	0.00	0.00	6.58	0.00	70.00	0.00
17	455.00	336.36	0.00	130.00	25.00	0.00	0.00	0.00	0.00	0.00	53.64	0.00	455.00	192.38	130.00	130.00	25.00	0.00	0.00	0.00	0.00	0.00	67.62	0.00	70.00	0.00
18	455.00	420.87	0.00	130.00	25.00	0.00	0.00	0.00	0.00	0.00	69.13	0.00	455.00	317.41	130.00	130.00	25.00	0.00	0.00	0.00	0.00	0.00	42.59	0.00	70.00	0.00
19	455.00	426.71	130.00	130.00	25.00	0.00	0.00	0.00	0.00	0.00	33.29	0.00	455.00	443.49	130.00	130.00	25.00	0.00	0.00	0.00	0.00	0.00	16.51	0.00	70.00	0.00
20	455.00	455.00	130.00	130.00	103.86	20.00	0.00	10.00	0.00	10.00	30.51	55.63	455.00	455.00	130.00	130.00	119.87	0.00	25.00	10.00	0.00	10.00	38.82	26.31	50.00	90.00
21	455.00	455.00	130.00	130.00	62.84	20.00	0.00	10.00	0.00	10.00	27.16	0.00	455.00	455.00	130.00	130.00	41.26	0.00	25.00	10.00	0.00	10.00	43.74	0.00	50.00	0.00
22	455.00	455.00	130.00	0.00	39.95	20.00	0.00	0.00	0.00	0.00	0.05	0.00	455.00	340.16	130.00	130.00	0.00	0.00	25.00	0.00	0.00	0.00	19.84	0.00	50.00	0.00
23	455.00	315.00	130.00	0.00	0.00	0.00	0.00	0.00	0.00	0.00	0.00	0.00	455.00	315.00	130.00	0.00	0.00	0.00	0.00	0.00	0.00	0.00	0.00	0.00	0.00	0.00
24	455.00	345.00	0.00	0.00	0.00	0.00	0.00	0.00	0.00	0.00	0.00	0.00	455.00	345.00	0.00	0.00	0.00	0.00	0.00	0.00	0.00	0.00	0.00	0.00	0.00	0.00
Fuel Cost	542905.6077												537127.0122													
Start-Up Cost	3460.00												2880.00													
C_{dm} **($)**	5197.0036												6899.5196													
L_{cost}^D **($)**	992.2421												1358.7409													
Total Cost	552554.8534												548265.2727													
Objective Function Cost	573633.5985												569628.4015													

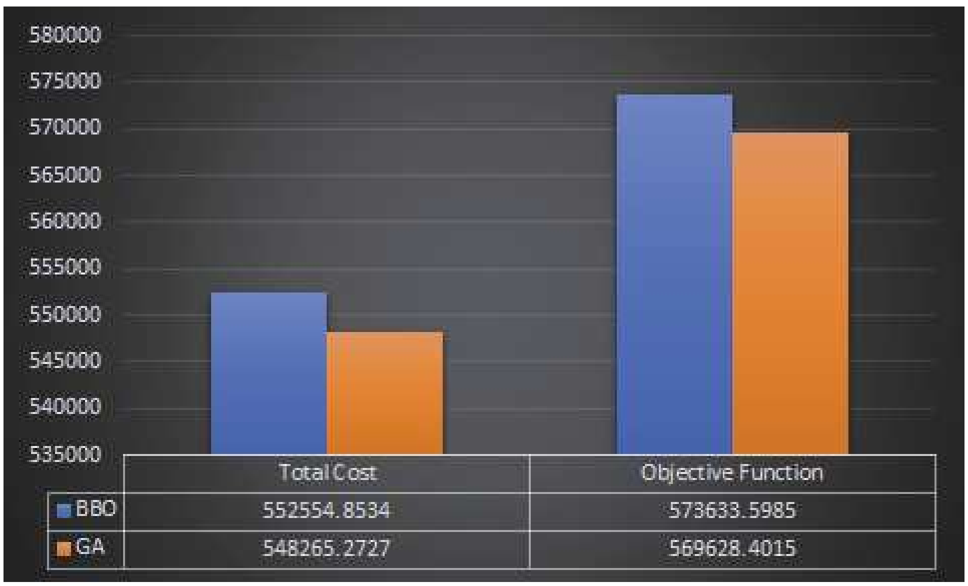

Figure 8.8: Optimal results of ten thermal generation units, a wind energy and the load reduction measures are active at peak loads for twenty-four periods of time and the spinning reserve on the thermal units is assumed to be 10% of the demand at each period

8.7 Conclusion

In this chapter, the unit commitment model for Smart Grid is modeled assuming the incorporation of significant amount of wind power and the load reduction measures are active at peak loads. Then, a procedure using any metaheuristic optimization was proposed to solve the problem. The Biogeography Based Optimization algorithm (BBO) and Genetic Algorithm (GA) were proposed and successfully utilized to solve the problem. The algorithms were applied to two systems to validate their accuracy and effectiveness, one consists of four thermal generation units, a wind turbine and a load reduction measures are active at peak loads with eight periods of time and the spinning reserve for the thermal units is assumed to be 10% of the demand at each period and the second consists of ten thermal generation units, a wind turbine and load reduction measures are active at peak loads with twenty-four periods of time and the spinning reserve on the thermal units is assumed to be 10% of the demand at each period. The simulation results of the proposed algorithms have been compared with other algorithms in the literature when the wind energy is not included and the load reduction measures are not active. Based on the results obtained in both test systems, there is not much difference to declare a clear superior method, instead, the methods BBO and GA offer similar sets of feasible near-optimal solutions. They also generate a better solutions compared with other algorithms in the literature when the wind energy is not included and the load reduction measures are not active for the first system. Also, the total cost decrease with the merging of wind energy and applying the load reduction measures.

Chapter 9

Hydrothermal Scheduling Problem for Smart Grid

9.1 Introduction

Hydrothermal scheduling (HTS) is finding the hour-by-hour optimal power allocation of the load among the available thermal units and hydro units for a time period between 1 day to 1 week, and the objective is to minimize the total fuel cost [129]. The wind power and the load reduction usually modeled as negative load due to the small contribution compared with the capacity of the system.

In smart grid the HTS problem will be finding the optimal power allocation of the load among the available thermal unit, renewable resources, assuming the load reduction measures are active at peak loads and hydro units for a period and the objective is to minimize the total fuel cost and the greenhouse gases emissions.

The integration of significant amount renewable energy and the integration of load reduction as demand side management measure increase the complexity of the problem and introduce many challenges in finding the optimal solution which accounts for the intermittent behavior of renewable resources and errors in the forecasting of the available renewable power and the forecasting of the amount of load reduction at peak loads. In this chapter, fixed head hydrothermal scheduling will be modeled and solved for smart grid network by assuming significant integration of wind energy to the network and the load reduction programs are active.

9.2 Smart Grid Hydrothermal Scheduling Mathematical Formulation

Suppose that there are N thermal generation units, and N_h hydro generation units that will feed the demand load over T periods and there are N_d areas for load reduction at peak load times. The hydrothermal scheduling objective function for smart grid network can be written as:

$$min\ \ C_{th} + C_{wind} + C_{LR} \tag{9.1}$$

where C_{th} is the total thermal power generation cost, C_{wind} is the total wind power generation cost and C_{LR} is the total load reduction cost.

9.2.1 Thermal Power Generation Cost

The total thermal power generation cost is shown in (9.2)[129].

$$C_{th} = \sum_{t=1}^{T}\sum_{j=1}^{N} F(P_j(t)) \tag{9.2}$$

where C_{th} is the total generation cost for N units in T periods (hours) and $F(P_j(t))$ is the fuel cost function for unit j at period t.

$$F(P_j) = a_j P_j^2 + b_j P_j + c_j \tag{9.3}$$

where a_j, b_j, c_j are the fuel cost coefficients of generator j, P_j is the the output power of generator j and $F(P_j)$ is the fuel cost of unit j.

9.2.2 Wind Power Generation Cost

There are two cost model shown in Chapter(6): the negative load model and the probabilistic model. Based on these models, the total wind cost for N_w units and in T periods can be calculated as follows:

$$C_{wind} = \sum_{t=1}^{T} W_{Cost}^{t} \tag{9.4}$$

Where W_{Cost}^{t} is the total wind power generation cost.

9.2.3 Load Reduction Cost

There are two main cost models proposed in Chapter(7): the negative load model and the probabilistic model. The probabilistic cost model was formulated to normal distribution, weibull distribution, and exponential distribution. Based on the selected model, the total wind cost for T periods can be calculated as follows:

$$C_{LR} = \sum_{t=1}^{T} LR_{Cost}^{t} \tag{9.5}$$

Where LR_{Cost}^{t} is the total cost of load reduction.

9.3 Equality Constraints

9.3.1 Real Power Balance Constraint

The total power generated from thermal and wind units should equal the load demand at each period of time as shown in (9.6), where the P_D represents the total load demand and P_L is the power losses.

$$\sum_{m=1}^{N_h} P_{H\,m} + \sum_{i=1}^{Nx} P_i + \sum_{j=1}^{Nw} w_j = P_D + P_L - \sum_{k=1}^{Nd} L_k \tag{9.6}$$

$$P_L = \sum_{k=1}^{N_t} \sum_{l=1}^{N_t} (P_k\, B_{kl}\, P_l + B_{0l}\, P_l + B_{00}) \tag{9.7}$$

Where $P_{H\,m}$ is the hydro power generation, w_j is the available wind power for the j^{th} wind turbine and L_k is the available load reduction from area k. B_{kl}, B_{0l} and B_{00} are the power loss coefficients and $N_t = N_x + N_h + N_w$.

9.3.2 Total Water Discharge Constraint

For fixed head reservoir the discharge rate is shown in (9.8) and the total volume for each hydro plant is fixed and the sum of the discharge rate for the total period should equal the total volume as shown in (9.9).

$$q_{m\,t} = \alpha_m\ P_{H\,m}^2(t) + \beta_m\ P_{H\,m}(t) + \gamma_m \tag{9.8}$$

$$\sum_{t=1}^{T} q_{m\,t}\ n_t = V_m \tag{9.9}$$

where $q_{m\,t}$ is the discharge rate for hydro generation unit m at time t and V_m is the total volume for hydro generation unit m.

9.4 Inequality Constraints

9.4.1 Thermal Unit Power Limit Constraint

Thermal generation units are restricted by their limits in term of generation active power as follows:

$$P_j^{min} \leq P_j \leq P_j^{max} \quad j = 1, 2 \cdots, N \tag{9.10}$$

where P_j^{min}, P_j^{max}, are the minimum active power output, maximum active power output of the j^{th} generating unit respectively.

9.4.2 Hydro Unit Power Limit Constraint

Hydro generation units are restricted by their limits in terms of generation active power as follows:

$$P_{Hm}^{min} \leq P_{Hm} \leq P_{Hm}^{max} \quad m = 1, 2 \cdots, N_h \tag{9.11}$$

where P_{Hm}^{min}, P_{Hm}^{max}, are the minimum active power output, maximum active power output of the m^{th} generating unit respectively.

9.4.3 Wind Turbine Power Limit Constraint

$$0 \leq w_j \leq w_j^r \quad j = 1, 2 \cdots, Nw \tag{9.12}$$

Here w_j^r, is the rated active power output of the j^{th} wind turbine unit.

9.4.4 Load Power Limit Constraint

$$L_k^{min} \leq L_k \leq L_k^{max} \quad k = 1, 2 \cdots, Nd \tag{9.13}$$

Here L_k^{min}, L_k^{max}, are the minimum active power reduction, maximum active power reduction of the k^{th} unit respectively.

9.5 Fixed Head Hydrothermal Scheduling Solution Procedure Incorporating Wind Energy and Load Reduction

‘The general procedure to solve the Fixed Head Hydrothermal Scheduling problem incorporating wind energy and load reduction measures are active at peak loads using any metaheuristic algorithm is shown in Procedure (5).

Procedure 5: Fixed Head Hydrothermal Scheduling

1. Initialize the algorithm parameters (population size, no of generations, no of iteration, mutation rate, cross over rate).
2. Generate a set of feasible solutions where each consist of a set of water discharge rate schedules, and on each hour in any schedule there are the wind power and the load reduction power, both generated randomly based on the forecast.
3. The economic dispatch is calculated using lambda iteration method for all the solutions to determine the thermal power generation values, the power loss and the fuel cost.
4. The direct cost, overestimation cost and the under estimation cost for wind power and load reduction power are calculated for all the solutions.
5. Calculate the objective function.
6. Save the best solution.
7. Apply the Algorithm operations on the set of the solutions.
8. Check the feasibility of the generated solutions and repeat steps (3-6).
9. Repeat steps (7-8) until the termination criterion is achieved.

9.6 Fixed Head Hydrothermal Scheduling Incorporating Wind Energy and Load Reduction

This section proposes a numerical example of the the fixed head hydrothermal scheduling problem incorporating wind energy and the load reduction measures are active at peak loads using the Biogeography based optimization algorithm (BBO), Genetic algorithm and the Khums Optimization Algorithm (KOA). Two benchmark systems were used and a comparison will be done between the results with other algorithms in the literature if possible. Probabilistic model will be used to represent the wind turbine cost model and the load reduction cost model.

9.6.1 Test 1

The study system consists of one thermal generation unit, one hydro generation unit and a wind turbine and the load reduction measures are active at peak loads with two periods of time. The data for the thermal generation units, the hydro units and load demand are shown in Appendix (C.3.1). The wind turbine cost model data and the load reduction cost model data are shown in Appendix (C.3.3).

Table (9.1) and Figure (9.1) show the obtained schedule using BBO algorithm, GA algorithm, KOA algorithm, LGIM[124] algorithm and IBFA[35] algorithm. The table shows the thermal power P_{TH}, the hydro power P_H, the power loss P_{Loss} and the water flow q for two periods. The BBO, GA and KOA result is higher than the two algorithm with 0.0164%, 0.0312% and 0.0052% respectively.

If the wind energy included the problem will be complex because of the inherent intermittent behavior of wind speed. Probabilistic cost model is used to minimize the effect of inaccurate wind speed forecasting. The rule here is to choose the solution with lower objective function which has lower overestimate and underestimate forecasting error. Table (9.2) shows the results when wind energy is included and the load reduction measures are not active. KOA algorithm introduce the best solution because it has the lowest objective function cost and the lowest total cost compared with BBO and GA as shown in Figure (9.2).

Table (9.3) shows the results in the case of load reduction measures are active and the wind energy is not included. The results again shows that the KOA algorithm introduce the best solution because it has the lowest objective function cost and the lowest total cost compared with BBO and GA as shown in Figure (9.3).

Table (9.4) and Figure (9.4) show the results in the case of wind energy is included and the load reduction measures are active at peak loads. The results shows that the KOA algorithm introduce the lowest objective function and BBO solution has the lowest total cost. The rule is to choose the lowest objective function even if the total cost is higher. Hence, the KOA solution is the recommended solution for this system at this situation.

Table 9.1: Comparison of BBO, GA, KOA, LGIM and IBFA algorithms results of test system 1 without wind energy and without load reduction

Load (MW)		BBO	GA	KOA	LGIM[124]	IBFA[35]
1200 (12 am to 12 pm)	P_{TH} (MW)	553.54	549.20	566.25	567.40	565.89
	P_H (MW)	683.88	688.75	669.62	668.30	670.03
	q (acre-ft/h)	3728.86	3753.09	3658.00	3651.50	3660.00
1500 (12 pm to 12 am)	P_{TH} (MW)	699.17	703.48	686.85	685.70	687.17
	P_H (MW)	860.00	855.00	874.30	875.60	873.93
	q (acre-ft/h)	4604.20	4579.35	4675.27	4681.70	4673.40
Total Cost ($)		169657.89	169683.00	169639.14	169630.00	169630.00

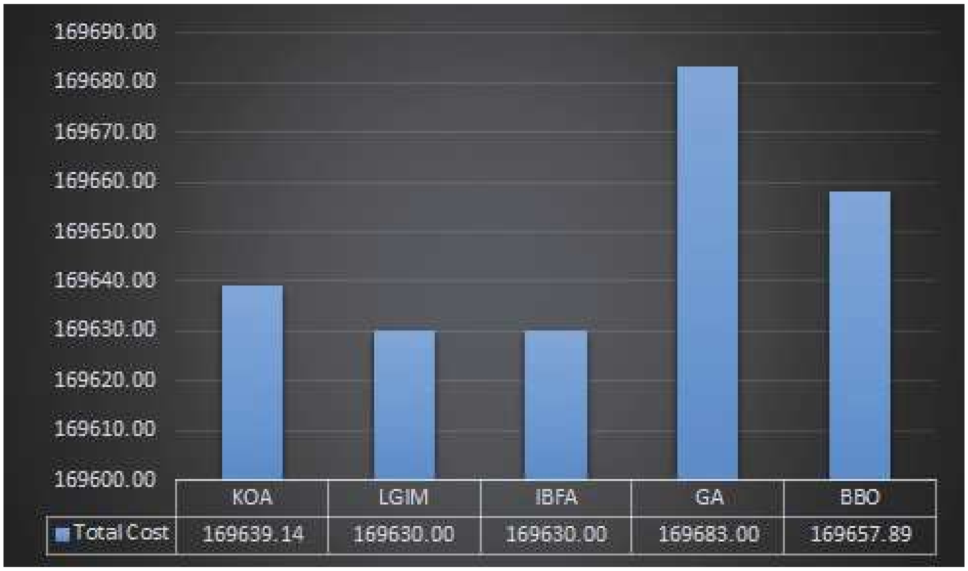

Figure 9.1: Comparison of BBO, GA, KOA, LGIM and IBFA algorithms results of test system 1 without wind energy and without load reduction

Table 9.2: BBO, GA and KOA algorithms results of test system 1 with wind energy and load reduction is not active

Load (MW)		BBO	GA	KOA
1200 (12 am to 12 pm)	P_{TH} (MW)	581.39	536.56	514.48
	P_H (MW)	627.00	677.50	700.62
	P_w (MW)	23.06	22.66	24.17
	P_{loss} (MW)	31.45	36.72	39.27
	q (acre-ft/h)	3446.19	3697.18	3812.10
1500 (12 pm to 12 am)	P_{TH} (MW)	631.66	672.41	685.84
	P_H (MW)	915.00	865.00	843.27
	P_w (MW)	20.32	22.44	27.78
	P_{loss} (MW)	66.98	59.86	56.89
	q (acre-ft/h)	4877.55	4629.05	4521.00
Total Cost ($)		168158.37	167940.76	167532.98
Objective Function Cost ($)		171384.20	171338.82	171255.09

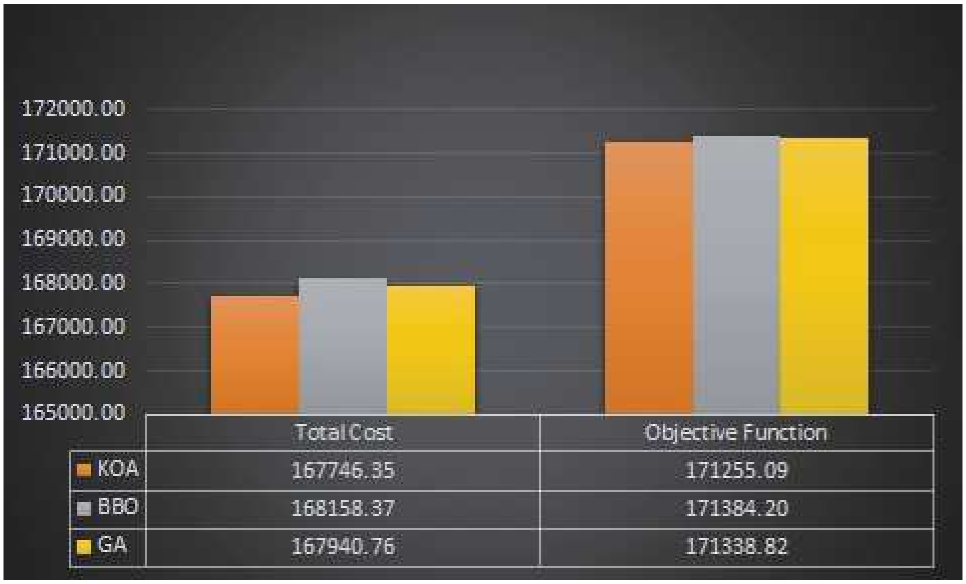

Figure 9.2: BBO, GA and KOA algorithms results of test system 1 with wind energy and load reduction is not active

Table 9.3: BBO, GA and KOA algorithms results of test system 1 without wind energy and with load reduction active at peak loads

Load (MW)		BBO	GA	KOA
1200 (12 am to 12 pm)	P_{TH} (MW)	555.66	550.09	554.31
	P_H (MW)	681.50	687.75	683.01
	P_{LR} (MW)	0.00	0.00	0.00
	P_{loss} (MW)	37.16	37.84	37.32
	q (acre-ft/h)	3717.06	3748.12	3724.54
1500 (12 pm to 12 am)	P_{TH} (MW)	680.27	685.33	681.09
	P_H (MW)	862.00	856.00	860.86
	P_{LR} (MW)	17.17	17.29	17.34
	P_{loss} (MW)	59.44	58.62	59.29
	q (acre-ft/h)	4614.14	4584.32	4608.48
Total Cost ($)		169136.03	169109.52	169087.81
Objective Function Cost ($)		170663.62	170653.22	170619.90

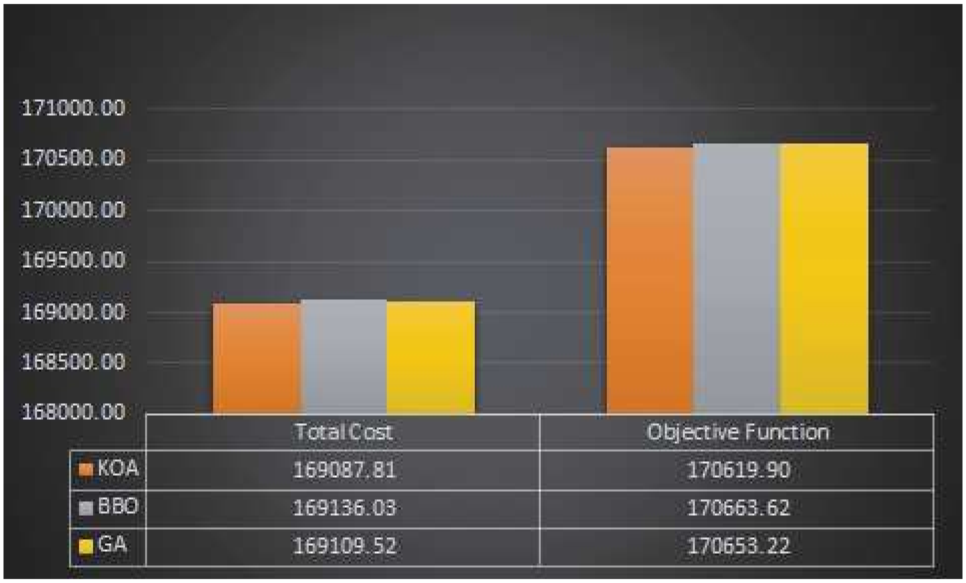

Figure 9.3: BBO, GA and KOA algorithms results of test system 1 without wind energy and with load reduction active at peak loads

Table 9.4: BBO, GA and KOA algorithms results of test system 1 with wind energy and with load reduction active at peak loads

Load (MW)		BBO	GA	KOA
1200 (12 am to 12 pm)	P_{TH} (MW)	536.93	603.13	561.44
	P_H (MW)	675.00	595.00	652.74
	P_w (MW)	24.52	30.19	19.90
	P_{LR} (MW)	0.00	0.00	0.00
	P_{loss} (MW)	36.45	28.32	34.09
	q (acre-ft/h)	3684.75	3287.15	3574.13
1500 (12 pm to 12 am)	P_{TH} (MW)	656.42	582.20	634.53
	P_H (MW)	868.00	947.00	891.17
	P_w (MW)	19.24	25.41	20.64
	P_{LR} (MW)	16.62	17.13	17.19
	P_{loss} (MW)	60.27	71.74	63.54
	q (acre-ft/h)	4643.96	5036.59	4759.13
Total Cost ($)		167420.68	167365.01	167434.11
Objective Function Cost ($)		172356.45	172476.27	172169.52

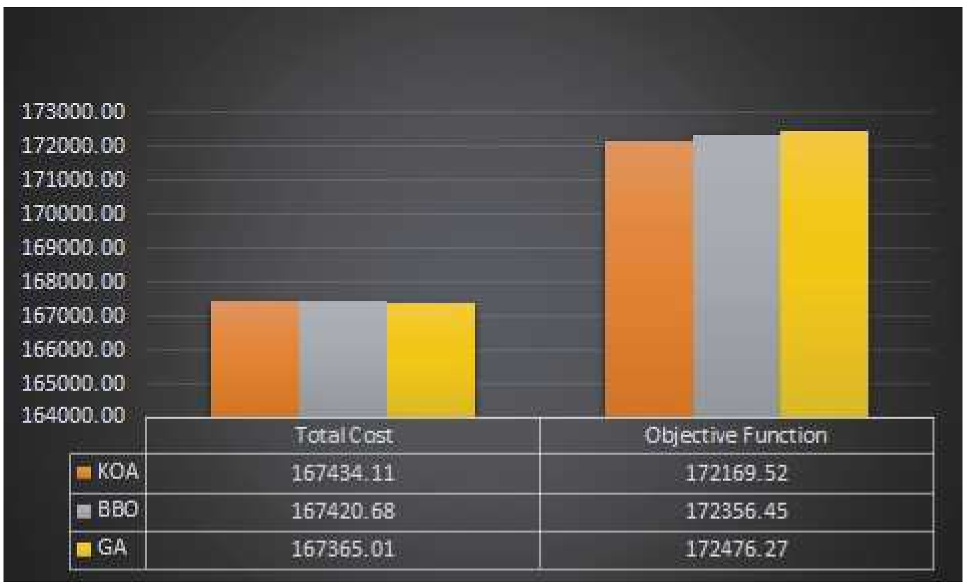

Figure 9.4: BBO, GA and KOA algorithms results of test system 1 with wind energy and with load reduction active at peak loads

9.6.2 Test 2

This study system consists of three thermal generation units, one hydro generation unit and a wind turbine. The data and load demand are shown in Appendix (C.3.2). The wind turbine cost model data and the load reduction cost model data are shown in Appendix (C.3.3).

The schedule obtained using BBO, GA and KOA without wind energy and without load reduction are shown in Table(9.6), Table(9.7) and Table(9.8) respectively and the results are illustrated in Figure (9.5). At each hour the thermal power P_i, the hydro power P_H, the power loss P_{Loss} and the water flow q are shown in the table. If the wind or the load reduction are included the actual value P_w for the wind and the P_{LR} for load reduction and forecast schedule P_w^F for the wind and P_{LR}^F for load reduction will be provided in the table. All the values are within limits and the solution is feasible. The total costs obtained is higher than the cost obtained in [35, 67] as shown in Table(9.5), but in both references the obtained result has unfeasible values. The infeasible point in [35] is in P_2 at H_{24} which is lower than the machine limit and there is also a small violation to the power balance constraint. In [67] the violation is in P_2 and P_H power limits.

Table (9.9), Table (9.10) and Table (9.11) show the obtained feasible schedule using BBO algorithm, GA algorithm and KOA algorithm respectively with wind power included and the load reduction is not active. The rule is to choose the solution with lower objective function as stated before, hence the best schedule achieved will be using GA algorithm as shown in Figure (9.6).

The best solution obtained in the case of the load reduction measures are active and the wind energy is not included will be the KOA algorithm schedule because it has the lowest objective function as shown in Figure (9.7) and shown in Table (9.12), Table (9.13) and Table (9.14) respectively.

Finally, the best solution obtained when the wind energy included and the load reduction measures are active is the BBO algorithm schedule as shown in Figure (9.8) and shown in Table (9.15), Table (9.16) and Table (9.17) respectively.

Table 9.5: Comparison of BBO, GA, KOA, IBFA and NRM algorithms results of test system 2 without wind energy and without load reduction

Algorithm	Cost (Rs)
BBO	24304.13
GA	24302.15
KOA	24303.72
IBFA[35]	24267.41
NRM[67]	24276.79

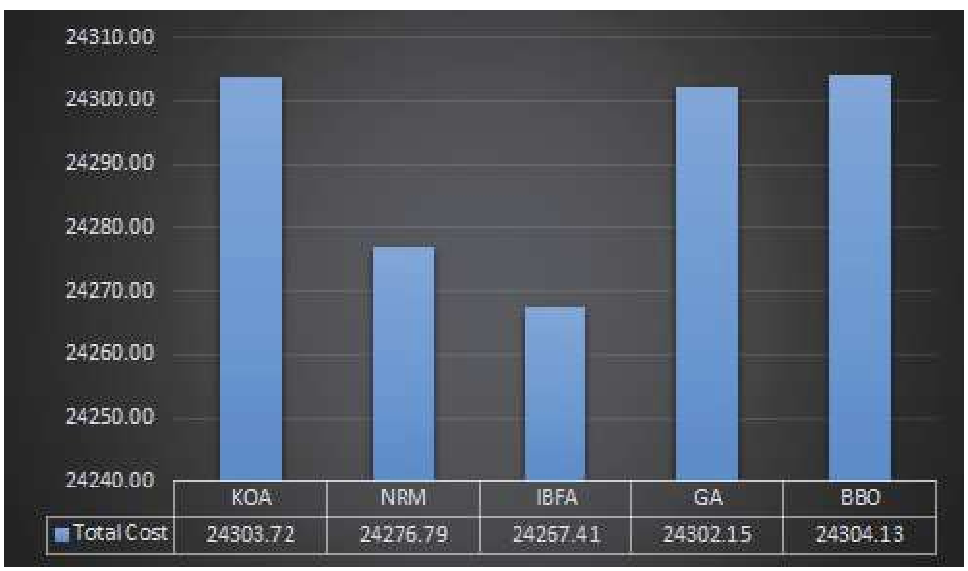

Figure 9.5: Comparison of BBO, GA, KOA, IBFA and NRM algorithms results of test system 2 without wind energy and without load reduction

Table 9.6: BBO algorithm result of test system 2 without wind energy and without load reduction

Time	P_1	P_2	P_3	P_H	P_{Loss}	q (m^3/h)
H1	68.77	40.00	63.42	10.00	7.20	346.00
H2	76.33	41.60	70.91	10.00	8.85	346.00
H3	89.28	49.37	83.59	10.00	12.26	346.00
H4	115.70	66.01	109.21	10.00	20.93	346.00
H5	133.69	77.99	126.47	10.00	28.16	346.00
H6	151.54	90.49	143.45	10.88	36.37	364.77
H7	165.30	100.56	156.39	11.18	43.43	371.04
H8	169.29	103.91	160.72	21.40	45.34	595.58
H9	168.06	104.00	161.28	50.81	44.17	1311.22
H10	174.94	109.98	168.91	69.00	47.83	1805.61
H11	184.75	118.85	179.89	95.04	53.54	2582.70
H12	194.26	126.91	189.19	99.00	59.37	2708.06
H13	200.00	133.29	196.36	99.00	63.66	2708.06
H14	190.66	123.81	185.64	97.00	57.12	2644.54
H15	173.34	109.68	168.96	95.00	46.98	2581.50
H16	170.03	105.69	163.46	56.00	45.19	1448.16
H17	167.68	103.27	160.18	38.00	44.13	986.64
H18	157.68	95.70	150.55	35.00	38.93	913.50
H19	155.33	93.41	147.35	17.00	38.11	497.34
H20	142.30	83.96	134.71	11.00	31.98	367.26
H21	124.66	71.90	117.83	10.00	24.40	346.00
H22	102.41	57.50	96.36	10.00	16.28	346.00
H23	80.63	44.15	75.13	10.00	9.92	346.00
H24	71.56	40.00	66.20	10.00	7.77	346.00
Total Cost (Rs)		24304.13		Total Volume (m^3)		24999.97

Table 9.7: GA algorithm result of test system 2 without wind energy and without load reduction

Time	P_1	P_2	P_3	P_H	P_{Loss}	q (m^3/h)
H1	68.77	40.00	63.42	10.00	7.20	346.00
H2	76.33	41.60	70.91	10.00	8.85	346.00
H3	89.28	49.37	83.59	10.00	12.26	346.00
H4	115.70	66.01	109.21	10.00	20.93	346.00
H5	133.54	77.89	126.33	10.32	28.09	352.75
H6	151.30	90.33	143.25	11.36	36.24	374.88
H7	164.90	100.29	156.06	11.94	43.20	387.35
H8	160.12	97.64	153.10	39.25	40.12	1017.49
H9	173.09	107.51	165.45	41.00	47.06	1060.86
H10	183.16	115.88	175.66	53.00	52.70	1368.41
H11	184.77	118.86	179.91	95.00	53.55	2581.50
H12	195.79	128.08	190.43	96.00	60.31	2612.96
H13	200.00	134.47	197.72	97.00	64.20	2644.54
H14	190.96	124.03	185.89	96.42	57.30	2626.12
H15	173.34	109.68	168.96	95.00	46.98	2581.50
H16	171.05	106.41	164.30	54.00	45.77	1394.96
H17	164.11	100.80	157.20	45.00	42.12	1161.50
H18	157.17	95.35	150.12	36.00	38.66	937.76
H19	152.78	91.72	145.21	22.00	36.72	609.04
H20	138.80	81.71	131.71	18.00	30.23	519.44
H21	124.66	71.90	117.83	10.00	24.40	346.00
H22	102.41	57.50	96.36	10.00	16.28	346.00
H23	80.63	44.15	75.13	10.00	9.92	346.00
H24	71.56	40.00	66.20	10.00	7.77	346.00
Total Cost (Rs)		24302.15		Total Volume (m^3)		24999.06

Table 9.8: KOA algorithm result of test system 2 without wind energy and without load reduction

Time	P_1	P_2	P_3	P_H	P_{Loss}	q (m^3/h)
H1	68.77	40.00	63.42	10.00	7.20	346.00
H2	76.33	41.60	70.91	10.00	8.85	346.00
H3	89.28	49.37	83.59	10.00	12.26	346.00
H4	115.70	66.01	109.21	10.00	20.93	346.00
H5	132.73	77.38	125.64	11.94	27.70	387.35
H6	150.61	89.88	142.67	12.71	35.87	403.97
H7	157.33	95.18	149.76	26.63	38.91	715.07
H8	163.78	100.13	156.16	32.08	42.15	843.30
H9	173.86	108.06	166.09	39.51	47.52	1023.79
H10	182.70	115.54	175.28	53.89	52.42	1392.00
H11	183.80	118.14	179.10	96.94	52.99	2642.64
H12	195.31	127.71	190.04	96.94	60.01	2642.64
H13	200.00	132.90	195.92	99.66	63.48	2729.00
H14	190.28	123.52	185.33	97.75	56.89	2668.43
H15	171.97	108.70	167.82	97.75	46.25	2668.43
H16	175.47	109.52	167.96	45.39	48.34	1171.38
H17	166.75	102.62	159.40	39.82	43.60	1031.54
H18	159.29	96.78	151.90	31.83	39.81	837.29
H19	153.42	92.15	145.75	20.74	37.07	580.69
H20	139.67	82.27	132.46	16.25	30.65	480.93
H21	124.66	71.90	117.83	10.00	24.40	346.00
H22	102.41	57.50	96.36	10.00	16.28	346.00
H23	80.63	44.15	75.13	10.00	9.92	346.00
H24	71.56	40.00	66.20	10.00	7.77	346.00
Total Cost (Rs)		24303.72		Total Volume (m^3)		24986.46

Table 9.9: BBO algorithm result of test system 2 with wind energy and the load reduction measures is not active

Time	P_1	P_2	P_3	P_H	P_w	P_{Loss}	q (m^3/h)	P_w^F
H1	68.77	40.00	63.42	10.00	0.00	7.20	346.00	0.00
H2	76.33	41.60	70.91	10.00	0.00	8.85	346.00	0.00
H3	89.28	49.37	83.59	10.00	0.00	12.26	346.00	0.00
H4	115.11	65.62	108.65	10.00	1.33	20.71	346.00	30.00
H5	131.10	76.24	124.01	10.25	5.44	27.05	351.40	30.00
H6	148.30	88.19	140.40	11.00	6.90	34.80	367.26	30.00
H7	156.38	94.02	148.07	12.00	18.29	38.76	388.64	50.00
H8	169.87	104.03	160.72	12.15	9.13	45.89	391.79	50.00
H9	170.61	105.12	162.30	27.32	20.57	45.93	731.15	50.00
H10	175.56	110.10	168.89	59.17	9.52	48.24	1533.41	20.00
H11	182.41	116.97	177.71	95.79	4.28	52.17	2606.23	20.00
H12	191.99	124.87	186.83	96.00	8.23	57.93	2612.96	40.00
H13	188.89	122.33	183.96	97.00	28.85	56.04	2644.54	40.00
H14	186.64	120.43	181.75	96.00	9.84	54.67	2612.96	20.00
H15	165.66	103.69	161.57	95.07	16.84	42.83	2583.57	20.00
H16	160.69	98.97	155.19	67.00	8.31	40.16	1749.34	20.00
H17	154.87	94.26	148.95	55.00	9.20	37.28	1421.50	20.00
H18	148.32	89.16	142.09	44.00	10.62	34.20	1136.16	20.00
H19	147.47	87.97	140.27	24.00	9.39	34.11	654.56	20.00
H20	138.78	81.59	131.51	14.00	4.41	30.31	431.76	10.00
H21	123.90	71.40	117.10	10.00	1.69	24.09	346.00	10.00
H22	100.07	56.03	94.09	10.00	5.32	15.52	346.00	10.00
H23	80.63	44.15	75.13	10.00	0.00	9.92	346.00	0.00
H24	71.56	40.00	66.20	10.00	0.00	7.77	346.00	0.00
Total Cost (Rs)		24215.53		Total Volume (m^3)			24985.23	
Objective Function Cost (Rs)				25649.05				

Table 9.10: GA algorithm result of test system 2 with wind energy and the load reduction measures is not active

Time	P_1	P_2	P_3	P_H	P_w	P_{Loss}	q (m^3/h)	P_w^F
H1	68.77	40.00	63.42	10.00	0.00	7.20	346.00	0.00
H2	76.33	41.60	70.91	10.00	0.00	8.85	346.00	0.00
H3	89.28	49.37	83.59	10.00	0.00	12.26	346.00	0.00
H4	115.21	65.69	108.74	10.00	1.11	20.75	346.00	30.00
H5	129.21	74.96	122.20	10.18	9.70	26.26	349.86	30.00
H6	147.60	87.66	139.69	10.18	9.35	34.48	349.86	30.00
H7	164.31	99.81	155.45	10.82	2.51	42.92	363.46	50.00
H8	165.44	100.86	156.85	16.83	13.37	43.36	493.68	50.00
H9	164.34	101.39	158.11	57.00	1.28	42.12	1474.88	50.00
H10	169.28	105.55	163.47	68.29	13.11	44.70	1785.63	20.00
H11	182.76	117.22	177.99	95.00	4.39	52.36	2581.50	20.00
H12	185.73	119.77	181.02	98.00	19.62	54.14	2676.24	40.00
H13	190.78	123.99	185.89	99.00	22.55	57.21	2708.06	40.00
H14	182.56	117.09	177.86	96.00	18.74	52.25	2612.96	20.00
H15	170.27	107.27	166.02	95.00	6.74	45.30	2581.50	20.00
H16	168.79	104.57	161.99	51.00	8.20	44.56	1316.06	20.00
H17	164.43	100.88	157.23	40.00	4.81	42.36	1036.00	20.00
H18	152.24	91.60	145.16	31.00	16.27	36.28	817.66	20.00
H19	147.45	87.90	140.15	22.00	11.63	34.14	609.04	20.00
H20	139.11	81.85	131.87	15.00	2.60	30.43	453.50	10.00
H21	121.77	69.99	115.06	10.00	6.43	23.25	346.00	10.00
H22	101.62	57.01	95.60	10.00	1.79	16.02	346.00	10.00
H23	80.63	44.15	75.13	10.00	0.00	9.92	346.00	0.00
H24	71.56	40.00	66.20	10.00	0.00	7.77	346.00	0.00
Total Cost (Rs)		24198.98		Total Volume (m^3)			24977.88	
Objective Function Cost (Rs)				25623.27				

Table 9.11: KOA algorithm result of test system 2 with wind energy and the load reduction measures is not active

Time	P_1	P_2	P_3	P_H	P_w	P_{Loss}	q (m^3/h)	P_w^F
H1	68.77	40.00	63.42	10.00	0.00	7.20	346.00	0.00
H2	76.33	41.60	70.91	10.00	0.00	8.85	346.00	0.00
H3	89.28	49.37	83.59	10.00	0.00	12.26	346.00	0.00
H4	113.97	64.88	107.55	10.00	3.89	20.29	346.00	30.00
H5	125.29	72.56	118.86	19.92	7.81	24.45	562.27	30.00
H6	138.69	81.76	131.83	22.59	15.21	30.09	622.34	30.00
H7	152.59	91.67	145.17	24.73	12.40	36.57	671.34	50.00
H8	164.48	100.57	156.69	29.83	0.99	42.56	789.88	50.00
H9	169.34	104.40	161.52	34.23	15.60	45.10	894.84	50.00
H10	178.19	111.64	170.50	45.07	19.50	49.90	1163.21	20.00
H11	183.48	117.88	178.80	96.88	0.75	52.80	2640.74	20.00
H12	188.82	122.27	183.88	96.88	14.14	56.00	2640.74	40.00
H13	195.00	127.54	189.90	99.13	13.25	59.83	2712.35	40.00
H14	188.97	122.39	184.02	96.88	3.81	56.09	2640.74	20.00
H15	164.91	103.18	160.95	96.88	16.53	42.45	2640.74	20.00
H16	172.71	107.32	165.25	43.65	7.87	46.81	1127.38	20.00
H17	163.05	99.84	155.90	39.78	8.06	41.63	1030.48	20.00
H18	153.32	92.56	146.50	36.82	7.51	36.72	957.67	20.00
H19	148.92	88.93	141.51	21.38	9.10	34.85	595.09	20.00
H20	135.72	79.52	128.66	15.61	9.40	28.91	466.74	10.00
H21	124.66	71.90	117.83	10.00	0.00	24.40	346.00	10.00
H22	99.41	55.62	93.45	10.00	6.81	15.31	346.00	10.00
H23	80.63	44.15	75.13	10.00	0.00	9.92	346.00	0.00
H24	71.56	40.00	66.20	10.00	0.00	7.77	346.00	0.00
Total Cost (Rs)		24249.24		Total Volume (m^3)			24924.58	
Objective Function Cost (Rs)				25657.92				

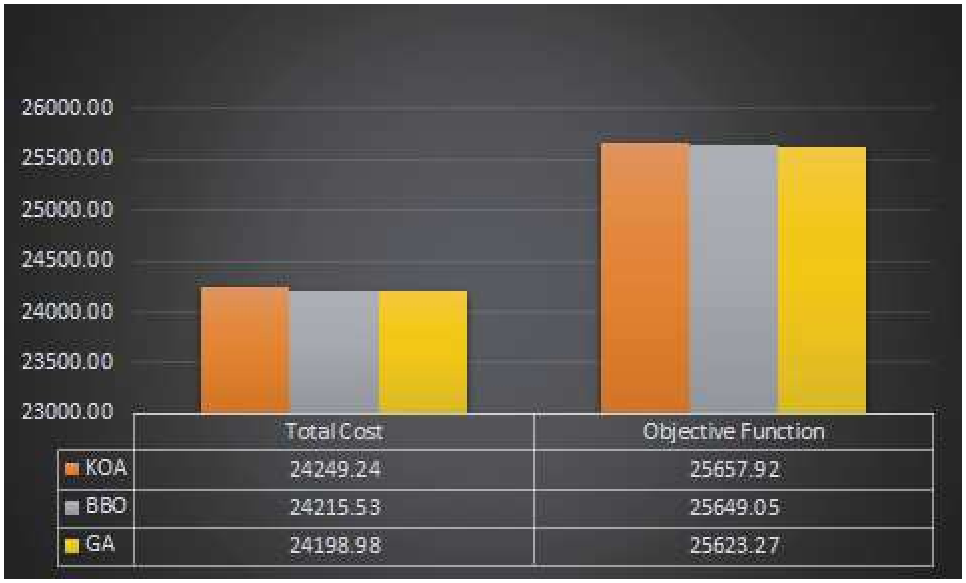

Figure 9.6: BBO, GA and KOA algorithms results of test system 2 with wind energy and without load reduction

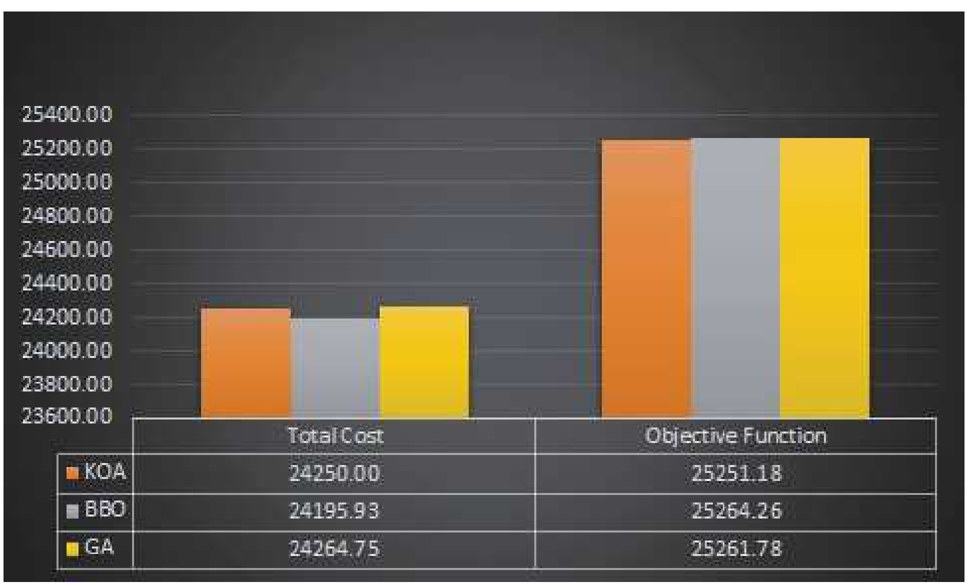

Figure 9.7: BBO, GA and KOA algorithms results of test system 2 without wind energy and the load reduction measures is active

Table 9.12: BBO algorithm result of test system 2 without wind energy and the load reduction measures is active

Time	P_1	P_2	P_3	P_H	P_{LR}	P_{Loss}	q (m^3/h)	P_{LR}^F
H1	68.77	40.00	63.42	10.00	0.00	7.20	346.00	0
H2	76.33	41.60	70.91	10.00	0.00	8.85	346.00	0
H3	89.28	49.37	83.59	10.00	0.00	12.26	346.00	0
H4	115.70	66.01	109.21	10.00	0.00	20.93	346.00	0
H5	133.45	77.84	126.26	10.49	0.00	28.05	356.38	0
H6	151.70	90.60	143.59	10.57	0.00	36.46	358.02	0
H7	164.22	99.82	155.50	13.25	0.00	42.80	415.55	0
H8	162.80	99.46	155.34	33.99	0.00	41.60	889.24	0
H9	176.39	109.84	168.16	34.64	0.00	49.04	904.69	0
H10	164.80	102.45	159.76	78.00	12.28	42.29	2065.04	18
H11	175.54	111.46	171.15	96.00	19.07	48.23	2612.96	20
H12	189.70	122.97	184.66	96.00	13.19	56.53	2612.96	20
H13	194.03	126.72	188.97	99.00	15.49	59.23	2708.06	18
H14	183.22	117.64	178.50	96.00	17.28	52.64	2612.96	20
H15	172.84	109.32	168.55	96.00	0.00	46.72	2612.96	0
H16	175.15	109.30	167.70	46.00	0.00	48.15	1186.96	0
H17	166.66	102.56	159.33	40.00	0.00	43.55	1036.00	0
H18	160.22	97.41	152.68	30.00	0.00	40.32	794.00	0
H19	152.78	91.72	145.21	22.00	0.00	36.72	609.04	0
H20	140.29	82.67	132.99	15.00	0.00	30.97	453.50	0
H21	124.66	71.90	117.83	10.00	0.00	24.40	346.00	0
H22	102.41	57.50	96.36	10.00	0.00	16.28	346.00	0
H23	80.63	44.15	75.13	10.00	0.00	9.92	346.00	0
H24	71.56	40.00	66.20	10.00	0.00	7.77	346.00	0
Total Cost (Rs)		24249.83		Total Volume (m^3)			24996.31	
Objective Function Cost (Rs)				25264.26				

Table 9.13: GA algorithm result of test system 2 without wind energy and the load reduction measures is active

Time	P_1	P_2	P_3	P_H	P_{LR}	P_{Loss}	q (m^3/h)	P_{LR}^F
H1	68.77	40.00	63.42	10.00	0.00	7.20	346.00	0
H2	76.33	41.60	70.91	10.00	0.00	8.85	346.00	0
H3	89.28	49.37	83.59	10.00	0.00	12.26	346.00	0
H4	115.70	66.01	109.21	10.00	0.00	20.93	346.00	0
H5	133.55	77.90	126.34	10.29	0.00	28.09	352.21	0
H6	151.61	90.54	143.52	10.74	0.00	36.41	361.62	0
H7	165.53	100.72	156.58	10.74	0.00	43.57	361.62	0
H8	166.28	101.84	158.24	27.21	0.00	43.58	728.60	0
H9	179.23	111.85	170.48	29.21	0.00	50.78	775.39	0
H10	180.28	113.31	172.51	45.99	14.00	51.10	1186.67	18
H11	177.52	113.03	173.04	95.91	14.83	49.34	2610.13	20
H12	188.53	121.99	183.55	96.00	15.73	55.82	2612.96	20
H13	193.63	126.34	188.52	98.00	17.47	58.97	2676.24	18
H14	183.18	117.60	178.45	96.00	17.37	52.62	2612.96	20
H15	172.98	109.42	168.66	95.72	0.00	46.79	2604.19	0
H16	161.00	99.43	155.87	74.00	0.00	40.31	1948.56	0
H17	165.63	101.85	158.47	42.00	0.00	42.97	1085.84	0
H18	157.17	95.35	150.12	36.00	0.00	38.66	937.76	0
H19	147.25	88.07	140.51	33.00	0.00	33.84	865.34	0
H20	139.79	82.35	132.57	16.00	0.00	30.72	475.36	0
H21	124.66	71.90	117.83	10.00	0.00	24.40	346.00	0
H22	102.41	57.50	96.36	10.00	0.00	16.28	346.00	0
H23	80.63	44.15	75.13	10.00	0.00	9.92	346.00	0
H24	71.56	40.00	66.20	10.00	0.00	7.77	346.00	0
Total Cost (Rs)		24264.75		Total Volume (m^3)			24963.46	
Objective Function Cost (Rs)				25261.78				

Table 9.14: KOA algorithm result of test system 2 without wind energy and the load reduction measures is active

Time	P_1	P_2	P_3	P_H	P_{LR}	P_{Loss}	q (m^3/h)	P_{LR}^F
H1	68.77	40.00	63.42	10.00	0.00	7.20	346.00	0
H2	76.33	41.60	70.91	10.00	0.00	8.85	346.00	0
H3	89.28	49.37	83.59	10.00	0.00	12.26	346.00	0
H4	115.70	66.01	109.21	10.00	0.00	20.93	346.00	0
H5	131.35	76.51	124.44	14.74	0.00	27.05	447.81	0
H6	146.60	87.26	139.27	20.62	0.00	33.76	578.01	0
H7	159.60	96.70	151.66	22.20	0.00	40.16	613.53	0
H8	160.69	98.02	153.58	38.13	0.00	40.43	989.84	0
H9	173.19	107.58	165.53	40.81	0.00	47.12	1056.15	0
H10	182.78	115.11	174.55	41.23	13.96	52.64	1066.71	18
H11	176.53	112.27	172.14	96.84	15.99	48.79	2639.48	20
H12	189.14	122.57	184.24	97.65	12.59	56.20	2665.16	20
H13	192.72	125.66	187.80	100.00	17.23	58.41	2740.00	18
H14	181.40	116.31	177.01	99.93	16.95	51.61	2737.76	20
H15	172.42	109.02	168.20	96.84	0.00	46.49	2639.48	0
H16	175.53	109.57	168.01	45.26	0.00	48.38	1168.09	0
H17	169.87	104.78	161.99	33.75	0.00	45.40	883.36	0
H18	160.32	97.48	152.76	29.81	0.00	40.38	789.46	0
H19	151.89	91.13	144.46	23.76	0.00	36.25	649.16	0
H20	137.88	81.12	130.92	19.85	0.00	29.78	560.54	0
H21	124.66	71.90	117.83	10.00	0.00	24.40	346.00	0
H22	102.41	57.50	96.36	10.00	0.00	16.28	346.00	0
H23	80.63	44.15	75.13	10.00	0.00	9.92	346.00	0
H24	71.56	40.00	66.20	10.00	0.00	7.77	346.00	0
Total Cost (Rs)		24250.00		Total Volume (m^3)			24992.54	
Objective Function Cost (Rs)				25251.18				

Table 9.15: BBO algorithm result of test system 2 with wind energy and the load reduction measures is active

Time	P_1	P_2	P_3	P_H	P_w	P_{LR}	P_{Loss}	q (m^3/h)	P_w^F	P_{LR}^F
H1	68.77	40.00	63.42	10.00	0.00	0.00	7.20	346.00	0.00	0.00
H2	76.33	41.60	70.91	10.00	0.00	0.00	8.85	346.00	0.00	0.00
H3	89.28	49.37	83.59	10.00	0.00	0.00	12.26	346.00	0.00	0.00
H4	111.05	63.00	104.72	10.00	10.46	0.00	19.23	346.00	30.00	0.00
H5	128.93	74.76	121.92	10.04	10.49	0.00	26.14	346.80	30.00	0.00
H6	145.02	85.85	137.27	10.50	14.60	0.00	33.26	356.53	30.00	0.00
H7	162.48	98.49	153.79	11.71	5.44	0.00	41.92	382.44	50.00	0.00
H8	162.34	98.51	153.88	15.78	21.22	0.00	41.74	470.44	50.00	0.00
H9	175.20	108.82	166.89	32.00	5.50	0.00	48.41	841.38	50.00	0.00
H10	180.00	112.83	171.81	39.00	7.79	14.61	51.04	1011.26	20.00	18.00
H11	174.02	110.22	169.62	95.00	5.28	18.21	47.37	2581.50	20.00	20.00
H12	178.67	113.99	174.20	96.99	20.29	15.85	50.01	2644.25	40.00	20.00
H13	183.26	117.74	178.66	98.00	22.65	17.36	52.68	2676.24	40.00	18.00
H14	174.00	110.24	169.66	96.00	19.91	17.55	47.36	2612.96	20.00	20.00
H15	167.77	105.34	163.64	95.65	11.56	0.00	43.95	2601.79	20.00	0.00
H16	157.43	96.75	152.44	73.99	7.87	0.00	38.49	1948.25	20.00	0.00
H17	153.81	93.79	148.47	65.02	0.60	0.00	36.71	1694.13	20.00	0.00
H18	145.32	86.95	139.12	42.00	19.41	0.00	32.81	1085.84	20.00	0.00
H19	151.00	90.44	143.52	22.00	3.88	0.00	35.85	609.04	20.00	0.00
H20	139.59	82.05	132.09	10.08	6.95	0.00	30.76	347.62	10.00	0.00
H21	120.68	69.27	114.01	10.00	8.86	0.00	22.82	346.00	10.00	0.00
H22	100.70	56.43	94.70	10.00	3.89	0.00	15.72	346.00	10.00	0.00
H23	80.63	44.15	75.13	10.00	0.00	0.00	9.92	346.00	0.00	0.00
H24	71.56	40.00	66.20	10.00	0.00	0.00	7.77	346.00	0.00	0.00
Total Cost (Rs)		24197.57		Total Volume (m^3)				24978.49		
Objective Function Cost (Rs)				26636.34						

Table 9.16: GA algorithm result of test system 2 with wind energy and the load reduction measures is active

Time	P_1	P_2	P_3	P_H	P_w	P_{LR}	P_{Loss}	q (m^3/h)	P_w^F	P_{LR}^F
H1	68.77	40.00	63.42	10.00	0.00	0.00	7.20	346.00	0.00	0.00
H2	76.33	41.60	70.91	10.00	0.00	0.00	8.85	346.00	0.00	0.00
H3	89.28	49.37	83.59	10.00	0.00	0.00	12.26	346.00	0.00	0.00
H4	106.84	60.31	100.66	10.00	19.95	0.00	17.76	346.00	30.00	0.00
H5	131.71	76.64	124.58	10.10	4.27	0.00	27.31	348.09	30.00	0.00
H6	151.03	90.13	142.97	10.89	1.09	0.00	36.13	364.95	30.00	0.00
H7	160.62	97.12	152.05	11.77	9.37	0.00	40.95	383.76	50.00	0.00
H8	166.64	101.60	157.70	12.12	16.07	0.00	44.13	391.12	50.00	0.00
H9	180.91	112.55	171.03	13.19	14.46	0.00	52.15	414.32	50.00	0.00
H10	165.32	102.46	159.60	66.72	8.59	14.89	42.58	1741.61	20.00	18.00
H11	174.17	110.33	169.76	95.00	4.96	18.22	47.45	2581.50	20.00	20.00
H12	182.22	116.78	177.48	95.00	14.46	16.10	52.05	2581.50	40.00	20.00
H13	191.84	124.88	186.90	99.00	14.23	6.01	57.86	2708.06	40.00	18.00
H14	177.30	112.86	172.83	96.03	14.93	15.26	49.22	2614.01	20.00	20.00
H15	166.88	104.63	162.75	95.00	14.20	0.00	43.48	2581.50	20.00	0.00
H16	157.38	96.71	152.39	74.00	7.99	0.00	38.47	1948.56	20.00	0.00
H17	154.43	93.75	148.21	49.00	16.72	0.00	37.12	1264.06	20.00	0.00
H18	153.57	92.69	146.65	35.00	8.95	0.00	36.87	913.50	20.00	0.00
H19	142.17	84.42	135.56	31.00	13.36	0.00	31.51	817.66	20.00	0.00
H20	137.77	80.86	130.49	13.00	7.75	0.00	29.88	410.14	10.00	0.00
H21	120.69	69.27	114.01	10.00	8.85	0.00	22.83	346.00	10.00	0.00
H22	99.34	55.58	93.38	10.00	6.98	0.00	15.29	346.00	10.00	0.00
H23	80.63	44.15	75.13	10.00	0.00	0.00	9.92	346.00	0.00	0.00
H24	71.56	40.00	66.20	10.00	0.00	0.00	7.77	346.00	0.00	0.00
Total Cost (Rs)		24263.96		Total Volume (m^3)				24832.34		
Objective Function Cost (Rs)				26703.92						

Table 9.17: KOA algorithm result of test system 2 with wind energy and the load reduction measures is active

Time	P_1	P_2	P_3	P_H	P_w	P_{LR}	P_{Loss}	q (m^3/h)	P_w^F	P_{LR}^F
H1	68.77	40.00	63.42	10.00	0.00	0.00	7.20	346.00	0.00	0.00
H2	76.33	41.60	70.91	10.00	0.00	0.00	8.85	346.00	0.00	0.00
H3	89.28	49.37	83.59	10.00	0.00	0.00	12.26	346.00	0.00	0.00
H4	105.95	59.74	99.79	10.00	21.97	0.00	17.46	346.00	30.00	0.00
H5	126.65	73.41	120.06	17.35	7.57	0.00	25.05	505.08	30.00	0.00
H6	137.07	80.71	130.40	25.36	15.77	0.00	29.31	685.68	30.00	0.00
H7	148.99	89.26	142.07	30.93	13.45	0.00	34.71	815.95	50.00	0.00
H8	156.00	94.42	148.88	33.81	14.97	0.00	38.10	884.88	50.00	0.00
H9	167.91	103.30	160.15	33.81	19.15	0.00	44.33	884.88	50.00	0.00
H10	173.55	108.08	166.23	46.58	12.03	15.77	47.24	1201.84	20.00	18.00
H11	177.11	112.74	172.70	96.84	12.53	2.19	49.12	2639.48	20.00	20.00
H12	177.74	113.35	173.48	99.62	18.21	17.08	49.50	2727.97	40.00	20.00
H13	184.76	119.05	180.22	100.00	16.87	17.68	53.58	2740.00	40.00	18.00
H14	182.53	117.11	177.89	96.84	7.03	10.83	52.24	2639.48	20.00	20.00
H15	165.29	103.46	161.31	96.84	15.74	0.00	42.65	2639.48	20.00	0.00
H16	171.39	106.00	163.52	35.48	19.80	0.00	46.21	925.22	20.00	0.00
H17	165.37	101.40	157.79	34.38	9.01	0.00	42.95	898.42	20.00	0.00
H18	156.73	94.74	149.20	26.83	11.08	0.00	38.60	719.83	20.00	0.00
H19	150.05	89.80	142.69	23.52	4.28	0.00	35.35	643.61	20.00	0.00
H20	133.44	78.11	126.75	21.57	7.93	0.00	27.81	599.25	10.00	0.00
H21	124.65	71.90	117.82	10.00	0.02	0.00	24.39	346.00	10.00	0.00
H22	100.65	56.39	94.65	10.00	4.01	0.00	15.70	346.00	10.00	0.00
H23	80.63	44.15	75.13	10.00	0.00	0.00	9.92	346.00	0.00	0.00
H24	71.56	40.00	66.20	10.00	0.00	0.00	7.77	346.00	0.00	0.00
Total Cost (Rs)		24195.93		Total Volume (m^3)				24919.04		
Objective Function Cost (Rs)				26687.80						

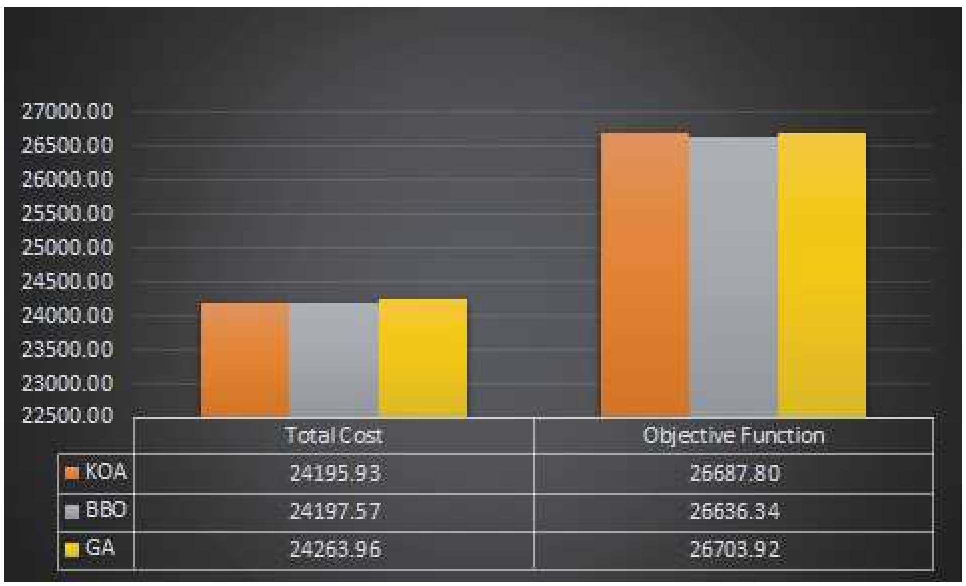

Figure 9.8: BBO, GA and KOA algorithms results of test system 2 with wind energy and the load reduction measures is active

9.7 Conclusion

In this chapter, the fixed head hydrothermal scheduling problem for Smart Grid is modeled assuming the incorporation of significant amount of wind power and the load reduction measures are active at peak loads. Then, a procedure using any meta-heuristic optimization was proposed to solve the problem. The Biogeography Based Optimization algorithm (BBO) and Genetic algorithm (GA) and Khums optimization algorithm (KOA) were proposed and successfully utilized to solve the problem. The algorithms were applied on two systems to validate their accuracy and effectiveness, one is composed of one thermal generation units, a hydro plant, a wind turbine and a load reduction measures are active at peak loads with two periods of time and the second consists of three thermal generation units, a hydro plant, a wind turbine and load reduction measures are active at peak loads with twenty-four periods of time. The simulation results of the proposed algorithms have been compared with other algorithms in the literature when the wind energy is not included and the load reduction measures are not active. Based on the results obtained in the first test systems, KOA succeeded in obtaining a good solution for the problem compared with BBO and GA. BBO, GA and KOA also generate a slightly higher cost solution compared with other algorithms in the literature when the wind energy is not included and the load reduction measures are not active for the first system. In the second test system, GA obtained the best schedule in the case of wind energy included and the load reduction measures are not active. KOA obtained the best solution in the case of wind energy not included and the load reduction is active. In the case of the wind energy is included and the load reduction measures are active, BBO obtained the best schedule.

Chapter 10

Optimal Power Flow Problem For Smart Grid

10.1 Introduction

Optimal power flow (OPF) is a nonlinear, non-convex and large-scale optimization problem and one of the most important optimization problems in power system operation and control. The main objective is to reduce the generation cost with or without reducing the system losses subjected to different equality constraints.

In smart grid the OPF objectives are modified to minimizing the total fuel cost and the greenhouse gases emissions. One way of achieving these objective is by the integration of a significant amount renewable energy and the integration of load reduction as demand side management measure which will increase the complexity of the problem and introduce many challenges in finding the optimal solution which accounts for the intermittent behavior of renewable resources and the error in the forecasting of the available renewable power and the forecasting of the amount of load reduction at peak loads.

In power systems with appreciable renewable energy and incentivising consumer driven load curtailment implementation of real time pricing are proposed as a smart grid function.

In this chapter, OPF will be modeled and solved for smart grid by assuming significant integration of wind energy to the network and the load reduction programs are active. It is assumed that the anticipated (forecast) wind power output is available in the studies of this thesis.

10.2 Smart Grid Optimal Power Flow Mathematical Formulation

The general formulation of the optimal power flow optimization problem for smart grid network can be stated as follows

$$min \quad J(x,u) \tag{10.1}$$

$$s.t \quad g(x,u) = 0 \tag{10.2}$$

$$and \;\; h(x,u) \leq 0 \tag{10.3}$$

where J is the OPF objective function, g is the equality constraints, h is the inequality constraints, x, and u are the system state and control vectors respectively. The state variable can be represented as

$$x_T = [P_{G1} \;\; Q_{G1} \cdot\cdot Q_{GNx} \;\; V_{L1} \cdot\cdot V_{LNy} \;\; S_{L1} \cdot\cdot S_{LNz}] \tag{10.4}$$

where P_{G1} is the slack bus generator output power, Q_G is the generator output reactive power, V_L is the PQ bus voltages, S_L is the transmission line power flow ,Nx,Ny and Nz are the number of generator units, the number of PQ buses, and the number of transmission lines respectively. The control vector is shown in (10.5), where the V_G is the voltage at controlled buses, P_G is the generator real output power, T is the transformers tap changers setting, Q_c the output reactive power generated by the shunt compensator, P_{wj} available wind power for the j^{th} wind turbine, P_{Lk} is the available load reduction from area k, Nt, Nc, N_x and N_d are the number of tap changing transformers, number of shunt compensators, number of wind turbines, and number of areas of load reduction respectively.

$$u_T = [V_{G1} \cdot\cdot V_{GNx} \;\; P_{G2} \cdot\cdot P_{GNx} \;\; T_1 \cdot\cdot T_{Nt} \;\; Q_{C1} \cdot\cdot Q_{CNc} \;\; P_{w1} \cdot\cdot P_{wN_w} \;\; P_{L1} \cdot\cdot P_{LN_d}] \tag{10.5}$$

10.3 The Objective Function

OPF problem usually solved with one of the four following objective functions: fuel cost minimization, voltage profile improvement, voltage stability limit enhancement and voltage stability enhancement during contingency condition.

10.3.1 Fuel Cost Minimization

In this case, the objective is to minimize the total fuel cost of the generation units as follows:

$$J_1 = W_{cost} + LR_{cost} + \sum_{i=1}^{Nx} f_i = W_{cost} + LR_{cost} + \sum_{i=1}^{Nx} a_i + b_i\, P_i + c_i\, P_i^2 \tag{10.6}$$

Where f_i is the fuel cost of generation unit i, N_x is the number of generator units, P_i is the out power of generation unit i, a_i, b_i and c_i are the fuel cost coefficients. W_{cost} is the total cost of wind power generation and LR_{cost} is the total cost of load reduction. W_{cost} model and LR_{cost} model will be discussed in chapter (6) and (7) respectively.

10.3.2 Voltage Profile Improvement

Minimizing the fuel cost may produce inappropriate voltage profile which means that the solution is not feasible because of the poor voltage profile. Hence, the objective function in (10.6) is modified by introducing the voltage deviation scaled weighting factor w as new term as shown in (10.7) which is selected to be 100 as proposed in [33].

$$J = J_1 + w \sum_{j=1}^{Ny} |V_j - 1| \tag{10.7}$$

Where V_j is the voltage of load bus j and N_y is the number of load buses.

10.3.3 Voltage Stability Enhancement

Voltage stability can be defined as the system ability to maintain steady voltages at all buses after being subjected to disturbances. The symptoms can be noticed as rise or fall of voltages of some buses which in turn can lead to loss of some loads, tripping of some transmission lines or loss of synchronism of some generators[3]. Assessing voltage stability can be achieved by calculating the L-index at all the load buses which serve as voltage stability indicators. The range of this index lies between 0 which represent the no load case and 1 which represents the voltage collapse condition. Hence, low value for L-index is recommended to insure the voltage stability of the network after a disturbances. L-index can be calculated as shown in[33]. The objective function is modified in this case to serve the required purpose by adding a scaled term represent the maximum L-index of the network and the scaling factor β is chosen to be 6000 as proposed in [33]. The objective function can be expressed as shown in (10.8).

$$J = J_1 + \beta \max (L_j) \quad j = 1, 2 \cdots Ny \tag{10.8}$$

10.3.4 Voltage Stability Enhancement During Contingency Condition

In this case, the objective function will be the same objective function as in case 3 and the contingency condition simulated is the outage of a transmission line. In the IEEE 30 bus system, for example, the line is line (2-6).

10.4 Equality Constraints

10.4.1 Power Flow Equality Constraints

The power flow equations (10.9) and (10.10) represent the set of equality constraints in the OPF problem, where the P_i represent the injected active power at bus i, Q_i is the injected reactive power at bus i, G_{im}, N is the total number of buses , G_{im} B_{im}, and θ_{im} represent the conductance and susceptance and voltage phase angle difference between bus i and m respectively.

$$P_i - V_i \sum_{m=1}^{N} V_m \; (G_{im} \; \cos\theta_{im} + B_{im} \; \sin\theta_{im}) = 0 \tag{10.9}$$

$$Q_i - V_i \sum_{m=1}^{N} V_m \; (G_{im} \; \sin\theta_{im} + B_{im} \; \cos\theta_{im}) = 0 \tag{10.10}$$

10.5 Inequality Constraints

10.5.1 Thermal Unit Power Limit Constraint

Generation units are restricted by their limits in term of generation voltage, active power and reactive power as follows:

$$V_{Gi}^{min} \leq V_{Gi} \leq V_{Gi}^{max} \quad i = 1, 2 \cdots, Nx \tag{10.11}$$

$$P_{Gi}^{min} \leq P_{Gi} \leq P_{Gi}^{max} \quad i = 1, 2 \cdots, Nx \tag{10.12}$$

$$Q_{Gi}^{min} \leq Q_{Gi} \leq Q_{Gi}^{max} \quad i = 1, 2 \cdots, Nx \tag{10.13}$$

Where V_{Gi}^{min}, V_{Gi}^{max}, P_{Gi}^{min}, P_{Gi}^{max}, Q_{Gi}^{min} and Q_{Gi}^{max} are the minimum voltage, maximum voltages, minimum active power output, maximum active power output, minimum reactive power output and maximum reactive power output of the i^{th} generating unit respectively.

10.5.2 Transformer Constraints

Transformer tap changers settings lower and upper limits are represented as follows:

$$T_i^{min} \leq T_i \leq T_i^{max} \quad i = 1, 2 \cdots, N_t \tag{10.14}$$

Where T_i^{min} and T_i^{max} are the minimum and maximum tab setting limits of the i^{th} transformer unit respectively. N_t is the number of transformer with tap changers.

10.5.3 Shunt Compensator Constraints

Shunt VAR compensators are constrained by their limits as follows:

$$Q_{ci}^{min} \leq Q_{ci} \leq Q_{ci}^{max} \quad i = 1, 2 \cdots, N_c \tag{10.15}$$

Where Q_{ci}^{min} and Q_{ci}^{max} are minimum and maximum Var injection limits of the i^{th} shunt capacitor unit respectively. N_c is the number of shunt VAR compensators.

10.5.4 Security Constraints

Security constraints includes the minimum and maximum voltage of the load buses, and the transmission line capacity limit which can be formulated as follows:

$$V_{Li}^{min} \leq V_{Li} \leq V_{Li}^{max} \quad i = 1, 2 \cdots, N_y \tag{10.16}$$

$$S_{Li} \leq S_{Li}^{max} \quad i = 1, 2 \cdots, N_z \tag{10.17}$$

where V_{Li}^{min}, V_{Li}^{max} and S_{Li}^{max} are the minimum voltage of the i^{th} load bus, maximum voltage of the i^{th} load bus and maximum apparent power flow limit of the i^{th} branch respectively. N_z is the number of shunt VAR compensators. N_z is the number of transmission lines.

10.5.5 Wind Turbine Power Limit Constraint

$$0 \leq P_{wj} \leq P_{wj}^{r} \quad j = 1, 2 \cdots, N_w \tag{10.18}$$

Here P_j^{wr}, is the rated active power output of the j^{th} wind turbine unit. N_w is the number of wind turbines.

10.5.6 Load Power Limit Constraint

$$P_{Lk}^{min} \leq P_{Lk} \leq P_{Lk}^{max} \quad k = 1, 2 \cdots, N_d \tag{10.19}$$

Here P_{Lk}^{min}, P_{Lk}^{max}, are the minimum active power reduction, maximum active power reduction of the k^{th} unit respectively. N_d is the number of load reduction areas.

10.6 Optimal Location for Wind Turbine

The optimal location of wind turbine is obtained here for modifying the IEEE benchmark system by adding a wind turbine or turbines in a locations which have the minimum operational cost based on the optimal power flow. The method is simply by connecting the wind turbine to a bus with a direct cost and solve for the optimal power flow with fuel cost minimization objective. All the buses will be tested in this case and the bus with minimum cost will be selected to add the wind turbine to it in the following sections. Fig(10.1) and Fig(10.2) show the results of solving the optimal power flow after connecting the wind turbine to a bus at a time saving the cost. The Figures show clearly that there will be a variation on the cost due to wind turbine connection based on the selected bus.

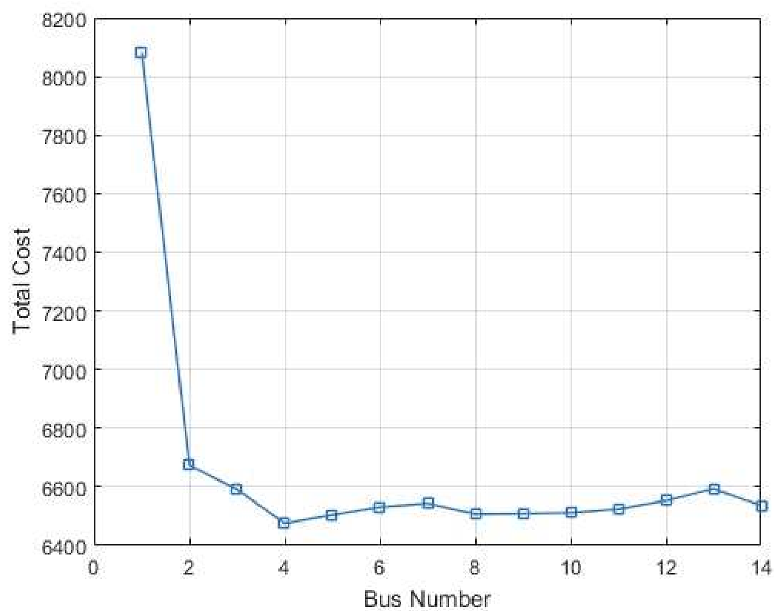

Figure 10.1: Total cost obtained from connecting a wind turbine in a bus and solving the OPF for total cost minimization

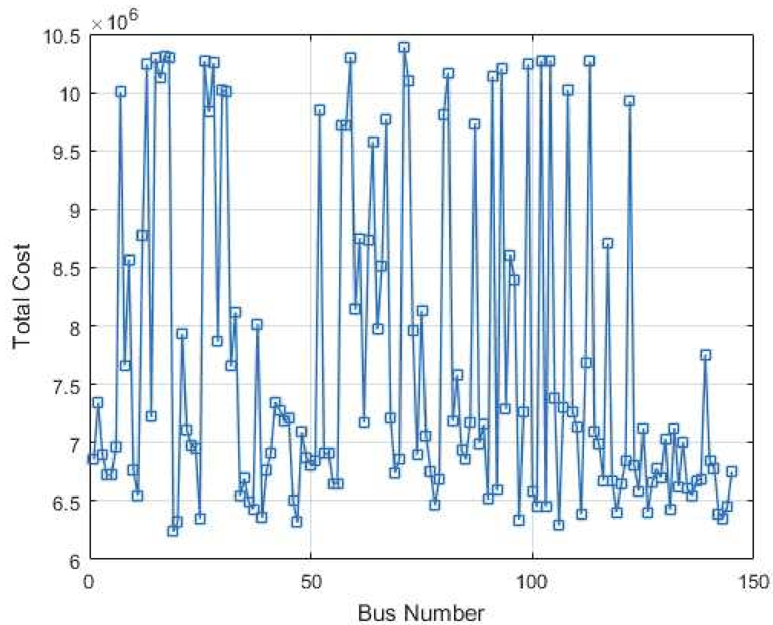

Figure 10.2: Total cost obtained from connecting a wind turbine in a bus and solving the OPF for total cost minimization

10.7 Optimal Location for Load Reduction

The optimal location to apply the load reduction measures is obtained here for modifying the Benchmark test system. The method is simply by reducing the load at a load bus and solve for the optimal power flow with fuel cost minimization objective. All the load buses will be tested in this case and the bus with minimum cost will be selected to add apply the load reduction measures on it. Fig(10.3) and Fig(10.4) show the results of applying a load reduction on a bus at a time and solve for optimal power flow and saving the cost. The Figures show clearly that there will be a variation on the cost due to load reduction based on the load bus.

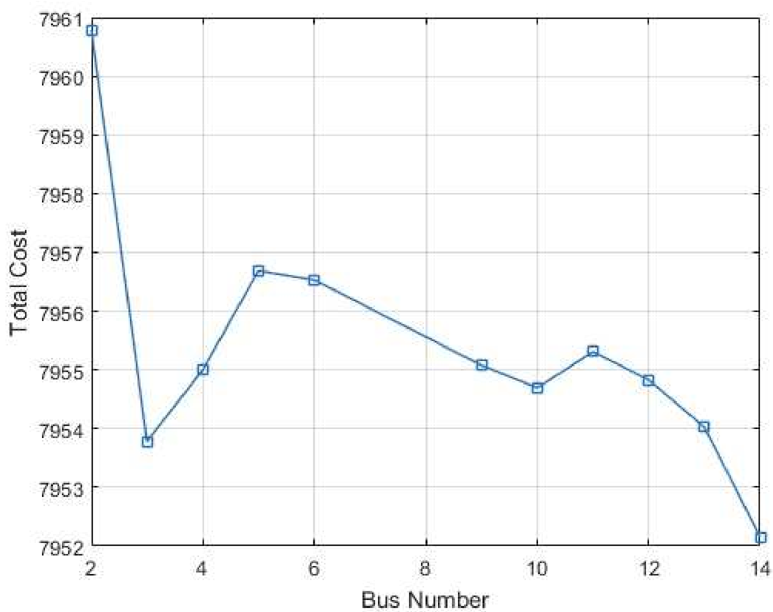

Figure 10.3: Total cost obtained from reducing the load in each load bus and solving the OPF for total cost minimization

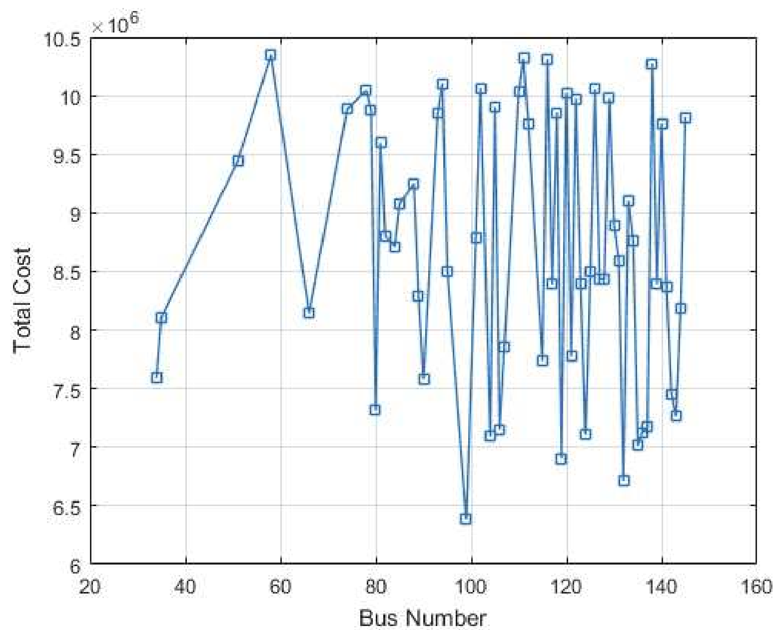

Figure 10.4: Total cost obtained from reducing the load in each load bus and solving the OPF for total cost minimization

10.8 Optimal Power Flow Solution Incorporating Wind Energy and Load Reduction

The general procedure to solve the optimal power flow problem incorporating wind energy and load reduction measures are active at peak loads using any metaheuristic algorithm is shown in Procedure (6).

Procedure 6: Optimal Power Flow

1. Initialize the algorithm parameters (population size, no of generations, no of iteration, mutation rate, cross over rate).
2. Generate a set of feasible solutions where each consist of a control vector shown in (10.5) where the wind power and the load reduction power, both generated randomly based on the forecast.
3. Optimal power flow is calculated for each solution.
4. The direct cost, overestimation cost and the under estimation cost for wind power and load reduction power are calculated for all the solutions.
5. Calculate the objective function.
6. Save the best solution.
7. Apply the Algorithm operations on the set of the solutions.
8. Check the feasibility of the generated solutions and repeat steps (3-6).
9. Repeat steps (7-8) until the termination criterion is achieved.

10.9 Optimal Power Flow Incorporating Wind Energy and Load Reduction by BH Algorithm and KOA Algorithm

In this section, numerical examples of the solution of the optimal power flow incorporating wind energy and the load reduction measures are active will be illustrated using the black hole optimization algorithm (BH) and the khums optimization algorithm (KOA). The IEEE 30 bus benchmark test system will be modified and used for the analysis. The optimal power flow simulation will be done by modifying the MATPOWER simulation package[143, 142] to use the evolutionary algorithms and to use different objective functions. The wind turbine cost model is assumed to be probabilistic based on the Weibull distribution and the load reduction model is also the probabilistic model but based on the Normal distribution.

10.9.1 Test System: IEEE 30-bus system

IEEE 30-bus system has six generation units, four off line tap changer transformers, and nine shunt reactive power compensators. The bus, line, fuel cost coefficients and parameters limits have been adopted from[33].

In this test system, the proposed algorithms have been utilized to solve the OPF problem with four separate objective functions: fuel cost minimization, voltage profile improvement, voltage stability limit enhancement and voltage stability enhancement during contingency condition.

Wind turbine farm will be added to the system at the bus which selected based on the OPF solution for the total cost minimization. Fig (10.5) shows the result obtained and it is clear that bus 5 has the lowest cost but the difference is very small and the wind turbine can be connected to any bus.

Similar decision will be obtained based on the result shown in Fig (10.6) where the difference in cost due to load reduction between the load buses is very small and the load reduction measures can be applied on any load bus. The selection criterion then will be based on the required load reduction amount.

The wind turbine will be connected to bus 7 and the load reduction bus will be applied to bus 5 since it has the largest load.

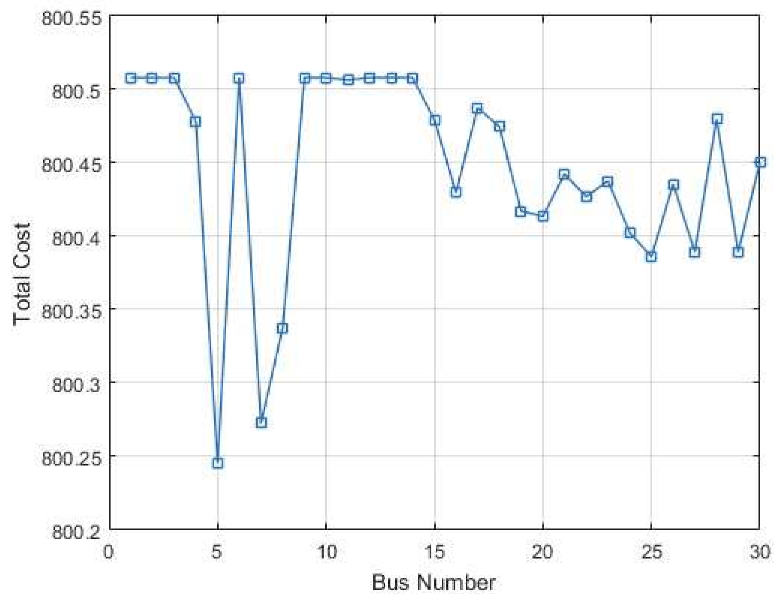

Figure 10.5: Total cost obtained from connecting a wind turbine in a bus and solving the OPF for total cost minimization

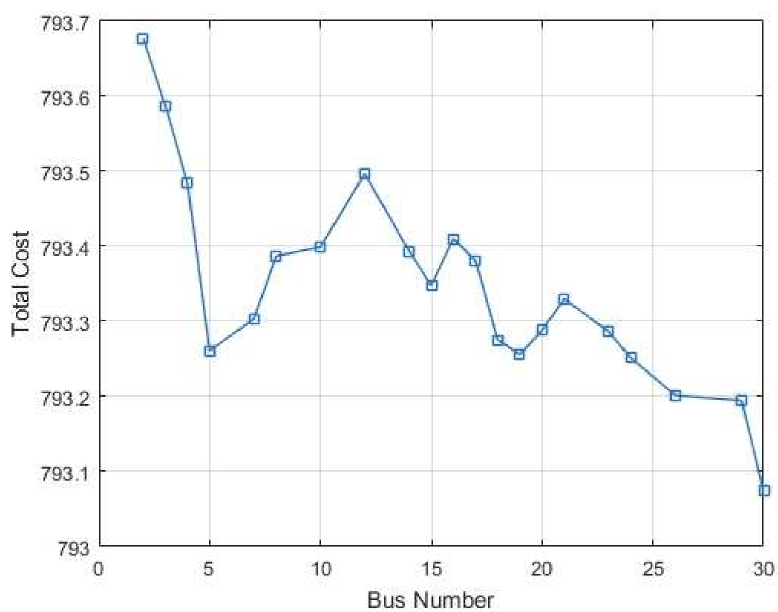

Figure 10.6: Total cost obtained from reducing the load in each load bus and solving the OPF for total cost minimization

The optimum control variable settings obtained by BH and KOA for the four cases without wind energy and without load reduction are shown in Table (10.3). In case 1, the objective is to minimize the total fuel cost of the generation units as shown in (10.6). The total fuel cost obtained for BH and KOA is higher than the best solution obtained in HFPSONM[58] by 0.62 % and 0.63 % respectively as shown in Table (10.1) and Figure (10.7). This work has been reported in [47] without the KOA algorithm.

Case 2 represent the Voltage profile improvement where the objective function of case 1 is modified by adding a scaled voltage deviation of load buses. The control variables are shown for case 2 in Table (10.3) while a comparison of the results with other techniques are shown in Table (10.1), Figure (10.7) and Figure (10.8). The results obtained using the BH and KOA algorithm are close to other algorithms. BH fuel cost is lower than the KOA and KOA has a lower voltage deviation than BH. The best result obtained is the HFPSONM[58] results because the choosing criterion will be based on the fuel cost and the voltage deviation and it has the best compromise solution as shown in Table (10.1).

Case 3 represents the voltage stability enhancement where the voltage stability defined as the system ability to maintain steady voltages at all buses after being subjected to disturbances. The control variable for case 3 is shown in Table (10.3). Since the best solution is decided based on the fuel cost value and the L_{max} value, BH, KOA and the HFPSONM[58] are the best solutions compared to other solutions as shown in Figure (10.7) and Figure (10.9).

Case 4 represents the voltage stability enhancement during contingency condition. In this case, the objective function will be the objective function in case 3 and the contingency condition simulated is the outage of line (2-6). The control variable is shown in Table (10.3). The total fuel cost obtained by BH and KOA is better than the other solutions because they have the lowest fuel cost with small difference in the L_{max} value as shown in Figure (10.7) and Figure (10.9). .

The optimum control variable settings obtained by BH and KOA for the four cases with wind energy and the load reduction measures are active are shown in Table (**??**), Figure (10.7) and Figure (10.11). .

The wind turbine cost model data and the load reduction cost model data are shown in Appendix (C.4.1). The wind turbine is connected to bus 7 and the load reduction measures are active on load bus 5. The forecast wind power for all the cases is 10 MW and the forecast load reduction is 13.19 MW.

In case 1, case 3 and case 4 BH has the optimum solution compared to KOA. In case 2 KOA the optimum solution compared to BH as shown in Figure (10.10). .

Table 10.1: Comparison of BH and KOA optimization algorithms result with other algorithms in literature without wind energy and the load reduction is not active

Case	Algorithm	Fuel cost ($/h)	P_{Loss} (MW)	Voltage deviations	L_{max}
1	BH	799.87	8.87	1.0932	0.1337
	KOA	799.95	8.89	1.1048	0.1327
	BBO[11]	799.1116	8.63	-	-
	DE[33]	799.2891	8.629	-	-
	HFPSONM[58]	794.9545	9.363	-	-
2	BH	803.07	9.72	0.3023	0.1357
	KOA	804.74	10.19	0.1763	0.1425
	BBO[11]	804.9982	9.95	0.102	-
	DE[33]	805.2619	10.4412	0.1357	-
	HFPSONM[58]	803.5278	9.794	0.0859	-
3	BH	800.29	8.99	1.1090	0.1318
	KOA	800.27	8.99	1.0406	0.1325
	BBO[11]	805.7252	10.21	-	0.1104
	DE[33]	807.5272	10.3142	-	0.1219
	HFPSONM[58]	801.7488	8.992	-	0.1023
4	BH	803.942	9.80	1.0886	0.1326
	KOA	803.82	9.79	1.0681	0.1334
	PSONM[58]	807.5284	9.823	-	0.1279
	DE[33]	810.2661	10.3142	-	0.1347
	HFPSONM[58]	805.7573	9.265	-	0.1078

Figure 10.7: Comparison of BH and KOA optimization algorithms fuel cost results with other algorithms in literature without wind energy and the load reduction is not active

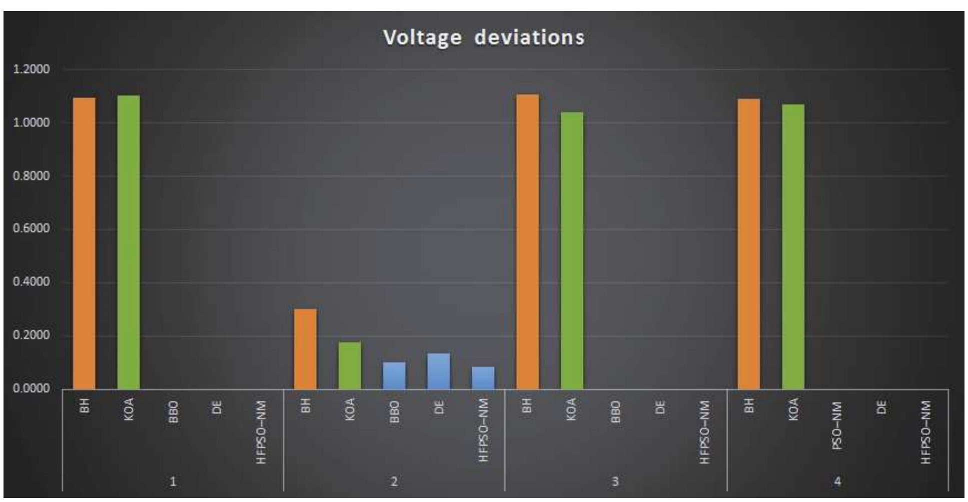

Figure 10.8: Comparison of BH and KOA optimization algorithms voltage deviation results with other algorithms in literature without wind energy and the load reduction is not active

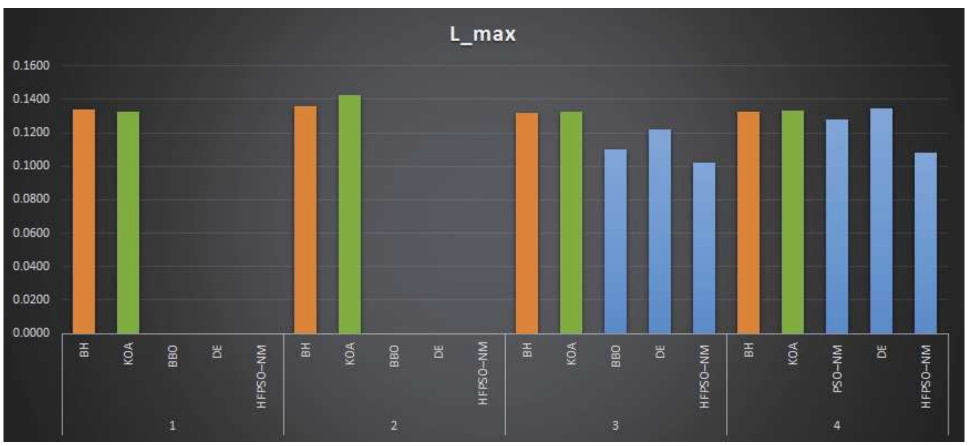

Figure 10.9: Comparison of BH and KOA optimization algorithms L_{max} results with other algorithms in literature without wind energy and the load reduction is not active

Table 10.2: Optimal control variable setting for IEEE 30 bus system without wind energy and without load reduction

Case	1		2		3		4	
Control variables	KOA	BH	KOA	BH	KOA	BH	KOA	BH
P_1	177.38	177.35	176.87	176.91	177.46	177.43	176.32	175.52
P_2	48.70	48.69	48.95	48.85	48.69	48.69	47.09	47.90
P_5	21.35	21.34	21.63	21.51	21.33	21.33	21.35	21.32
P_8	21.00	21.03	21.86	21.67	21.02	21.06	23.66	23.69
P_{11}	11.86	11.86	12.25	12.18	11.88	11.88	12.76	12.77
P_{13}	12.00	12.00	12.03	12.01	12.00	12.00	12.00	12.00
V_1	1.09	1.09	1.03	1.06	1.10	1.10	1.10	1.10
V_2	1.07	1.07	1.01	1.04	1.08	1.08	1.08	1.09
V_5	1.04	1.04	0.98	1.00	1.05	1.05	1.05	1.05
V_8	1.04	1.05	0.96	1.00	1.05	1.06	1.04	1.05
V_{11}	1.00	1.03	1.02	0.99	1.10	1.04	1.09	1.06
V_{13}	1.06	1.06	1.06	1.02	1.05	1.04	1.05	1.05
T_{11}	1.0719	1.0035	1.0135	1.0051	1.0251	0.9793	1.0490	0.9792
T_{12}	0.9136	0.9774	1.0351	1.0725	0.9756	0.9703	1.0801	0.9944
T_{15}	0.9883	0.9693	1.0635	0.9933	0.9320	0.9341	0.9530	0.9545
T_{36}	0.9820	0.9854	0.9280	0.9136	0.9680	0.9682	0.9740	0.9627
Q_{c10}	4.54	2.55	3.84	2.99	0.00	1.31	3.93	1.30
Q_{c12}	4.14	2.51	4.85	3.57	0.00	1.42	3.29	0.85
Q_{c15}	3.65	3.16	4.29	3.27	0.00	0.92	3.12	1.24
Q_{c17}	3.41	3.07	3.40	3.85	0.00	1.08	4.70	0.88
Q_{c20}	4.39	2.41	4.89	3.52	0.00	1.15	3.89	1.01
Q_{c21}	3.78	3.51	3.87	3.90	0.00	1.06	3.26	0.96
Q_{c23}	4.69	3.09	3.65	3.51	0.00	0.99	3.05	1.25
Q_{c24}	3.83	2.32	3.61	3.92	0.00	0.96	4.25	0.95
Q_{c29}	4.76	3.07	4.25	3.67	0.00	1.39	3.23	1.12
Fuel cost (\$/h)	799.95	799.87	804.74	803.07	800.27	800.29	803.82	803.94
P_{Loss} (MW)	8.89	8.87	10.19	9.72	8.99	8.99	9.79	9.80
Voltage deviations	1.1048	1.0932	0.1763	0.3023	1.0406	1.1090	1.0681	1.0886
L_{max}	0.1327	0.1337	0.1425	0.1357	0.1325	0.1318	0.1334	0.1326

Table 10.3: Optimal control variable setting for IEEE 30 bus system with wind energy and with load reduction

Case	1		2		3		4	
Control variables	KOA	BH	KOA	BH	KOA	BH	KOA	BH
P_1	166.74	166.81	169.83	167.98	170.05	167.00	167.60	165.88
P_2	46.10	46.10	47.07	46.42	47.03	46.14	45.94	45.51
P_5	20.35	20.34	20.88	20.45	20.75	20.34	20.52	20.37
P_8	15.43	15.33	18.71	16.22	15.51	15.58	19.53	18.43
P_{11}	10.07	10.08	11.05	10.26	10.77	10.13	11.35	10.96
P_{13}	12.00	12.00	12.00	12.00	12.00	12.00	12.00	12.00
P_{w7}	9.57	8.70	4.06	5.67	5.82	6.81	2.36	6.12
V_1	1.09	1.09	1.04	1.09	1.07	1.09	1.10	1.10
V_2	1.07	1.07	1.02	1.07	1.04	1.08	1.09	1.09
V_5	1.05	1.04	1.00	1.04	1.01	1.05	1.06	1.06
V_8	1.05	1.04	1.00	1.04	1.01	1.05	1.05	1.05
V_{11}	1.03	1.05	1.08	0.97	1.04	1.04	1.10	1.06
V_{13}	1.05	1.04	1.05	1.04	1.07	1.05	1.04	1.06
V_{w7}	1.04	1.04	1.00	1.04	1.01	1.04	1.05	1.04
T_{11}	0.9726	1.0317	1.1000	1.0862	0.9260	0.9805	1.1000	0.9767
T_{12}	1.1000	1.0145	0.9547	0.9517	1.1000	0.9992	0.9000	0.9809
T_{15}	0.9780	0.9508	1.0121	1.0548	0.9935	0.9657	0.9320	0.9590
T_{36}	1.0140	0.9555	0.9680	1.0398	0.9380	0.9744	0.9680	0.9583
Q_{c10}	4.17	2.32	5.00	4.08	5.00	2.18	3.13	0.44
Q_{c12}	5.00	2.06	0.82	3.02	3.57	2.33	0.00	0.40
Q_{c15}	3.78	1.76	0.00	2.95	5.00	2.59	0.00	0.47
Q_{c17}	5.00	2.15	0.10	4.10	3.96	2.23	0.15	0.43
Q_{c20}	4.46	1.65	0.04	3.06	5.00	2.22	0.00	0.52
Q_{c21}	5.00	2.03	0.00	3.97	3.94	2.23	0.00	0.38
Q_{c23}	5.00	1.74	0.04	4.09	5.00	2.11	0.00	0.38
Q_{c24}	3.40	2.33	0.70	3.59	0.27	2.32	0.70	0.48
Q_{c29}	3.30	2.12	0.00	4.27	3.47	2.74	0.00	0.47
P_{L5}	10.90	11.96	8.76	12.37	10.00	13.16	13.09	12.92
V_{L5}	1.05	1.04	1.00	1.04	1.01	1.05	1.06	1.06
Fuel cost (\$/h)	734.92	734.02	760.23	740.33	749.68	734.13	750.37	740.84
Wind cost (\$/h)	8.61	7.83	3.65	5.10	12.00	6.13	8.00	5.51
Load Reduction cost (\$/h)	10.90	11.96	8.76	12.37	12.00	13.16	20.00	12.92
P_{Loss} (MW)	7.76	7.91	8.94	7.97	8.53	7.77	8.99	8.78
Voltage deviations	0.9563	0.8628	0.2040	0.3614	0.9266	1.1395	1.0400	1.0643
L_{max}	0.1382	0.1328	0.1457	0.1469	0.1335	0.1321	0.1333	0.1326
Total cost (\$/h)	754.44	753.81	772.64	757.81	773.68	753.43	778.37	759.26
Objective Function cost (\$/h)	765.48	757.25	800.67	801.06	1574.49	1553.26	1578.29	1562.27

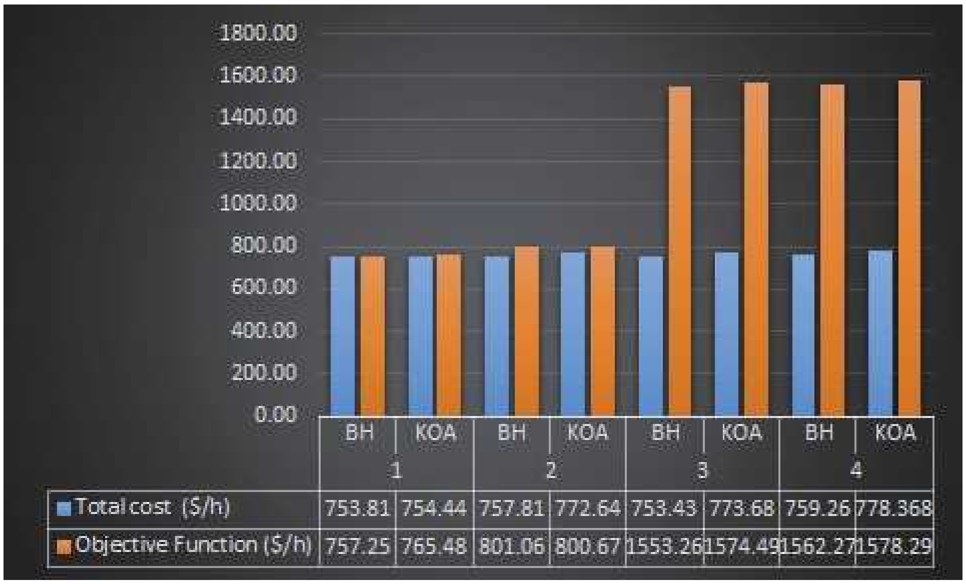

Figure 10.10: Objective function and total cost for IEEE 30 bus system with wind energy and with load reduction for the four cases

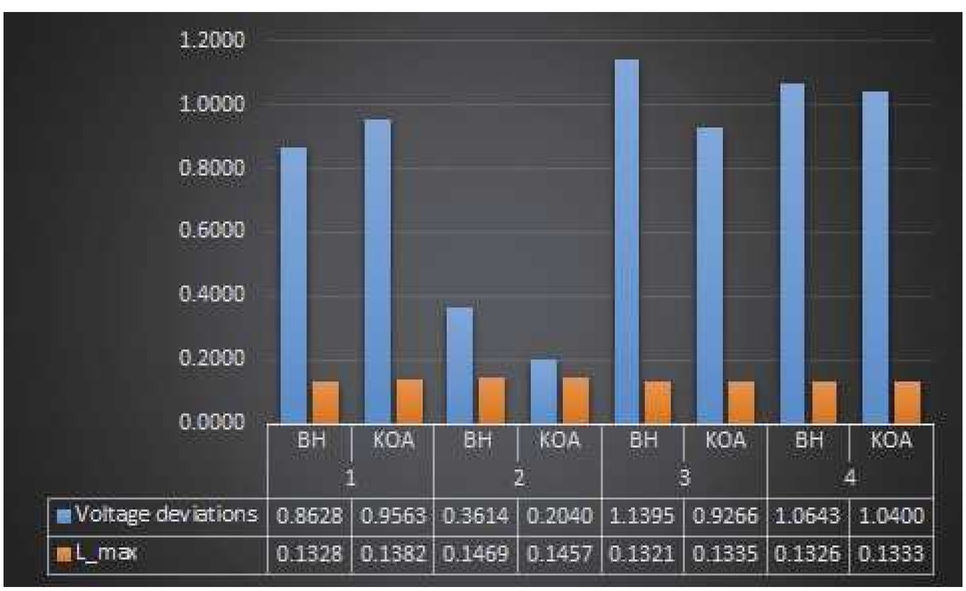

Figure 10.11: voltage deviation and L_{max} for IEEE 30 bus system with wind energy and with load reduction for the four cases

10.10 Conclusion

In this chapter, the optimal power flow problem for Smart Grid is modeled assuming the incorporation of significant amount of wind power and the load reduction measures are active at peak loads with different objective functions including minimizing the fuel cost, enhancing the voltage profile and improving the voltage stability under both normal and contingency conditions. Then, a procedure using any metaheuristic optimization was proposed to solve the problem. The BH and KOA algorithms have been tested on the IEEE 30-bus system. The simulation results of the proposed algorithms have been compared with those reported in literature. Based on the results obtained, BH and KOA succeeded in solving the problem and the solution obtained is close to the solution obtained using other algorithms when the wind energy is not included and the load reduction is not active. BH obtain better solution compared to KOA when the wind energy is included and the load reduction measures are active.

Chapter 11

Conclusion

11.1 Conclusion

In this research work, a formulation of economic dispatch problem for smart grid is proposed, and the different equality and inequality constraints were defined. The objective function and the constrains were modified based on the significant contribution of both wind energy and load reduction at peak loads.

Two wind turbine cost models proposed in the literature for solving the economic dispatch problem were introduced and they are: negative load model and the probabilistic wind turbine cost model. Comparisons between the probabilistic wind turbine cost model and the negative load model in solving the economic dispatch problem were done for three test systems. For all the cases, the behavior of the probabilistic model at low wind forecast will be equivalent or following the negative load model till the forecast wind power reach a critical point. Then the negative load will start to become costly compared to the probabilistic model which will schedule the wind at fix power equal to the critical wind power forecast even if the wind power forecast increased to a higher value because the overestimation forecast error is high and the overestimation cost is also high.

Two models were proposed for the load reduction as demand side management measure for economic dispatch problem in smart grid at peak load time and they are the negative load cost model and the probabilistic cost model based on Normal distribution. The general response of the objective function and the total cost function obtained without wind energy, is similar in general to the response obtained by the wind turbine only. The general response of the objective function and the total cost function obtained with wind energy is more complex and result into four possible model combinations: N-N, N-P, P-N and P-P. Where N stand for negative load cost model and P stand for probabilistic cost model based on Normal distribution. Among the four combinations, P-P are the most reliable in dealing with the forecasting errors because it is either the cheapest choice or the second cheapest choice in the objective function for the three test systems in the four regions.

Since the economic dispatch is a main operation on the unit commitment (UC) problem solving and it affects the UC problem results, a unit commitment model for Smart Grid is modeled assuming the incorporation of significant amount of wind power and the load reduction measures are active at peak loads. Then, a procedure using any metaheuristic optimization was proposed to solve the problem. The Biogeography Based Optimization algorithm (BBO) and Genetic Algorithm (GA) were proposed and successfully utilized to solve the problem. The algorithms were applied to two test systems. Based on the results obtained in both test systems, BBO and GA succeeded in obtaining a good solution for the problem with a slight difference between them. Also, the total cost decrease with the merging of wind energy and applying the load reduction measures.

The fixed head hydrothermal scheduling problem is also affected by the economic dispatch model which motivate the modeling of the fixed head hydrothermal scheduling problem for Smart Grid assuming the incorporation of significant amount of wind power and the load reduction measures are active at peak loads. Then, a procedure using any metaheuristic optimization was proposed to solve the problem. The Biogeography Based Optimization algorithm (BBO) and Genetic algorithm (GA) and Khums optimization algorithm (KOA) were proposed and successfully utilized to solve the problem on to two test systems to validate their accuracy and effectiveness. Based on the results obtained in the first test systems, KOA succeed in obtaining a good solution for the problem compared with BBO and GA. In the second test system, GA obtained the best schedule in the case of wind energy included and the load reduction measures are not active. KOA obtained the best solution in the case of wind energy not included and the load reduction is active. In the case of the wind energy is included and the load reduction measures are active, BBO obtained the best schedule. All the solutions obtained for both test systems are feasible solutions and the differences is on the amount of wind energy and load reduction overestimation and underestimation forecasting error.

Optimal power flow for Smart Grid is modeled. Then, a procedure using any metaheuristic optimization was proposed to solve the problem. The BH and KOA algorithms have been tested on the IEEE 30-bus system. The simulation results of the proposed algorithms have been compared with those reported in literature. Based on results obtained, BH and KOA succeeded in solving the problem and the solution obtained is close to the solution obtained using other algorithms when the wind energy is not included and the load reduction is not active. BH obtained better solution compared to KOA when the wind energy is included and the load reduction measures are active.

In this research work, new optimization algorithm called Khums optimization algorithm proposed. KOA has two operations to search for optimal solution, collection and distribution. In collection, new solution will be generated from cutting the tax from the solutions based on their earning and in distribution the generated solution will be as result from distributing these taxes among the poor solutions. The algorithm was applied to solve 14 benchmark from the literature and compare the performance with other methods. Then the KOA algorithm applied to solve the economic dispatch with valve point effect for two systems. The results show that the new algorithm can be applied to solve practical optimization problems. Although, KOA has better performance on solving the benchmark systems but we cannot conclude that it is better than other algorithms based on the no free lunch theorem.

11.2 Scope of Future Work

- Develop probabilistic model for other renewable resources (if needed) to incorporate them in the economic dispatch model.
- Study and develop model for the energy storage elements to incorporate in the economic dispatch model.
- Develop an environmental multi fuel economic dispatch model for smart grid which will be more complicated multi objective economic dispatch model.
- Study the consumer behavior on load reduction to decide accurately the load reduction probability distribution function.
- Three interesting modifications can be studied in the future for the Khums optimization algorithm:

  1. The first modification is about the Khums tax rate where it is assumed in this work to be constant 20%. The khums rate can be random but within this range and a comparison between the performance of the algorithm based on these two tax rates observed.
  2. The second modification is in the way of ranking the good solutions and poor solutions. Other methods can be used to study the effects on the performance of the algorithms.
  3. Finally, the last modification can be done by adding the effects of death of tax payers and the effect of joining new tax payers which is like the mutation process in other algorithms which may affect the performance of the algorithm and need to be studied as future work.

Appendix A

Wind Turbine Probabilistic Cost Models

A.1 Introduction

- The source of the derivation for the probabilistic model
- Assume that the wind speed is V and $V \sim W(c,k)$.
- The wind Power $P_w(v) = 0.5\,\rho\,A_s\,v^3$ (w).
  where ρ is the air density in (kg/m^3), A_s is the cross sectional area in (m^2) through which the wind pass and V is the wind speed in (m/s).
- The pdf and cdf of the weibull distribution is shown in(A.1) and (A.2) while the expected (mean) and the variance are shown in (A.3) and (A.4) respectively [73].

$$f(v) = \frac{k}{c}\,\left(\frac{v}{c}\right)^{k-1} \exp[-(\frac{v}{c})^k]\ u(v) \tag{A.1}$$

$$F(v) = P(V \leq v) = \int_{-\infty}^{v} \frac{k}{c}\,\left(\frac{m}{c}\right)^{k-1} \exp[-(\frac{m}{c})^k]\ u(m)\ dm$$
$$F(v) = \int_{0}^{v} \frac{k}{c}\,\left(\frac{m}{c}\right)^{k-1} \exp[-(\frac{m}{c})^k]\ dm = \Big[-\exp[-(\frac{m}{c})^k]\Big]_0^v$$

$$F(v) = (1-\exp[-(\frac{v}{c})^k])\ u(v) \tag{A.2}$$

$$E(V^n) = \int_{-\infty}^{\infty} m^n\,\frac{k}{c}\,\left(\frac{m}{c}\right)^{k-1} \exp[-(\frac{m}{c})^k]\ u(m)\ dm$$

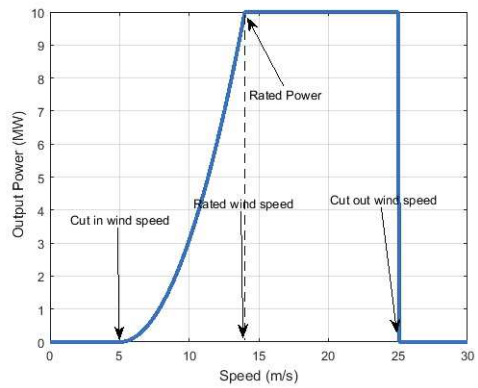

Figure A.1: Wind Turbine Power Curve

$$(\frac{m}{c})^k = Z \quad \Rightarrow \quad \frac{m}{c} = Z^{\frac{1}{k}} \Rightarrow \; m^n = c^n \; Z^{\frac{n}{k}}$$

$$dZ = \frac{k}{c} \; (\frac{m}{c})^{k-1} \; dm$$

$$E(V^n) = c^n \; \int_0^\infty Z^{\frac{n}{k}} \; \exp[-Z] \; dZ$$

$$E(V^n) = c^n \; \int_0^\infty Z^{\frac{n}{k}+1-1} \; \exp[-Z] \; dZ = c^n \; \Gamma(1 + \frac{n}{k})$$

$$E(V^n) = c^n \; \Gamma(1 + \frac{n}{k}) \tag{A.3}$$

$$Var(V) = E(V^2) - E(V)^2 = c^2 \; [\Gamma(1 + \frac{2}{k}) - (\Gamma(1 + \frac{1}{k}))^2] \tag{A.4}$$

$$w = \begin{cases} 0 & \text{if } v < V_{in} \\ \frac{(V-V_{in})\, w_r}{(V_r - V_{in})} & \text{if } V_{in} \le v < V_r \\ w_r & \text{if } V_r \le v < V_o \\ 0 & \text{if } v \ge V_o \end{cases} \tag{A.5}$$

Fig(A.1) shows the speed power curve of the wind turbine. while (A.5) shows the simplified speed power mathematical model. Using the power curve the target is to find the cdf of the power of the wind turbine knowing that the $P_w \propto V^3$ and the $V \sim W(c,k)$. From the mathematical model we observe that the there are two regions where the $w = 0$, one region with constant power $w = w_r$ and one linear region between V_{in} and V_r. First we will find the probability of $w = 0$:

$$P(W = 0) = P(v < V_{in}) + P(v \geq V_o) - P(v < V_{in} \cap v \geq V_o)$$
$$P(v < V_{in} \cap v \geq V_o) = 0$$
$$P(v < V_{in}) = P(v \leq V_{in}) = F(V_{in}) = 1 - \exp[-(\frac{V_{in}}{c})^k]$$
$$P(v \geq V_o) = 1 - F(V_o) = 1 - (1 - \exp[-(\frac{V_o}{c})^k]) = \exp[-(\frac{V_o}{c})^k]$$
$$P(W = 0) = 1 - \exp[-(\frac{V_{in}}{c})^k] + \exp[-(\frac{V_o}{c})^k]$$

Second we will find the probability of $w = w_r$:

$$\begin{aligned} P(W = w_r) &= P(V_r \leq v < V_o) \\ &= F(V_o) - F(V_r) \\ &= 1 - \exp[-(\frac{V_o}{c})^k] - ((1 - \exp[-(\frac{V_r}{c})^k])) \\ &= \exp[-(\frac{V_r}{c})^k]) - \exp[-(\frac{V_o}{c})^k]) \end{aligned}$$

Between V_{in} and V_r the cdf can be calculated by linear transformation as follow:

$$\begin{aligned} w &= \frac{(V - V_{in})\, w_r}{(V_r - V_{in})} \\ V - V_{in} &= \frac{w}{w_r}(V_r - V_{in}) \\ V &= V_{in} + \frac{w}{w_r}(\frac{V_r}{V_{in}} - 1) \\ h &= \frac{V_r}{V_{in}} - 1 \\ V &= (1 + \frac{w\ h}{w_r})V_{in} \end{aligned}$$

Substituting in (B.9) by $V = (1 + \frac{w\ h}{w_r})V_{in}$ as follow:

$$\phi(w) = F((1 + \frac{w\ h}{w_r})V_{in}) = (1 - \exp[-(\frac{(1 + \frac{w\ h}{w_r})V_{in}}{c})^k])$$

The cdf of the wind power $F_w(w) = P(W \leq w)$:

First $w \leq 0$ and since the event is not possible, then

$$P(W < 0) = 0$$

For $0 \leq w < w_r$

$$\begin{aligned}
P(0 \leq W < w_r) &= P(W = 0 \cup 0 < W \leq w_r) \\
&= P(W = 0) + P(0 < W \leq w_r) - P(W = 0 \cap 0 < W \leq w_r) \\
&= P(w = 0) + \int_0^w f(u)du \\
&= P(W = 0) + \phi(w) - \phi(0) \\
&= 1 - \exp[-(\frac{V_{in}}{c})^k] + \exp[-(\frac{V_o}{c})^k] \\
&+ (1 - \exp[-(\frac{(1 + \frac{w\,h}{w_r})V_{in}}{c})^k]) - (1 - \exp[-(\frac{V_{in}}{c})^k]) \\
&= 1 - \exp[-(\frac{(1 + \frac{w\,h}{w_r})V_{in}}{c})^k] + \exp[-(\frac{V_o}{c})^k]
\end{aligned}$$

For $w \geq w_r$, and since $P(W > w_r)$ is not possible

$$\begin{aligned}
P(W \leq w_r) + P(W > w_r) &= 1 \\
P(W > w_r) &= 0 \\
P(W \leq w_r) &= 1
\end{aligned}$$

Hence the the wind power cdf can be written as follows:

$$F_w(w) = \begin{cases} 0 & \text{if } w < 0 \\ 1 - \exp(-(\frac{(1+\frac{h\,w}{w_r})V_{in}}{c})^k) + \exp(-(\frac{V_o}{c})^k) & \text{if } 0 \leq w < w_r \\ 1 & \text{if } w \geq w_r \end{cases} \tag{A.6}$$

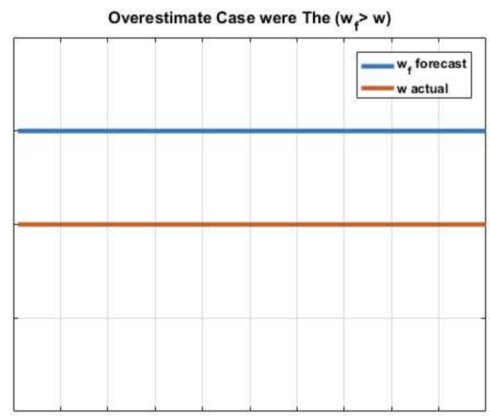

Figure A.2: Over estimate case where the forecast Value w_F is grater than the actual value w

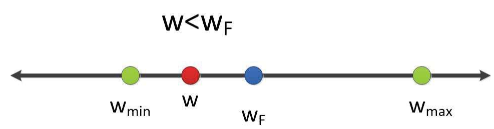

Figure A.3: When the actual value lies between w_{min} and w_F

A.2 Overestimation of w:

From Fig(B.8) it is obvious that the forecast value is grater than the actual value $(w_F > w)$. which leads to financial loss due to buying unplanned power from other utilities. To account for this events we should calculate the expected value of $w_F > w$ and merge it with our cost model for the wind turbine. But according to fig(A.3) and fig(A.5), this will happen only in the region from (w_{min}, w_{sc}). Hence, the expected value of overestimation [73] will be as follows:

$$E^{oe} = I_1 + I_2$$

At $w = 0$

$$I_1 = w_F \ P(w = 0)$$
$$I_1 = w_F \ [1 - \exp(-(\frac{V_{in}}{c})^k) + \exp(-(\frac{V_o}{c})^k)]$$

$$
\begin{aligned}
I_2 &= \int_0^{w_r} max(w_F - w\,,\,0)\,f(w)\;dw \\
&= \int_0^{w_F} (w_F - w)\,f(w)\,dw \\
&= \int_0^{w_F} w_F\,f(w)\;dw - \int_0^{w_F} w\,f(w)\;dw
\end{aligned}
$$

$$
\begin{aligned}
I_2 &= w_F\;(F_w(w_F) - F_w(0)) - I_3 \\
&= w_F\;(1 - \exp(-(\frac{(1+\frac{h\,w_F}{w_r})V_{in}}{c})^k) + \exp(-(\frac{V_o}{c})^k) - (1 - \exp(-(\frac{V_{in}}{c})^k) + \exp(-(\frac{V_o}{c})^k))) - I_3 \\
&= w_F\;[\exp(-(\frac{V_{in}}{c})^k) - \exp(-(\frac{V_F}{c})^k)] - I_3
\end{aligned}
$$

$$
\begin{aligned}
I_3 &= \int_0^{w_F} w\,f(w)\;dw \\
&= \int_0^{w_F} w\;\frac{k\,h\,V_{in}}{w_F\;c}\;\left(\frac{(1+\frac{h\,w}{w_r})V_{in}}{c}\right)^{k-1} \exp[-(\frac{(1+\frac{h\,w}{w_r})V_{in}}{c})^k]
\end{aligned}
$$

to simplify the integration, let $V = (1+\frac{h\,w}{w_r})V_{in}$

$$
\begin{aligned}
V &= (1+\frac{h\,w}{w_r})V_{in} \\
dV &= \frac{h\,V_{in}}{w_r}\;dw \\
w &= \frac{w_r}{h\,V_{in}}\,(V - V_{in})
\end{aligned}
$$

I_3 will become as follow:

$$
\begin{aligned}
I_3 &= \int_{V_{in}}^{V_F} \frac{k}{c}\ \frac{w_r}{h\,V_{in}}\,(V - V_{in})\ \left(\frac{V}{c}\right)^{k-1} \exp[-(\frac{V}{c})^k]\ dV \\
&= \int_{V_{in}}^{V_F} \frac{k}{c}\ \frac{w_r}{h\,V_{in}}\,V\ \left(\frac{V}{c}\right)^{k-1} \exp[-(\frac{V}{c})^k]\ dV \\
&\quad - \frac{w_r}{h} \int_{V_{in}}^{V_F} \frac{k}{c}\ \left(\frac{V}{c}\right)^{k-1} \exp[-(\frac{V}{c})^k]\ dV \\
I_3 &= I_4 - \frac{w_r}{h}\,[F(V_F) - F(V_{in})] \\
I_3 &= I_4 - \frac{w_r}{h}\,[1 - \exp(-(\frac{V_F}{c})^k) - (1 - \exp(-(\frac{V_{in}}{c})^k))] \\
I_3 &= I_4 - \frac{w_r}{h}\,[\exp(-(\frac{V_{in}}{c})^k) - \exp(-(\frac{V_F}{c})^k)]
\end{aligned}
$$

$$
V_F = (1 + \frac{h\,w_F}{w_r})V_{in}
$$

$$
\begin{aligned}
I_4 &= \int_{V_{in}}^{V_F} \frac{k}{c}\ \frac{w_r}{h\,V_{in}}\,V\ \left(\frac{V}{c}\right)^{k-1} \exp[-(\frac{V}{c})^k]\ dV \\
&= \frac{k\,w_r}{h\,V_{in}} \int_{V_{in}}^{V_F} \left(\frac{V}{c}\right)^{k} \exp[-(\frac{V}{c})^k]\ dV
\end{aligned}
$$

to simplify the integration, let $y = (1 + \frac{h\,w}{w_r})V_{in}$

$$
\begin{aligned}
y &= \left(\frac{V}{c}\right)^k \Rightarrow y^{\frac{1}{k}} = \frac{V}{c} \\
dy &= \left(\frac{V}{c}\right)^{k-1}\ \frac{k}{c}\ dV
\end{aligned}
$$

$$
I_4 = \frac{k\,w_r}{h\,V_{in}} \int_{(\frac{V_{in}}{c})^k}^{(\frac{V_F}{c})^k} y\ \exp[-y]\ y^{-k+1}\ \frac{c}{k}\ dy
$$

$$
I_4 = \frac{c\,w_r}{h\,V_{in}} \int_{(\frac{V_{in}}{c})^k}^{(\frac{V_F}{c})^k} y^{\frac{1}{k}}\ \exp[-y]\ dy
$$

Incomplete Gamma function is shown here:

$$\Gamma(\alpha, x) = \int_x^{\infty} y^{\alpha-1}\ exp(-y)\ dy$$

$$\int_a^b y^{\alpha-1}\ exp(-y)\ dy = \int_a^{\infty} y^{\alpha-1}\ exp(-y)\ dy - \int_b^{\infty} y^{\alpha-1}\ exp(-y)\ dy$$
$$= \Gamma(\alpha, a) - \Gamma(\alpha, b)$$

$$I_4 = \frac{k\, w_r}{h\, V_{in}} \int_{(\frac{V_{in}}{c})^k}^{(\frac{V_F}{c})^k} y\ \ \exp[-y]\ y^{-k+1}\ \frac{c}{k}\ dy$$
$$I_4 = \frac{c\, w_r}{h\, V_{in}} \int_{(\frac{V_{in}}{c})^k}^{(\frac{V_F}{c})^k} y^{\frac{1}{k}}\ \ \exp[-y]\ dy$$

Using the incomplete Gamma function

$$\frac{1}{k} = \alpha - 1$$
$$\alpha = 1 + \frac{1}{k}$$

$$I_4 = \frac{c\, w_r}{h\, V_{in}}\ [\Gamma(1 + \frac{1}{k}, (\frac{V_{in}}{c})^k) - \Gamma(1 + \frac{1}{k}, (\frac{V_F}{c})^k)]$$

Back substitution of I_4 in I_3 and I_3 in I_2 as follow:

$$I_3 = I_4 - \frac{w_r}{h}\, [\exp(-(\frac{V_{in}}{c})^k) - \exp(-(\frac{V_F}{c})^k)]$$
$$I_3 = \frac{c\, w_r}{h\, V_{in}}\ [\Gamma(1 + \frac{1}{k}, (\frac{V_{in}}{c})^k) - \Gamma(1 + \frac{1}{k}, (\frac{V_F}{c})^k)] - \frac{w_r}{h}\, [\exp(-(\frac{V_{in}}{c})^k) - \exp(-(\frac{V_F}{c})^k)]$$

$$I_2 = w_F\ [\exp(-(\frac{V_{in}}{c})^k) - \exp(-(\frac{V_F}{c})^k)]$$
$$-[\frac{c\, w_r}{h\, V_{in}}\ [\Gamma(1+\frac{1}{k}, (\frac{V_{in}}{c})^k) - \Gamma(1+\frac{1}{k}, (\frac{V_F}{c})^k)] - \frac{w_r}{h}\, [\exp(-(\frac{V_{in}}{c})^k) - \exp(-(\frac{V_F}{c})^k)]]$$

Back substitution of I_2 and I_1 in E^{oe} as follow:

$$E^{oe} = I_1 + I_2$$

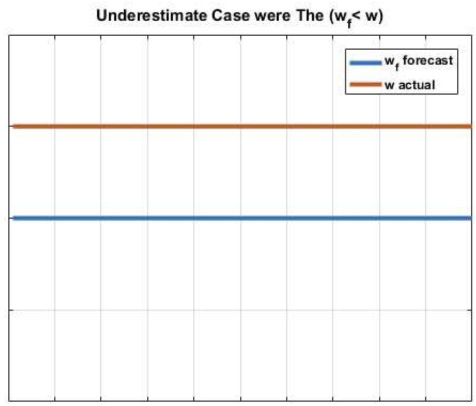

Figure A.4: under estimate case where the forecast Value w_F is smaller than the actual value w

$$
\begin{aligned}
E^{oe} = {} & w_F\ [1 - \exp(-(\frac{V_{in}}{c})^k) + \exp(-(\frac{V_o}{c})^k)] + w_F\ [\exp(-(\frac{V_{in}}{c})^k) - \exp(-(\frac{V_F}{c})^k)] \\
& - \frac{c\, w_r}{h\, V_{in}}\ [\Gamma(1+\frac{1}{k},(\frac{V_{in}}{c})^k) - \Gamma(1+\frac{1}{k},(\frac{V_F}{c})^k)] + \frac{w_r}{h}\ [\exp(-(\frac{V_{in}}{c})^k) - \exp(-(\frac{V_F}{c})^k)]
\end{aligned}
$$

$$
\begin{aligned}
E^{oe} = {} & w_F\ [1 - \exp(-(\frac{V_{in}}{c})^k) + \exp(-(\frac{V_o}{c})^k)] \\
& + (w_F + \frac{w_r}{h})\ [\exp(-(\frac{V_{in}}{c})^k) - \exp(-(\frac{V_F}{c})^k)] \\
& - \frac{c\, w_r}{h\, V_{in}}\ [\Gamma(1+\frac{1}{k},(\frac{V_{in}}{c})^k) - \Gamma(1+\frac{1}{k},(\frac{V_F}{c})^k)]
\end{aligned}
$$

Or we can simplify it more as follows:

$$
\begin{aligned}
E^{oe} = {} & w_F\ [1 - \exp(-(\frac{V_F}{c})^k) + \exp(-(\frac{V_o}{c})^k)] + \frac{w_r}{h}\ [\exp(-(\frac{V_{in}}{c})^k) - \exp(-(\frac{V_F}{c})^k)] \\
& - \frac{c\, w_r}{h\, V_{in}}\ [\Gamma(1+\frac{1}{k},(\frac{V_{in}}{c})^k) - \Gamma(1+\frac{1}{k},(\frac{V_F}{c})^k)]
\end{aligned}
$$

A.3 Underestimation of w:

From Fig(B.8) it is obvious that the forecast value is less than the actual value ($w_F < w$). which leads to a problem of wasting the available power by not using it. To account for this events we should calculate the expected value of $w_F < w$ and merge it with our cost model for the load reduction. But according to fig(A.3) and fig(A.5), this will happen only in the region from (w_F, w_{max}). Hence, the expected value of underestimation will be as follows:

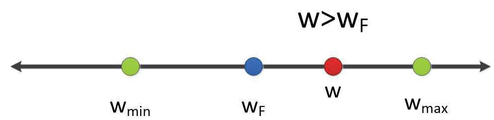

Figure A.5: When the actual value lies between w_F and w_{max}

$$E^{ue} = M_1 + M_2$$

At $w = w_r$

$$M_1 = (w_r - w_F)\ P(w = w_r)$$
$$M_1 = (w_r - w_F)\ [\exp(-(\frac{V_r}{c})^k) - \exp(-(\frac{V_o}{c})^k)]$$

$$\begin{aligned} M_2 &= \int_0^{w_r} max(w - w_F\ ,\ 0)\ f(w)\ dw \\ &= \int_{w_F}^{w_r} (w - w_F)\ f(w)\ dw \\ &= \int_{w_F}^{w_r} w\ f(w)\ dw - \int_{w_F}^{w_r} w_F\ f(w)\ dw \end{aligned}$$

$$\begin{aligned} M_2 &= M_3 - w_F\ (F_w(w_r) - F_w(w_F)) \\ &= M_3 - w_F\ [1 - \exp(-(\frac{(1 + \frac{h\,w_r}{w_r})V_{in}}{c})^k) + \exp(-(\frac{V_o}{c})^k \\ &- (1 - \exp(-(\frac{(1 + \frac{h\,w_F}{w_r})V_{in}}{c})^k) + \exp(-(\frac{V_o}{c})^k))] \\ &= M_3 + w_F\ [\exp(-(\frac{V_r}{c})^k) - \exp(-(\frac{V_F}{c})^k)] \end{aligned}$$

$$\begin{aligned} M_3 &= \int_{w_F}^{w_r} w\ f(w)\ dw \\ &= \int_{w_F}^{w_r} w\ \frac{k\,h\,V_{in}}{w_F\ c} \left(\frac{(1 + \frac{h\,w}{w_r})V_{in}}{c}\right)^{k-1} \exp[-(\frac{(1 + \frac{h\,w}{w_r})V_{in}}{c})^k] \end{aligned}$$

to simplify the integration, let $V = (1 + \frac{h\,w}{w_r})V_{in}$

$$
\begin{aligned}
V &= (1 + \frac{h\,w}{w_r}) V_{in} \\
dV &= \frac{h\,V_{in}}{w_r}\; dw \\
w &= \frac{w_r}{h\,V_{in}}\,(V - V_{in})
\end{aligned}
$$

M_3 will become as follow:

$$
\begin{aligned}
M_3 &= \int_{V_F}^{V_r} \frac{k}{c}\; \frac{w_r}{h\,V_{in}}\,(V - V_{in}) \left(\frac{V}{c}\right)^{k-1} \exp[-(\frac{V}{c})^k]\; dV \\
&= \int_{V_F}^{V_r} \frac{k}{c}\; \frac{w_r}{h\,V_{in}}\,V \left(\frac{V}{c}\right)^{k-1} \exp[-(\frac{V}{c})^k]\; dV \\
&\quad - \frac{w_r}{h} \int_{V_F}^{V_r} \frac{k}{c}\; \left(\frac{V}{c}\right)^{k-1} \exp[-(\frac{V}{c})^k]\; dV \\
M_3 &= M_4 - \frac{w_r}{h}\,[F(V_r) - F(V_F)] \\
M_3 &= M_4 - \frac{w_r}{h}\,[1 - \exp(-(\frac{V_r}{c})^k) - (1 - \exp(-(\frac{V_F}{c})^k))] \\
M_3 &= M_4 - \frac{w_r}{h}\,[\exp(-(\frac{V_F}{c})^k) - \exp(-(\frac{V_r}{c})^k)]
\end{aligned}
$$

$$
V_F = (1 + \frac{h\,w_F}{w_r}) V_{in}
$$

$$
\begin{aligned}
M_4 &= \int_{V_F}^{V_r} \frac{k}{c}\; \frac{w_r}{h\,V_{in}}\,V \left(\frac{V}{c}\right)^{k-1} \exp[-(\frac{V}{c})^k]\; dV \\
&= \frac{k\,w_r}{h\,V_{in}} \int_{V_F}^{V_r} \left(\frac{V}{c}\right)^{k} \exp[-(\frac{V}{c})^k]\; dV
\end{aligned}
$$

to simplify the integration, let $y = (1 + \frac{h\,w}{w_r}) V_{in}$

$$
\begin{aligned}
y &= \left(\frac{V}{c}\right)^k \Rightarrow y^{\frac{1}{k}} = \frac{V}{c} \\
dy &= \left(\frac{V}{c}\right)^{k-1}\; \frac{k}{c}\; dV
\end{aligned}
$$

$$M_4 = \frac{k\,w_r}{h\,V_{in}} \int_{(\frac{V_F}{c})^k}^{(\frac{V_r}{c})^k} y \;\; \exp[-y] \; y^{-k+1} \; \frac{c}{k} \; dy$$
$$M_4 = \frac{c\,w_r}{h\,V_{in}} \int_{(\frac{V_F}{c})^k}^{(\frac{V_r}{c})^k} y^{\frac{1}{k}} \;\; \exp[-y] \; dy$$

Incomplete Gamma function is shown here:

$$\Gamma(\alpha, x) = \int_x^{\infty} y^{\alpha-1} \; exp(-y) \; dy$$
$$\int_a^b y^{\alpha-1} \; exp(-y) \; dy = \int_a^{\infty} y^{\alpha-1} \; exp(-y) \; dy - \int_b^{\infty} y^{\alpha-1} \; exp(-y) \; dy$$
$$= \Gamma(\alpha, a) - \Gamma(\alpha, b)$$

$$M_4 = \frac{k\,w_r}{h\,V_{in}} \int_{(\frac{V_F}{c})^k}^{(\frac{V_r}{c})^k} y \;\; \exp[-y] \; y^{-k+1} \; \frac{c}{k} \; dy$$
$$M_4 = \frac{c\,w_r}{h\,V_{in}} \int_{(\frac{V_F}{c})^k}^{(\frac{V_r}{c})^k} y^{\frac{1}{k}} \;\; \exp[-y] \; dy$$

Using the incomplete Gamma function

$$\frac{1}{k} = \alpha - 1$$
$$\alpha = 1 + \frac{1}{k}$$

$$M_4 = \frac{c\,w_r}{h\,V_{in}} \; [\Gamma(1 + \frac{1}{k}, (\frac{V_F}{c})^k) - \Gamma(1 + \frac{1}{k}, (\frac{V_r}{c})^k)]$$

Back substitution of M_4 in M_3 and M_3 in M_2 as follow:

$$M_3 = M_4 - \; \frac{w_r}{h} [\exp(-(\frac{V_F}{c})^k) - \exp(-(\frac{V_r}{c})^k)]$$
$$M_3 = \frac{c\,w_r}{h\,V_{in}} \; [\Gamma(1 + \frac{1}{k}, (\frac{V_F}{c})^k) - \Gamma(1 + \frac{1}{k}, (\frac{V_r}{c})^k)] - \; \frac{w_r}{h} [\exp(-(\frac{V_F}{c})^k) - \exp(-(\frac{V_r}{c})^k)]$$

$$M_2 = \frac{c\,w_r}{h\,V_{in}} \; [\Gamma(1 + \frac{1}{k}, (\frac{V_F}{c})^k) - \Gamma(1 + \frac{1}{k}, (\frac{V_r}{c})^k)]$$
$$- \; \frac{w_r}{h} [\exp(-(\frac{V_F}{c})^k) - \exp(-(\frac{V_r}{c})^k)] + w_F \; [\exp(-(\frac{V_r}{c})^k) - \exp(-(\frac{V_F}{c})^k)]$$

Back substitution of M_2 and M_1 in E^{oe} as follow:

$$E^{ue} = M_1 + M_2$$

$$\begin{aligned}
E^{ue} = {} & (w_r - w_F)\ [\exp(-(\frac{V_r}{c})^k) - \exp(-(\frac{V_o}{c})^k)] \\
& + \frac{c\, w_r}{h\, V_{in}}\ [\Gamma(1+\frac{1}{k},(\frac{V_F}{c})^k) - \Gamma(1+\frac{1}{k},(\frac{V_r}{c})^k)] \\
& -\ \frac{w_r}{h}\,[\exp(-(\frac{V_F}{c})^k) - \exp(-(\frac{V_r}{c})^k)] + w_F\ [\exp(-(\frac{V_r}{c})^k) - \exp(-(\frac{V_F}{c})^k)]
\end{aligned}$$

$$\begin{aligned}
E^{ue} = {} & (w_r - w_F)\ [\exp(-(\frac{V_r}{c})^k) - \exp(-(\frac{V_o}{c})^k)] \\
& + (w_F + \frac{w_r}{h})\ [\exp(-(\frac{V_r}{c})^k) - \exp(-(\frac{V_F}{c})^k)] \\
& + \frac{c\, w_r}{h\, V_{in}}\ [\Gamma(1+\frac{1}{k},(\frac{V_F}{c})^k) - \Gamma(1+\frac{1}{k},(\frac{V_r}{c})^k)]
\end{aligned}$$

Appendix B

Load Reduction Probabilistic Cost Models

B.1 Probabilistic Model of the Load Reduction using Normal Distribution

- Assume that load reduction Power is L and $L \sim N(\mu, \sigma^2)$.

- Assume that the Load reduction Power is $L_{min} \leq L \leq L_{max}$.

- The pdf of the normal distribution is shown in(B.1) while the expected (mean) and the variance shown in (B.2) and (B.3) respectively.

$$f(x) = \frac{1}{\sigma\sqrt{2\pi}}\; e^{\frac{-(x-\mu)^2}{2\,\sigma^2}} \tag{B.1}$$

$$E(X) = \int_{-\infty}^{\infty} x\; f(x)\; dx = \mu \tag{B.2}$$

$$Var(X) = E(X^2) - E(X)^2 = \sigma^2 \tag{B.3}$$

B.1.1 Overestimation of L

From Fig(B.5) it is obvious that the forecast value is grater than the actual value $(L_F > L)$. which leads to financial losses due to buying unplanned power from other utilities. To account for this events we should calculate the expected value of $L_F > L$ and merge it with our cost model for the load reduction. But according to fig(B.2) and fig(B.4), this will happen only in the region from (L_{min}, L_F). Hence, the expected value of overestimation will be as follows:

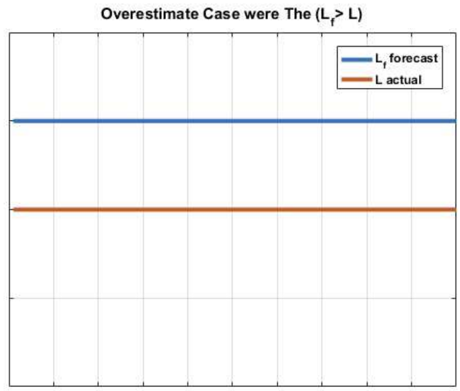

Figure B.1: Over estimate case where the forecast Value L_F is grater than the actual value L

$$E_{oe} = \int_{-\infty}^{\infty} max(0, L_F - L)\ f(L)\ dL$$
$$E_{oe} = \int_{L_{min}}^{L_F} (L_F - L)\ f(L)\ dL$$
$$E_{oe} = L_F \int_{L_{min}}^{L_F} f(L)\ dL - \int_{L_{min}}^{L_F} L\ f(L)\ dL$$
$$E_{oe} = L_F\ (F(L_F) - F(L_{min})) - X_{11}$$

$$X_{11} = \int_{L_{min}}^{L_F} L\ f(L)\ dL$$
$$X_{11} = \int_{L_{min}}^{L_F} (L - \mu + \mu)\ f(L)\ dL$$

$$X_{11} = \int_{L_{min}}^{L_F} (L-\mu)\ \frac{1}{\sigma\sqrt{2\pi}}\ e^{\frac{-(L-\mu)^2}{2\,\sigma^2}}\ dL + \mu\ \int_{L_{min}}^{L_F} f(L)\ dL$$

$$X_{11} = \frac{-\sigma}{\sqrt{2\pi}} \int_{L_{min}}^{L_F} \frac{-(L-\mu)}{\sigma^2}\ \ e^{\frac{-(L-\mu)^2}{2\,\sigma^2}}\ dL + \mu\,(F(L_F) - F(L_{min}))$$

$$X_{11} = \mu\,(F(L_F) - F(L_{min})) + \frac{-\sigma}{\sqrt{2\pi}} \left[e^{\frac{-(L-\mu)^2}{2\,\sigma^2}} \right]_{L_{min}}^{L_F}$$

$$X_{11} = \mu\,(F(L_F) - F(L_{min})) - \frac{\sigma}{\sqrt{2\pi}} \left[e^{\frac{-(L_F-\mu)^2}{2\,\sigma^2}} - e^{\frac{-(L_{min}-\mu)^2}{2\,\sigma^2}} \right]$$

$$E_{oe} = L_F\ (F(L_F) - F(L_{min})) - (\mu\,(F(L_F) - F(L_{min})) - \frac{\sigma}{\sqrt{2\pi}} \left[e^{\frac{-(L_F-\mu)^2}{2\,\sigma^2}} - e^{\frac{-(L_{min}-\mu)^2}{2\,\sigma^2}} \right])$$

$$E_{oe} = (L_F - \mu)\ (F(L_F) - F(L_{min})) + \frac{\sigma}{\sqrt{2\pi}} \left[e^{\frac{-(L_F-\mu)^2}{2\,\sigma^2}} - e^{\frac{-(L_{min}-\mu)^2}{2\,\sigma^2}} \right]$$

$$\boxed{E_{oe} = (L_F - \mu)\ (F(L_F) - F(L_{min})) + \frac{\sigma}{\sqrt{2\pi}} \left[e^{\frac{-(L_F-\mu)^2}{2\,\sigma^2}} - e^{\frac{-(L_{min}-\mu)^2}{2\,\sigma^2}} \right]}$$

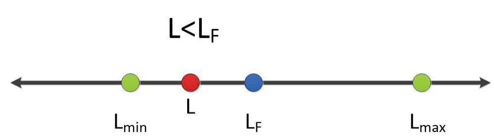

Figure B.2: When the actual value lies between L_{min} and L_F

B.1.2 Underestimation of L

From Fig(B.5) it is obvious that the forecast value is less than the actual value ($L_F < L$). which leads to a problem of wasting the available power by not using it. To account for this events we should calculate the expected value of $L_F < L$ and merge it with our cost model for the load reduction. But according to fig(B.2) and fig(B.4), this will happen only in the region from (L_F, L_{max}). Hence, the expected value of underestimation will be as follows:

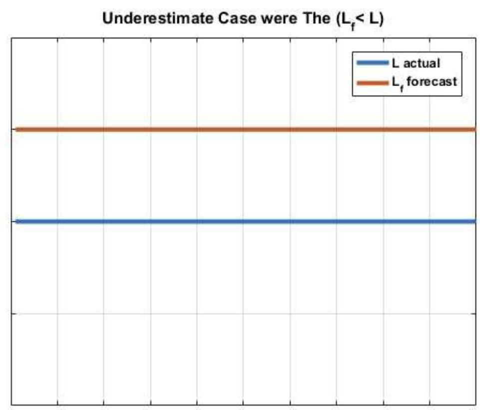

Figure B.3: Underestimate case where the forecast Value L_F is grater than the actual value L

$$E_{ue} = \int_{-\infty}^{\infty} max(0, L - L_F)\ f(L)\ dL$$

$$E_{ue} = \int_{L_F}^{L_{max}} (L - L_F)\ f(L)\ dL$$

$$E_{ue} = \int_{L_F}^{L_{max}} L\ f(L)\ dL - L_F \int_{L_F}^{L_{max}} f(L)\ dL$$

$$E_{ue} = X_{11} - L_F\ (F(L_{max}) - F(L_F))$$

$$X_{11} = \int_{L_F}^{L_{max}} L\ f(L)\ dL$$

$$X_{11} = \int_{L_F}^{L_{max}} (L - \mu + \mu)\ f(L)\ dL$$

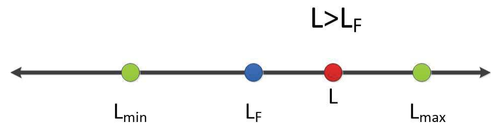

Figure B.4: When the actual value lies between L_F and L_{max}

$$X_{11} = \int_{L_F}^{L_{max}} (L-\mu)\ \frac{1}{\sigma\sqrt{2\pi}}\ e^{\frac{-(L-\mu)^2}{2\,\sigma^2}}\ dL + \mu \int_{L_F}^{L_{max}} f(L)\ dL$$

$$X_{11} = \frac{-\sigma}{\sqrt{2\pi}} \int_{L_F}^{L_{max}} \frac{-(L-\mu)}{\sigma^2}\ \ e^{\frac{-(L-\mu)^2}{2\,\sigma^2}}\ dL + \mu\,(F(L_{max}) - F(L_F))$$

$$X_{11} = \mu\,(F(L_{max}) - F(L_F)) + \frac{-\sigma}{\sqrt{2\pi}} \left[e^{\frac{-(L-\mu)^2}{2\,\sigma^2}} \right]_{L_F}^{L_{max}}$$

$$X_{11} = \mu\,(F(L_{max}) - F(L_F)) - \frac{\sigma}{\sqrt{2\pi}} \left[e^{\frac{-(L_{max}-\mu)^2}{2\,\sigma^2}} - e^{\frac{-(L_F-\mu)^2}{2\,\sigma^2}} \right]$$

$$E_{ue} = \mu\,((F(L_{max}) - F(L_F)) - \frac{\sigma}{\sqrt{2\pi}} \left[e^{\frac{-(L_{max}-\mu)^2}{2\,\sigma^2}} - e^{\frac{-(L_F-\mu)^2}{2\,\sigma^2}} \right] - L_F\ (F(L_{max}) - F(L_F))$$

$$E_{ue} = (\mu - L_F)\ (F(L_{max}) - F(L_F)) - \frac{\sigma}{\sqrt{2\pi}} \left[e^{\frac{-(L_{max}-\mu)^2}{2\,\sigma^2}} - e^{\frac{-(L_F-\mu)^2}{2\,\sigma^2}} \right]$$

$$\boxed{E_{ue} = (\mu - L_F)\ (F(L_{max}) - F(L_F)) - \frac{\sigma}{\sqrt{2\pi}} \left[e^{\frac{-(L_{max}-\mu)^2}{2\,\sigma^2}} - e^{\frac{-(L_F-\mu)^2}{2\,\sigma^2}} \right]}$$

B.2 Probabilistic Model of the Load Reduction using Exponential Distribution

- Assume that load reduction Power is L and $L \sim Exp(\lambda)$.
- Assume that the Load reduction Power is $L_{min} \leq L \leq L_{max}$.
- The pdf and cdf of the exponential distribution is shown in(B.8) and (B.9) while the expected (mean) and the variance shown in (B.10) and (B.11) respectively.

$$f(x) = \lambda \; e^{-\lambda \; x} \; u(x) \tag{B.4}$$

$$F(x) = P(X \leq x) = \int_{-\infty}^{x} \lambda \; e^{-\lambda \; m} \; u(m) \; dm$$
$$F(x) = \int_{0}^{x} \lambda \; e^{-\lambda \; m} \; dm = \left[-e^{-\lambda \; m}\right]_{0}^{x}$$

$$F(x) = (1 - e^{-\lambda \; x}) \; u(x) \tag{B.5}$$

$$E(X) = \int_{-\infty}^{\infty} x \; f(x) \; dx = \frac{1}{\lambda} \tag{B.6}$$

$$Var(X) = E(X^2) - E(X)^2 = \frac{1}{\lambda^2} \tag{B.7}$$

B.2.1 Overestimation of L

From Fig(B.5) it is obvious that the forecast value is grater than the actual value ($L_F > L$). which leads to financial loss due to buying unplanned power from other utilities. To account for this events we should calculate the expected value of $L_F > L$ and merge it with our cost model for the load reduction. But according to fig(B.2) and fig(B.4), this will happen only in the region from (L_{min}, L_F). Hence, the expected value of overestimation will be as follows:

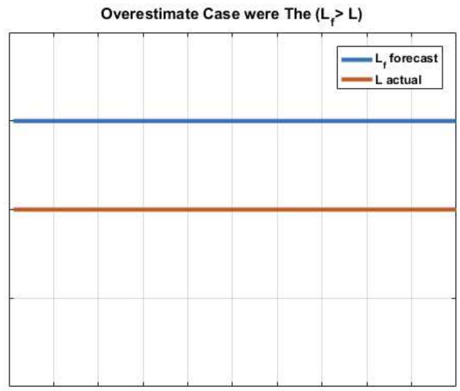

Figure B.5: Over estimate case where the forecast Value L_F is grater than the actual value L

$$E_{oe} = \int_{-\infty}^{\infty} max(0, L_F - L)\ f(L)\ dL$$
$$E_{oe} = \int_{L_{min}}^{L_F} (L_F - L)\ f(L)\ dL$$
$$E_{oe} = L_F \int_{L_{min}}^{L_F} f(L)\ dL - \int_{L_{min}}^{L_F} L\ f(L)\ dL$$
$$E_{oe} = L_F\ (F(L_F) - F(L_{min})) - X_{11}$$

$$X_{11} = \int_{L_{min}}^{L_F} L\ f(L)\ dL$$
$$X_{11} = \int_{L_{min}}^{L_F} L\ \lambda\ e^{-\lambda\ L}\ u(L)\ dL$$

Using Integration by Parts:

$$\int_a^b u\ dv = [u\ v]_a^b - \int_a^b v\ du$$
$$u = L \Rightarrow du = dL$$
$$dv = \lambda\ e^{-\lambda\ L}\ dL \Rightarrow v = -e^{-\lambda\ L}$$

$$X_{11} = \left[-L\ e^{-\lambda\ L}\right]_{L_{min}}^{L_F} - \int_{L_{min}}^{L_F} -e^{-\lambda\ L}\ dL$$
$$X_{11} = L_{min}\ e^{-\lambda\ L_{min}} - L_F\ e^{-\lambda\ L_F} - \frac{1}{\lambda}(e^{-\lambda\ L_F} - e^{-\lambda\ L_{min}})$$

$$E_{oe} = L_F\ (F(L_F) - F(L_{min})) - (L_{min}\ e^{-\lambda\ L_{min}} - L_F\ e^{-\lambda\ L_F} - \frac{1}{\lambda}(e^{-\lambda\ L_F} - e^{-\lambda\ L_{min}}))$$
$$E_{oe} = (L_F - L_{min})\ e^{-\lambda\ L_{min}} - \frac{1}{\lambda}(F(L_F) - F(L_{min}))$$

$$\boxed{E_{oe} = (L_F - L_{min})\ e^{-\lambda\ L_{min}} - \frac{1}{\lambda}(F(L_F) - F(L_{min}))}$$

B.2.2 Underestimation of L

From Fig(B.6) it is obvious that the forecast value is less than the actual value ($L_F < L$). which leads to a problem of wasting the available power by not using it. To account for this events we should calculate the expected value of $L_F < L$ and merge it with our cost model for the load reduction. But according to fig(B.2) and fig(B.4), this will happen only in the region from (L_F, L_{max}). Hence, the expected value of underestimation will be as follows:

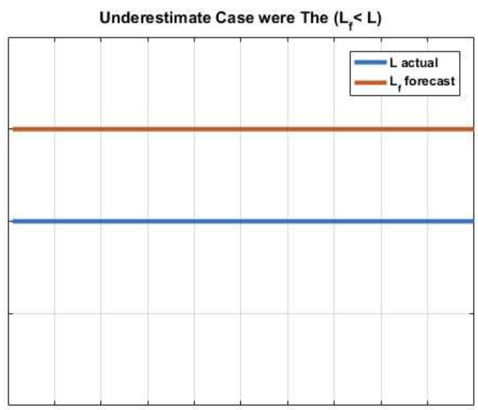

Figure B.6: Over estimate case where the forecast Value L_F is smaller than the actual value L

$$E_{ue} = \int_{-\infty}^{\infty} max(0, L - L_F)\ f(L)\ dL$$

$$E_{ue} = \int_{L_F}^{L_{max}} (L - L_F)\ f(L)\ dL$$

$$E_{ue} = \int_{L_F}^{L_{max}} L\ f(L)\ dL - L_F \int_{L_F}^{L_{max}} f(L)\ dL$$

$$E_{ue} = X_{11} - L_F\ (F(L_{max}) - F(L_F))$$

$$X_{11} = \int_{L_F}^{L_{max}} L\ f(L)\ dL$$

$$X_{11} = \int_{L_F}^{L_{max}} L\ f(L)\ dL$$
$$X_{11} = \int_{L_F}^{L_{max}} L\ \lambda\ e^{-\lambda\ L}\ u(L)\ dL$$

Using Integration by Parts:

$$\int_a^b u\ dv = [u\ v]_a^b - \int_a^b v\ du$$
$$u = L \Rightarrow du = dL$$
$$dv = \lambda\ e^{-\lambda\ L}\ dL \Rightarrow v = -e^{-\lambda\ L}$$

$$X_{11} = \left[-L\ e^{-\lambda\ L}\right]_{L_F}^{L_{max}} - \int_{L_F}^{L_{max}} -e^{-\lambda\ L}\ dL$$
$$X_{11} = L_F\ e^{-\lambda\ L_F} - L_{max}\ e^{-\lambda\ L_{max}} - \frac{1}{\lambda}(e^{-\lambda\ L_{max}} - e^{-\lambda\ L_F})$$

$$E_{ue} = L_F\ e^{-\lambda\ L_F} - L_{max}\ e^{-\lambda\ L_{max}} - \frac{1}{\lambda}(e^{-\lambda\ L_{max}} - e^{-\lambda\ L_F}) - L_F\ (F(L_{max}) - F(L_F))$$

$$\boxed{E_{ue} = (L_F - L_{max})\ e^{-\lambda\ L_{max}} - \frac{1}{\lambda}(F(L_F) - F(L_{max}))}$$

B.3 Probabilistic Model of the Load Reduction using Weibull Distribution

- Assume that load reduction Power is L and $L \sim W(c,k)$.
- Assume that the Load reduction Power is $L_{min} \leq L \leq L_{max}$.
- The pdf and cdf of the weibull distribution is shown in(B.8) and (B.9) while the expected (mean) and the variance shown in (B.10) and (B.11) respectively.

$$f(x) = \frac{k}{c}\ \left(\frac{x}{c}\right)^{k-1}\ exp[-(\frac{x}{c})^k]\ u(x) \tag{B.8}$$

$$F(x) = P(X \leq x) = \int_{-\infty}^{x} \frac{k}{c}\ \left(\frac{m}{c}\right)^{k-1}\ exp[-(\frac{m}{c})^k]\ u(m)\ dm$$
$$F(x) = \int_{0}^{x} \frac{k}{c}\ \left(\frac{m}{c}\right)^{k-1}\ exp[-(\frac{m}{c})^k]\ dm = \Big[-exp[-(\frac{m}{c})^k]\Big]_0^x$$

$$F(x) = (1 - exp[-(\frac{m}{c})^k])\ u(x) \tag{B.9}$$

$$E(X^n) = \int_{-\infty}^{\infty} m^n\ \frac{k}{c}\ \left(\frac{m}{c}\right)^{k-1}\ exp[-(\frac{m}{c})^k]\ u(m)\ dm$$

$$(\frac{m}{c})^k = Z\ \Rightarrow\ \frac{m}{c} = Z^{\frac{1}{k}} \Rightarrow\ m^n = c^n\ Z^{\frac{n}{k}}$$
$$dZ = \frac{k}{c}\ (\frac{m}{c})^{k-1}\ dm$$

$$E(X^n) = c^n\ \int_0^{\infty} Z^{\frac{n}{k}}\ exp[-Z]\ dZ$$
$$E(X^n) = c^n\ \int_0^{\infty} Z^{\frac{n}{k}+1-1}\ exp[-Z]\ dZ = c^n\ \Gamma(1+\frac{n}{k})$$

$$E(X^n) = c^n \; \Gamma(1 + \frac{n}{k}) \tag{B.10}$$

$$Var(X) = E(X^2) - E(X)^2 = c^2 \; (\Gamma(1 + \frac{2}{k}) - (\Gamma(1 + \frac{1}{k}))^2) \tag{B.11}$$

B.3.1 Overestimation of L

From Fig(B.5) it is obvious that the forecast value is grater than the actual value ($L_F > L$). which leads to financial loss due to buying unplanned power from other utilities. To account for this events we should calculate the expected value of $L_F > L$ and merge it with our cost model for the load reduction. But according to fig(B.2) and fig(B.4), this will happen only in the region from (L_{min}, L_F). Hence, the expected value of overestimation will be as follows:

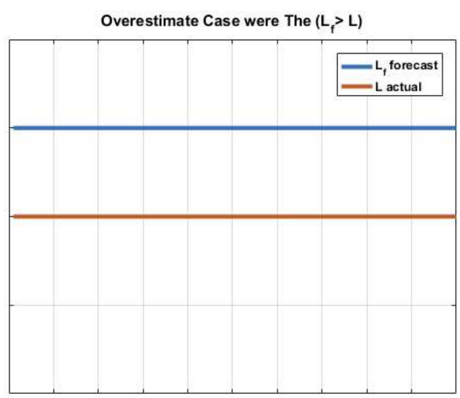

Figure B.7: Over estimate case where the forecast Value L_F is grater than the actual value L

$$E_{oe} = \int_{-\infty}^{\infty} max(0, L_F - L) \; f(L) \; dL$$

$$E_{oe} = \int_{L_{min}}^{L_F} (L_F - L) \; f(L) \; dL$$

$$E_{oe} = L_F \int_{L_{min}}^{L_F} f(L) \; dL - \int_{L_{min}}^{L_F} L \; f(L) \; dL$$

$$E_{oe} = L_F \; (F(L_F) - F(L_{min})) - X_{11}$$

$$X_{11} = \int_{L_{min}}^{L_F} L \ f(L) \ dL$$

$$X_{11} = \int_{L_{min}}^{L_F} L \ \frac{k}{c} \ \left(\frac{L}{c}\right)^{k-1} \ exp[-(\frac{L}{c})^k] \ u(L) \ dL$$

Gamma function is shown here:

$$\Gamma(\alpha, x) = \int_x^{\infty} y^{\alpha-1} \ exp(-y) \ dy$$

$$\int_a^b y^{\alpha-1} \ exp(-y) \ dy = \int_a^{\infty} y^{\alpha-1} \ exp(-y) \ dy - \int_b^{\infty} y^{\alpha-1} \ exp(-y) \ dy$$
$$= \Gamma(\alpha, a) - \Gamma(\alpha, b)$$

$$X_{11} = \int_{L_{min}}^{L_F} L \ \frac{k}{c} \ \left(\frac{L}{c}\right)^{k-1} \ exp[-(\frac{L}{c})^k] \ \ dL$$

$$Z = (\frac{L}{c})^k \Rightarrow L = c \ Z^{\frac{1}{k}}$$
$$dZ = \frac{k}{c} \ \ (\frac{L}{c})^{k-1} \ dL$$

$$X_{11} = \int_{(\frac{L_{min}}{c})^k}^{(\frac{L_F}{c})^k} c \ Z^{\frac{1}{k}} \ exp[-Z] \ \ dZ$$
$$X_{11} = \int_{(\frac{L_{min}}{c})^k}^{(\frac{L_F}{c})^k} c \ Z^{\frac{1}{k}+1-1} \ exp[-Z] \ \ dZ$$
$$X_{11} = c \ (\Gamma(1 + \frac{1}{k}, (\frac{L_{min}}{c})^k) - \Gamma(1 + \frac{1}{k}, (\frac{L_F}{c})^k))$$

$$E_{oe} = L_F \ (F(L_F) - F(L_{min})) - c \ (\Gamma(1 + \frac{1}{k}, (\frac{L_{min}}{c})^k) - \Gamma(1 + \frac{1}{k}, (\frac{L_F}{c})^k))$$

$$\boxed{E_{oe} = L_F \ (F(L_F) - F(L_{min})) - c \ (\Gamma(1 + \frac{1}{k}, (\frac{L_{min}}{c})^k) - \Gamma(1 + \frac{1}{k}, (\frac{L_F}{c})^k))}$$

B.3.2 Underestimation of L

From Fig(B.5) it is obvious that the forecast value is less than the actual value ($L_F < L$). which leads to a problem of wasting the available power by not using it. To account for this events we should calculate the expected value of $L_F < L$ and merge it with our cost model for the load reduction. But according to fig(B.2) and fig(B.4), this will happen only in the region from (L_F, L_{max}). Hence, the expected value of underestimation will be as follows:

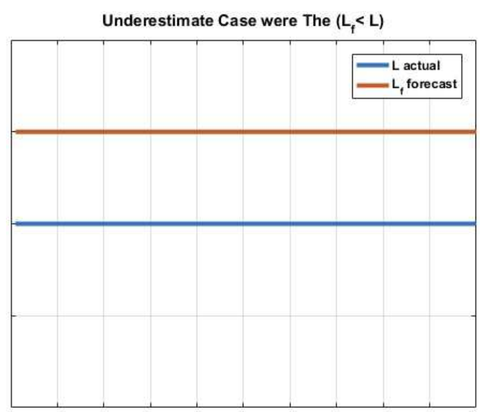

Figure B.8: Over estimate case where the forecast Value L_F is grater than the actual value L

$$E_{ue} = \int_{-\infty}^{\infty} max(0, L - L_F)\ f(L)\ dL$$

$$E_{ue} = \int_{L_F}^{L_{max}} (L - L_F)\ f(L)\ dL$$

$$E_{ue} = \int_{L_F}^{L_{max}} L\ f(L)\ dL - L_F \int_{L_F}^{L_{max}} f(L)\ dL$$

$$E_{ue} = X_{11} - L_F\ (F(L_{max}) - F(L_F))$$

$$X_{11} = \int_{L_F}^{L_{max}} L\ f(L)\ dL$$

$$X_{11} = \int_{L_F}^{L_{max}} L \ f(L) \ dL$$

$$X_{11} = \int_{L_F}^{L_{max}} L \ \frac{k}{c} \ \left(\frac{L}{c}\right)^{k-1} \ exp[-(\frac{L}{c})^k] \ u(L) \ dL$$

Gamma function is shown here:

$$\Gamma(\alpha, x) = \int_x^{\infty} y^{\alpha-1} \ exp(-y) \ dy$$

$$\int_a^b y^{\alpha-1} \ exp(-y) \ dy = \int_a^{\infty} y^{\alpha-1} \ exp(-y) \ dy - \int_b^{\infty} y^{\alpha-1} \ exp(-y) \ dy$$
$$= \Gamma(\alpha, a) - \Gamma(\alpha, b)$$

$$X_{11} = \int_{L_F}^{L_{max}} L \ \frac{k}{c} \ \left(\frac{L}{c}\right)^{k-1} \ exp[-(\frac{L}{c})^k] \ \ dL$$

$$Z = (\frac{L}{c})^k \Rightarrow L = c \ Z^{\frac{1}{k}}$$
$$dZ = \frac{k}{c} \ \ (\frac{L}{c})^{k-1} \ dL$$

$$X_{11} = \int_{(\frac{L_F}{c})^k}^{(\frac{L_{max}}{c})^k} c \ Z^{\frac{1}{k}} \ exp[-Z] \ \ dZ$$

$$X_{11} = \int_{(\frac{L_F}{c})^k}^{(\frac{L_{max}}{c})^k} c \ Z^{\frac{1}{k}+1-1} \ exp[-Z] \ \ dZ$$

$$X_{11} = c \ (\Gamma(1 + \frac{1}{k}, (\frac{L_F}{c})^k) - \Gamma(1 + \frac{1}{k}, (\frac{L_{max}}{c})^k))$$

$$E_{ue} = c \ (\Gamma(1 + \frac{1}{k}, (\frac{L_F}{c})^k) - \Gamma(1 + \frac{1}{k}, (\frac{L_{max}}{c})^k)) - L_F \ (F(L_{max}) - F(L_F))$$

$$\boxed{E_{ue} = c \ (\Gamma(1 + \frac{1}{k}, (\frac{L_F}{c})^k) - \Gamma(1 + \frac{1}{k}, (\frac{L_{max}}{c})^k)) - L_F \ (F(L_{max}) - F(L_F))}$$

Appendix C

Test Systems Data

C.1 Economic Dispatch Test Systems

C.1.1 Three Unit System

This system consists of three generation units with quadratic cost functions the demand load is 850 MW. The unit characteristics of cost coefficients, and generators operating limits were taken from [104].

Table C.1: Generation units cost coefficients and capacity limits

Unit	a_i	b_i	c_i	P_i^{min}	P_i^{max}
1	0.001562	7.92	561	100	600
2	0.00482	7.97	78	50	200
3	0.00194	7.85	310	100	400

C.1.2 Three Unit System with Valve Point Effect

This system consists of three generation units with quadratic cost functions and the effects of valve-point loading is considered. The unit characteristics cost coefficients, and generators operating limits were taken from [104]. The demand load is 850 MW.

Table C.2: Generation units cost coefficients and capacity limits

Unit	a_i	b_i	c_i	e_i	f_i	P_i^{min}	P_i^{max}
1	0.001562	7.92	561	300	0.0315	100	600
2	0.00482	7.97	78	150	0.063	50	200
3	0.00194	7.85	310	200	0.042	100	400

C.1.3 Six Unit System

This test system consists of six generation units with quadratic cost functions, transmission losses, ramp rates limits and prohibited operating zones. The unit characteristics cost coefficients, and generators operating limits were taken from [40]. The demand load is 1263 MW. The power loss coefficients are in per unit and the base is equal to the system base which is equal to 100 MVA.

Table C.3: Generation units cost coefficients, capacity limits, prohibited operation zones, and ramp rate limits

Unit	a_i	b_i	c_i	P_i^{min}	$P_{i,1}^l$	$P_{i,1}^u$	$P_{i,2}^l$	$P_{i,2}^u$	P_i^{max}	$P_{i\ now}$	DR_i	UR_i
1	0.007	7	240	100	210	240	350	380	500	440	120	80
2	0.0095	10	200	50	90	110	140	160	200	170	90	50
3	0.009	8.5	220	80	150	170	210	240	300	200	100	65
4	0.009	11	200	50	80	90	110	120	150	150	90	50
5	0.008	10.5	220	50	90	110	140	150	200	190	90	50
6	0.0075	12	190	50	75	85	100	105	120	110	90	50

Power loss coefficients:

$$B_{ij} = \begin{bmatrix} 0.0017 & 0.0012 & 0.0007 & -0.0001 & -0.0005 & -0.0002 \\ 0.0012 & 0.0014 & 0.0009 & 0.0001 & -0.0006 & -0.0001 \\ 0.0007 & 0.0009 & 0.0031 & 0 & -0.001 & -0.0006 \\ -0.0001 & 0.0001 & 0 & 0.0024 & -0.0006 & -0.0008 \\ -0.0005 & -0.0006 & -0.001 & -0.0006 & 0.0129 & -0.0002 \\ -0.0002 & -0.0001 & -0.0006 & -0.0008 & -0.0002 & 0.015 \end{bmatrix}$$

$$B_{0j} = \begin{bmatrix} -0.0003908 & -0.0001297 & 0.0007047 & 5.91E-05 & 0.0002161 & -0.0006635 \end{bmatrix}$$

$$B_{00} = 0.0056$$

C.1.4 Thirteen Unit System with Valve Point Effect

This system consists of thirteen generation units with quadratic cost functions and the effects of valve-point loading is considered. The unit characteristics cost coefficients, and generators operating limits were taken from [104]. The demand load is 1800 MW.

Table C.4: Generation units cost coefficients and capacity limits

Unit	a_i	b_i	c_i	e_i	f_i	P_i^{min}	P_i^{max}
1	0.00028	8.1	550	300	0.035	0	680
2	0.00056	8.1	309	200	0.042	0	360
3	0.00056	8.1	307	200	0.042	0	360
4	0.00324	7.74	240	150	0.063	60	180
5	0.00324	7.74	240	150	0.063	60	180
6	0.00324	7.74	240	150	0.063	60	180
7	0.00324	7.74	240	150	0.063	60	180
8	0.00324	7.74	240	150	0.063	60	180
9	0.00324	7.74	240	150	0.063	60	180
10	0.00284	8.6	126	100	0.084	40	120
11	0.00284	8.6	126	100	0.084	40	120
12	0.00284	8.6	126	100	0.084	55	120
13	0.00284	8.6	126	100	0.084	55	120

C.1.5 Wind Turbine and Load Reduction Cost Model Data

Wind turbine cost model data and load reduction cost model data based on Normal distribution are shown in Table (C.5) and Table (C.6) respectively. These are the default model data for solving the economic dispatch problem and if there are any changes, they will be specified.

Table C.5: Wind turbine cost model data for economic dispatch problem

k	c	k_p	k_r	d	V_i	V_r	V_0	W_r
2	10	6	10	8	5	15	45	165

Table C.6: Load reduction cost model data for economic dispatch problem

h	kue	koe	μ	σ	$L_{min}(MW)$	$L_{max}(MW)$
9	7	11	75	5	0	200

C.2 Unit Commitment Test Systems

C.2.1 Four Unit System

This system consists of four generation units with quadratic cost functions. The unit characteristics cost coefficients, generators operating limits, minimum up time, minimum down time, hot start cost, cold start cost and initial state were taken from [64].

Table C.7: Generation Units characteristics for four units system

Unit	1	2	3	4
P_{max} (MW)	300	250	80	60
P_{min} (MW)	75	60	25	20
a	0.0021	0.0042	0.0018	0.0034
b	16.83	16.95	20.74	23.6
c	684.74	585.62	213	252
Minimum up time (h)	4	3	2	1
Minimum down time (h)	5	5	4	1
Hot start up cost ($)	500	170	150	0
Cold start up cost ($)	1100	400	350	0.02
Cold start time(h)	5	5	4	0
Initial state	8	8	-5	-6

Table C.8: Load Demand (MW)

Hour	1	2	3	4	5	6	7	8
Load (MW)	450	530	600	540	400	280	290	500

C.2.2 Ten Unit System

This system consists of ten generation units with quadratic cost functions. The unit characteristics cost coefficients, generators operating limits, minimum up time, minimum down time, hot start cost, cold start cost and initial state were taken from [64].

Table C.9: Generation Units characteristics for ten units system

Unit	1	2	3	4	5	6	7	8	9	10
P_{max} (MW)	455	455	130	130	162	80	85	55	55	55
P_{min} (MW)	150	150	20	20	25	20	25	10	10	10
a	0.00048	0.00031	0.002	0.00211	0.00398	0.00712	0.00079	0.00413	0.00222	0.00173
b	16.19	17.26	16.6	16.5	19.7	22.26	27.74	25.92	27.27	27.79
c	1000	970	700	680	450	370	480	660	665	670
Minimum up time (h)	8	8	5	5	6	3	3	1	1	1
Minimum down time (h)	8	8	5	5	6	3	3	1	1	1
Hot start up cost ($)	4500	5000	550	560	900	170	260	30	30	30
Cold start up cost ($)	9000	10000	1100	1120	1800	340	520	60	60	60
Cold start time(h)	5	5	4	4	4	2	2	0	0	0
Initial state	8	8	-5	-5	-6	-3	-3	-1	-1	-1

Table C.10: Load Demand (MW)

Hour	1	2	3	4	5	6	7	8	9	10	11	12
Load	700	750	850	950	1000	1100	1150	1200	1300	1400	1450	1500
Hour	13	14	15	16	17	18	19	20	21	22	23	24
Load	1400	1300	1200	1050	1000	1100	1200	1400	1300	1100	900	800

C.2.3 Wind Turbine and Load Reduction Cost Model Data

Wind turbine cost model data and load reduction cost model data based on Normal distribution are shown in Table (C.11) and Table (C.12) respectively. These are the default model data for solving the unit commitment problem and if there are any changes, they will be specified.

Table C.11: Wind turbine cost model data for unit commitment problem

Test System	k	c	k_p	k_r	d	V_i	V_r	V_0	W_r
C.2.1	2	10	6	10	8	5	15	45	165
C.2.2	2	10	6	10	8	5	15	45	495

Table C.12: Load reduction cost model data for unit commitment problem

System	h	kue	koe	μ	σ	$L_{min}(MW)$	$L_{max}(MW)$
C.2.1	9	7	11	75	5	0	90
C.2.2	9	7	11	170	10	0	200

C.3 Fixed Head Hydrothermal Scheduling Test Systems

C.3.1 One Hydro Unit One Thermal Unit System

The study system consists of one thermal generation unit and one hydro generation unit with two periods of time. The data and load demand are given in [124].The water volume of the hydroplant is 100,000 acre-ft over the scheduling period and the fuel cost is 1.15 $/MBtu.

Thermal unit System:

$$H(P) = 0.0016\,P^2 + 8\,P + 500$$
$$150\,\text{MW} \leq P \leq 1500\,\text{MW}$$

Hydroplant:

$$q = 330 + 4.97\,P_H \quad \text{acre-ft/h}$$
$$\text{for} \qquad 0\ \text{MW} \leq P_H \leq 1000\ \text{MW}$$
$$q = 5300 + 12\,(P_H - 1000) + 0.05\,(P_H - 1000)^2 \quad \text{acre-ft/h}$$
$$\text{for} \quad 1000\ \text{MW} \leq P_H \leq 1100\ \text{MW}$$
$$\text{Power Loss:} \quad P_L = 0.00008\,P_H^2$$

The load demand is as follows:

$$\text{12 am-12 pm:} \quad P_D = 1200\ \text{MW}$$
$$\text{12 pm-12 am:} \quad P_D = 1500\ \text{MW}$$

The wind forecast for C.3.2 system is as follows:

$$\text{12 am-12 pm:} \quad w^F = 40\ \text{MW}$$
$$\text{12 pm-12 am:} \quad w^F = 47.5\ \text{MW}$$

The load reduction forecast for C.3.2 system is as follows:

$$\text{12 am-12 pm:} \quad L^F = 0 \text{ MW}$$
$$\text{12 pm-12 am:} \quad L^F = 20 \text{ MW}$$

C.3.2 One Hydro Unit Three Thermal Unit System

The study system consists of three thermal generation units and one hydro generation unit. The data and load demand are given in [35]. The load demand is shown in Table (C.15). The total water volume of the hydroplant is 25,000 m^3 and the fuel cost is 1 \$/MBtu.

Thermal units System:

$$H(P_1) = 0.01\,P_1^2 + 0.1\,P_1 + 100$$
$$H(P_2) = 0.02\,P_2^2 + 0.1\,P_2 + 120$$
$$H(P_3) = 0.01\,P_3^2 + 0.2\,P_3 + 150$$

Hydroplant:

$$q = 140 + 20\,P_H + 0.06\,P_H^2 \quad m^3/h$$

$$50\,\text{MW} \le P_1 \le 200\,\text{MW}$$
$$40\,\text{MW} \le P_2 \le 170\,\text{MW}$$
$$30\,\text{MW} \le P_3 \le 215\,\text{MW}$$
$$10\,\text{MW} \le P_H \le 100\,\text{MW}$$

Table C.13: Load demand for test system 2

Hour	Load	Hour	Load	Hour	Load	Hour	Load
1	175	7	390	13	565	19	375
2	190	8	410	14	540	20	340
3	220	9	440	15	500	21	300
4	280	10	475	16	450	22	250
5	320	11	525	17	425	23	200
6	360	12	550	18	400	24	180

Table C.14: Wind forecast for test system 2

Hour	P_w^F	Hour	P_w^F	Hour	P_w^F	Hour	P_w^F
1	0	7	50	13	40	19	20
2	0	8	50	14	20	20	10
3	0	9	50	15	20	21	10
4	30	10	20	16	20	22	10
5	30	11	20	17	20	23	0
6	30	12	40	18	20	24	0

Table C.15: Load reduction forecast for test system 2

Hour	P_{LR}^F	Hour	P_{LR}^F	Hour	P_{LR}^F	Hour	P_{LR}^F
1	0	7	0	13	18	19	0
2	0	8	0	14	20	20	0
3	0	9	0	15	0	21	0
4	0	10	18	16	0	22	0
5	0	11	20	17	0	23	0
6	0	12	20	18	0	24	0

C.3.3 Wind Turbine and Load Reduction Cost Model Data

Wind turbine cost model data and load reduction cost model data based on Normal distribution are shown in Table (C.16) and Table (C.17) respectively. These are the default model data for solving the fixed head hydrothermal scheduling problem and if there are any changes, they will be specified.

Table C.16: Wind turbine data used for hydrothermal scheduling problem benchmark test systems

Test System	k	c	k_p	k_r	d	V_i	V_r	V_0	W_r
C.3.1	2	10	6	11	8	5	15	45	50
C.3.2	2	10	3	6	4	5	15	45	50

Table C.17: Load reduction cost model data for fixed head hydrothermal scheduling problem

Test System	h	kue	koe	μ	σ	$L_{min}(MW)$	$L_{max}(MW)$
C.3.1	9	7	11	17	1	0	20
C.3.2	4.5	3	6	17	1	0	20

C.4 Optimal Power Flow Test Systems

C.4.1 Wind Turbine and Load Reduction Cost Model Data

Wind turbine cost model data and load reduction cost model data based on Normal distribution are shown in Table (C.18) and Table (C.19) respectively. These are the default model data for solving the optimal power flow problem and if there are any changes, they will be specified.

Table C.18: Wind turbine data used for optimal power flow problem benchmark test systems

Test System	k	c	k_p	k_r	d	V_i	V_r	V_0	W_r	Bus Number
IEEE 30-Bus	2	10	0.6	1.75	0.9	4	11.5	30	20	7

Table C.19: Load reduction cost model data for optimal power flow problem

Test System	h	kue	koe	μ	σ	$L_{min}(MW)$	$L_{max}(MW)$	Bus Number
IEEE 30-Bus	1	0.6	1.75	9.42	1.88	0	15.06	5

Bibliography

[1] Saleh Y. Abujarad, M.W. Mustafa, and J.J. Jamian. Recent approaches of unit commitment in the presence of intermittent renewable energy resources: A review. *Renewable and Sustainable Energy Reviews*, 70:215 – 223, 2017.

[2] S. K. Agarwal and I. J. Nagrath. Optimal scheduling of hydrothermal systems. *Electrical Engineers, Proceedings of the Institution of*, 119(2):169–173, February 1972.

[3] Venkataramana Ajjarapu. *Computational techniques for voltage stability assessment and control*. Springer, 2007.

[4] O. Alsac, J. Bright, M. Prais, and B. Stott. Further developments in lp-based optimal power flow. *Power Systems, IEEE Transactions on*, 5(3):697–711, Aug 1990.

[5] O. Alsac and B. Stott. Optimal load flow with steady-state security. *Power Apparatus and Systems, IEEE Transactions on*, PAS-93(3):745–751, May 1974.

[6] T. Back. *Evolutionary Algorithms in Theory and Practice: Evolution Strategies, Evolutionary Programming, Genetic Algorithms*. Oxford University Press, 1996.

[7] A.K. Barisal. Dynamic search space squeezing strategy based intelligent algorithm solutions to economic dispatch with multiple fuels. *International Journal of Electrical Power & Energy Systems*, 45(1):50 – 59, 2013.

[8] A. Bhattacharya and P. K. Chattopadhyay. Hybrid differential evolution with biogeography-based optimization for solution of economic load dispatch. *IEEE Transactions on Power Systems*, 25(4):1955–1964, Nov 2010.

[9] A. Bhattacharya and P.K. Chattopadhyay. Biogeography-based optimization for different economic load dispatch problems. *Power Systems, IEEE Transactions on*, 25(2):1064–1077, May 2010.

[10] A. Bhattacharya and P.K. Chattopadhyay. Application of biogeography-based optimisation to solve different optimal power flow problems. *Generation, Transmission Distribution, IET*, 5(1):70–80, Jan 2011.

[11] A. Bhattacharya and P.K. Chattopadhyay. Application of biogeography-based optimisation to solve different optimal power flow problems. *Generation, Transmission Distribution, IET*, 5(1):70–80, Jan 2011.

[12] R.C. Burchett, H.H. Happ, and D. R. Vierath. Quadratically convergent optimal power flow. *Power Apparatus and Systems, IEEE Transactions on*, PAS-103(11):3267–3275, Nov 1984.

[13] R.C. Burchett, H.H. Happ, D. R. Vierath, and K.A. Wirgau. Developments in optimal power flow. *Power Apparatus and Systems, IEEE Transactions on*, PAS-101(2):406–414, Feb 1982.

[14] J Carpentier. Optimal power flows. *International Journal of Electrical Power & Energy Systems*, 1(1):3 – 15, 1979.

[15] M. Carrion and J. M. Arroyo. A computationally efficient mixed-integer linear formulation for the thermal unit commitment problem. *IEEE Transactions on Power Systems*, 21(3):1371–1378, Aug 2006.

[16] S.-K. Chang, F. Albuyeh, M.L. Gilles, G.E. Marks, and K. Kato. Optimal real-time voltage control. *Power Systems, IEEE Transactions on*, 5(3):750–758, Aug 1990.

[17] C. H. Chen and S. N. Yeh. Particle swarm optimization for economic power dispatch with valve-point effects. In *2006 IEEE/PES Transmission Distribution Conference and Exposition: Latin America*, pages 1–5, Aug 2006.

[18] H. Chen, H. Ngan, and Y. Zhang. *Power System Optimization: Large-scale Complex Systems Approaches*. Wiley, 2016.

[19] Po-Hung Chen and Hong-Chan Chang. Large-scale economic dispatch by genetic algorithm. *Power Systems, IEEE Transactions on*, 10(4):1919–1926, Nov 1995.

[20] Chuan-Ping Cheng, Chih-Wen Liu, and Chun-Chang Liu. Unit commitment by lagrangian relaxation and genetic algorithms. *IEEE Transactions on Power Systems*, 15(2):707–714, May 2000.

[21] Arthur I. Cohen and Miki Yoshimura. A branch-and-bound algorithm for unit commitment. *Power Apparatus and Systems, IEEE Transactions on*, PAS-102(2):444–451, Feb 1983.

[22] I. N. da Silva and L. Nepomuceno. An efficient neural approach to economic load dispatch in power systems. In *2001 Power Engineering Society Summer Meeting. Conference Proceedings (Cat. No.01CH37262)*, volume 2, pages 1269–1274 vol.2, July 2001.

[23] K. Dasgupta, S. Banerjee, and C. K. Chanda. Short-term hydrothermal scheduling using time varying acceleration coefficient based particle swarm optimization with constriction factor and inertia weight approach. In *2015 International Conference on Energy, Power and Environment: Towards Sustainable Growth (ICEPE)*, pages 1–6, June 2015.

[24] M. Djukanovic, M. Calovic, B. Milosevic, and D. J. Sobajic. Neural-net based real-time economic dispatch for thermal power plants. *IEEE Transactions on Energy Conversion*, 11(4):755–761, Dec 1996.

[25] R. Doherty, E. Denny, and M. O'Malley. System operation with a significant wind power penetration. In *Power Engineering Society General Meeting, 2004. IEEE*, pages 1002–1007 Vol.1, June 2004.

[26] H.W. Dommel and W.F. Tinney. Optimal power flow solutions. *Power Apparatus and Systems, IEEE Transactions on*, PAS-87(10):1866–1876, Oct 1968.

[27] M. Dorigo, V. Maniezzo, and A. Colorni. Ant system: optimization by a colony of cooperating agents. *Systems, Man, and Cybernetics, Part B: Cybernetics, IEEE Transactions on*, 26(1):29–41, Feb 1996.

[28] M. Dorigo and T. Stutzle. *Ant Colony Optimization*. A Bradford book. BRADFORD BOOK, 2004.

[29] R. Eberhart and J. Kennedy. A new optimizer using particle swarm theory. In *Micro Machine and Human Science, 1995. MHS '95., Proceedings of the Sixth International Symposium on*, pages 39–43, Oct 1995.

[30] A.E. Eiben. *Parallel Problem Solving from Nature - PPSN V: 5th International Conference, Amsterdam, The Netherlands, September 27-30, 1998, Proceedings*. Lecture Notes in Computer Science. Springer, 1998.

[31] M.E. El-Hawary. Optimal economic operation of large scale electric power systems: A review. In *Athens Power Tech, 1993. APT 93. Proceedings. Joint International Power Conference*, volume 1, pages 206–210, Sep 1993.

[32] A.A. Abou El Ela, M.A. Abido, and S.R. Spea. Optimal power flow using differential evolution algorithm. *Electric Power Systems Research*, 80(7):878 – 885, 2010.

[33] A.A. Abou El Ela, M.A. Abido, and S.R. Spea. Optimal power flow using differential evolution algorithm. *Electric Power Systems Research*, 80(7):878 – 885, 2010.

[34] B. Priya Esther and K. Sathish Kumar. A survey on residential demand side management architecture, approaches, optimization models and methods. *Renewable and Sustainable Energy Reviews*, 59:342 – 351, 2016.

[35] I. A. Farhat and M. E. El-Hawary. Short-term hydro-thermal scheduling using an improved bacterial foraging algorithm. In *Electrical Power Energy Conference (EPEC), 2009 IEEE*, pages 1–5, Oct 2009.

[36] I. A. Farhat and M. E. El-Hawary. Fixed-head hydro-thermal scheduling using a modified bacterial foraging algorithm. In *Electric Power and Energy Conference (EPEC), 2010 IEEE*, pages 1–6, Aug 2010.

[37] I. A. Farhat and M. E. El-Hawary. Short-term hydro-thermal scheduling with environmental considerations using bacterial foraging algorithm. In *Electrical and Computer Engineering (CCECE), 2011 24th Canadian Conference on*, pages 000425–000429, May 2011.

[38] R.A. Fernandes, H.H. Happ, and Wirgau K.A. Optimal reactive power flow for improved system operations. *International Journal of Electrical Power & Energy Systems*, 2(3):133 – 139, 1980.

[39] David B Fogel. *Evolutionary computation: toward a new philosophy of machine intelligence*, volume 1. John Wiley & Sons, 2006.

[40] Zwe-Lee Gaing. Particle swarm optimization to solving the economic dispatch considering the generator constraints. *Power Systems, IEEE Transactions on*, 18(3):1187–1195, Aug 2003.

[41] Zwe-Lee Gaing and Rung-Fang Chang. Security-constrained optimal power flow by mixed-integer genetic algorithm with arithmetic operators. In *Power Engineering Society General Meeting, 2006. IEEE*, pages 8 pp.–, 2006.

[42] Brahim Gasbaoui and Boumediène Allaoua. Ant colony optimization applied on combinatorial problem for optimal power flow solution. *Leonardo Journal of Sciences*, (14), 2009.

[43] Zong Woo Geem, Joong Hoon Kim, and GV Loganathan. A new heuristic optimization algorithm: harmony search. *Simulation*, 76(2):60–68, 2001.

[44] E. Gil, J. Bustos, and H. Rudnick. Short-term hydrothermal generation scheduling model using a genetic algorithm. *IEEE Transactions on Power Systems*, 18(4):1256–1264, Nov 2003.

[45] Xiaohong Guan, Ernan Ni, Renhou Li, and P. B. Luh. An optimization-based algorithm for scheduling hydrothermal power systems with cascaded reservoirs and discrete hydro constraints. *IEEE Transactions on Power Systems*, 12(4):1775–1780, Nov 1997.

[46] H. Hajian-Hoseinabadi, S.H. Hosseini, and Mehdi Hajian. Optimal power flow solution by a modified particle swarm optimization algorithm. In *Universities Power Engineering Conference, 2008. UPEC 2008. 43rd International*, pages 1–4, Sept 2008.

[47] Z. Hasan and M. E. El-Hawary. Optimal power flow by black hole optimization algorithm. In *2014 IEEE Electrical Power and Energy Conference*, pages 134–141, Nov 2014.

[48] Z. Hasan and M. E. El-Hawary. Comparison of wind turbine probabilistic model with negative model in economic dispatch problem using differential evolution (de). In *2016 IEEE Electrical Power and Energy Conference (EPEC)*, pages 1–5, Oct 2016.

[49] Z. Hasan and M. E. El-Hawary. Economic dispatch incorporating wind energy by bh, bbo and de. In *2016 IEEE Canadian Conference on Electrical and Computer Engineering (CCECE)*, pages 1–6, May 2016.

[50] Z. Hasan and M. E. El-Hawary. Unit commitment incorporating wind energy by bbo and ga. In *2016 IEEE Electrical Power and Energy Conference (EPEC)*, pages 1–7, Oct 2016.

[51] Z. Hasan and M. E. El-Hawary. Khums optimization algorithm. In *2017 IEEE 30th Canadian Conference on Electrical and Computer Engineering (CCECE)*, pages 1–5, April 2017.

[52] Z. Hasan and M.E. El-Hawary. Optimal power flow by black hole optimization algorithm. In *Electrical Power and Energy Conference (EPEC), 2014 IEEE*, pages 134–141, Nov 2014.

[53] Abdolreza Hatamlou. Black hole: A new heuristic optimization approach for data clustering. *Information Sciences*, 222:175 – 184, 2013. Including Special Section on New Trends in Ambient Intelligence and Bio-inspired Systems.

[54] J. Hetzer, D.C. Yu, and K. Bhattarai. An economic dispatch model incorporating wind power. *Energy Conversion, IEEE Transactions on*, 23(2):603–611, June 2008.

[55] John H Holland. *Adaptation in natural and artificial systems: An introductory analysis with applications to biology, control, and artificial intelligence.* U Michigan Press, 1975.

[56] E.C. Housos and G.D. Irisarri. A sparse variable metric optimization method applied to the solution of power system problems. *Power Apparatus and Systems, IEEE Transactions on*, PAS-101(1):195–202, Jan 1982.

[57] Yang Jin-Shyr and Chen Nanming. Short term hydrothermal coordination using multi-pass dynamic programming. *IEEE Transactions on Power Systems*, 4(3):1050–1056, Aug 1989.

[58] Mahmood Joorabian and Ehsan Afzalan. Optimal power flow under both normal and contingent operation conditions using the hybrid fuzzy particle swarm optimisation and neldermead algorithm (hfpsonm). *Applied Soft Computing*, 14, Part C(0):623 – 633, 2014.

[59] H. T. Kahraman, M. K. Dosoglu, U. Guvenc, S. Duman, and Y. Sonmez. Optimal scheduling of short-term hydrothermal generation using symbiotic organisms search algorithm. In *2016 4th International Istanbul Smart Grid Congress and Fair (ICSG)*, pages 1–5, April 2016.

[60] MOHD ROZELY Kalil, Ismail Musirin, and Muhammad Murtadha Othman. Ant colony based optimization technique for voltage stability control. In *Proceeding of the WSEAS International Conference on Power System, Lisbon, Portugal*, pages 149–154, 2002.

[61] Abdollah Kavousi-Fard, Mohammad-Reza Akbari-Zadeh, Farzaneh Kavousi-Fard, and Mohammad-Ali Rostami. Effect of wind turbine on the economic load dispatch problem considering the wind speed uncertainty. *J. Intell. Fuzzy Syst.*, 28(2):693–705, March 2015.

[62] J. Kennedy and R. Eberhart. Particle swarm optimization. In *Neural Networks, 1995. Proceedings., IEEE International Conference on*, volume 4, pages 1942–1948 vol.4, Nov 1995.

[63] Ahsan Raza Khan, Anzar Mahmood, Awais Safdar, Zafar A. Khan, and Naveed Ahmed Khan. Load forecasting, dynamic pricing and {DSM} in smart grid: A review. *Renewable and Sustainable Energy Reviews*, 54:1311 – 1322, 2016.

[64] S. Khanmohammadi, M. Amiri, and M. Tarafdar Haque. A new three-stage method for solving unit commitment problem. *Energy*, 35(7):3072 – 3080, 2010.

[65] A.H. Khazali and M. Kalantar. Optimal reactive power dispatch based on harmony search algorithm. *International Journal of Electrical Power & Energy Systems*, 33(3):684 – 692, 2011.

[66] Jong-Yul Kim, Hee-Myung Jeong, Hwa-Seok Lee, and June-Ho Park. Pc cluster based parallel pso algorithm for optimal power flow. In *Intelligent Systems Applications to Power Systems, 2007. ISAP 2007. International Conference on*, pages 1–6, Nov 2007.

[67] D.P. Kothari and J.S. Dhillon. *Power System Optimization*. Prentice-Hall of India, 2004.

[68] B. R. Kuanr, H. Shekhar, and N. Chakraborty. Imperialistic competition based short-term economic emission dispatch of hydrothermal power system with cascaded reservoirs. In *2015 IEEE Power, Communication and Information Technology Conference (PCITC)*, pages 795–800, Oct 2015.

[69] L.L. Lai, J.T. Ma, R. Yokoyama, and M. Zhao. Improved genetic algorithms for optimal power flow under both normal and contingent operation states. *International Journal of Electrical Power & Energy Systems*, 19(5):287 – 292, 1997.

[70] K. Y. Lee and J. b. Park. Application of particle swarm optimization to economic dispatch problem: Advantages and disadvantages. In *2006 IEEE PES Power Systems Conference and Exposition*, pages 188–192, Oct 2006.

[71] C. H. Liang, C.Y. Chung, K.P. Wong, and X.Z. Duan. Parallel optimal reactive power flow based on cooperative co-evolutionary differential evolution and power system decomposition. *Power Systems, IEEE Transactions on*, 22(1):249–257, Feb 2007.

[72] R. H. Liang and Y. Y. Hsu. Short-term hydro-scheduling using hopfield neural network. *IEE Proceedings - Generation, Transmission and Distribution*, 143(3):269–275, May 1996.

[73] Xian Liu and Wilsun Xu. Minimum emission dispatch constrained by stochastic wind power availability and cost. *Power Systems, IEEE Transactions on*, 25(3):1705–1713, Aug 2010.

[74] M. Madrigal and V.H. Quintana. An interior-point/cutting-plane method to solve unit commitment problems. *Power Systems, IEEE Transactions on*, 15(3):1022–1027, Aug 2000.

[75] Z. Mohammed and J. Talaq. Unit commitment by biogeography based optimization method. In *Electrotechnical Conference (MELECON), 2012 16th IEEE Mediterranean*, pages 551–554, March 2012.

[76] Zakaryia Mohammed and J Talaq. Economic dispatch by biogeography based optimization method. In *International Conference on Signal, Image Processing and Applications With workshop of ICEEA*, 2011.

[77] Zakaryia Mohammed and J Talaq. Economic dispatch by biogeography based optimization method. *IPCSIT IACSIT Press*, 21:161–165, 2011.

[78] Zakaryia Mohammed and J Talaq. Economic dispatch by biogeography based optimization method. In *International Conference on Signal, Image Processing and Applications With workshop of ICEEA*, 2011.

[79] S. Mokhtari, J. Sing, and B. Wollenberg. A unit commitment expert system [power system control]. *Power Systems, IEEE Transactions on*, 3(1):272–277, Feb 1988.

[80] H. Mori and T. Horiguchi. A genetic algorithm based approach to economic load dispatching. In *[1993] Proceedings of the Second International Forum on Applications of Neural Networks to Power Systems*, pages 145–150, 1993.

[81] R. Naresh and J. Sharma. Two-phase neural network based solution technique for short term hydrothermal scheduling. *IEE Proceedings - Generation, Transmission and Distribution*, 146(6):657–663, Nov 1999.

[82] P. Naveen, A. K. Chandel, B. Vedik, and K. Topwal. Economic dispatch with valve point effect using symbiotic oragnisms search algorithm. In *2016 International Conference on Energy Efficient Technologies for Sustainability (ICEETS)*, pages 430–435, April 2016.

[83] Taher Niknam. A new fuzzy adaptive hybrid particle swarm optimization algorithm for non-linear, non-smooth and non-convex economic dispatch problem. *Applied Energy*, 87(1):327 – 339, 2010.

[84] O. Nilsson and D. Sjelvgren. Mixed-integer programming applied to short-term planning of a hydro-thermal system. *IEEE Transactions on Power Systems*, 11(1):281–286, Feb 1996.

[85] S. O. Orero and M. R. Irving. A genetic algorithm modelling framework and solution technique for short term optimal hydrothermal scheduling. *IEEE Transactions on Power Systems*, 13(2):501–518, May 1998.

[86] R. E. Perez-Guerrero and J. R. Cedeno-Maldonado. Differential evolution based economic environmental power dispatch. In *Proceedings of the 37th Annual North American Power Symposium, 2005.*, pages 191–197, Oct 2005.

[87] R. E. Perez-Guerrero and J. R. Cedeno-Maldonado. Economic power dispatch with non-smooth cost functions using differential evolution. In *Proceedings of the 37th Annual North American Power Symposium, 2005.*, pages 183–190, Oct 2005.

[88] J. Peschon, D.W. Bree, and L.P. Hajdu. Optimal power-flow solutions for power system planning. *Proceedings of the IEEE*, 60(1):64–70, Jan 1972.

[89] P. K. Rao and B. R. Teja. Teaching learning based optimization for short term hydro-thermal scheduling. In *2015 Conference on Power, Control, Communication and Computational Technologies for Sustainable Growth (PCCCTSG)*, pages 26–31, Dec 2015.

[90] Singiresu S Rao and SS Rao. *Engineering optimization: theory and practice*. John Wiley & Sons, 2009.

[91] A. Rathi, A. Agarwal, A. Sharma, and P. Jain. A new hybrid technique for solution of economic load dispatch problems based on biogeography based optimization. In *TENCON 2011 - 2011 IEEE Region 10 Conference*, pages 19–24, Nov 2011.

[92] P.K. Roy, S.P. Ghoshal, and S.S. Thakur. Biogeography based optimization for multi-constraint optimal power flow with emission and non-smooth cost function. *Expert Systems with Applications*, 37(12):8221 – 8228, 2010.

[93] S. Ruzic and R. Rajakovic. Optimal distance method for lagrangian multipliers updating in short-term hydro-thermal coordination. *IEEE Transactions on Power Systems*, 13(4):1439–1444, Nov 1998.

[94] S. Ruzic, A. Vuckovic, and N. Rajakovic. A flexible approach to short-term hydro-thermal coordination. ii. dual problem solution procedure. *IEEE Transactions on Power Systems*, 11(3):1572–1578, Aug 1996.

[95] A.A. Sachedina. *The Just Ruler in Shi'ite Islam: The Comprehensive Authority of the Jurist in Imamite Jurisprudence*. Oxford University Press, 1998.

[96] T. N. Saha and S. A. Khaparde. An application of a direct method to the optimal scheduling of hydrothermal system. *IEEE Transactions on Power Apparatus and Systems*, PAS-97(3):977–983, May 1978.

[97] Musoke H. Sendaula, Saroj K. Biswas, Ahmed Eltom, Cliff Parten, and Wilson Kazibwe. Simultaneous solution of unit commitment and dispatch problems using artificial neural networks. *International Journal of Electrical Power & Energy Systems*, 15(3):193 – 199, 1993.

[98] G.B. Sheble and G.N. Fahd. Unit commitment literature synopsis. *Power Systems, IEEE Transactions on*, 9(1):128–135, Feb 1994.

[99] A. Shukla, R. Tiwari, and R. Kala. *Towards Hybrid and Adaptive Computing: A Perspective*. Studies in Computational Intelligence. Springer, 2010.

[100] D. Simon. Biogeography-based optimization. *IEEE Transactions on Evolutionary Computation*, 12(6):702–713, Dec 2008.

[101] Dan Simon. *Evolutionary Optimization Algorithms*. John Wiley & Sons, 2013.

[102] D.N. Simopoulos, S.D. Kavatza, and C.D. Vournas. Reliability constrained unit commitment using simulated annealing. *Power Systems, IEEE Transactions on*, 21(4):1699–1706, Nov 2006.

[103] N. Sinha, R. Chakrabarti, and P.K. Chattopadhyay. Evolutionary programming techniques for economic load dispatch. *Evolutionary Computation, IEEE Transactions on*, 7(1):83–94, Feb 2003.

[104] N. Sinha, R. Chakrabarti, and P.K. Chattopadhyay. Evolutionary programming techniques for economic load dispatch. *Evolutionary Computation, IEEE Transactions on*, 7(1):83–94, Feb 2003.

[105] S. Sivasubramani and K.S. Swarup. Multi-objective harmony search algorithm for optimal power flow problem. *International Journal of Electrical Power & Energy Systems*, 33(3):745 – 752, 2011.

[106] Rainer Storn and Kenneth Price. *Differential evolution-a simple and efficient adaptive scheme for global optimization over continuous spaces*, volume 3. ICSI Berkeley, 1995.

[107] Rainer Storn and Kenneth Price. *Differential evolution-a simple and efficient adaptive scheme for global optimization over continuous spaces*, volume 3. ICSI Berkeley, 1995.

[108] Rainer Storn and Kenneth Price. Differential evolution- a simple and efficient heuristic for global optimization over continuous spaces. *Journal of Global Optimization*, 11(4):341–359, 1997.

[109] P. Subbaraj and P.N. Rajnarayanan. Optimal reactive power dispatch using self-adaptive real coded genetic algorithm. *Electric Power Systems Research*, 79(2):374 – 381, 2009.

[110] T. Sum-im and W. Ongsakul. Ant colony search algorithm for unit commitment. In *IEEE International Conference on Industrial Technology, 2003*, volume 1, pages 72–77 Vol.1, Dec 2003.

[111] Chengfu Sun, Haiyan Zhou, and Liqing Chen. Improved differential evolution algorithms. In *Computer Science and Automation Engineering (CSAE), 2012 IEEE International Conference on*, volume 3, pages 142–145, May 2012.

[112] D.I. Sun, Bruce Ashley, Brian Brewer, Art Hughes, and William F. Tinney. Optimal power flow by newton approach. *Power Apparatus and Systems, IEEE Transactions on*, PAS-103(10):2864–2880, Oct 1984.

[113] S. Sutradhar, N. B. DevChoudhury, and N. Sinha. Grey wolf optimizer for short term hydrothermal scheduling problems. In *Michael Faraday IET International Summit 2015*, pages 522–527, Sept 2015.

[114] K.S. Swarup and S. Yamashiro. Unit commitment solution methodology using genetic algorithm. *Power Systems, IEEE Transactions on*, 17(1):87–91, Feb 2002.

[115] Jianxin Tang and P. B. Luh. Hydrothermal scheduling via extended differential dynamic programming and mixed coordination. *IEEE Transactions on Power Systems*, 10(4):2021–2028, Nov 1995.

[116] K. Tangpatiphan and A. Yokoyama. Optimal power flow with steady-state voltage stability consideration using improved evolutionary programming. In *PowerTech, 2009 IEEE Bucharest*, pages 1–7, June 2009.

[117] G.L. Torres and V.H. Quintana. On a nonlinear multiple-centrality-corrections interior-point method for optimal power flow. *Power Systems, IEEE Transactions on*, 16(2):222–228, May 2001.

[118] E. Tsoi, Kit Po Wong, and Chun Che Fung. Hybrid ga/sa algorithms for evaluating trade-off between economic cost and environmental impact in generation dispatch. In *Proceedings of 1995 IEEE International Conference on Evolutionary Computation*, volume 1, pages 132–, Nov 1995.

[119] K. Vu, M.M. Begouic, and D. Novosel. Grids get smart protection and control. *Computer Applications in Power, IEEE*, 10(4):40–44, Oct 1997.

[120] D. C. Walters and G. B. Sheble. Genetic algorithm solution of economic dispatch with valve point loading. *IEEE Transactions on Power Systems*, 8(3):1325–1332, Aug 1993.

[121] Kit Po Wang and J. Yuryevich. Evolutionary-programming-based algorithm for environmentally-constrained economic dispatch. *IEEE Transactions on Power Systems*, 13(2):301–306, May 1998.

[122] Warsono, D.J. King, C.S. Ozveren, and D.A. Bradley. Economic load dispatch optimization of renewable energy in power system using genetic algorithm. In *Power Tech, 2007 IEEE Lausanne*, pages 2174–2179, July 2007.

[123] T. G. Werner and J. F. Verstege. An evolution strategy for short-term operation planning of hydrothermal power systems. *IEEE Transactions on Power Systems*, 14(4):1362–1368, Nov 1999.

[124] A.J.W.B. Wollenberg. *POWER GENERATION OPERATION & CONTROL, 2ND ED (With CD)*. Wiley India Pvt. Limited, 2006.

[125] K. P. Wong and C. C. Fung. Simulated annealing based economic dispatch algorithm. *IEE Proceedings C - Generation, Transmission and Distribution*, 140(6):509–515, Nov 1993.

[126] K. P. Wong and Y. W. Wong. Short-term hydrothermal scheduling. ii. parallel simulated annealing approach. *IEE Proceedings - Generation, Transmission and Distribution*, 141(5):502–506, Sep 1994.

[127] K. P. Wong and Y. W. Wong. Short-term hydrothermal scheduling part. i. simulated annealing approach. *IEE Proceedings - Generation, Transmission and Distribution*, 141(5):497–501, Sep 1994.

[128] Kit Po Wong and Jason Yuryevich. Optimal power flow method using evolutionary programming. In *Simulated Evolution and Learning*, pages 405–412. Springer, 1999.

[129] Allen J. Wood and Bruce F. Wollenberg. *Power Generation Operation and Control (2nd Edition)*. Wiley India Pvt. Limited, 2006.

[130] Yong-Gang Wu, Chun-Ying Ho, and Ding-Yo Wang. A diploid genetic approach to short-term scheduling of hydro-thermal system. *IEEE Transactions on Power Systems*, 15(4):1268–1274, Nov 2000.

[131] Le Xie and M.D. Ilic? Model predictive dispatch in electric energy systems with intermittent resources. In *Systems, Man and Cybernetics, 2008. SMC 2008. IEEE International Conference on*, pages 42–47, Oct 2008.

[132] M. y. El-Sharkh, N. S. Sisworahardjo, A. Rahman, and M. S. Alam. An improved ant colony search algorithm for unit commitment application. In *2006 IEEE PES Power Systems Conference and Exposition*, pages 1741–1746, Oct 2006.

[133] Hong-Tzer Yang, Pai-Chuan Yang, and Ching-Lien Huang. Evolutionary programming based economic dispatch for units with non-smooth fuel cost functions. *IEEE Transactions on Power Systems*, 11(1):112–118, Feb 1996.

[134] P. C. Yang, H. T. Yang, and C. L. Huang. Scheduling short-term hydrothermal generation using evolutionary programming techniques. *IEE Proceedings - Generation, Transmission and Distribution*, 143(4):371–376, Jul 1996.

[135] Xin-She Yang. *Engineering optimization: an introduction with metaheuristic applications*. John Wiley & Sons, 2010.

[136] Binghui Yu, Xiaohui Yuan, and Jinwen Wang. Short-term hydro-thermal scheduling using particle swarm optimization method. *Energy Conversion and Management*, 48(7):1902 – 1908, 2007.

[137] Haibo Zhang, Li-Zi Zhang, and Fanling Meng. Reactive power optimization based on genetic algorithm. In *Power System Technology, 1998. Proceedings. POWERCON '98. 1998 International Conference on*, volume 2, pages 1448–1453 vol.2, Aug 1998.

[138] J. Zhang, J. Wang, and C. Yue. Small population-based particle swarm optimization for short-term hydrothermal scheduling. *IEEE Transactions on Power Systems*, 27(1):142–152, Feb 2012.

[139] Wen Zhang and Yutian Liu. Reactive power optimization based on pso in a practical power system. In *Power Engineering Society General Meeting, 2004. IEEE*, pages 239–243 Vol.1, June 2004.

[140] Jizhong Zhu. *Optimization of power system operation*. John Wiley & Sons, 2015.

[141] F. Zia, M. Nasir, and A.A. Bhatti. Optimization methods for constrained stochastic wind power economic dispatch. In *Power Engineering and Optimization Conference (PEOCO), 2013 IEEE 7th International*, pages 129–133, June 2013.

[142] R. D. Zimmerman, C. E. Murillo-Sanchez, and R. J. Thomas. Matpower: Steady-state operations, planning, and analysis tools for power systems research and education. *IEEE Transactions on Power Systems*, 26(1):12–19, Feb 2011.

[143] Ray D Zimmerman, Carlos E Murillo-Sánchez, and Deqiang Gan. A matlab power system simulation package, 1997.